FINAL
IN-39-CR

NASA CONTRACTOR REPORT

NASA-CR-197229

DEVELOPMENT AND APPLICATION OF STRUCTURAL DYNAMICS ANALYSIS CAPABILITIES

Klaus W. Heinemann
and Shig Hozaki

Eloret Institute
3788 Fabian Way
Palo Alto, CA 94303

Prepared for

NASA Dryden Flight Research Facility
under **Cooperative Agreement NCC2-518**

National Aeronautics and
Space Administration

Ames Research Center
Moffett Field, California 94035

NASA CONTRACTOR REPORT

DEVELOPMENT AND APPLICATION OF STRUCTURAL DYNAMICS ANALYSIS CAPABILITIES

Klaus W. Heinemann
and Shig Hozaki

CONTRACT NAS2–

NASA

1. Report No.	2. Government Accession No.	3. Recipient's Catalog No.
4. Title and Subtitle Development and Application of Structural Dynamics Analysis Capabilities		5. Report Date 11/15/94
		6. Performing Organization Code
7. Author(s) K. Heinemann and S. Hozaki		8. Performing Organization Report No.
		10. Work Unit No.
9. Performing Organization Name and Address Eloret Institute 3788 Fabian Way Palo Alto CA 94303		11. Contract or Grant No. NCC2-518
		13. Type of Report and Period Covered 2/1/88 to 9/30/94
12. Sponsoring Agency Name and Address National Aeronautics and Space Administration, Washington, D.C. 20456		14. Sponsoring Agency Code

15. Supplementary Notes

Point of Contact: Dr. K. Gupta, c/o D-2131 NASA Dryden Flight Research Facility, Edwards, CA 93523-0273

16. Abstract

Extensive research activities were performed in the area of multidisciplinary modeling and simulation of aerospace vehicles that are relevant to NASA Dryden Flight Research Facility. The efforts involved theoretical development, computer coding, and debugging of the STARS code. New solution procedures were developed in such areas as structures, CFD, and graphics, among others. Furthermore, systems-oriented codes were developed for rendering the code truly multidisciplinary and rather automated in nature. Also, work was performed in pre- and post-processing of engineering analysis data.

17. Key Words (Suggested by Author(s))	18. Distribution Statement
STARS program modeling of aerospace vehicles simulation of aerospace vehicles CFD codes	unclassified, unlimited

19. Security Classif. (of this report)	20. Security Classif. (of this page)	21. No. of Pages	22. Price*
unclassified	unclassified		

*For sale by the National Technical Information Service, Springfield, Virginia 22161

DEVELOPMENT AND APPLICATION OF STRUCTURAL DYNAMICS ANALYSIS CAPABILITIES

Final Technical Report

for
Cooperative Agreement NCC2-518

for the period
February 1, 1988 - September 30, 1994

Submitted to

National Aeronautics and Space Administration
Dryden Flight Research Facility
Edwards, California 93523

Kevin L. Petersen, NASA Technical Officer

Prepared by

ELORET INSTITUTE
1178 Maraschino Drive
Sunnyvale, CA 94087
Phone: 408 730-8422 and 415 493-4710
Fax: 408 730-1441
K. Heinemann, Principal Investigator and Grant Administrator

15 November, 1994

SUMMARY

Eloret Institute has been engaged in extensive research activities in the area of multidisciplinary modeling and simulation of aerospace vehicles that are relevant to NASA Dryden Flight Research Facility. This effort involved theoretical development, computer coding, and debugging of the STARS code. New solution procedures were developed in such areas as structures, CFD, and graphics, among others. Furthermore, systems-oriented codes were developed for rendering the code truly multidisciplinary and rather automated in nature. Also, work was performed in pre- and post-processing of engineering analysis data.

A. STARS CFD RESEARCH

A novel accelerated Euler solution technique and a resulting code were developed that proved to be rather efficient as convergence was achieved at a much faster rate than the usual Euler solution. This code was based on a double-precision version of the STARS Euler solution module and involves implementation of the acceleration of solution convergence for each degree of freedom. The resulting code can now routinely solve large order NASA CFD problems, effecting savings of more than 50% in solution time. This accelerated solution module is now an integral part of the STARS program, being extensively used for solution of day-to-day NASA problems.

B. STARS SYSTEM MODULE DEVELOPMENT

Over the past few years, Eloret Institute performed continuous and extensive research as follows:

I. Development of a "shell" system code for integrating all submodules in the STARS-SOLIDS program. Also, an enhanced version of the shell has recently been successfully introduced that enables effortless implementation of a versatile, nonlinear analysis capability in the following two aspects:

(a) geometric nonlinearity that includes large displacement and rotation effects in a structure, and

(b) material nonlinearity, including elasto-plasticity.

II. Maintenance of the STARS program. This involved continuous improvement of program performance from a systems point of view.

III. Graphics. Much effort has been devoted to the development of a pre-processor that involves automated generation of 2D- and 3-D finite element grids for subsequent structural and CFD analyses. Research activities were performed in this area to optimize mesh generation time. For example, in the CFD area, a new discretization technique was developed that reduces generation time of the tetrahedral elements by approximately a factor of eight (8). These modules are now an integral part of the STARS code and are routinely used for the solution of practical NASA problems.

At the other end of the analysis spectrum, a STARS post-processor module was developed for IBM as well as DEC computer systems, to enable effective color post-processing of solution results. These were developed for both SOLIDS and CFD modules. Further development has been initiated for post-processing of linear aerodynamic and controls engineering problems.

C. STARS HEAT TRANSFER ANALYSIS

Some effort was expended toward the development of a heat transfer analysis module of the STARS code for solution of steady-state as well as transient problems. Some nonlinear effects, such as radiation boundary conditions, were also incorporated in the computer program, which becomes a new module for the STARS code.

D. PUBLICATIONS AND REPORTS

A number of publications resulted from this research activity, including:

1. K.K. Gupta and C.L. Lawson, *Development of a Block Lanczos Algorithm for Free Vibration Analysis of Spinning Structures*," Int. Journal for Numerical Methods in Engineering, **26** (1988) 1029.

2. STARS (STructural Analysis RoutineS), Eloret Institute Research Report 10/1989.

3. K.K. Gupta and C.L. Lawson, *Solution of Finite Dynamic Element Quadratic Matrix Eigenproblem by a Block Lanczos Procedure*," Int. Journal for Numerical Methods in Engineering (1991), Eloret Institute Research Report 1990.

4. K.K. Gupta, K. Petersen, and C.L. Lawson, *"Multidisciplinary Modeling and Simulation of a Generic Hypersonic Vehicle,"* AIAA 3rd Int. Aerospace Planes Conference, Orlando, 12/1991, AIAA-Paper 91-5015.

5. K.K. Gupta, K. Petersen, and C.L. Lawson, *"On Some Recent Advances in multidisciplinary Analysis of Hypersonic Vehicles,"* AIAA 4th Int. Aerospace Planes Conference, Orlando, 12/1992, AIAA-Paper 92-5026.

6. K.K. Gupta, *"STARS - An Integrated General-Purpose Finite Element Structural, Aeroelastic, and Aeroservoelastic Analysis Computer Program,"* NASA Technical Memorandum 101709, 7/12/93.
(A copy of this report, to which ELORET personnel heavily contributed, is attached as APPENDIX A).

7. P. Arentzen, *"NO_x Emissions from Aircraft Engines: Exhaust Emissions and Engine Efficiency for Aircraft Gas Turbine Engines, a Literature Review,"* Eloret Institute Report, May 1994. (A copy is attached as APPENDIX B).

APPENDIX A

NASA Technical Memorandum 101709
Revised 7/12/93

STARS - An Integrated General-Purpose Finite Element Structural, Aeroelastic, and Aeroservoelastic Analysis Computer Program

K.K. Gupta

January 1991

National Aeronautics and
Space Administration

CONTENTS

FIGURES

TABLES

SUMMARY

A multidisciplinary, finite element based and highly graphics oriented analysis capability that includes such disciplines as structures, heat transfer, CFD, aerodynamics and controls engineering, among others, has been achieved by integrating several new modules in the original STARS (STructual Analysis RoutineS) computer program (ref.1). Each individual analysis module is general-purpose in nature; which are also effectively integrated to yield aeroelastic and aeroservoelastic (ASE) solution of complex engineering problems. Examples of advanced NASA-DFRF projects analyzed by the code in recent years include X-29A, F18 HARV/TVCS, B-52/Pegasus, Generic Hypersonics, NASP, SR-71/Halo, and the high speed civil transport (HSCT), among others. Extensive graphics capabilities exist for convenient model development as well as postprocessing of analysis results.

The program is written in modular form in standard FORTRAN language to run on a variety of computers such as the IBM RISC/6000, DEC, and Cray Y-MP; associated graphics codes utilize standard PHIGS as well as the IBM/graPHIGS language for color depiction.

1. INTRODUCTION

The highly-integrated digital computer program, STARS, has been designed as an efficient tool for analyzing practical engineering problems, as well as for supporting relevant research and development activities; it has also proved to be an effective teaching aid, all such activities being mutually enhancing and interrelated (fig. 1). Each individual module (fig. 2) of the program is general-purpose in nature, being capable of solving a wide array of problems. Such finite element analysis modules are also appropriately combined to yield unique multidisciplinary modeling and simulation capabilities of complex engineering problems.

The STRUCTURES (SOLIDS) module is capable of analyzing static, stability, vibration and dynamic response problems of all types of structures including spinning ones subjected to mechanical as well as thermal loading. The element library consists of a number of 1-, 2-, and 3-D elements with general material properties that also includes composite and sandwich elements. Structural as well as viscous damping may be included in the analysis. Figure 3 provides an overview of the SOLIDS link.

The heat conduction analysis capability in the program is effected through the HEAT TRANSFER module. Both steady state as well as transient analyses may be performed, that also include nonlinear solution of problems with radiation boundary conditions. The element library consists of line, shell, and solid elements, including composites.

A schematic of the associated aeroelastic and aeroservoelastic (ASE) analyses is depicted in figure 4. Thus, once the frequencies and mode shapes of the structure are derived from finite element analysis employing the STARS-SOLIDS module, the STARS-AERO module is next utilized to compute the unsteady aerodynamic forces on the structure. An alternative option enables input of measured modal data in lieu of calculated data. A flutter solution is then achieved using the k and/or p-k methods. The user has to input details of the aerodynamic paneling to achieve the aeroelastic analysis.

Subsequent ASE analysis may be achieved by first employing the STARS-CONTROLS-PADÉ submodule. The user provides essential data to perform a polynomial curve fitting of unsteady aerodynamic forces resulting in the state-space matrices. For an alternative open-loop flutter analysis, such data consist of information on polynomial tension coefficients, previously calculated generalized masses, and damping and modal characteristics as well as a set of velocity values. Additional data, in lieu of velocity values, relating to coordinate transformations from earth- to body-centered coordinate systems and also sensor locations, are needed for the subsequent ASE analysis for frequency response calculations and also for determination of damping and frequency values. This is achieved by the STARS-CONTROLS-FRESP submodule in which the primary data input relates to analog and/or digital controller blocks connectivity, associated transfer function polynomial descriptions as well as gain input, specifications for system output and input, and also connection details between the plant and the blocks. This ASE analysis procedure may also be effectively utilized as the third flutter solution option. The CONTROLS module also has a control law design capability based on the Eigenstructure Assignment procedure.

The CFD (computational fluid dynamics) module of the program, that employs unstructured grids for domain discretizaion, may be effectively employed for the solution of fluid flow problems. Related nonlinear aeroelastic and aeroservoelastic analysis capability has also been implemented in the program. Associated PROPULSION module essentially employs CFD techniques for simulation of flow mixing phenomenon. Data pertaining to temperature dependent material properties are stored in the MATERIALS module.

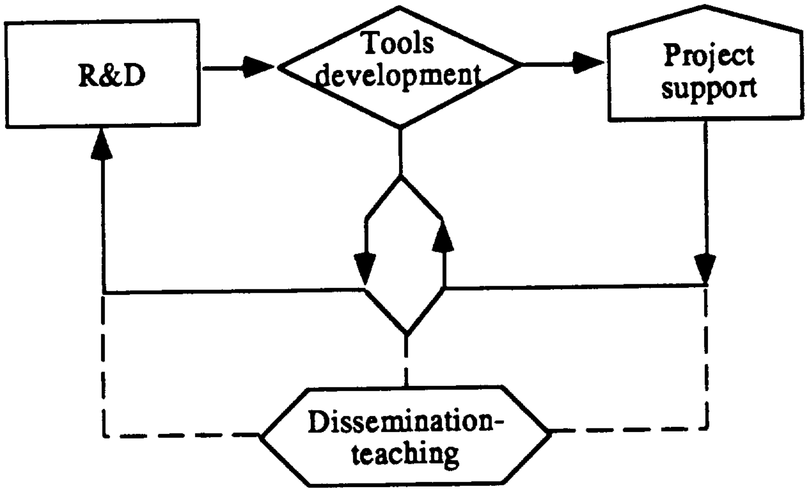

Figure 1. Structural synthesis.

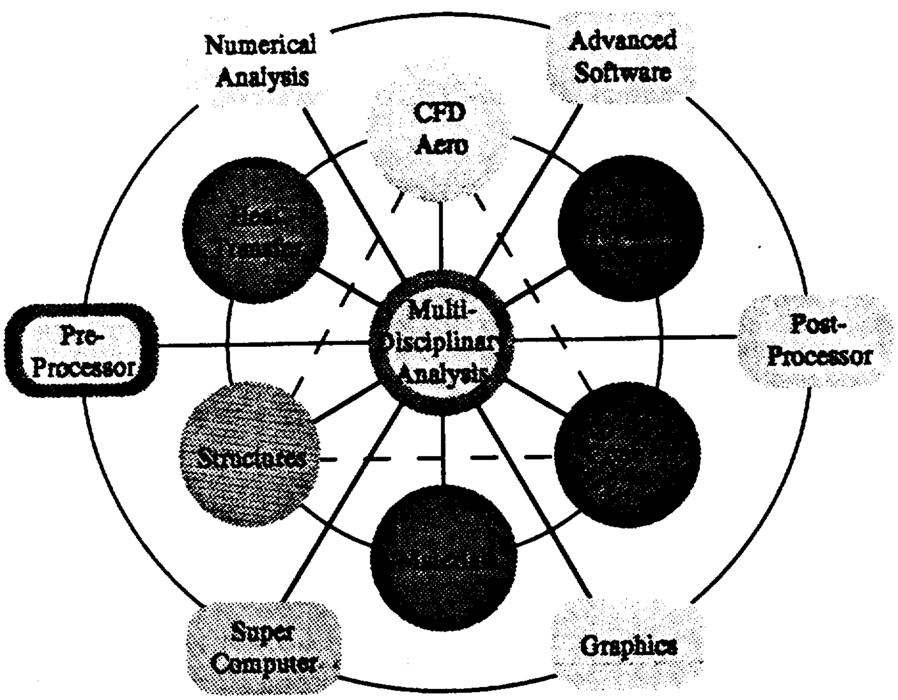

FE Structural Analysis
Spinning structures
Mechanical and thermal loading
General and composite materials

Static, buckling
Vibration, dynamic responses

Aeroelasticity -
Flutter and divergence

Aeroservoelasticity -
Frequency response, damping and frequencies, digital and analog controllers

FE Heat transfer
FE Computational fluid dynamics

Preprocessor - automatic FEM model data generation
Postprocessor - color graphical depiction of analysis results

Figure 2. Major modules of STARS.

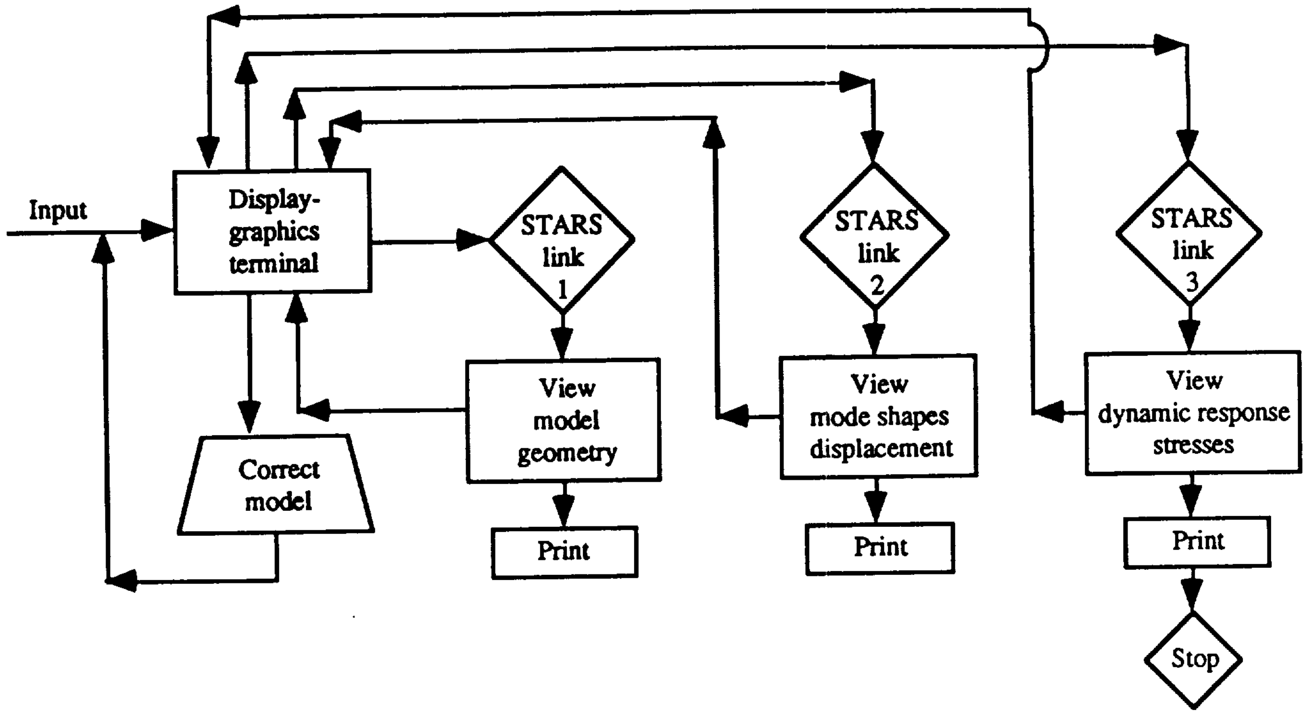

Figure 3. STARS-SOLIDS overview.

The NUMERICAL ANALYSIS module contains a number of efficient solution procedures for large sparse matrix linear equations as well as eigenvalue problems. Thus a block Lanczos procedure is available for solution of free vibration problems of nonspinning and spinning structures as well as the quadratic matrix eigenvalue problem associated with a finite dynamic element formulation. An alternative procedure, based on a combined Sturm sequence and inverse iteration technique, is also available that enables extraction of roots, as well as associated vectors lying within any specified bound.

A separate preprocessor routine, PREPROC, has been developed for automated generation of nodal, element, and other associated input data for any continuum. It is capable of generating complex structural forms through duplication, mirror-imaging, and cross-sectioning of modular representative structures. A fully automated 3-D mesh generation capability is also an important feature of this module. The STARS postprocessor program, POSTPLOT, on the other hand, is utilized for extensive color plotting of various structual, heat transfer and CFD related solution results.

Section 2 provides a concise description of the STARS-SOLIDS module of the program as well as highlights of some of its important features, and section 3 depicts the data input procedure. Section 4 provides summaries of input data and analysis results for a number of sample test cases relevant to this module. Section 5 describes the various features of the aeroelastic (AERO) and ASE analyses capabilities, whereas section 6 provides data input details of various related submodules. A representative, integrated aero-structural-control sample problem is worked out in detail in section 7. Some details of CFD analysis as well as nonlinear aeroelasticity and aeroservoelasticity (ASE) are provided in section 8.

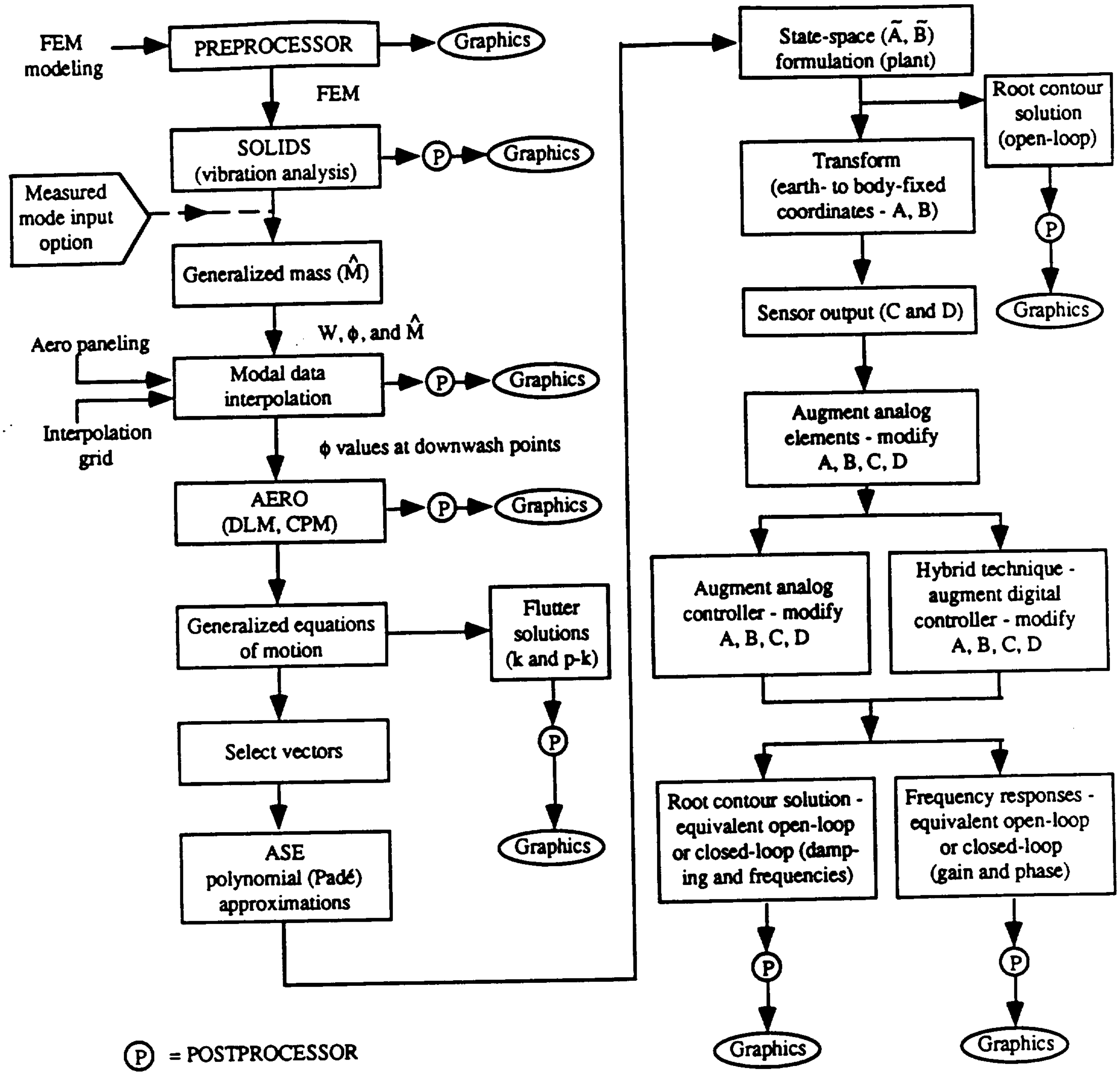

Figure 4. STARS-ASE flowchart.

2. STARS-SOLIDS PROGRAM DESCRIPTION

The structure to be analyzed by STARS may be composed of any suitable combination of one-, two-, and three-dimensional (1-, 2-, and 3-D) elements. The general features of the STARS-SOLIDS module include the following:

1. A general-purpose, compact, finite element program.
2. Elements: bars, rods, beams, 3-D line elements, rigid bars, membrane, triangular and quadrilateral plane, plate, shells, as well as sandwich panels and composite elements, tetrahedral and hexahedral solids.
3. Geometry: any relevant structure formed by a suitable combination of the elements in (2).
4. Material: general, isotropic, orthotropic, and anisotropic material.
5. Analysis: natural frequencies and mode shapes of nonrotating and rotating structures with or without structural damping, viscous damping, or both, including initial load (prestress) effect; stability (buckling) analysis; dynamic-response analysis of nonrotating and rotating structures; and static analysis for multiple sets of mechanical and thermal loading. Also steady-state and transient heat transfer analysis including non-linear radiation boundary conditions.

Special features of the STARS program include the following:

1. Random data input within a subset.
2. Matrix bandwidth minimization.
3. Automatic node and element generation.
4. General nodal deflection boundary conditions.
5. Multiple sets of static load input.
6. Preprocessor and postprocessor.
7. Plot of initial geometry.
8. Plots of mode shapes, nodal deformations, and element stresses as a function of time, as required.

Structural geometry is described in terms of the global and/or the local-global coordinate system (GCS/LGCS) having a right-handed Cartesian set of X-, Y-, and Z-coordinate axes. Each structural node is assumed to have six degrees of freedom (DOF) consisting of three translations, UX, UY, UZ, and three rotations, UXR, UYR, UZR, which are the undetermined quantities in the associated solution process. Details of some important features of the program are summarized below.

2.1 Nodal and Element Data Generation

The STARS program provides simple linear interpolation schemes that enable automatic generation of nodal and element data. Generation of nodal data is dependent on the occurrence of such features as nodes lying on straight lines and common nodal displacement boundary conditions, whereas generation of element data is possible if the finite element mesh is repetitive in nature with elements possessing common basic properties. The program enables input of data employing a number of rectangular local-global coordinate systems (LGCS) relevant to various substructures.

A separate preprocessor routine, PREPROC, has been developed for automated generation of nodal, element, and other associated input data for any continuum. The preprocessor is an interactive graphics structures modeling program. It is capable of generating complex structures through duplication, mirror-imaging, and cross-sectioning of modular representative structures.

2.2 Matrix Bandwidth Minimization

This feature enables effective bandwidth minimization of the stiffness, inertia, and all other relevant system matrices by reordering input nodal numbers, taking into consideration first-order as well as second-order nodal connectivity conditions. With reference to figure 5, the existing nodal numbering may be modified (ref. 2) to minimize bandwidth of associated matrices. Therefore, any node with minimum first-order connectivity may be chosen as the starting node. Accordingly, any one of nodes 1, 4, 7, 10, 13, and 16, all of which have a minimum first-order nodal connectivity of two, may be selected as the first node to start the nodal numbering scheme. However, nodes 1, 4, 10, and 13 possess a higher second-order connectivity condition than do nodes 7 and 16. For example, nodes connected to node 1 (namely nodes 2 and 18) are, in turn, connected to a total of seven nodes, whereas such a connectivity number for either node 7 or 16 happens to be only six. As such, either node 7 or 16 may be chosen as the starting node for the renumbering scheme. A revised nodal numbering that minimizes matrix bandwidth is shown in parentheses in figure 5. The present minimization scheme also takes into consideration the presence of nodal interdependent displacement boundary conditions.

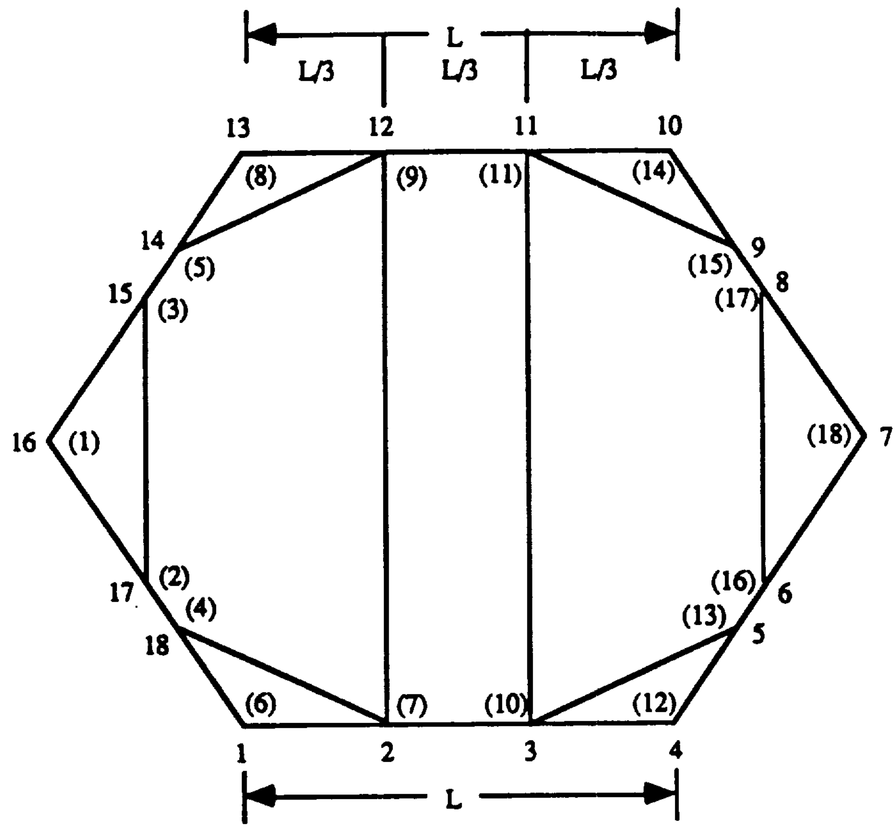

Figure 5. Bandwidth minimization scheme.

2.3 Deflection Boundary Conditions

The nodal displacement relationships may be classified as zero, finite, and interdependent deflection boundary conditions (ZDBC, FDBC, and IDBC). Details of such a formulation are provided in section 3.4. Thus, in addition to prescribed zero and finite displacements, the motion of any node in a particular degree of freedom can be related in any desired manner to the motion of the same or any other combination of nodes in any set of specified directions.

2.4 Prescribed Loads

A structure may be subjected to any combination of mechanical and thermal loadings. The loads in the mechanical category may be either concentrated at nodes or distributed. Thus, uniform pressure may be applied along the length of line elements acting in the direction of the local y- and z-axes. Such uniform surface loads are assumed to act in the direction of the local z-axis of the shell and solid elements, acting respectively on the shell and solid base surfaces.

The effect of thermal loading can be incorporated by the appropriate input of data pertaining to uniform element temperature increases, as well as thermal gradients.

2.5 Static Analysis

Static analysis, performed by setting the parameter IPROB = 8 in the input data, is effected by solving the set of linear simultaneous equations

$$\mathbf{KU} = \mathbf{P} \tag{1}$$

where

K	=	system elastic stiffness matrix
U	=	nodal displacement vector
P	=	external nodal load vector
IPROB	=	integer designating problem type (defined in section 3.1)

A multiple set of load vectors is represented by the matrix **P** incorporating effects of both mechanical and thermal loading. The equations are solved once, initially by Gaussian elimination, and solutions pertaining to multiple nodal load cases are obtained by simple back substitution.

2.6 Elastic Buckling Analysis

A buckling analysis is performed by solving the eigenvalue problem

$$(\mathbf{K_E} + \gamma \mathbf{K_G})\mathbf{U} = 0 \tag{2}$$

in which $\mathbf{K_E}$ and $\mathbf{K_G}$ are elastic stiffness and geometric stiffness matrices, respectively; **U** represents the buckled mode shapes and γ is the buckling load. This is achieved by setting IPROB = 9.

2.7 Free Vibration Analysis

The matrix equation of free vibration for the general case of a spinning structure with viscous and structural damping is expressed (ref. 3) as

$$\left[\mathbf{K_E}(1 + i^* g) + \mathbf{K_G} + \mathbf{K'}\right]\mathbf{U} + (\mathbf{C_C} + \mathbf{C_D})\dot{\mathbf{U}} + \mathbf{M}\ddot{\mathbf{U}} = 0 \tag{3}$$

in which a dot indicates differentiation with respect to time; the previously undefined terms are described as follows:

$\mathbf{K'}$	=	centrifugal force matrix
$\mathbf{C_C}$	=	Coriolis matrix
$\mathbf{C_D}$	=	viscous damping matrix
M	=	inertia matrix
g	=	structural damping parameter
i*	=	imaginary number, $\sqrt{-1}$

Such a structure may have individual nonrotating and also rotating components spinning with different spin rates along arbitrary axes.

Various reduced sets of equations pertaining to specific cases of free vibration are given as follows:

1. Free, undamped vibration of nonspinning structures (IPROB = 1):

$$\mathbf{K_E U + M\ddot{U} = 0} \tag{4}$$

2. Free, undamped vibration of spinning structures (IPROB = 2):

$$\mathbf{KU + C_C\dot{U} + M\ddot{U} = 0} \tag{5}$$

with $\mathbf{K = K_E + K_G + K'}$.

3. Free, damped vibration of spinning structures (IPROB = 4, 5), defined by equation (3).

4. Free, damped vibration of nonspinning structures (IPROB = 6, 7):

$$\mathbf{K_E(1 + i^* g)U + C_D\dot{U} + M\ddot{U} = 0} \tag{6}$$

The eigenvalue problems pertaining to the IPROB = 1 and 9 cases are real in nature, but the rest of the above problems involve complex-conjugate roots and vectors. In the special case of a prestressed structure, the matrix $\mathbf{K_G}$ is automatically included in equation (6).

In addition, STARS solves the quadratic matrix eigenvalue problem (IPROB = 3) associated with a dynamic element formulation (ref. 4),

$$\mathbf{\left[K_E - \lambda^2 M - \lambda^4 (M_2 - K_4)\right]U = 0} \tag{7}$$

which is quadratic in terms of the eigenvalues $\chi = \lambda^2$ and where both $\mathbf{M_2}$ and $\mathbf{K_4}$ are the higher order dynamic correction matrices, λ being the natural frequencies. This option is currently being updated to include a number of elements.

Structures prestressed by initial loads may also be analyzed; in which cases the relevant eigenvalue problem for undamped structures has the form

$$\mathbf{\left(K_E + K_G - \lambda^2 M\right)U = 0} \tag{8}$$

in which the geometrical stiffness matrix $\mathbf{K_G}$ is a function of initial stresses; similar formulations are obtained for structures with various forms of damping.

2.8 Dynamic Response Analysis

The modal superposition method is employed for the dynamic response analysis following the computation of structural frequencies and modes. As an example, for a nonrotating, undamped structure, the associated eigenvalue problem of equation (4) is first solved to obtain the first few eigenvectors Φ and also the eigenvalues. The vectors may consist of a set of rigid body modes Φ_r and a number of elastic modes Φ_e which are next mass-orthonormalized so that the matrix product

$$\Phi^T M \Phi = [I] \tag{9}$$

is a unit matrix. A transformation relationship

$$U = \Phi\eta \tag{10}$$

is substituted in the dynamic equation

$$M\ddot{U} + KU = P(t) \tag{11}$$

and when premultiplied by Φ^T, yields a set of uncoupled equations

$$\ddot{\eta}_r = \Phi_r{}^T P(t) \tag{12}$$

and

$$\ddot{\eta}_e + \Omega^2 \eta_e = \Phi_e{}^T P(t) \tag{13}$$

incorporating rigid body and elastic mode effects, respectively; $P(t)$ is the externally applied, time-dependent forcing function, and Ω^2 is a diagonal matrix, with ω_i being the natural frequencies. Solutions of equations (12) and (13) can be expressed in terms of Duhamel's integrals, which, in turn, may be evaluated by standard procedures (ref. 5). In the present analysis, the externally applied, time-dependent forcing function must be applied to the structure in appropriate small, incremental steps of rectangular pulses. The forcing function may be either load or acceleration vectors; the program also allows application of initial displacement and velocity vectors to the structure. For spinning and damped structures, identified as IPROB = 2, 4, 5, 6, and 7, Φ^T is replaced by its transjugate $\overline{\Phi}^T$ in the relevant dynamic response formulation.

2.9 Shift Synthesis

The program provides special eigenvalue switching provisions in the analysis to ensure numerical stability. Such a problem may be encountered in the analysis of aerospace structures, which are designed to be strong and lightweight. For example, the elements of the mass matrix of equation (4) may have numerical values much smaller than those of the stiffness matrix. In such cases, the effect of the mass matrix in the $(K - \lambda^2 M)y = 0$ formulation may be insignificant. Such a problem also occurs in the presence of rigid body modes characterized by "zero" frequencies. An eigenvalue shift strategy has been developed to accommodate such situations.

Thus, the eigenvalue problem pertaining to equation (4) representing the problem defined as IPROB = 1 may be written as

$$(K - \lambda^2 M)y = 0 \tag{14}$$

in which λ is the natural frequency of free vibration, and y is the eigenvector. The stiffness and mass matrices must be suitably perturbed to handle rigid body modes and to maintain numerical stability by negating effects of rounding error. Thus, equation (14) is rearranged as

$$\left[\mathbf{K} + 4\hat{\mathbf{M}} - (\tilde{\lambda} + 4)\hat{\mathbf{M}}\right]\mathbf{y} = 0 \tag{15}$$

or

$$\left(\hat{\mathbf{K}} - \hat{\lambda}\hat{\mathbf{M}}\right)\mathbf{y} = 0 \tag{16}$$

in which

$$\hat{\mathbf{K}} = \mathbf{K} + 4\hat{\mathbf{M}} \tag{17}$$

$$\hat{\mathbf{M}} = \mathbf{F}\mathbf{M} \tag{18}$$

$$\tilde{\lambda} = \frac{\lambda^2}{F} \tag{19}$$

$$\hat{\lambda} = \frac{\lambda^2}{F} + 4 \tag{20}$$

$$F = \frac{\max\left(\frac{|K_{i,i}|}{|M_{i,i}|}\right)}{10^7} \tag{21}$$

where $|K_{i,i}|$ and $|M_{i,i}|$ typically denote the norms of the diagonal elements and the number 10^7 relates to the computational accuracy of the VAX 11 computer. Once the eigenvalue problem defined by equation (16) is solved, the natural frequencies are simply obtained as

$$\lambda = \sqrt{\left(\hat{\lambda} - 4\right)F} \tag{22}$$

A similar procedure is adopted for the analysis of free vibration problems defined by IPROB = 6 and 7, as well as for the buckling analysis (IPROB = 9).

In the case of spinning structures, a somewhat similar strategy is used in perturbing appropriate matrices to ensure effective computation of rigid body modes, as well as numerical stability.

2.10 Formulation for Nodal Centrifugal Forces in Finite Elements

The STARS program can perform dynamic analyses of structures with nonrotating and rotating parts having different spin rates. A general derivation for the in-plane centrifugal forces generated in various elements due to the arbitrary spin rate, along with related formulation of the associated normal components, is given in detail in reference 6. Reference 7 provides details of a block Lanczos algorithm developed for efficient, free vibration analysis of spinning structures.

Once the nodal centrifugal forces have been derived, as previously mentioned, and stored in array **P**, the element stresses in the structure caused by these forces are simply obtained by solving equation (1) (repeated here for convenience),

$$\mathbf{KU} = \mathbf{P}$$

The stresses are next utilized to derive the structural geometrical stiffness matrix $\mathbf{K_G}$ required for solving the free vibration problems defined in section 2.7.

2.11 Material Properties

The structural material may be general in nature. Thus, the finite element material properties may be isotropic, orthotropic, or anisotropic. In the most general case of solid elements having anisotropic material properties, defined as material type 3, the stress-strain matrix is expressed as

$$\boldsymbol{\delta} = \mathbf{E}\boldsymbol{\varepsilon} \tag{23}$$

with $\mathbf{E}_{ij}$ being elements of the general material matrix of order 6 by 6, defining the relationship between the stress vector δ and the strain vector ε. The elements of the upper symmetric half of the **E** matrix, as well as coefficients of thermal expansion and material density consisting of 28 coefficients, are the required data input for the pertinent material type. In this connection, it may be noted that the material data input is designed in such a way as to be quite general; the user may easily incorporate effects of various related features, such as varying material axes orientation, by appropriately calculating the elements of the material matrix. If the material is orthotropic, the input scheme remains the same as for the anisotropic case.

Material type 2 pertains to thin shell elements displaying anisotropic or orthotropic material properties; it requires an input of 13 coefficients. For isotropic material classified as material type 1, only four coefficients constitute the required input data. The isotropic case for sandwich shell elements is designated as material type 4, whereas type 5 pertains to the corresponding orthotropic-anisotropic case. For the heat transfer case, material types 6, 7 and 8 refer to isotropic line, isotropic shell and orthotropic-anisotropic shell element, respectively.

2.12 Heat Transfer Analysis

A heat conduction analysis capability for solids has been incorporated in the STARS program. Figure 6 depicts a typical heat transfer problem in a three-dimensional anisotropic solid solution domain, D, bounded by a surface, S. The corresponding thermal energy equation is derived from the law of conservation of energy and Fourier's law, and the resulting parabolic heat conduction equation is solved subject to an initial condition and boundary conditions on all portions of the surface. A finite element discretization of the continuum is achieved by the method of weighted residuals (ref. 8,9).

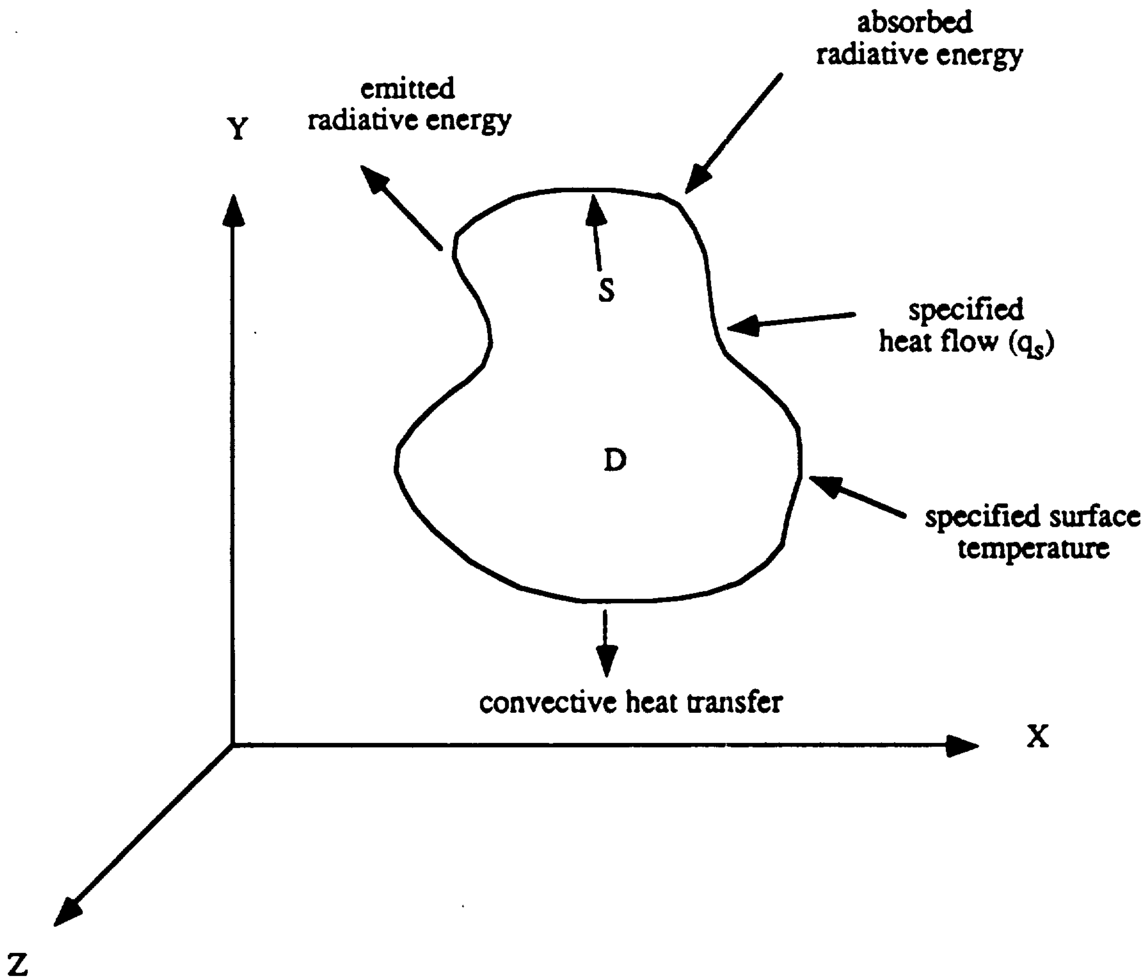

Figure 6. 3-D general heat conduction.

The following analysis types are relevant to the current heat transfer solution effort:

Linear steady-state analysis

$$[[K_c]+[K_h]]\{T\}=\{R_Q\}+\{R_q\}+\{R_h\} \tag{24}$$

in which the element conductance matrix has contributions from conduction and convection, and the heat load vector has contributions from internal heat generation, surface heating and surface convection. The element matrices and heat load vectors are constant and a linear solution of a set of simultaneous equations is required.

Linear transient analysis

$$[C]\{\dot{T}(t)\}+[[K_c]+[K_h(t)]]\{T(t)\}=\{R_Q(t)\}+\{R_q(t)\}+\{R_h(t)\} \tag{25}$$

in which the element capacitance matrices are also required, element convection matrices and heat load vectors are time dependent, and a solution of the equations by a time-marching scheme is required.

Nonlinear steady-state analysis

$$[[K_c(T)]+[K_h(T)]+[K_r(T)]]\{T\}=\{R_Q(T)\}+\{R_q(T)\}+\{R_h(T)\}+\{R_r(T)\} \tag{26}$$

in which the element matrices and heat load vectors have contributions from radiation, and the matrices and vectors are temperature dependent; thus the equations are nonlinear and require solution by an iterative scheme.

Nonlinear transient analysis

$$[C(T)]\{\dot{T}\}+[[K_c(T)]+[K_h(T,t)]+[K_r(T)]]\{T(t)\}=$$

$$\{R_Q(T,t)\}+\{R_q(T,t)\}+\{R_h(T,t)\}+\{R_r(T,t)\} \tag{27}$$

in which the element matrices and heat load vectors are both temperature and time dependent, and solution by an iterative, time-marching scheme is required. In general, nonlinearities are caused by temperature dependent anisotropic material properties and convection coefficients as well as nonlinear radiation boundary conditions.

The following definitions pertain to the above numerical formulations and figure 6:

C	=	element capacitance matrix.
K_c, K_h, K_r	=	element conductance matrices related to conduction, convection, and radiation, respectively.
R_T, R_Q, R_q R_h, R_r	=	Heat load vectors arising from specified nodal temperatures, internal heat generation, specified surface heating, surface convection, and incident surface radiant heating, respectively.
q_s, q_r	=	specified surface and incident radiant heat flow rates/unit area, respectively.
n_x, n_y, n_z	=	direction cosines of the outward normal to the surface.

2.13 Output of Analysis Results

A dynamic response analysis, in general, yields an output of nodal deformations and element stresses as appropriate functions of time. Additional printouts provide summaries of maximum deformations and stresses/loads, as appropriate, as well as principal stresses and relevant angles. For line elements, member endloads and moments constitute the usual output of results. In the case of thin shell elements, the stresses σ_{xx}, σ_{yy}, and σ_{xy} are calculated at the centroid of the element and at both its top and bottom surfaces. For solid elements, all six components of stresses (σ_{xx}, σ_{yy}, σ_{zz}, σ_{xy}, σ_{yz}, σ_{zx}) are computed at the center of the volume of the element. Since free vibration analysis constitutes a vital preliminary for the dynamic response analysis, the natural frequencies and associated modes are computed by the program and printed out, as desired. Similar results are obtained for elastic buckling analysis. For static problems, the nodal displacements and element stresses are computed for multiple-load cases. A heat transfer analysis yields unknown nodal temperatures as the solution.

Special printout options make possible a selective output of analysis results. Thus, such computed data as stiffness and inertia matrices may be printed out, as desired. Initially, the program automatically prints out the generated nodal coordinates, element data, and other relevant input data. The POSTPLOT program may be effectively used for color graphics depiction of solution results.

2.14 Discussion

Additional analysis features such as finite, dynamic element discretizations, improved dynamic analysis capabilities, and various efficient numerical techniques are continuously being implemented in the program. A nonlinear analysis capability is also being developed in parallel. Improved preprocessing and postprocessing of data, using IBM RISC, E/S PS 390, DEC-VT, CIT, Tektronix, or other graphics terminals, are being used to permit efficient modeling and analysis, as well as display, of the results pertaining to practical structural problems.

An automatic data conversion program has also been developed to convert NASTRAN (ref. 10) program data into STARS format.

3.1 Basic Data

3.1.1 PRIMARY JOB TITLE
Format (FREE)

3.1.1.1 ADDITIONAL JOB DETAILS
Format (A1, FREE)

1. Description: Various job-related descriptions, any number of input lines.

2. Notes:

   First line input is required, and subsequent lines of input must have a C in the first column; up to 80 characters per line are accepted.

3.1.2 NN, NEL, NMAT, NMECN, NEP, NET, NLGCS, NMANGL, NSTACK, MAXLEL
Format (FREE)

1. Description: Basic data parameters (structural).

2. Notes:

NN = total number of nodes

NEL = total number of elements

NMAT = total number of element material types

NMECN = number of material elastic or heat transfer constants, a maximum of numbers, as follows:
= 4, for isotropic material
= 13, for orthotropic-anisotropic material for 2-D shell elements (types 2, 3, 6, and 7)
= 10, for isotropic sandwich panel material for shell elements (types 2 & 3)
= 25, for orthotropic-anisotropic sandwich panel material for shell elements (types 2 & 3)
= 28, for orthotropic-anisotropic material for 3-D solid elements (types 4 & 5)
= 11, for isotropic heat transfer problem pertaining to line elements (type 1)
= 31, for isotropic heat transfer problem pertaining to shell elements (types 2, 3, 6, and 7)
= 34, for orthotropic-anisotropic heat transfer problem pertaining to shell elements (types 2, 3, 6, and 7)

NEP = total number of line element property types (type 1)

NET = total number of shell element thickness types (types 2 & 3)

NLGCS = total number of local-global coordinate systems (LGCS)

NMANGL = total number of material angle types

NSTACK = total number of composite shell element stack types

MAXLEL = maximum number of layers in a composite shell element

3.1.3 NTMP, NPR, NSPIN, NC, NBUN, NLSEC, NCNTRL, NOUT, NEXP
Format (FREE)

1. Description: Basic data parameters (loads and displacements).

2. Notes:

NTMP = total number of element temperature types

NPR = total number of element uniform pressure types

NSPIN = total number of different element spin types

NC = number of sets of nodal loads for IPROB = 8, 10
= 0, for IPROB = 1 through 7
= 1, for IPROB = 9, 10
= NTTS, for NTTS $\neq$ 0

NBUN = total number of interdependent and finite nodal displacement connectivity conditions (includes IDBC and FDBC in section 2.3, being equal to number of lines of input)
= total number of nodal temperature inputs for IPROB = 10, being equivalent to FDBC case

NLSEC = total number of line element special end conditions excluding commonly occurring cases of purely rigid or hinged ends

NCNTRL = total number of control surface rigid body modes used for ASE analyses; may also be utilized for generating perfect rigid body modes

NOUT = total number of output nodes where direct modal interpolation is effected; to be set to 0 for alternative interpolation scheme effected by GRIDCHG submodule

NEXP = total number of uniform external in-plane pressures for membranes

3.1.4 IPROB, IEIG, IDRS, IBAN, IPLUMP, IMLUMP, INMM, IINTP
Format (FREE)

1. Description: Data defining nature of required solution.

2. Notes:

IPROB = index for problem type, to be set as follows:
= 1, undamped, free vibration analysis of nonspinning structures
= 2, undamped, free vibration analysis of spinning structures
= 3, quadratic matrix eigenproblem option for DEM (dynamic element method) analysis
= 4, free vibration analysis of spinning structures with diagonal viscous damping matrix

= 5, as for IPROB = 4 with structural damping
= 6, free vibration analysis of nonspinning structures with general viscous damping
= 7, as for IPROB = 6 with structural damping
= 8, static analysis of structures with thermal and multiple mechanical load cases
= 9, elastic buckling analysis
= 10, heat transfer analysis

IEIG = integer defining eigenproblem solution type
= 0, for solution based on a modified, combined Sturm sequence and inverse iteration method
= 1, for an alternative solution technique based on a block Lanczos procedure (recommended for computation of first few roots and vectors when the lower bound PL = 0 for cases IPROB = 1, 2, 3, and 9)

IDRS = index for dynamic response analysis
= 0, no response analysis required
= 1, performs response analysis

IBAN = bandwidth minimization option
= 0, performs minimization
= 1, minimization not required
= -1, option to perform minimization only and exit

IPLUMP = index for nodal external loads
= 0, no load input
= 1, concentrated nodal load input for IPROB = 8 and 9, as well as for IPROB = 1 through 7 for prestressed structures

IMLUMP = index for nodal lumped scalar mass
= 0, no lumped mass
= 1, lumped nodal mass input (IPROB = 1 through 7)

INMM = index for nodal 6 by 6 mass matrix
= 0, no mass matrix
= 1, nodal mass matrix input (IPROB = 1 through 7)

IINTP = integer defining modal data for direct interpolation
= 0, no interpolation required
= 1, performs interpolation on STARS calculated modal data
= 2, performs interpolation on externally supplied modal data; for example, GVS results

3. Additional notes:

A dynamic response analysis is achieved by specifying appropriate values for IPROB and IDRS; at the end of problem solution, extensive options are available for plotting nodal deformations, mode shapes, and element stresses by utilizing the postprocessor routine, POSTPLOT.

Initial static load (prestress) effect: in the case of dynamic problems, the presence of nonzero values of integers IPLUMP, NPR, and/or NTMP activates computation of prestressing effect.

Mass matrix: nodal lumped mass matrix is added to consistent mass matrix to evolve the final mass matrix.

3.1.5 IPREC, IPLOT, IPRINT, INDATA, IERCHK, INCFOR
Format (FREE)

1. Description: Additional basic data.

2. Notes:

IPREC = specification for solution precision
= 1, single precision
= 2, double precision

IPLOT = index for graphics display
= 0, no plotting needed
= 1, performs display of input geometry; if satisfactory, a restart option enables continuation of current analysis

IPRINT = output print option
= 0, prints final results output only
= 1, prints global stiffness (K), mass (M), damping or Coriolis (C) matrices, as well as detailed output on deformations, stresses, and root convergence characteristics
= 2, prints output as in IPRINT = 1, but omits K, M, and C matrices
= 3, output as in IPRINT = 0, but omits eigenvector printouts

INDATA = input data option
= 0, basic matrices are automatically computed
= 1, to read upper symmetric banded half of basic matrices K, M, and C from user input files, row-wise

IERCHK = integer defining level of error checks in input data specified by user
= 0, usual level of error checkouts
= 1, additional extensive data checkouts

INCFOR = integer defining input data format
= 0, basic format
= 1, alternative format

3.1.6 INDEX, NR, INORM, PU, PL, TOL
Format (FREE)

(Required if IDRS = 1 with IPROB ≠ 8)

1. Description: Data specifications for eigenproblem solution.

2. Notes:

INDEX = indicator for number of eigenvalues and vectors to be computed
= 1, computes NR smallest roots (and vectors) lying within bounds PU, PL
= 2, computes all roots (and vectors) lying within bounds PU, PL

NR = number of roots to be computed (any arbitrary root number input for INDEX = 2)

INORM = index for vector normalization; any desired vector row number
= 0, normalizes with respect to a scalar of displacement vector **Y** having largest modulus
= -1, normalizes with respect to a scalar of **Y** or **YD** (velocity) vector having largest modulus

PU = upper bound of roots

PL = lower bound of roots

TOL = tolerance factor (eq. (21))
= 0, defaults to 25.0E + 08
= X, defaults to X (X = 1.0E + 07 may be useful for computation)

3.1.7 IUV, IDDI, NTTS, NDELT (Required if IDRS = 1)
Format (FREE)

1. Description: Data related to dynamic response analysis.

2. Notes:

IUV = index for initial displacement (U) and velocity (V) input
= 0, no initial data
= 1, either initial displacement or velocity or both are nonzero vectors

IDDI = index for dynamic data input
= 1, nodal load input
= 2, nodal acceleration input

NTTS = total number of sets of load or acceleration data input

NDELT = number of sets of uniform time increments for response calculation

3.1.8 G (Required if IPROB = 5 or 7)
Format (FREE)

1. Description: Structural damping in formulation **[K = K(1 + i*G)]**.

2. Notes:

G = structural damping parameter

i* = imaginary number, $\sqrt{-1}$

K = system stiffness matrix

3.1.9 M11 (Required if INDATA = 1)
Format (FREE)

1. Description: Half-bandwidth of **K**, **M**, or **C**.

3.1.10 ((**B**(I,J), I = 1, N), J = 1, NC) (Required if INDATA = 1 and IPROB = 8)
Format (6E10.4)

1. Description: Load matrix of order N = NN × 6.

3.1.11 ((**K**(I,J), J = 1, M11), I = 1, N) (Required if INDATA = 1 and IPROB = 1 through 8)
Format (6E10.4)

1. Description: Stiffness matrix.

3.1.12 ((**M**(I,J), J = 1, M11), I = 1, N) (Required if INDATA = 1 and IPROB = 1 through 7)
Format (6E10.4)

1. Description: Mass matrix.

3.1.13 ((**C**(I,J), J = 1, M11), I = 1, N) (Required if INDATA = 1 and IPROB = 2 through 5)
Format (6E10.4)

1. Description: Coriolis (IPROB = 2, 4, 5) or dynamic correction (IPROB = 3) matrix.

3.1.14 ((**CD**(I,J), J = 1, M11), I = 1, N) (Required if INDATA = 1 and IPROB = 4 through 7)
Format (6E10.4)

1. Description: Viscous damping matrix.

2. General note:

   Each set of data input in succeeding sections is preceded with a relevant comment statement having a dollar sign ($) at the first column, followed by optional descriptive words.

3. Note:

   If INDATA = 1, no further input is required.

3.2 Nodal Data

3.2.1 $ NODAL DATA

3.2.2 IN, X, Y, Z, UX, UY, UZ, UXR, UYR, UZR, ILGCS, IZDRCS, IINC

Format (I5,3E10.4,9I5) (INCFOR = 0)
or (I5,3E15.8,6I2,3I5) (INCFOR = 1)

1. Description: NN sets of nodal data input in GCS/LGCS, at random; table 1 provides a description of the input data.

Table 1. Arrangement of nodal data input.

Node number (IN)	Nodal coordinates			Nodal zero displacement boundary conditions (ZDBC)						Local-global coordinate system type (ILGCS)	ZDBC reference coordinate system (IZDRCS)	Increment (IINC)
	(X)	(Y)	(Z)	(UX) 1	(UY) 2	(UZ) 3	(UXR) 4	(UYR) 5	(UZR) 6			
*	*	*	*	*	*	*	*	*	*	*	*	*

2. Notes:

a. A right-handed Cartesian coordinate system (X, Y, Z) is to be chosen to define the global coordinate system (GCS).

b. The asterisk (*) indicates required data input in GCS/LGCS.

c. Each structural node is assumed to have six degrees of freedom (DOF) consisting of three translations, UX, UY, UZ, and three rotations, UXR, UYR, UZR, usually labeled as displacement degrees of freedom 1, 2, 3, and 4, 5, 6, respectively.

d. For nodal zero displacement boundary conditions (ZDBC) defined in coordinate system referred to as IZDRCS, set value to
   = 0, for free motion,
   = 1, for constrained motion.

e. For node generation by increment, set IINC
   = 0, for no increment,
   = I, to increment node number of previous input by I until current node number is attained; coordinates of intermediate nodes are linearly interpolated.

f. In automatic node generation (note (e)), all relevant data of generated intermediate nodes pertain to that of the last data set of the sequence.

g. Third-point nodes for line elements are assumed to lie on element local x-y plane and may be chosen as any existing active node or dummy nodes with UX through UZR set to 1.

h. Final data are automatically formed in increasing sequence of node numbers.

3. Additional notes:

ILGCS = integer specifying local-global coordinate system number (set to 0 if data is in GCS), defining nodal data

IZDRCS = integer defining zero displacement boundary condition reference coordinate system (set to 0 for data in GCS or an ILGCS number)

3.2.3 $ LOCAL-GLOBAL COORDINATE SYSTEM DATA (Required if NLGCS $\neq$ 0)

3.2.4 ILGCS, IDMOD
Format (2I5)

3.2.5 XOR, YOR, ZOR, X2, Y2, Z2, (IDMOD = 1)
X3, Y3, Z3
or
XOR, YOR, ZOR, D11, D12, D13, (IDMOD = 2)
D21, D22, D23, D31, D32, D33
Format (2(6E10.4, /))

1. Description: NLGCS sets of local-global coordinate system (LGCS) definition data, at random.

2. Notes:

IDMOD = integer specifying nature of input data
= 1, input involves global coordinates of the origin of the LGCS (XOR, YOR, ZOR) and two data points (X2 through Z3, pertaining to two points located on LGCS X-axis and X-Y plane, respectively) in GCS
= 2, involves input of origin of LGCS (XOR, YOR, ZOR) and elements of direction cosine matrix of the LGCS

3. Special note:

If IINTP = 2, no further data input is required until 3.5.7.

3.3. Element Data

General note: Element data input may be at random within each data group.

3.3.1 $ ELEMENT CONNECTIVITY

3.3.2 IET, IEN, ND1, ND2, ND3, ND4, ND5, ND6, ND7, ND8, IMPP, IEPP/ITHTH, ITMPP, IPRR, IST, INC
Format (16I5)

1. Description: NEL sets of element data input; definition of input data is given in table 2.

Table 2. Element data layout.

Element type (IET)	Element number (IEN)	Node number for vertices 1 (ND1)	2 (ND2)	3 (ND3)	4 (ND4)	5 (ND5)	6 (ND6)	7 (ND7)	8 (ND8)	IMPP	IEPP/ ITHTH	ITMPP	IPRR	IST	INC
Line (bars, rods, beams, 3-D lines) 1	*	*	*	**	IEC1	IEC2	▼			*	X	*	*	*	*
Shell quadrilateral (plane, plate, shear, shell - usual and sandwich) 2, 22	*	*	*	*	*				▲	*	†	*	*	*	*
Shell triangular (plane, plate, shear, shell - sandwich) 3, 33	*	*	*	*					▲	*	†	*	*	*	*
Solid hexahedron 4	*	*	*	*	*	*	*	*	*	*		*	*	*	*
Solid tetrahedron 5	*	*	*	*	*					*		*	*	*	*
Shell quadrilateral composite element (plane, plate, shear, and shell) 6	*	*	*	*	*				■	*		*	*	*	*
Shell triangular composite element (plane, plate, shear, and shell) 7	*	*	*	*					■	*		*	*	*	*
Rigid element (pin-ended bar, rigid body) 8	*	*	*	**	IEC1	IEC2	◆								*
Prestressed rectangular membrane 11	*	*	*	*	*				●	*	†	*	*	*	*

2. Notes:

*	= data as defined; under element type 8, individual rigid elements are characterized by appropriate data entry
**	= third point node for element types 1 and 8
IECI	= integer defining line element end condition pertaining to end I = 0, rigid-ended = 1, pin-ended in three rotational degrees of freedom = J, denoting special end condition number, to be set greater than 1; for scalar springs, set IEC1 to a negative value less than -1
IMPP	= integer defining material property type number
IEPP(x)	= integer defining line element property type
ITHTH(†)	= integer defining shell element thickness type
ITMPP	= integer defining element temperature type
IPRR	= integer defining element pressure type
IST	= integer defining element spin type
INC	= integer for element generation by increment = 0, no increment = J, increments node numbers of previous elements by J until current element nodal numbers are reached
▼	= ILGCS, integer defining LGCS associated with a zero-length scalar spring element; defaults to GCS
▲	= IMANG, integer defining material angle type number, suitable for layered elements
■	= ISTACK, stack type number, used for integrated composite elements (types 6 and 7)
◆	= dependent degree of freedom at ND1 to be rigidly connected to all six degrees of freedom at ND2; rules concerning interdependence of nodes and degrees of freedom are defined in section 3.4.4 = -1, if all six degrees of freedom at ND1 are involved = 0, for pin-ended rigid bar elements
●	= integer defining prestress type

Rigid elements may be specified to span any length, including 0. Rigid pin-ended bar elements may be simulated by setting IEC1 = IEC2 = 1.

In automatic element generation (see INC, above), the generated intermediate elements acquire the same properties as the last element in current sequence. Also, a special option enables repetitive use of an element with an input format (I3, I2, 15I5); the integer IET is then replaced by NELN0 and IET, where NELN0 is the total number of similar elements connecting the specified nodes.

Sandwich shell elements may be generated by individual inputs of membrane, bending, and transverse shear effects. Furthermore, the composite shell elements consisting of layered composites can be formed for varying stacks of materials.

For element type 8, defined by two nodes, if the first node has some ZDBC constraints, the latter should also be applied to the second node.

3. Element description:

   The various elements and associated degrees of freedom are depicted in figure 7. The global coordinate system (GCS) is represented by X, Y, Z, whereas x, y, z relates to local coordinate system (LCS).

4. Notes:

   a. A right-handed Cartesian coordinate system (x, y, z) is to be chosen to define any element local coordinate system (LCS).

   b. Any node may be chosen as the first vertex of an element, the local x-axis being along the line connecting vertices 1 and 2.

   c. For line elements, the local x-y plane is defined as the plane contained by vertices 1, 2, and the specified third-point node.

   d. The vertices of thin shell elements are usually numbered in a counter-clockwise sequence when observed from any point along the local positive z-axis; they are also utilized as plane and plate-bending elements, as appropriate. For highly ill-conditioned problems, alternative elements 22 and 33 may yield better results than the preferred element types 2 and 3, respectively.

   e. For solid elements, the y-axis lies in the plane formed by vertices 1-2-3 and 1-2-3-4 for the tetrahedral and hexahedral elements, respectively; the z-axis is perpendicular to the x-y-plane, heading toward the fourth node for the tetrahedron element, and toward the plane containing the other four nodes for the hexahedral element.

   f. The vertices of the solid elements are also numbered in a counter-clockwise sequence when viewed from any point on the positive z-axis lying above the plane under consideration; the fifth vertex of the hexahedron is to be chosen as the node directly above vertex 1.

   g. For layered composite shell element types 6 and 7, the layering sequence starts with the layer that has maximum -z coordinate expressed in element LCS.

   h. For element type 7, for heat transfer analysis, the element also caters to radiation and surface heat flow on all five surfaces. The averaged internal heat generation rate may be applied to the element.

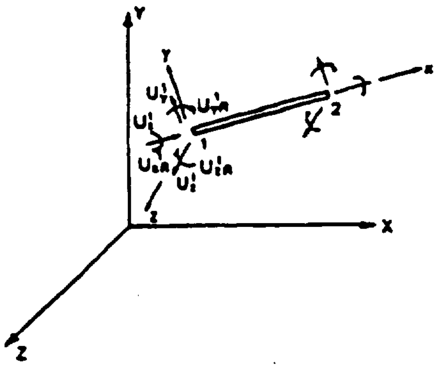

(a) Line element

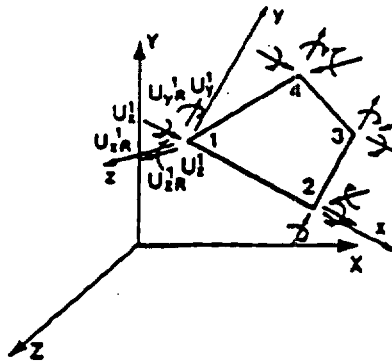

(b) Quadrilateral shell element

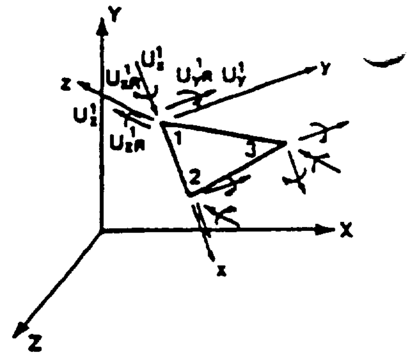

(c) Triangular shell element

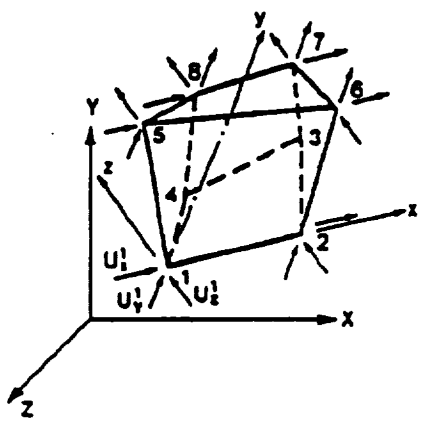

(d) Hexahedral solid element

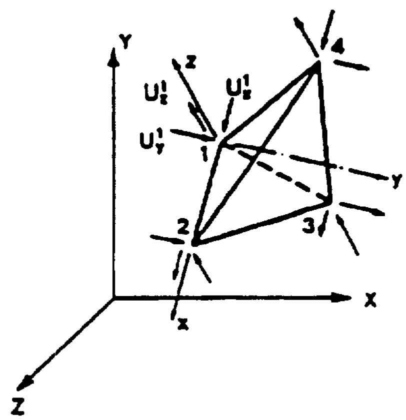

(e) Tetrahedral solid element

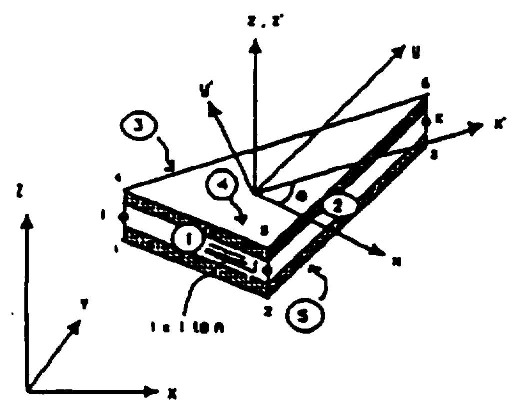

(f.1) Basic composite triangular shell/ prism element (6 d.o.f. per node for shell element, 2 d.o.f. per node at top & bottom for heat transfer case)

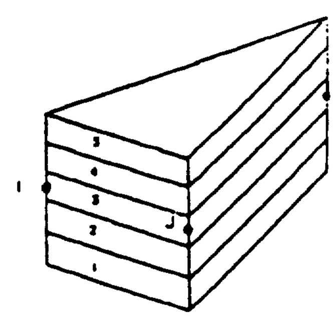

(f.2) Substack description for heat transfer case only (maximum of 5 substacks and 6 d.o.f. per node)

(f) Composite shell/prism element

Figure 7. STARS-SOLIDS element types

5. Structural modeling:

Since each node is assumed to possess six displacement degrees of freedom, any individual structural form may be simply represented by suppressing appropriate displacement terms. The following rules may be adopted:

Truss structures: to allow only two nodal translational deformations in the plane of the structure; to use line elements.

Plane frame: all three in-plane displacements, namely, two translations and one rotation, are retained in the formulation; to use line elements.

Plane stress/strain: displacement boundary conditions are similar to truss structures; to use shell elements.

Plate bending: only the three out-of-plane displacements consisting of one translation and two rotations are considered for the analysis; to use shell elements.

Solid structures: the three translational degrees of freedom are retained in the analysis; to use solid elements.

Shell, space frame: all six degrees of freedom are to be retained in the solution process; to use shell and line elements, respectively.

Heat transfer analysis: Only first two nodal degrees of freedom are used for two-dimensional or linear gradient in three dimensional heat transfer analysis. If different temperature gradients in Z direction are desired, the number of degrees of freedom can be increased accordingly. It can have a maximum of six degrees of freedom and five different temperature gradients through the thickness.

Suppression of derived nodal motion may be achieved by using zero and interdependent displacement boundary conditions (ZBDC, IDBC) defined in sections 3.2 and 3.4, respectively.

3.3.3 $ COMPOSITE SHELL ELEMENT STACK DESCRIPTION DATA (Required for composite shell elements (types 6 and 7), and only if NSTACK ≠ 0)

3.3.4 ISTACK, NLAYER, NSUBST, SBT1NL, SBT2NL, SBT3NL, SBT4NL, SBT5NL
Format (8I5)

3.3.5 (IMATC(I), THCL(I), IMANGC(I), I = 1, NLAYER)
Format (I5, E10.4, I5)

1. Description: NSTACK sets of composite shell element data; layers to be read from bottom of element.

2. Notes:

ISTACK	=	stack number
NLAYER	=	total number of layers in the stack
NSUBST	=	number of substacks in the stack (heat transfer case only, a maximum of 5)

SBT1NL through
SBT5NL = number of layers in the Ith substack; any number of layers allowed within a substack (required for heat transfer case only)

IMATC(I) = material type number for the composite layer

THCL(I) = thickness of the composite layer

IMANGC(I) = integer specifying material angle type number (IMANG)

Since the program allows a maximum of 5 substacks, six temperatures at a node are the usual requirement (a substack is allowed to have any number of layers) using all six DOF, starting from the bottom.

3.3.6 $ SPECIFICATION FOR MATERIAL AXES ORIENTATION (Required if NMANGL ≠ 0)

3.3.7 IMANG, IMAMD, ILGCS
Format (3I5)

3.3.8 D11, D12, D13, D21, D22, D23, (IMAMD = 1)
D31, D32, D33
Format (2(6E10.4, /))
or
THETA (IMAMD = 2)
Format (E10.4)

1. Description: NMANGL sets of material angle definition data.

2. Notes:

IMAMD = integer defining material angle data input mode
= 1, involves input of elements of direction cosine matrix of material axes with respect to LGCS/GCS (set ILGCS = 0 for data in GCS)
= 2, requires input of material axis angle (THETA) with shell element local x-axis

ILGCS = integer specifying local-global coordinate system number (set to 0 if data is in GCS)

THETA = material axis angle with respect to shell element local x-axis

3.3.9 $ LINE ELEMENT BASIC PROPERTIES (Required for line elements only)

3.3.10 IEPP, A, JX, IY, IZ, SFY, SFZ
Format (I5, 6E10.4)

1. Description: NEP sets of line element basic property data in element local coordinate system (LCS).

2. Notes:

IEPP = integer denoting line element property type

A = area of cross section

JX = torsional moment of inertia about element x-axis
= (P, perimeter for IPROB = 10)

IY = moment of inertia about element y-axis

IZ = moment of inertia about element z-axis

SFY = A/ASY, shear area (ASY) factor along y-axis

SFZ = A/ASZ, shear area (ASZ) factor along z-axis

For no shear area effect, SFY and SFZ are to be set at 0.0. Also for heat transfer problems (IPROB = 10), only A and P are the required input.

3.3.11 $ LINE ELEMENT SPECIAL END CONDITIONS (Required for line elements only if NLSEC ≠ 0)

3.3.12 ILSEC, (k(I), I = 1, 6)
Format (I5, 6E10.4)

1. Description: NLSEC sets of line element special end conditions data in LCS.

2. Notes:

ILSEC = element end condition type (to be set greater than 1), referring to members attached at the nodes by flexible connections, or members with free end degrees of freedom in LCS (corresponds to IEC1 and IEC2)
= set to a negative value, less than -1, for scalar springs connecting two nodes (corresponds to IEC1)

k(I) = additional spring stiffness along Ith translational (x-, y-, and z-direction) degree of freedom and actual rotational Ith spring stiffness (x, y, and z rotational constraint)
= -2, for rigid rotational Ith constraint
= -1, for release of corresponding member end degree of freedom, relevant also to ILSEC value set greater than 1
= stiffness values for scalar springs associated with a negative ILSEC value less than -2

Such elements may have 0 or any finite length.

To simulate only specified end condition, set Young's modulus E = 0 for the corresponding material type, IMPP.

3.3.13 $ SHELL ELEMENT THICKNESS (Required for shell elements (types 2, 22 and 3, 33) only)

3.3.14 ITHTH, TM, TB, TS
Format (I5, 3E10.4)

1. Description: NET sets of element thickness data.

2. Notes:

   ITHTH = element thickness type

   TM = membrane element thickness

   TB = bending element thickness

   TS = transverse shear element thickness

   Above shell thickness pertains to sandwich elements; in the absence of data for TB and TS, the shell element thickness T is taken as TM.

   For consistent mass matrix formulation, shell thickness T is taken as TM.

3.3.15 $ ELEMENT MATERIAL PROPERTIES

3.3.16 IMPP, MT
Format (2I5)

3.3.17 E, MU, ALP, RHO (material type 1); or

E11, E12, E14, E22, E24, E44, E55,
E56, E66, ALPX, ALPY, ALPXY, RHO (material type 2); or

E11, E12, E13, E14, E15, E16, E22,
E23, E24, E25, E26, E33, E34, E35,
E36, E44, E45, E46, E55, E56, E66,
ALP1, ALP2, ALP3, ALP4, ALP5, ALP6, RHO (material type 3); or

EM, EB, ES, MUM, MUB, MUS,
ALPM, ALPB, ALPS, RHO (material type 4); or

E11M, E12M, E14M, E22M, E24M, E44M,
E11B, E12B, E14B, E22B, E24B, E44B,
E55S, E56S, E66S, ALPXM, ALPYM, ALPXYM,
ALPXB, ALPYB, ALPXYB, ALPXS, ALPYS, ALPXYS,
RHO (material type 5); or

KL, H, Q, QS, TE, QR, STB,
EMS, SABS, CP, RHO (material type 6); or

KS, H1, H2, H3, H4, HT, HB,
Q,QS1, QS2, QS3, QS4, QST, QSB,
T1, T2, T3, T4, TT, TB, QR1,
QR2, QR3, QR4, QRT, QRB, STB1, STB2,
STB3, STB4, STBT, STBB, EMS1, EMS2, EMS3,
EMS4, EMST, EMSB,SABS, CP, RHO (material type 7); or

KS11, KS12, KS22, KS66, H1, H2, H3,
H4, HT, HB, Q, QS1, QS2, QS3,
QS4,QST, QSB, T1, T2, T3, T4,

TT, TB, QR1, QR2, QR3, QR4, QRT,
QRB, STB1, STB2, STB3, STB4, STBT, STBB,
EMS1, EMS2, EMS3, EMS4, EMST, EMSB,SABS,
CP, RHO (material type 8)

Format (5(7E10.4,/))

1. Description: NMAT sets of element material property data; the individual material matrices are derived from the 6 by 6 symmetric matrix for general solid material.

2. Notes:

IMPP = material number

MT = material type
= 1, isotropic
= 2, orthotropic-anisotropic, shell elements
= 3, orthotropic-anisotropic, solid elements
= 4, isotropic, sandwich shell elements incorporating individual membrane, bending, and transverse shear effects
= 5, orthotropic-anisotropic sandwich shell elements with individual effects, as above
= 6, isotropic heat transfer, line elements
= 7, isotropic heat transfer, shell elements
= 8, orthotropic-anisotropic heat transfer, shell elements

E = Young's modulus

EIJ = elements of material stress-strain matrix (I = 1, 6 ; J = 1, 6)

MU = Poisson's ratio

ALP = coefficient of thermal expansion for isotropic material

ALPX, ALPY,
ALPXY = coefficients of thermal expansion, shell elements

ALP1 through
ALP6 = coefficients of thermal expansion, solid elements

RHO = mass per unit volume

For sandwich elements (material types 4 and 5), relevant notations defining such properties utilize a postscript of M, B, or S for membrane, bending, or transverse shear stiffness, respectively.

For heat transfer problems:
KL, KS,
KSIJ = relevant elements of symmetric conductivity tensor (I = 1, 2, 6; J = 1, 2, 6)
H, HI = convective heat transfer coefficient for line element and quadrilateral/triangular shell element, as pertaining to the edges and the top and bottom surfaces, respectively (I = 1-4 and T and B)
TE, TI = convective exchange temperature, for line and other elements, as defined for H, HI

QS, QSI	=	specified surface heat flow, for line and other elements, defined as above
QR, QRI	=	specified incident surface radiant heat flow, for line and other elements, defined as above
STB, STBI	=	Stefan-Boltzmann constant, for line and other elements, defined as above
EMS, EMSI	=	surface emissivity, for line and other elements, defined as above
Q	=	appropriate internal heat generation rate/unit volume
SABS	=	surface absorptivity
CP	=	specific heat

3. Additional notes:

For radiation problems, in the absence of specified temperature, an initial temperature input is needed on the radiating surface.

3.3.18 $ ELEMENT TEMPERATURE DATA/INITIAL NODAL TEMPERATURE DATA (Required if NTMP ≠ 0)

3.3.19 ITMPP, T, DTDY, DTDZ (If IPROB ≠ 10)
Format (2(I5,3E10.4))

IN, NDOF, TEMP (If IPROB = 10)
Format(2I5,E10.4)

1. Description: NTMP number of element temperature types; table 3 shows compatible input data.

Table 3. Element temperature data input.

Element type	T	DTDY	DTDZ
1	*	*	*
2,3,6,7	*		*
4,5	*		

2. Notes:

ITMPP	=	element temperature increase type
T	=	uniform temperature increase; relates to all elements
DTDY	=	temperature gradient along element local y-axis; relates to line elements only
DTDZ	=	temperature gradient along element local z-axis; relates to line and shell elements
*	=	compatible input data
IN	=	node number
NDOF	=	nodal degree of freedom

TEMP = temperature

3.3.20 $ ELEMENT PRESSURE DATA (Required if NPR ≠ 0)

3.3.21 IPRR, PR
Format (5(I5,E10.4))

1. Description: NPR sets of element pressure data.

2. Notes:

IPRR = element pressure type

PR = uniform pressure

Pressure directions for line elements: uniform pressure is allowed in local y- and z-directions only, and the program calculates as input both end loads and moments; while pressure corresponding to a first nodal input pertains to y-direction, a subsequent input for the same node signifies pressure acting in the z-direction.

Pressure directions for shell elements: uniform pressure is allowed in local z-direction only; the program computes nodal load input.

Pressure directions for solid elements: uniform pressure is allowed on base surfaces defined by nodes 1-2-3-4 and 1-2-3 for hexahedral and tetrahedral elements, respectively, acting in local z-direction; the program computes nodal load input data.

3.3.22 $ PRESTRESSED RECTANGULAR MEMBRANE ELEMENT DATA
(Required if NEXP ≠ 0)

3.3.23 IIEXP, SX, SY
Format (I5,2E10.4)

1. Description: NEXP sets of prestressed membrane stress data.

2. Notes:

IIEXP = integer defining stress combination type

SX, SY = membrane stresses in the element x- and y-directions, respectively

3.4 Data in Global or Local-Global Coordinate System

General note: Data input may be at random within each data group.

3.4.1 $ ELEMENT SPIN RATE DATA (Required if NSPIN ≠ 0)

3.4.2 IST, SPX, SPY, SPZ, ILGCS
Format (I5, 3E10.4, I5)

1. Description: NSPIN sets of spin data.

2. Notes:

IST	=	spin type
SPX, SPY, SPZ	=	components of element spin rate in global/local-global X-, Y-, and Z-directions, respectively
ILGCS	=	local-global coordinate system number, as defined in section 3.2.2

3.4.3 $ DISPLACEMENT BOUNDARY CONDITION DATA (Required if NBUN ≠ 0)

3.4.4 INI, IDOFJ, INIP, IDOFJP, CONFCT, IDRCS, NDBCON
Format (4I5, E10.4, 2I5)

1. Description: NBUN sets of nodal interdependent displacement boundary condition (IDBC) data.

2. Notes:

INI	=	node number I
IDOFJ	=	Jth DOF associated with node I
INIP	=	node number I'
IDOFJP	=	J'th DOF associated with node I'
CONFCT	=	connectivity factor
IDRCS	=	displacement boundary condition reference coordinate system
NDBCON	=	integer defining displacement boundary condition increment
	=	0, no increment
	=	an integer, to increment IDOFJ and IDOFJP by 1 until IDOFJ reaches NDBCON value

J and J' vary between 1 and 6. For IPROB = 10, only INI and CONFCT (nodal temperature) are the required input.

3. Additional notes:

The nodal displacement boundary conditions relationship is expressed as

$$U_{i,j} = a_{m,n} U_{m,n}$$

$$= a_{i,j} U_{i,j} + a_{i',j'} U_{i',j'} + \ldots$$

The input scheme is shown in table 4.

Table 4. Data layout for displacement boundary conditions.

Node 1	DOF	Node 2	DOF	Connectivity Coefficient	Reference Coordinate System	Incremental DOF Value	Terminology
i	j	i'	j'	$a_{i'j'}$	IDRCS	NDBCON	IDBC
i	j	i	j	a_{ij}	IDRCS	NDBCON	FDBC
i	j	i	j	0	IDRCS	NDBCON	ZDBC

in which

i, i' = node numbers,

j, j' = degrees of freedom,

$a_{i,j}$, $a_{i'j'}$ = connectivity coefficients.

IDBC, FDBC, and ZDBC are, respectively, the interdependent, finite, and zero displacement boundary conditions. The ZDBC may also be conveniently implemented by following the rules given in table 1, which is generally recommended for such cases. It should be noted that the dependent degrees of freedom appearing in columns 1 and 2 may not appear subsequently in columns 3 and 4 as independent degrees of freedom. However, the independent degrees of freedom may be subsequently related.

3.4.5 $ NODAL LOAD DATA (Required if IPLUMP ≠ 0)

3.4.6 IN, IDOF, P, IDOFE, ILGCS
Format (2I5, E10.4, 2I5)

1. Description: NC sets of nodal force data.

2. Notes:

IN = node number

IDOF and IDOFE are, respectively, the start and end degrees of freedom assigned with the same P value; default value for IDOFE is IDOF.

P = nodal load

Each data set is to be terminated by setting a negative value for IN.

3.4.7 $ NODAL MASS DATA (Required if IMLUMP ≠ 0)

3.4.8 IN, IDOF, M, IDOFE, ILGCS
Format (2I5, E10.4, 2I5)

1. Description: Nodal lumped mass data.

2. Notes:

M = nodal mass

Other definitions are as in section 3.4.6.

3.4.9 $ NODAL MASS MATRIX IN LGCS/GCS (Required if INMM ≠ 0)

3.4.10 IN, ILGCS
Format (2I5)

3.4.11 (VNMDAT(I), I = 1, 36)
Format (6(6E10.4,/))

1. Description: User input of 6 by 6 nodal mass matrix.

2. Notes:

The user may input data for only the upper symmetric elements; numbers in lower half may be set to zero as the program automatically symmetrizes the matrix.

For data in GCS, set ILGCS = 0.

Each data set is to be terminated by setting a negative value for IN.

3.4.12 $ NODAL INITIAL DISPLACEMENT AND VELOCITY DATA (Required if IUV = 1 and IDRS = 1)

3.4.13 IN, IDOF, UI, VI
Format (2I5, 2E15.5)

1. Description: Initial displacements and velocities data.

2. Notes:

IN = node number

IDOF = degree of freedom

UI = initial displacement value

VI = initial velocity value

Data set is terminated if IN is read as -1.

3.4.14 $ NODAL FORCE ACCELERATION DATA/ELEMENT HEAT TRANSFER DATA (Required if NTTS ≠ 0 and IDRS = 1)

3.4.15 TZ
Format (E15.5)

3.4.16 IN, IDOF, PZ (If IPROB ≠ 10)
Format (2I5, E15.5)

IEN, ISURF, Q, QS, TI (If IPROB = 10)
Format(2I5,3E15.5)

1. Description: NTTS sets of dynamic nodal load (IDDI = 1) or acceleration (IDDI = 2) input data

2. Notes:

TZ = time-duration of load application

PZ = nodal force or acceleration data

IEN = element number

ISURF = element surface indicator (Fig. 7, f.1)

Each data set is terminated by setting IN value to -1; other definitions are as given in section 3.3.17 and 3.4.6.

3.4.17 $ INCREMENTAL TIME DATA FOR RESPONSE CALCULATION (Required if NDELT ≠ 0 and IDRS = 1)

3.4.18 DELT, IDELT
Format (E15.5, I5)

1. Description: NDELT sets of uniform incremental time input data for dynamic response calculations.

2. Notes:

DELT = uniform incremental time step

IDELT = total number of uniform time steps in the data set

3.5 Additional Basic Data

3.5.1 $ VISCOUS DAMPING DATA (Required if IPROB = 4 or 5)

3.5.2 (C(I,I),I = 1, N)
Format (6E10.4)

1. Description: User input of diagonal viscous damping matrix.

2. Notes:

C = diagonal viscous damping matrix

N = order of matrix

3.5.3 $ COEFFICIENTS FOR PROPORTIONAL VISCOUS DAMPING (Required if IPROB = 6 or 7)

3.5.4 ALPHA, BETA
Format (2E10.4)

1. Description: Proportional viscous damping formulation C = ALPHA*K + BETA*M

2. Notes:

ALPHA and BETA are damping parameters.

K and M are system stiffness and mass matrices.

3.5.5 $ USER INPUT OPTION FOR VISCOUS DAMPING MATRIX (Required if IPROB = 6 or 7 and ALPHA and BETA set to 0)

3.5.6 ((C(I,J), J = 1, M11), I = 1, 6)
Format (6E10.4)

1. Description: NN sets of user input of banded viscous damping matrix C(N,M11) in blocks of six rows of bandwidth M11, one row at a time ($N = 6 \times NN$).

2. Notes:

Data file must conform to IDBC, FDBC, and ZDBC, inherent in the problem.

3.5.7 $ MEASURED MODAL DATA INPUT (Required if IINTP = 2)

3.5.8 (INODM(I), (DISPLM(I,J), J = 1, 6), I = 1, NN)
Format (I5, 6E10.4)

1. Description: Measured modal displacement data input, NR sets of data.

2. Notes:

Each data set to be terminated by setting INODM(I) value to -1.

3.5.9 $ OUTPUT POINTS SPECIFICATION FOR DIRECT INTERPOLATION OF MODAL DATA (Required if NOUT ≠ 0)

3.5.10 (IOUTP(I), (ICONP(I,J), J = 1, 6), I = 1, NOUT)
Format (7I5)

1. Description: To read output point and up to six connecting points

2. Notes:

IOUTP(I) = output points on AERO interpolation lines

ICONP(I,J) = STARS finite element nodes whose deflections will be averaged to calculate the deflection value at the interpolation point

3.5.11 $ RIGID CONTROL MODES DATA INPUT (Required if NCNTRL ≠ 0)

3.5.12 INS, IDOF, DISP, INE, ININC
Format (2I5, E10.4, 2I5)

1. Description: Modal displacement data for NCNTRL number of modes.

2. Notes:

INS, INE	=	start and end node numbers; default value for INE is INS
IDOF	=	degree of freedom, a value between 1 and 6
DISP	=	associated displacement
ININC	=	integer defining nodal incremental value; to increment INS by ININC until INE is attained

Each data set is to be terminated by setting INS value to -1.

4. SAMPLE PROBLEMS

A. STARS-SOLIDS

This section provides the input data as well as relevant outputs of several typical test cases involving static, stability, free vibration, and dynamic response analyses of representative structures. The input data is prepared in accordance with the procedures described in section 3. Details of such analyses are in the descriptions that follow in which each structural geometry is described in a right-handed, rectangular coordinate system, and the associated input data are defined in consistent unit form.

4.1 Space Truss: Static Analysis

The static analysis of the space truss depicted in figure 8 (ref. 11) was performed to yield nodal deformations and element forces. A load of 300 lb acts at node 7 along the axial direction of the member connecting nodes 7 and 9; another load of 500 lb is applied at node 10 in the direction of the structural base centerline. Also, the three members in the upper tier of the structure are subjected to a uniform temperature increase of 100°. Two rigid elements are, however, introduced between nodes 5 and 8 and nodes 7 and 9.

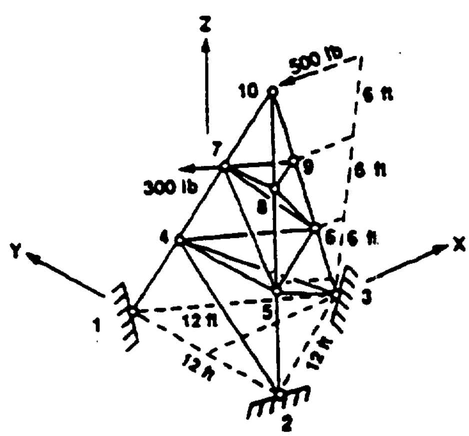

Figure 8. Space truss.

Important data parameters:

Young's modulus, E	=	1.0×10^7
Poisson's ratio, μ	=	0.3
Coefficient of thermal expansion, α	=	12.5×10^{-6}

STARS input data:

```
SPACE TRUSS - MECHANICAL AND THERMAL LOADING  - RBARS FROM NODES 5-8, 7-9
11,21,1,4,1,0,0,0,0,0
1,0,0,1,0,0,0,0,0
8,0,0,1,1,0,0,0
2,0,1,0,1,0
$ NODAL DATA
   1      0.0      72.0      0.0   1   1   1   0   0   0
   2      0.0     -72.0      0.0   1   1   1   0   0   0
   3   124.68       0.0      0.0   1   1   1   0   0   0
   4    13.86      48.0     72.0
   5    13.86     -48.0     72.0
   6   96.972       0.0     72.0
   7   27.708      24.0    144.0
   8   27.708     -24.0    144.0
   9   69.276       0.0    144.0
  10   41.568       0.0    216.0
  11    144.0      36.0      0.0   1   1   1   1   1   1
$ ELEMENT CONNECTIVITY
   1   1   1   4  11   1   1   0   0   0   1   1
   1   2   2   4  11   1   1               1   1
   1   3   2   5  11   1   1               1   1
   1   4   3   5  11   1   1               1   1
   1   5   3   6  11   1   1               1   1
   1   6   3   4  11   1   1               1   1
   1   7   4   5  11   1   1               1   1
   1   8   5   6  11   1   1               1   1
   1   9   6   4  11   1   1               1   1
   1  10   4   7  11   1   1               1   1
   1  11   5   7  11   1   1               1   1
   8  12   5   8  11          -1
   1  13   6   8  11   1   1               1   1
   1  14   6   9  11   1   1               1   1
   1  15   6   7  11   1   1               1   1
   1  16   7   8  11   1   1               1   1
   1  17   8   9  11   1   1               1   1
   8  18   9   7  11   1   1
   1  19   7  10  11   1   1               1   1   1
   1  20   8  10  11   1   1               1   1   1
   1  21   9  10  11   1   1               1   1   1
$ LINE ELEMENT BASIC PROPERTIES
   1   0.01389
$ ELEMENT MATERIAL PROPERTIES
   1   1
  10.0E6        0.3  12.5E-06
$ ELEMENT TEMPERATURE DATA
   1     100.0
$ NODAL LOAD DATA
  10   1   -500.0
   7   1   -259.8
   7   2    150.0
  -1
```

STARS analysis results - nodal deformations and element stresses:

LOAD CASE NO. 1

NODE EXT	NODE INT	X-DISPL.	Y-DISPL.	Z-DISPL.	X-ROTN.	Y-ROTN.	Z-ROTN.
1	1	0.000000E+00	0.000000E+00	0.000000E+00	0.000000E+00	0.000000E+00	0.000000E+00
2	2	0.000000E+00	0.000000E+00	0.000000E+00	0.000000E+00	0.000000E+00	0.000000E+00
3	3	0.000000E+00	0.000000E+00	0.000000E+00	0.000000E+00	0.000000E+00	0.000000E+00
4	4	-0.302075E+00	0.233780E+00	-0.331469E+00	0.000000E+00	0.000000E+00	0.000000E+00
5	5	-0.294402E+00	0.233737E+00	-0.297469E+00	-0.533925E-01	-0.976475E-01	-0.252952E+00
6	6	-0.358100E+00	0.344029E+00	0.558126E+00	0.000000E+00	0.000000E+00	0.000000E+00
7	7	-0.161162E+01	0.575101E+00	-0.385535E+00	0.000000E+00	0.000000E+00	0.000000E+00
8	8	-0.125416E+01	0.575116E+00	-0.226667E+00	-0.533925E-01	-0.976475E-01	-0.252952E+00
9	9	-0.143291E+01	0.884640E+00	0.696849E+00	0.000000E+00	0.000000E+00	0.000000E+00
10	10	-0.460499E+01	0.916627E+00	0.131711E+00	0.000000E+00	0.000000E+00	0.000000E+00
11	11	0.000000E+00	0.000000E+00	0.000000E+00	0.000000E+00	0.000000E+00	0.000000E+00
12	12	0.000000E+00	0.000000E+00	0.000000E+00	0.000000E+00	0.000000E+00	0.000000E+00

ORIGINAL PAGE IS
OF POOR QUALITY

ELEMENT STRESSES

ELEMENT NO.	END1 END5	END2 END6	END3 END7	END4 END8	PX1/PX2 SXT SXX	PY1/PY2 SYT SYY	PZ1/PZ2 SXYT SZZ	MX1/MX2 SXB SXY	MY1/MY2 SYB SYZ	MZ1/MZ2 SXYB SZX
1	1	4			0.785577E+03	0.000000E+00	0.000000E+00	0.000000E+00	0.000000E+00	0.000000E+00
					-0.785577E+03	0.000000E+00	0.000000E+00	0.000000E+00	0.000000E+00	0.000000E+00
2	2	4			-0.756511E-02	0.000000E+00	0.000000E+00	0.000000E+00	0.000000E+00	0.000000E+00
					0.756511E-02	0.000000E+00	0.000000E+00	0.000000E+00	0.000000E+00	0.000000E+00
3	2	5			0.464123E+03	0.000000E+00	0.000000E+00	0.000000E+00	0.000000E+00	0.000000E+00
					-0.464123E+03	0.000000E+00	0.000000E+00	0.000000E+00	0.000000E+00	0.000000E+00
4	3	5			0.807432E-01	0.000000E+00	0.000000E+00	0.000000E+00	0.000000E+00	0.000000E+00
					-0.807432E-01	0.000000E+00	0.000000E+00	0.000000E+00	0.000000E+00	0.000000E+00
5	3	6			-0.116939E+04	0.000000E+00	0.000000E+00	0.000000E+00	0.000000E+00	0.000000E+00
					0.116939E+04	0.000000E+00	0.000000E+00	0.000000E+00	0.000000E+00	0.000000E+00
6	3	4			-0.146366E+03	0.000000E+00	0.000000E+00	0.000000E+00	0.000000E+00	0.000000E+00
					0.146366E+03	0.000000E+00	0.000000E+00	0.000000E+00	0.000000E+00	0.000000E+00
7	4	5			-0.627136E-01	0.000000E+00	0.000000E+00	0.000000E+00	0.000000E+00	0.000000E+00
					0.627136E-01	0.000000E+00	0.000000E+00	0.000000E+00	0.000000E+00	0.000000E+00
8	5	6			0.177002E-02	0.000000E+00	0.000000E+00	0.000000E+00	0.000000E+00	0.000000E+00
					-0.177002E-02	0.000000E+00	0.000000E+00	0.000000E+00	0.000000E+00	0.000000E+00
9	6	4			0.150008E+03	0.000000E+00	0.000000E+00	0.000000E+00	0.000000E+00	0.000000E+00
					-0.150008E+03	0.000000E+00	0.000000E+00	0.000000E+00	0.000000E+00	0.000000E+00
10	4	7			0.705240E+03	0.000000E+00	0.000000E+00	0.000000E+00	0.000000E+00	0.000000E+00
					-0.705240E+03	0.000000E+00	0.000000E+00	0.000000E+00	0.000000E+00	0.000000E+00
11	5	7			0.452271E-01	0.000000E+00	0.000000E+00	0.000000E+00	0.000000E+00	0.000000E+00
					-0.452271E-01	0.000000E+00	0.000000E+00	0.000000E+00	0.000000E+00	0.000000E+00
12	5	8			0.000000E+00	0.000000E+00	0.000000E+00	0.000000E+00	0.000000E+00	0.000000E+00
					0.000000E+00	0.000000E+00	0.000000E+00	0.000000E+00	0.000000E+00	0.000000E+00
13	6	8			-0.180786E+00	0.000000E+00	0.000000E+00	0.000000E+00	0.000000E+00	0.000000E+00
					0.180786E+00	0.000000E+00	0.000000E+00	0.000000E+00	0.000000E+00	0.000000E+00
14	6	9			-0.927916E+03	0.000000E+00	0.000000E+00	0.000000E+00	0.000000E+00	0.000000E+00
					0.927916E+03	0.000000E+00	0.000000E+00	0.000000E+00	0.000000E+00	0.000000E+00
15	6	7			-0.321364E+03	0.000000E+00	0.000000E+00	0.000000E+00	0.000000E+00	0.000000E+00
					0.321364E+03	0.000000E+00	0.000000E+00	0.000000E+00	0.000000E+00	0.000000E+00
16	7	8			0.424805E-01	0.000000E+00	0.000000E+00	0.000000E+00	0.000000E+00	0.000000E+00
					-0.424805E-01	0.000000E+00	0.000000E+00	0.000000E+00	0.000000E+00	0.000000E+00
17	8	9			0.837402E-01	0.000000E+00	0.000000E+00	0.000000E+00	0.000000E+00	0.000000E+00
					-0.837402E-01	0.000000E+00	0.000000E+00	0.000000E+00	0.000000E+00	0.000000E+00
18	9	7			0.000000E+00	0.000000E+00	0.000000E+00	0.000000E+00	0.000000E+00	0.000000E+00
					0.000000E+00	0.000000E+00	0.000000E+00	0.000000E+00	0.000000E+00	0.000000E+00
19	7	10			0.463998E+03	0.000000E+00	0.000000E+00	0.000000E+00	0.000000E+00	0.000000E+00
					-0.463998E+03	0.000000E+00	0.000000E+00	0.000000E+00	0.000000E+00	0.000000E+00
20	8	10			0.463998E+03	0.000000E+00	0.000000E+00	0.000000E+00	0.000000E+00	0.000000E+00
					-0.463998E+03	0.000000E+00	0.000000E+00	0.000000E+00	0.000000E+00	0.000000E+00
21	9	10			-0.927967E+03	0.000000E+00	0.000000E+00	0.000000E+00	0.000000E+00	0.000000E+00
					0.927967E+03	0.000000E+00	0.000000E+00	0.000000E+00	0.000000E+00	0.000000E+00

4.2 Space Frame: Static Analysis

A space frame with rigid connections, shown in figure 9 (ref. 12), is subjected to nodal forces and moments. Results of such an analysis are presented below.

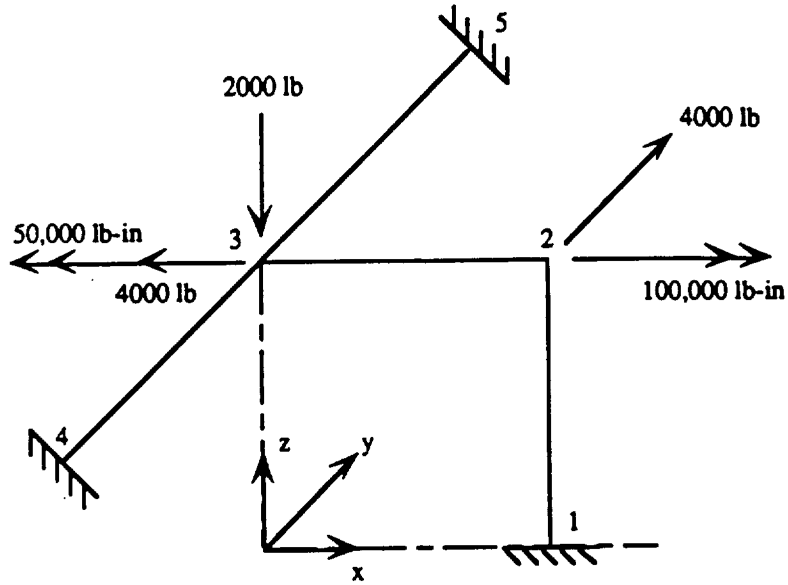

Figure 9. Space frame structure.

Important data parameters:

Young's modulus, E	= 30.24×10^6
Poisson's ratio, μ	= 0.2273
Cross-sectional area, A	= 25.13
Member length, ℓ	= 120

STARS input data:

```
SPACE FRAME CASE
6,4,1,4,1,0,0,0,0,0
0,0,0,1,0,0,0,0,0
8,0,0,1,1,0,0,0
2,0,1,0,1,0
$ NODAL DATA
   1     120.0       0.0       0.0    1    1    1    1    1    1
   2     120.0       0.0     120.0    0    0    0    0    0    0
   3       0.0       0.0     120.0    0    0    0    0    0    0
   4       0.0    -120.0     120.0    1    1    1    1    1    1
   5       0.0     120.0     120.0    1    1    1    1    1    1
   6      10.0      10.0       0.0    1    1    1    1    1    1
$ ELEMENT CONNECTIVITY
   1   1   1   2   6   0   0                     1   1
   1   2   2   3   6   0   0                     1   1
   1   3   3   4   6   0   0                     1   1
   1   4   3   5   6   0   0                     1   1
$ LINE ELEMENT BASIC PROPERTIES
   1     25.13     125.7     62.83     62.83
$ ELEMENT MATERIAL PROPERTIES
   1   1
  30.24E06    0.2273
$ NODAL LOAD DATA
   2   4  100000.0
   2   2    4000.0
   3   1   -4000.0
   3   3   -2000.0
   3   4  -50000.0
  -1
```

STARS analysis results:

LOAD CASE NO. 1

NODE EXT	INT	X-DISPL.	Y-DISPL.	Z-DISPL.	X-ROTN.	Y-ROTN.	Z-ROTN.
1	1	0.000000E+00	0.000000E+00	0.000000E+00	0.000000E+00	0.000000E+00	0.000000E+00
2	2	-0.125288E+00	0.347953E+00	0.196027E-04	-0.239969E-02	-0.121545E-02	0.323397E-02
3	3	-0.125397E+00	0.103330E-03	-0.804946E-01	-0.580122E-03	-0.283265E-03	0.910380E-03
4	4	0.000000E+00	0.000000E+00	0.000000E+00	0.000000E+00	0.000000E+00	0.000000E+00
5	5	0.000000E+00	0.000000E+00	0.000000E+00	0.000000E+00	0.000000E+00	0.000000E+00
6	6	0.000000E+00	0.000000E+00	0.000000E+00	0.000000E+00	0.000000E+00	0.000000E+00

ELEMENT STRESSES

ELEMENT NO.	END1 / END5	END2 / END6	END3 / END7	END4 / END8	PX1/PX2 SXT SXX	PY1/PY2 SYT SYY	PZ1/PZ2 SXYT SZZ	MX1/MX2 SXB SXY	MY1/MY2 SYB SYZ	MZ1/MZ2 SXYB SZX
1	1	2			-0.124139E+03 0.124139E+03	-0.931688E+03 0.931688E+03	0.261767E+04 -0.261767E+04	-0.417341E+05 0.417341E+05	-0.193156E+06 -0.120964E+06	-0.785065E+05 -0.332961E+05
2	2	3			-0.690013E+03 0.690013E+03	0.232395E+03 -0.232395E+03	-0.129390E+04 0.129390E+04	0.234814E+05 -0.234814E+05	0.397457E+05 0.115522E+06	0.255969E+05 0.229051E+04
3	3	4			-0.654366E+03 0.654366E+03	0.523179E+03 -0.523179E+03	-0.980653E+03 0.980653E+03	0.365551E+04 -0.365551E+04	0.437120E+05 0.739664E+05	0.234344E+05 0.393472E+05
4	3	5			0.654366E+03 -0.654366E+03	0.131882E+04 -0.131882E+04	0.249337E+04 -0.249337E+04	-0.365551E+04 0.365551E+04	-0.164730E+06 -0.134475E+06	0.870056E+05 0.711728E+05

4.3 Plate Bending: Vibration Analysis

A square cantilever plate was analyzed to yield the natural frequencies and associated mode shapes. Figure 10 depicts the plate with a 4 by 4 finite element mesh, the bottom edge along the x-axis being clamped.

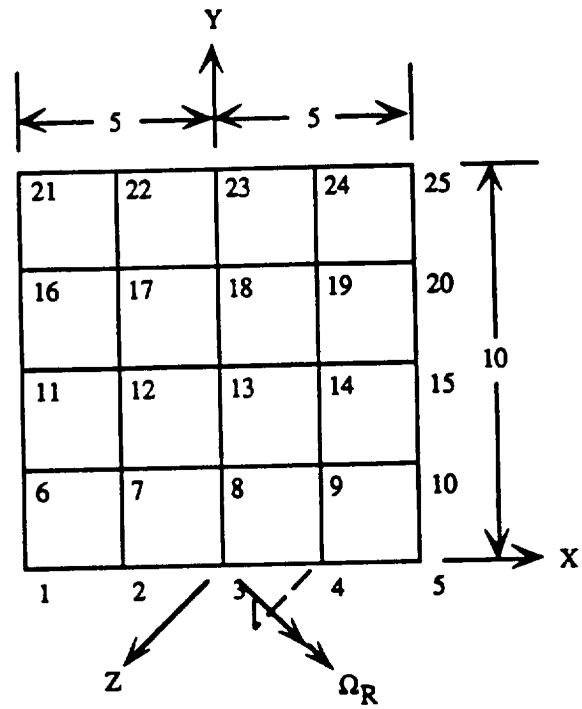

Figure 10. Square cantilever plate.

Important data parameters:

Young's modulus, E	$= 10 \times 10^6$
Side length, ℓ	= 10
Plate thickness, t	= 0.1
Poisson's ratio, μ	= 0.3
Mass density, ρ	$= 0.259 \times 10^{-3}$

STARS input data:

```
SQUARE 4 BY 4 PLATE    NONSPINNING STRUCTURE
 25, 16, 1, 4, 0, 1, 0, 0, 0, 0
  0,  0, 0, 1, 0, 0, 0, 0, 0
  1,  1, 0, 1, 0, 0, 0, 0
  2,  0, 2, 0, 1, 0
  1,  6, 0, 6000.0, 0.0, 0, 0.0
$ NODAL DATA
    1      -5.0      0.0      0.0   1   1   1   1   1   1   0   0   0
    5       5.0      0.0      0.0   1   1   1   1   1   1   0   0   1
    6      -5.0      2.5      0.0   0   0   0   0   0   0   0   0   0
   10       5.0      2.5      0.0   0   0   0   0   0   0   0   0   1
   11      -5.0      5.0      0.0   0   0   0   0   0   0   0   0   0
   15       5.0      5.0      0.0   0   0   0   0   0   0   0   0   1
   16      -5.0      7.5      0.0   0   0   0   0   0   0   0   0   0
   20       5.0      7.5      0.0   0   0   0   0   0   0   0   0   1
   21      -5.0     10.0      0.0   0   0   0   0   0   0   0   0   0
   25       5.0     10.0      0.0   0   0   0   0   0   0   0   0   1
$ ELEMENT CONNECTIVITY
    2    1    1    2    7    6   0   0   0   0   1   1   0   0   0
    2    4    4    5   10    9   0   0   0   0   1   1   0   0   0   1
    2    5    6    7   12   11   0   0   0   0   1   1   0   0   0
    2    8    9   10   15   14   0   0   0   0   1   1   0   0   0   1
    2    9   11   12   17   16   0   0   0   0   1   1   0   0   0
    2   12   14   15   20   19   0   0   0   0   1   1   0   0   0   1
    2   13   16   17   22   21   0   0   0   0   1   1   0   0   0
    2   16   19   20   25   24   0   0   0   0   1   1   0   0   0   1
$ SHELL ELEMENT THICKNESSES
    1      0.1
$ ELEMENT MATERIAL PROPERTIES
    1    1
   1.0E+07      0.30       0.0  0.259E-3
```

STARS output summary - The output summary is presented in table 5.

Table 5. Natural frequencies of a square cantilever plate.

Mode	Natural frequency ω, rad/sec	Nondimensional parameter $\gamma = \omega^2 \sqrt{\rho t / D}$
1	214.02	3.60
2	506.62	8.52
3	1248.40	20.99
4	1538.29	25.87
5	1765.53	29.69

Note: D = plate flexural rigidity
= $Et^3/12(1 - \mu^2)$

4.4 General Shell: Vibration Analysis

A cantilevered circular cylindrical shell is shown in figure 11 in which quadrilateral shell elements are used for structural discretization to perform a free vibration analysis.

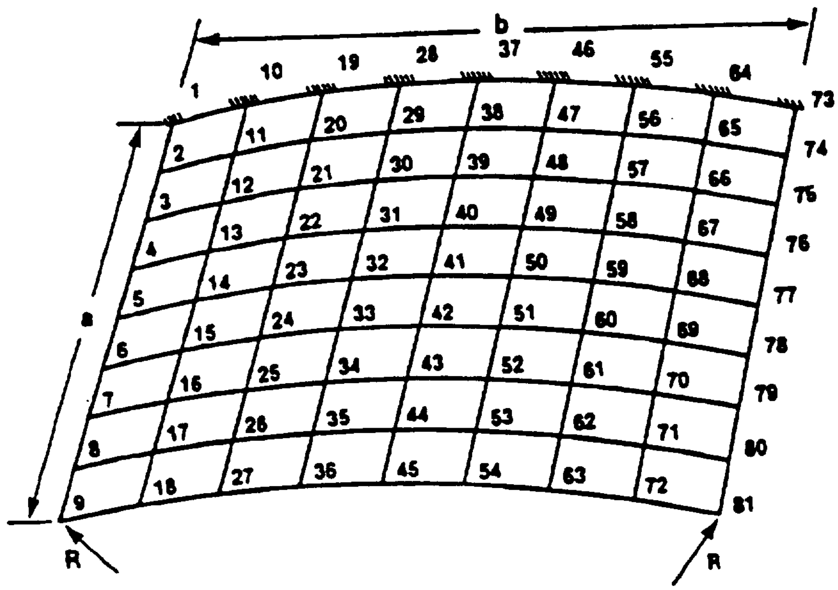

Figure 11. Finite element model of cylindrical shell.

Important data parameters:

Side length, a, b	= 10
Radius, R	= 20
Thickness, t	= 0.1
Young's modulus, E	= 29.5×10^6
Poisson's ratio, μ	= 0.3
Mass density, ρ	= 0.733×10^{-3}

STARS input data:

```
SHELL ELEMENT       8 BY 8    CURVED SHELL     FREE VIBRATION ANALYSIS
 81, 64, 1, 4, 0, 1, 0, 0, 0, 0
  0,  0, 0, 1, 0, 0, 0, 0, 0
  1,  1, 0, 1, 0, 0, 0, 0
  2,  0, 2, 0, 1, 0
  1,  6, 0, 90000.0, 0.0, 0.0
$ NODAL DATA
    1       0.0       0.0        0.0    1    1    1    1    1    1    0    0    0
    2      1.25       0.0        0.0    0    0    0    0    0    0    0    0    0
    9      10.0       0.0        0.0    0    0    0    0    0    0    0    0    1
   10       0.0      1.25  0.2803754    1    1    1    1    1    1    0    0    0
   11      1.25      1.25  0.2803754    0    0    0    0    0    0    0    0    0
   18      10.0      1.25  0.2803754    0    0    0    0    0    0    0    0    1
   19       0.0       2.5   0.478218    1    1    1    1    1    1    0    0    0
   20      1.25       2.5   0.478218    0    0    0    0    0    0    0    0    0
   27      10.0       2.5   0.478218    0    0    0    0    0    0    0    0    1
   28       0.0      3.75  0.5959826    1    1    1    1    1    1    0    0    0
   29      1.25      3.75  0.5959826    0    0    0    0    0    0    0    0    0
   36      10.0      3.75  0.5959826    0    0    0    0    0    0    0    0    1
   37       0.0       5.0  0.6350833    1    1    1    1    1    1    0    0    0
   38      1.25       5.0  0.6350833    0    0    0    0    0    0    0    0    0
   45      10.0       5.0  0.6350833    0    0    0    0    0    0    0    0    1
   46       0.0      6.25  0.5959826    1    1    1    1    1    1    0    0    0
   47      1.25      6.25  0.5959826    0    0    0    0    0    0    0    0    0
   54      10.0      6.25  0.5959826    0    0    0    0    0    0    0    0    1
   55       0.0       7.5   0.478218    1    1    1    1    1    1    0    0    0
   56      1.25       7.5   0.478218    0    0    0    0    0    0    0    0    0
   63      10.0       7.5   0.478218    0    0    0    0    0    0    0    0    1
   64       0.0      8.75  0.2803754    1    1    1    1    1    1    0    0    0
   65      1.25      8.75  0.2803754    0    0    0    0    0    0    0    0    0
   72      10.0      8.75  0.2803754    0    0    0    0    0    0    0    0    1
   73       0.0      10.0        0.0    1    1    1    1    1    1    0    0    0
   74      1.25      10.0        0.0    0    0    0    0    0    0    0    0    0
   81      10.0      10.0        0.0    0    0    0    0    0    0    0    0    1
$ ELEMENT CONNECTIVITY
    2    1    1    2   11   10    0    0    0    0    1    1
    2    8    8    9   18   17    0    0    0    0    1    1    0    0    0    1
    2    9   10   11   20   19    0    0    0    0    1    1
    2   16   17   18   27   26    0    0    0    0    1    1    0    0    0    1
    2   17   19   20   29   28    0    0    0    0    1    1
    2   24   26   27   36   35    0    0    0    0    1    1    0    0    0    1
    2   25   28   29   38   37    0    0    0    0    1    1
    2   32   35   36   45   44    0    0    0    0    1    1    0    0    0    1
    2   33   37   38   47   46    0    0    0    0    1    1
    2   40   44   45   54   53    0    0    0    0    1    1    0    0    0    1
    2   41   46   47   56   55    0    0    0    0    1    1
    2   48   53   54   63   62    0    0    0    0    1    1    0    0    0    1
    2   49   55   56   65   64    0    0    0    0    1    1
    2   56   62   63   72   71    0    0    0    0    1    1    0    0    0    1
    2   57   64   65   74   73    0    0    0    0    1    1
    2   64   71   72   81   80    0    0    0    0    1    1    0    0    0    1
$ SHELL ELEMENT THICKNESSES
    1       0.1
$ ELEMENT MATERIAL PROPERTIES
    1    1
0.2950E+080.3000E+000.0000E+000.7332E-03
```

STARS output summary - The output summary is presented in table 6.

Table 6. Natural frequencies of a cylindrical cantilever shell.

Mode	Natural frequency ω, rad/sec	Nondimensional parameter $\gamma = \omega a^2 \sqrt{\rho t / D}$
1	686.0745	11.30
2	1108.5908	18.26
3	1918.0797	31.60
4	2703.7155	44.54
5	2962.7536	48.81
6	3904.4432	64.32

4.5 General Solid: Vibration Analysis

A cube idealized by hexahedral solid elements is shown in figure 12. The nodes lying in the X-Y plane are assumed to be fixed. Details of the natural frequency analysis of the cube are presented herein.

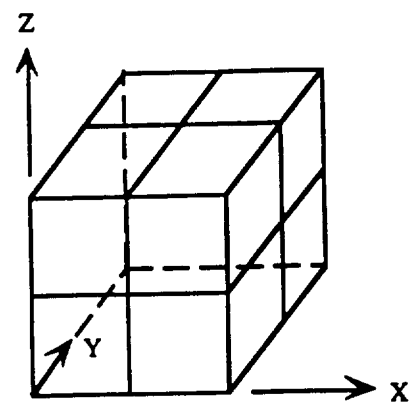

Figure 12. Cube discretized by hexahedral elements.

Important data parameters:

Side length, ℓ	= 10
Young's modulus, E	= 10×10^6
Poisson's ratio, μ	= 0.3
Mass density, ρ	= 2.349×10^{-4}

STARS input data:

```
HEXAHEDRON CASE - 2 BY 2
27,8,1,4,0,0,0,0,0,0
0,0,0,1,0,0,0,0,0
1,1,0,1,0,0,0,0
2,0,2,0,1,0
1,6,0,150000.0,0.0,0.0
$ NODAL DATA
  1    00.0    00.0    00.0   1   1   1   1   1   1
  2     5.0    00.0    00.0   1   1   1   1   1   1
  3    10.0    00.0    00.0   1   1   1   1   1   1
  4    10.0     5.0    00.0   1   1   1   1   1   1
  5    10.0    10.0    00.0   1   1   1   1   1   1
  6     5.0    10.0    00.0   1   1   1   1   1   1
  7    00.0    10.0    00.0   1   1   1   1   1   1
  8    00.0     5.0    00.0   1   1   1   1   1   1
  9     5.0     5.0    00.0   1   1   1   1   1   1
 10    00.0    00.0     5.0               1   1   1
 11     5.0    00.0     5.0               1   1   1
 12    10.0    00.0     5.0               1   1   1
 13    10.0     5.0     5.0               1   1   1
 14    10.0    10.0     5.0               1   1   1
 15     5.0    10.0     5.0               1   1   1
 16    00.0    10.0     5.0               1   1   1
 17    00.0     5.0     5.0               1   1   1
 18     5.0     5.0     5.0               1   1   1
 19    00.0    00.0    10.0               1   1   1
 20     5.0    00.0    10.0               1   1   1
 21    10.0    00.0    10.0               1   1   1
 22    10.0     5.0    10.0               1   1   1
 23    10.0    10.0    10.0               1   1   1
 24     5.0    10.0    10.0               1   1   1
 25    00.0    10.0    10.0               1   1   1
 26    00.0     5.0    10.0               1   1   1
 27     5.0     5.0    10.0               1   1   1
$ ELEMENT CONNECTIVITY
  4   1   1   2   9   8  10  11  18  17   1
  4   2   2   3   4   9  11  12  13  18   1
  4   3   9   4   5   6  18  13  14  15   1
  4   4   8   9   6   7  17  18  15  16   1
  4   5  10  11  18  17  19  20  27  26   1
  4   6  11  12  13  18  20  21  22  27   1
  4   7  18  13  14  15  27  22  23  24   1
  4   8  17  18  15  16  26  27  24  25   1
$ ELEMENT MATERIAL PROPERTIES
  1   1
  1.0E+7      0.3      0.0  2.349E-4
```

STARS output summary - The output summary is presented in table 7.

Table 7. Natural frequencies of a solid cube.

Mode	Natural frequency parameter $\hat{\omega} = \omega / \sqrt{(E/\rho)}$, rad / sec — Mesh size: 2 by 2	4 by 4	6 by 6	Exact solution $\hat{\omega}$
1	0.07975	0.07195	0.06958	0.06801
2	0.07975	0.07195	0.06958	0.06801
3	0.13150	0.10430	0.09762	0.09288
4	0.17200	0.16450	0.16230	0.16110
5	0.22800	0.19330	0.18500	0.18190
6	0.22800	0.19330	0.18500	0.18190

4.6 Cantilever Beam (Spinning and Nonspinning Cases): Vibration Analysis

A cantilever beam spinning about the Y-axis is shown in figure 13.

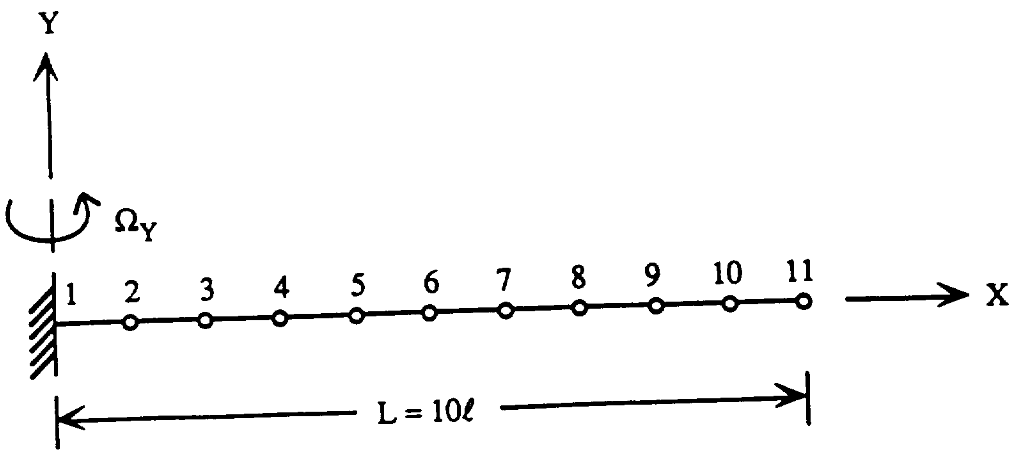

Figure 13. Spinning cantilever beam.

Important data parameters - The structure is assumed to possess both viscous and structural damping.

Young's modulus, E	$= 30 \times 10^6$
Cross-sectional area, A	= 1.0
Moment of inertia:	
About Y-axis	= 1/12
About Z-axis	= 1/24
Element length, ℓ	= 6
Nodal translational mass	= 1
Nodal mass moment of inertia	= 1/35
Scalar viscous damping	= 0.628318
Structural damping coefficient	= 0.01
Spin rate, Hz	= 0.1

STARS input data:

```
SPINNING CANTILEVER BEAM - 10-ELEMENT IDEALIZATION - VISC AND STRUCT DAMPING
12,10,1,4,1,0,0,0,0,0
0,0,1,1,0,0,0,0,0
5,0,0,0,0,1,0,0
2,0,2,0,1,0
1,6,0,500.0,0.0,0.0
0.01
$ NODAL DATA
    1      0.0      0.0      0.0   1   1   1   1   1   1
    2      6.0      0.0      0.0   0   0   0   0   0   0
    3     12.0      0.0      0.0   0   0   0   0   0   0
    4     18.0      0.0      0.0   0   0   0   0   0   0
    5     24.0      0.0      0.0   0   0   0   0   0   0
    6     30.0      0.0      0.0   0   0   0   0   0   0
    7     36.0      0.0      0.0   0   0   0   0   0   0
    8     42.0      0.0      0.0   0   0   0   0   0   0
    9     48.0      0.0      0.0   0   0   0   0   0   0
   10     54.0      0.0      0.0   0   0   0   0   0   0
   11     60.0      0.0      0.0   0   0   0   0   0   0
   12     25.0     15.0      0.0   1   1   1   1   1   1
$ ELEMENT CONNECTIVITY
    1   1   1   2  12   0   0   0   0   0   1   1   0   0   1   0
    1  10  10  11  12   0   0   0   0   0   1   1   0   0   1   1
$ LINE ELEMENT BASIC PROPERTIES
    1       1.0   0.125000.083333330.04166667
$ ELEMENT MATERIAL PROPERTIES
    1   1
  30.0E+06      0.30
$ ELEMENT SPIN RATE DATA
    1       0.0  0.628318       0.0
$ NODAL MASS DATA
    2   1        1.0   3
    3   1        1.0   3
    4   1        1.0   3
    5   1        1.0   3
    6   1        1.0   3
    7   1        1.0   3
    8   1        1.0   3
    9   1        1.0   3
   10   1        1.0   3
   11   1        1.0   3
    2   4 0.0285714    6
    3   4 0.0285714    6
    4   4 0.0285714    6
    5   4 0.0285714    6
    6   4 0.0285714    6
    7   4 0.0285714    6
    8   4 0.0285714    6
    9   4 0.0285714    6
   10   4 0.0285714    6
   11   4 0.0285714    6
   -1
$ VISCOUS DAMPING DATA
0.0000E+000.0000E+000.0000E+000.0000E+000.0000E+000.0000E+00
0.628318000.628318000.628318000.628318000.628318000.62831800
0.628318000.628318000.628318000.628318000.628318000.62831800
0.628318000.628318000.628318000.628318000.628318000.62831800
0.628318000.628318000.628318000.628318000.628318000.62831800
0.628318000.628318000.628318000.628318000.628318000.62831800
0.628318000.628318000.628318000.628318000.628318000.62831800
0.628318000.628318000.628318000.628318000.628318000.62831800
0.628318000.628318000.628318000.628318000.628318000.62831800
0.628318000.628318000.628318000.628318000.628318000.62831800
0.628318000.628318000.628318000.628318000.628318000.62831800
0.0000E+000.0000E+000.0000E+000.0000E+000.0000E+000.0000E+00
```

STARS output summary - The output summary is presented in table 8.

Table 8. Natural frequencies of a spinning cantilever beam.

Mode	Structure without damping, IPROB = 2	Structure with viscous damping, IPROB = 4	Structure with viscous and structural damping, IPROB = 5
1	2.526	-.3107 ± 2.4886i*	-.3195 ± 2.4820i*
2	3.448	-.3116 ± 3.4200i*	-.3255 ± 3.4123i*
3	15.396	-.3169 ± 15.3865i*	-.3930 ± 15.3831i*
4	21.705	-.3166 ± 21.7002i*	-.4243 ± 21.6912i*
5	43.161	-.3202 ± 43.1398i*	-.4848 ± 43.0627i*
6	60.951	-.3202 ± 60.9491i*	-.6246 ± 60.9390i*

Notes: Natural frequencies for various problem types are due to a spin rate $\Omega = 0.1$ Hz (0.6283 rad/sec).
$i^* = \sqrt{-1}$.

Additionally, table 9 provides a parametric study of vibration analysis of the nonspinning beam using both the IPROB = 1 and 3 (dynamic element) cases using consistent mass formulation (density ρ = 0.1666).

Table 9. Natural frequencies of a nonspinning cantilever beam.

No. of elements	IPROB	Natural frequencies ω, rad/sec					
		ω_1	ω_2	ω_3	ω_4	ω_5	ω_6
2	1	2.676	3.784	16.901	23.897	57.144	80.770
	3	2.675	3.782	16.766	23.707	49.864	70.494
4	1	2.675	3.783	16.779	23.724	47.277	66.829
	3	2.675	3.782	16.759	23.697	46.924	66.332
6	1	2.675	3.782	16.763	23.702	46.999	66.438
	3	2.675	3.782	16.759	23.696	46.914	66.317
8	1	2.675	3.782	16.760	23.698	46.942	66.357
	3	2.675	3.782	16.759	23.696	46.914	66.317
10	1	2.675	3.782	16.760	23.697	46.926	66.333
	3	2.675	3.782	16.759	23.696	46.914	66.317

4.7 Spinning Cantilever Plate: Vibration Analysis

The cantilever plate model described in section 4.3 is chosen for this sample problem. The plate is spun along the Z-axis with a uniform spin rate $\Omega_Z = 0.8 \times \omega_n^1$, ω_n^1 being the first natural frequency of vibration of the nonrotating plate. Table 10 provides the first few natural frequencies of the plate in nondimensional form, ω being the natural frequencies. Also presented in the table are the results of the free vibration analysis of the plate rotating along an arbitrary axis, the spin rate being $\Omega_R = 0.8 \times \omega_n^1$, with components $\Omega_X = \Omega_Y = \Omega_Z = 0.8 \times \omega_n^1 / \sqrt{3}$.

STARS input data:

```
SQUARE 4 BY 4 PLATE    SPINNING STRUCTURE
25,16,1,4,0,1,0,0,0,0
0,0,1,1,0,0,0,0,0
2,0,0,1,0,0,0,0
2,0,2,0,1,0
1,6,0,6000.0,0.0,0.0
$ NODAL DATA
   1      -5.0      0.0      0.0   1   1   1   1   1   1   0   0   0
   5       5.0      0.0      0.0   1   1   1   1   1   1   0   0   1
   6      -5.0      2.5      0.0   0   0   0   0   0   0   0   0   0
  10       5.0      2.5      0.0   0   0   0   0   0   0   0   0   1
  11      -5.0      5.0      0.0   0   0   0   0   0   0   0   0   0
  15       5.0      5.0      0.0   0   0   0   0   0   0   0   0   1
  16      -5.0      7.5      0.0   0   0   0   0   0   0   0   0   0
  20       5.0      7.5      0.0   0   0   0   0   0   0   0   0   1
  21      -5.0     10.0      0.0   0   0   0   0   0   0   0   0   0
  25       5.0     10.0      0.0   0   0   0   0   0   0   0   0   1
$ ELEMENT CONNECTIVITY
   2   1   1   2   7   6   0   0   0   0   1   1   0   0   1
   2   4   4   5  10   9   0   0   0   0   1   1   0   0   1   1
   2   5   6   7  12  11   0   0   0   0   1   1   0   0   1
   2   8   9  10  15  14   0   0   0   0   1   1   0   0   1   1
   2   9  11  12  17  16   0   0   0   0   1   1   0   0   1
   2  12  14  15  20  19   0   0   0   0   1   1   0   0   1   1
   2  13  16  17  22  21   0   0   0   0   1   1   0   0   1
   2  16  19  20  25  24   0   0   0   0   1   1   0   0   1   1
$ SHELL ELEMENT THICKNESSES
   1      0.1
$ ELEMENT MATERIAL PROPERTIES
   1   1
   1.0E+07      0.30      0.0  0.259E-3
$ ELEMENT SPIN RATE DATA
   1      0.        0.     100.0
```

STARS output summary - The output is presented in table 10.

Table 10. Natural frequency parameters of a spinning square cantilever plate.

Mode	Natural frequency parameter $\gamma = \omega \ell^2 \sqrt{\rho t / D}$			
	$\Omega_Z = 0.8\omega_N^1$ = 100.00 rad/sec		Ω_R = 100.00 rad/sec, $\Omega_X = \Omega_Y = \Omega_Z$ = 57.735 rad/sec	
	ω	γ	ω	γ
1	242.32	4.0752	155.48	2.6148
2	526.82	8.8598	489.05	8.2246
3	1271.00	21.3750	1250.40	21.0286
4	1551.90	26.0991	1536.40	25.8384
5	1784.50	30.0108	1768.60	29.7434
6	2902.60	48.8144	2891.60	48.6295

4.8 Helicopter Structure: Vibration Analysis

A coupled helicopter rotor-fuselage system is shown in figure 14 (ref. 14) along with relevant stiffness and mass distributions, which are suitably approximated for the discrete element modeling of the structure. Numerical free vibration analysis was performed for the structure with the rotor spinning at 10 rad/sec ($\Omega_Y = 10$); such results are presented in table 11, along with the results for the corresponding nonspinning case.

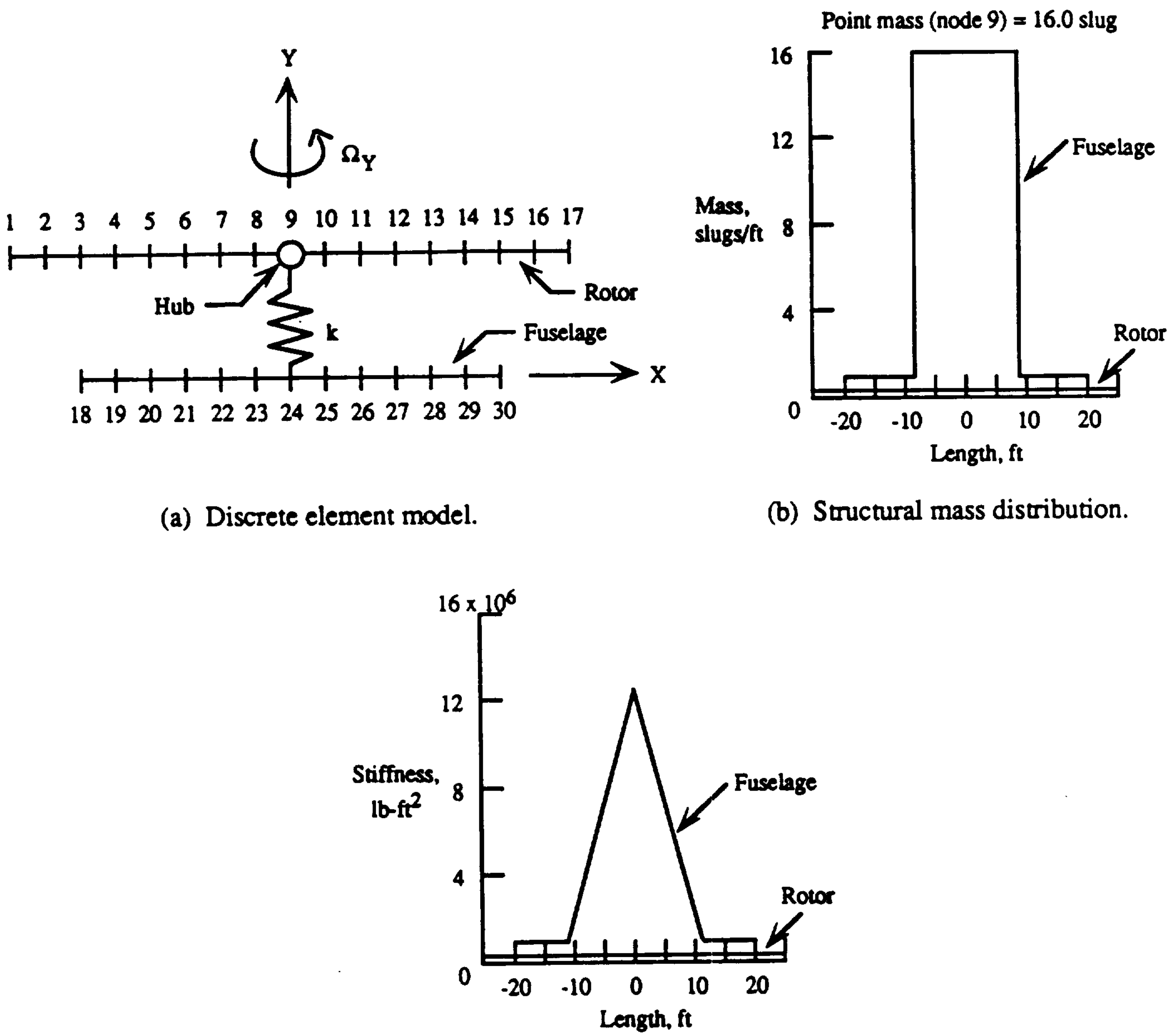

(a) Discrete element model.

(b) Structural mass distribution.

(c) Structural stiffness distribution.

Figure 14. Coupled helicopter rotor-fuselage system.

STARS input data:

```
HELICOPTER STRUCTURE, JOURNAL CASE,  SPIN - 10.0 (FIXED UZ, UXR, UYR)
31,29,7,4,2,0,0,0,0,0
0,0,1,0,0,0,0,0,0
2,0,0,1,0,1,0,0
2,0,2,0,1,0
1,12,0,53.15,0.0,0.0
$ NODAL DATA
   1 -25.00000      1.0       0.0   0   0   1   1   1   0   0
   8  -3.12500      1.0       0.0   0   0   1   1   1   0   0   0   1
   9   0.00000      1.0       0.0   0   0   1   1   1   0   0
  10   3.12500      1.0       0.0   0   0   1   1   1   0   0
  17  25.00000      1.0       0.0   0   0   1   1   1   0   0   0   1
  18 -20.00000      0.0       0.0   0   0   1   1   1   0   0
  23  -3.33333      0.0       0.0   0   0   1   1   1   0   0   0   1
  24   0.00000      0.0       0.0   0   0   1   1   1   0   0
  25   3.33333      0.0       0.0   0   0   1   1   1   0   0
  30  20.00000      0.0       0.0   0   0   1   1   1   0   0   0   1
  31  10.00000      0.5       0.0   1   1   1   1   1   1   0
$ ELEMENT CONNECTIVITY
   1   1   1   2  24                      1   1   0   0   1   0
   1  16  16  17  24                      1   1   0   0   1   1
   1  17  18  19   9                      2   1
   1  18  19  20   9                      2   1
   1  19  20  21   9                      3   1
   1  20  21  22   9                      4   1
   1  21  22  23   9                      5   1
   1  22  23  24   9                      6   1
   1  23  24  25   9                      6   1
   1  24  25  26   9                      5   1
   1  25  26  27   9                      4   1
   1  26  27  28   9                      3   1
   1  27  28  29   9                      2   1
   1  28  29  30   9                      2   1
   1  29   9  24  31                      7   2
$ LINE ELEMENT BASIC PROPERTIES
   1      1.       1.       1.       1.
   2    100.       1.       1.       1.
$ ELEMENT MATERIAL PROPERTIES
   1   1
  2.0E05      0.3      0.      0.3
   2   1
 1.53E06      0.3      0.      1.23
   3   1
  2.E06       0.3      0.      1.23
   4   1
  4.8E06      0.3      0.      8.6
   5   1
  7.8E06      0.3      0.      16.
   6   1
  11.E06      0.3      0.      16.
   7   1
   1.E08      0.3      0.      0.
$ ELEMENT SPIN RATE DATA
   1      0.0     10.0      0.0
$ NODAL MASS DATA
   9   1      16.    3
  -1
```

STARS output summary - The output summary is presented in table 11.

Table 11. Natural frequencies of a helicopter structure.

Mode number	Natural frequencies, spin rates		Mode shape
	$\Omega_Y = 0$	$\Omega_Y = 10$	
1,2,3	0	0	Rigid body
4	4.642	11.789	Rotor 1st symmetric bending
5	5.041	11.793	Rotor 1st antisymmetric bending
6	22.138	22.229	Fuselage 1st bending
7	27.892	36.199	Rotor 2nd antisymmetric bending
8	28.278	37.800	Rotor 2nd symmetric bending
9	37.176	38.478	Rotor 3rd antisymmetric bending

4.9 Rocket Structure: Dynamic Response Analysis

A rocket idealized simply by four line elements, as shown in figure 15 (ref. 5), is subjected to a pulse loading function at the base. Results of the dynamic response analysis are shown in figures 16 and 17.

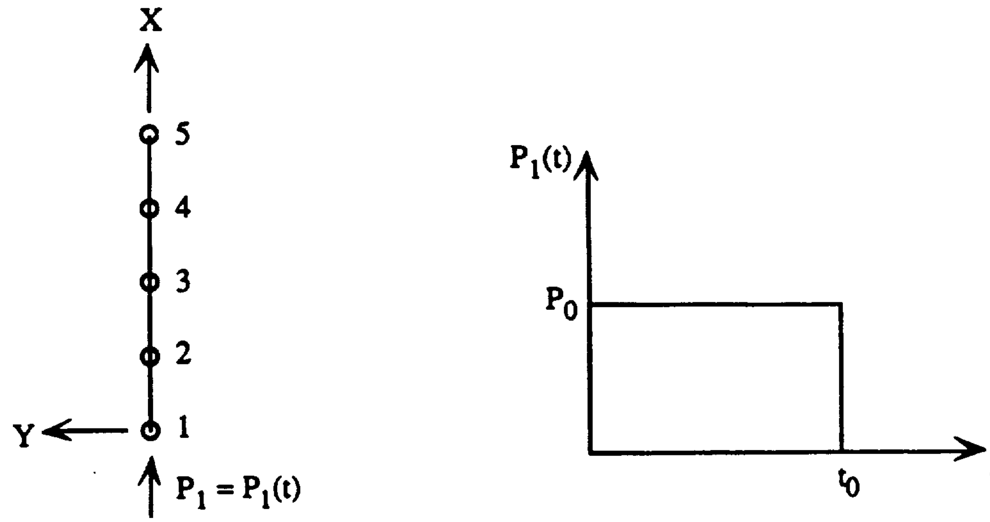

(a) Rocket structure. (b) Pulse loading.

Figure 15. Rocket subjected to dynamic loading.

Important data parameters - Arbitrary element and material properties data are assumed for the analysis to correlate results with available ones expressed in parametric form.

Young's modulus, E	= 100
Poisson's ratio, μ	= 0.3
Cross-sectional area, A	= 1.0
Mass density, ρ	= 1.0
Length of an element, ℓ	= 2.5
Pulse load intensity, P_0	= 10.0
Duration of load, sec	= 1.0
Total time period for response evaluation	= 2.0

STARS input data:

```
DYNAMIC RESPONSE CASE - PRZEMIENIECKI
6,4,1,4,1,0,0,0,0,0
0,0,0,0,0,0,0,0,0
1,0,1,1,0,0,0,0
2,0,2,0,1,0
1,3,0,20.0,0.0,0.0
0,1,1,2
$ NODAL DATA
   1       0.0       0.0       0.0   0   1   1   1   1   1
   5      10.0       0.0       0.0   0   1   1   1   1   1   0   0   1
   6       5.0       5.0       0.0   1   1   1   1   1   1
$ ELEMENT CONNECTIVITY
   1   1   1   2   6   0   0                 1   1
   1   4   4   5   6   0   0                 1   1   0   0   0   1
$ LINE ELEMENT BASIC PROPERTIES
   1       1.0       0.0       0.0       0.0
$ ELEMENT MATERIAL PROPERTIES
   1   1
    100.0      0.3       0.0       1.0
$ DYNAMIC NODAL FORCE DATA
           1.0
   1   1             10.0
  -1
$ INCREMENTAL TIME DATA FOR DYNAMIC RESPONSE ANALYSIS
          0.10   10
          0.20    5
```

STARS analysis results at a typical time step:

DYNAMIC RESPONSE AT TIME = 0.7000E+00

NODE EXT	NODE INT	X-DISPL.	Y-DISPL.	Z-DISPL.	X-ROTN.	Y-ROTN.	Z-ROTN.
1	1	0.646322E+00	0.000000E+00	0.000000E+00	0.000000E+00	0.000000E+00	0.000000E+00
2	2	0.490999E+00	0.000000E+00	0.000000E+00	0.000000E+00	0.000000E+00	0.000000E+00
3	3	0.191562E+00	0.000000E+00	0.000000E+00	0.000000E+00	0.000000E+00	0.000000E+00
4	4	-0.102987E-02	0.000000E+00	0.000000E+00	0.000000E+00	0.000000E+00	0.000000E+00
5	5	-0.495080E-01	0.000000E+00	0.000000E+00	0.000000E+00	0.000000E+00	0.000000E+00
6	6	0.000000E+00	0.000000E+00	0.000000E+00	0.000000E+00	0.000000E+00	0.000000E+00

ELEMENT STRESSES

ELEMENT NO.	END1 / END5	END2 / END6	END3 / END7	END4 / END8	PX1/PX2 SXT SXX	PY1/PY2 SYT SYY	PZ1/PZ2 SXYT SZZ	MX1/MX2 SXB SXY	MY1/MY2 SYB SYZ	MZ1/MZ2 SXYB SZX
1	1	2			0.621289E+01	0.000000E+00	0.000000E+00	0.000000E+00	0.000000E+00	0.000000E+00
					-0.621289E+01	0.000000E+00	0.000000E+00	0.000000E+00	0.000000E+00	0.000000E+00
2	2	3			0.119775E+02	0.000000E+00	0.000000E+00	0.000000E+00	0.000000E+00	0.000000E+00
					-0.119775E+02	0.000000E+00	0.000000E+00	0.000000E+00	0.000000E+00	0.000000E+00
3	3	4			0.770366E+01	0.000000E+00	0.000000E+00	0.000000E+00	0.000000E+00	0.000000E+00
					-0.770366E+01	0.000000E+00	0.000000E+00	0.000000E+00	0.000000E+00	0.000000E+00
4	4	5			0.193913E+01	0.000000E+00	0.000000E+00	0.000000E+00	0.000000E+00	0.000000E+00
					-0.193913E+01	0.000000E+00	0.000000E+00	0.000000E+00	0.000000E+00	0.000000E+00

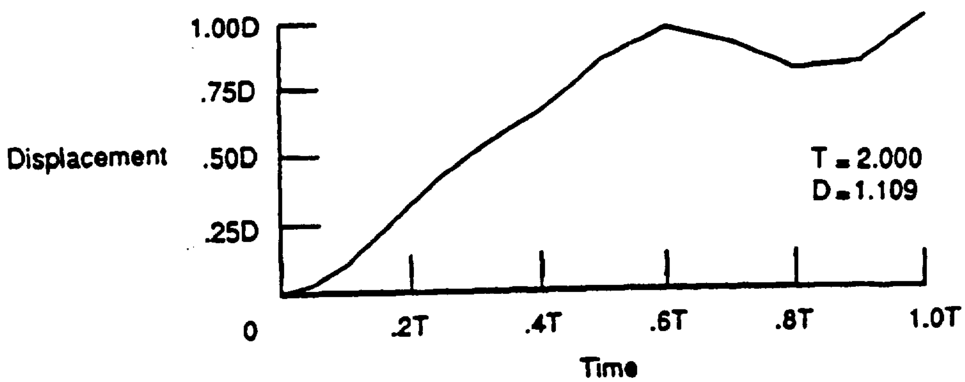

Figure 16. Rocket nodal displacement as a function of time, node 1.

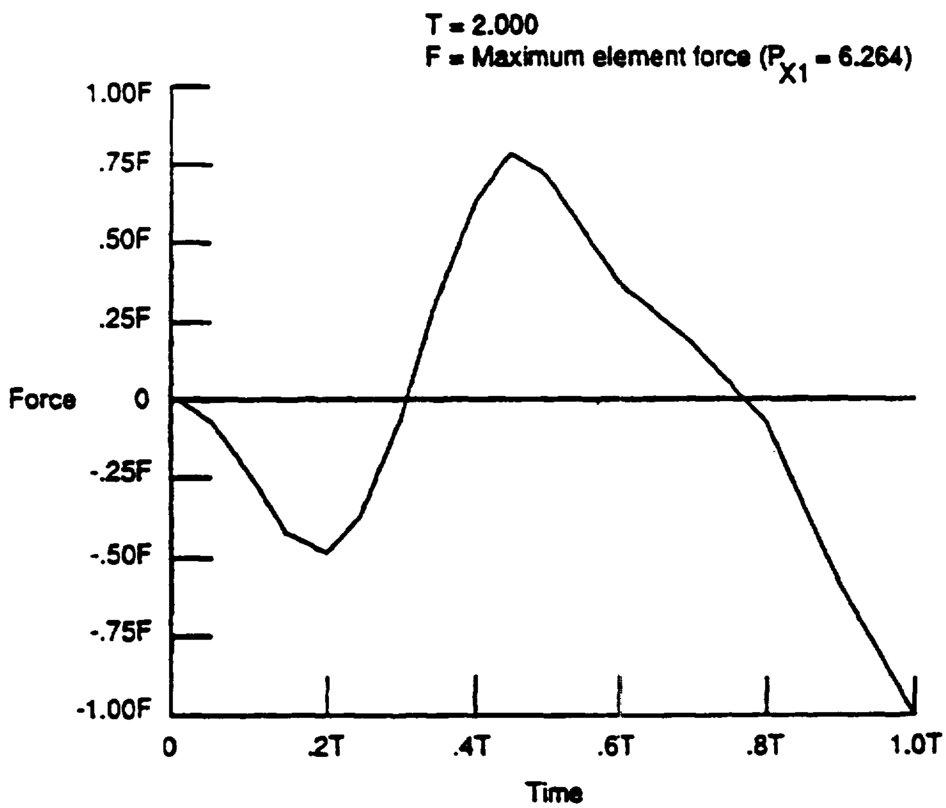

Figure 17. Rocket element force as a function of time, element 4.

4.10 Plate, Beam, and Truss Structures: Buckling Analysis

4.10.1 Simply supported square plate

A buckling analysis was performed for a simply-supported square plate model, described in section 4.3, subjected to a uniform unit stress acting along the two edges parallel to the y-axis; relevant input data and analysis results are as follows.

STARS input data:

```
SQUARE 4 BY 4 PLATE,BC W=0, midline x=0,Y(13)=5.0, BUCKLING ANALYSIS
25,16,1,4,0,1,0,0,0,0
0,0,0,1,0,0,0,0,0
9,1,0,1,1,0,0,0
2,0,2,0,1,0
1,1,0,20000.0,0.0,0.0
$ NODAL DATA
   1    -5.00    0.0     0.0   0   0   1   0   0   1   0   0   0
   2    -2.50    0.0     0.0   0   0   1   0   0   1   0   0   0
   3     0.0     0.0     0.0   1   0   1   0   1   1   0   0   0
   4     2.50    0.0     0.0   0   0   1   0   0   1   0   0   0
   5     5.00    0.0     0.0   0   0   1   0   0   1   0   0   0
   6    -5.00    2.50    0.0   0   0   1   0   0   1   0   0   0
   7    -2.50    2.50    0.0   0   0   0   0   0   1   0   0   0
   8     0.0     2.5     0.0   1   0   0   0   1   1   0   0   0
   9     2.50    2.50    0.0   0   0   0   0   0   1   0   0   0
  10     5.00    2.50    0.0   0   0   1   0   0   1   0   0   0
  11    -5.00    5.00    0.0   0   1   1   1   0   1   0   0   0
  12    -2.50    5.00    0.0   0   1   0   1   0   1   0   0   0
  13     0.0     5.00    0.0   1   1   0   1   1   1   0   0   0
  14     2.50    5.00    0.0   0   1   0   1   0   1   0   0   0
  15     5.00    5.00    0.0   0   1   1   1   0   1   0   0   0
  16    -5.00    7.50    0.0   0   0   1   0   0   1   0   0   0
  17    -2.50    7.50    0.0   0   0   0   0   0   1   0   0   0
  18     0.0     7.5     0.0   1   0   0   0   1   1   0   0   0
  19     2.50    7.50    0.0   0   0   0   0   0   1   0   0   0
  20     5.00    7.50    0.0   0   0   1   0   0   1   0   0   0
  21    -5.00   10.00    0.0   0   0   1   0   0   1   0   0   0
  22    -2.50   10.00    0.0   0   0   1   0   0   1   0   0   0
  23     0.0    10.0     0.0   1   0   1   0   1   1   0   0   0
  24     2.50   10.00    0.0   0   0   1   0   0   1   0   0   0
  25     5.00   10.00    0.0   0   0   1   0   0   1   0   0   0
$ ELEMENT CONNECTIVITY
   2   1   1   2   7   6   0   0   0   0   1   1   0   0   0
   2   4   4   5  10   9   0   0   0   0   1   1   0   0   0   1
   2   5   6   7  12  11   0   0   0   0   1   1   0   0   0
   2   8   9  10  15  14   0   0   0   0   1   1   0   0   0   1
   2   9  11  12  17  16   0   0   0   0   1   1   0   0   0
   2  12  14  15  20  19   0   0   0   0   1   1   0   0   0   1
   2  13  16  17  22  21   0   0   0   0   1   1   0   0   0
   2  16  19  20  25  24   0   0   0   0   1   1   0   0   0   1
$ SHELL ELEMENT THICKNESSES
   1      0.1
$ ELEMENT MATERIAL PROPERTIES
   1   1
   1.0E+07     0.30
$ NODAL LOAD DATA
   1   1    .125
   6   1    .250
  11   1    .250
  16   1    .250
  21   1    .125
   5   1   -.125
  10   1   -.250
  15   1   -.250
  20   1   -.250
  25   1   -.125
  -1
```

STARS analytical results - The analytical results pertaining to the buckling load are presented in table 12.

Table 12. Critical load of a simply supported square plate.

Buckling load parameter for Mode 1			
STARS solution			Exact solution
4 by 4	8 by 8	14 by 14	
3530.695	3552.620	3570.558	3615.240

4.10.2 Cantilever beam

The cantilever beam described in section 4.6 is the subject of a buckling analysis; the relevant details are given below.

STARS input data:

```
CANTILEVER BEAM - 10-ELEMENT IDEALIZATION - BUCKLING ANALYSIS
C
C TEMPERATURE LOADING ADDED
C
12,10,1,4,1,0,0,0,0,0
1,0,0,1,0,0,0,0,0
9,1,0,1,1,0,0,0
2,0,2,0,1,0
1,1,0,12000.0,0.0,0.0
$ NODAL DATA
   1      0.0      0.0      0.0   1   1   1   1   1   1
   2      6.0      0.0      0.0   0   0   1   1   1   0
   3     12.0      0.0      0.0   0   0   1   1   1   0
   4     18.0      0.0      0.0   0   0   1   1   1   0
   5     24.0      0.0      0.0   0   0   1   1   1   0
   6     30.0      0.0      0.0   0   0   1   1   1   0
   7     36.0      0.0      0.0   0   0   1   1   1   0
   8     42.0      0.0      0.0   0   0   1   1   1   0
   9     48.0      0.0      0.0   0   0   1   1   1   0
  10     54.0      0.0      0.0   0   0   1   1   1   0
  11     60.0      0.0      0.0   0   1   1   1   1   0
  12     25.0     15.0      0.0   1   1   1   1   1   1
$ ELEMENT CONNECTIVITY
   1   1   1   2  12   0   0   0   0   0   1   1   1   0   0   0
   1  10  10  11  12   0   0   0   0   0   1   1   1   0   0   1
$ LINE ELEMENT BASIC PROPERTIES
   1      1.0      0.125  0.083333  0.041667
$ ELEMENT MATERIAL PROPERTIES
   1   1
  30.0E+06      0.30   6.6E-06
$ ELEMENT TEMPERATURE DATA
   1      -1.0
$ NODAL LOAD DATA
  11   1      -1.0
  -1
```

STARS analytical results - The analytical results are presented in table 13.

Table 13. Critical load of a cantilever beam.

Mode	Buckling load parameter	
	STARS solution	Exact solution
1	7011.14	7010.42

4.10.3 Truss problem

The simple truss of figure 18 (ref. 5) is also analyzed to determine the critical loads. The associated input data and analytical results are given below.

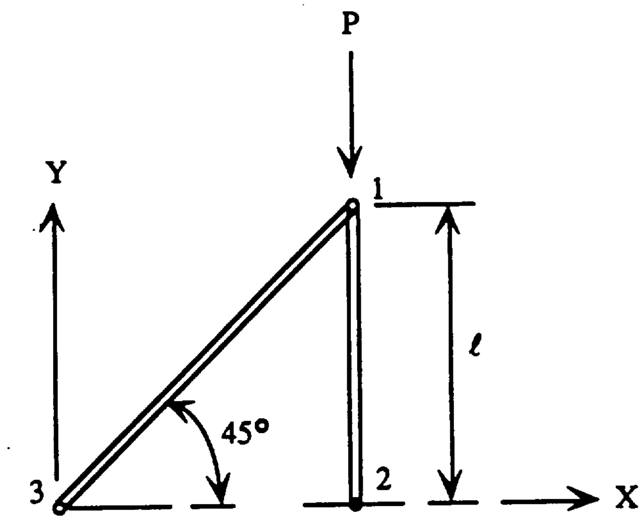

Figure 18. Truss structure.

STARS input data:

```
PRZ - TRUSS BUCKLING ANALYSIS
4,2,1,4,1,0,0,0,0,0
0,0,0,1,0,0,0,0,0
9,0,0,1,1,0,0,0
2,0,2,0,1,0
1,2,0,20000.0,0.0,0.0
$ NODAL DATA
   1     100.0     100.0      0.0   0   0   1   1   1   1
   2     100.0       0.0      0.0   1   1   1   1   1   1
   3       0.0       0.0      0.0   1   1   1   1   1   1
   4       0.0      50.0      0.0   1   1   1   1   1   1
$ ELEMENT CONNECTIVITY
   1   1   3   1   4   1   1   0   0   0   1   1
   1   2   2   1   4   1   1   0   0   0   1   1
$ LINE ELEMENT BASIC PROPERTIES
   1      0.1
$ ELEMENT MATERIAL PROPERTIES
   1   1
  10.0E03      0.2
$ NODAL LOAD DATA
   1   2      -1.0
  -1
```

STARS analytical results - The analytical results are presented in table 14.

Table 14. Critical load of a simple truss.

Mode	Buckling load parameter	
	STARS solution	Exact solution
1	261.20388	261.20387

4.11 Composite Plate Bending: Vibration Analysis

To illustrate the use of multiple material angle (as in layered elements) and the diverse coordinate system capabilities, a square composite plate (fig. 19) similar to that in section 4.3 is considered for vibration analysis; the plate, fixed along two opposite edges, is analysed for uniform temperature loading.

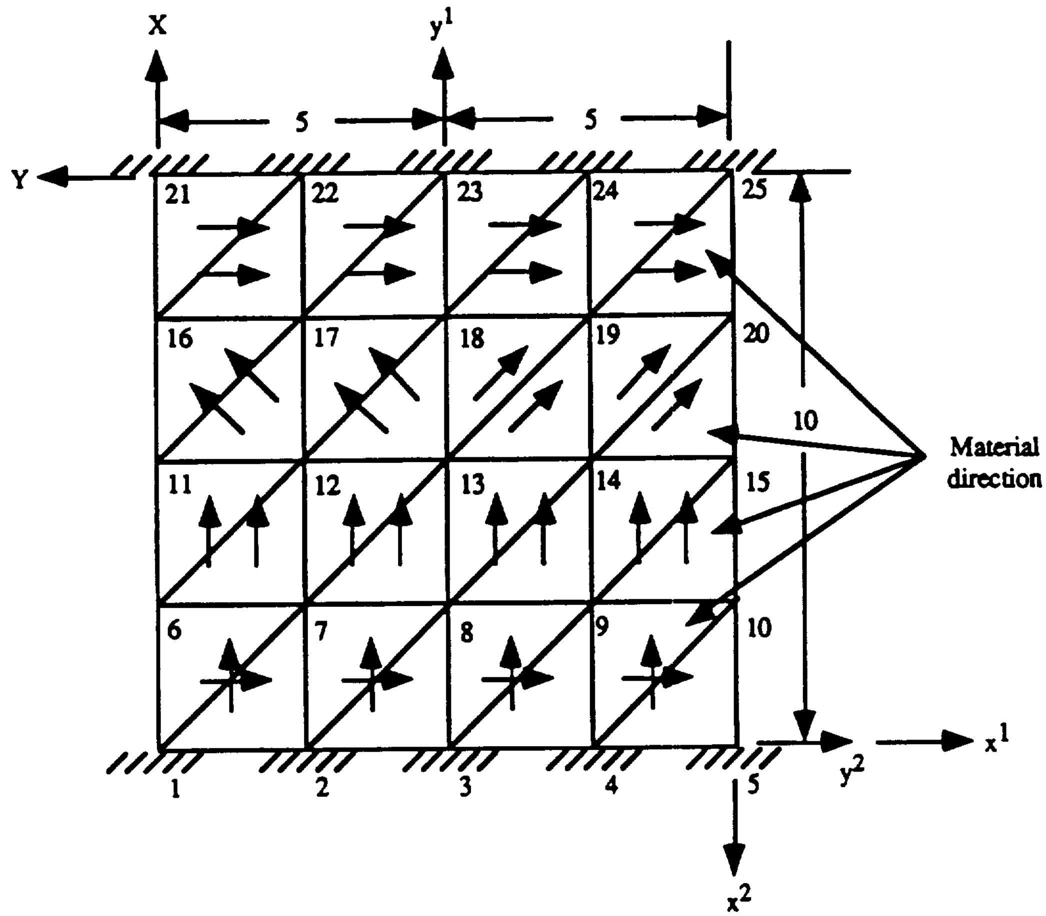

Figure 19. Square composite plate.

Important data parameters:

Side length, ℓ = 10
Plate thickness, t = 0.063
Mass density, ρ = 0.259×10^{-3}
Material properties - anisotropic, as shown in input data.

STARS input data:

```
TRIANGULAR 4 BY 4 PLATE / COMPOSITE LAYERS / ILGCS TEST CASE / NMANGL TEST CASE
 25, 32, 1, 13, 0, 0, 2, 8, 10, 2
  1,  0, 0,  0, 0, 0, 0, 0,  0
  1,  1, 0,  1, 0, 0, 0, 0
  2,  0, 2,  0, 1, 0
  1, 10, 0, 6000.0, 0.0, 0.0
$ NODAL DATA
    1      -5.0       0.0        0.0   1   1   1   1   1   1   1   0   0
    5       5.0       0.0        0.0   1   1   1   1   1   1   1   0   1
    6      -2.5     -10.0        0.0   0   0   0   0   0   0   2   0   0
   10      -2.5       0.0        0.0   0   0   0   0   0   0   2   0   1
   11      -5.0       5.0        0.0   0   0   0   0   0   0   1   0   0
   15       5.0       5.0        0.0   0   0   0   0   0   0   1   0   1
   16      -2.5       0.0        0.0   0   0   0   0   0   0   0   0   0
   20      -2.5     -10.0        0.0   0   0   0   0   0   0   0   0   1
   21      -5.0      10.0        0.0   1   1   1   1   1   1   1   0   0
   25       5.0      10.0        0.0   1   1   1   1   1   1   1   0   1
$ LOCAL-GLOBAL COORDINATE SYSTEM DATA
    1    2
     -10.0      -5.0       0.0       0.0      -1.0       0.0
       1.0       0.0       0.0       0.0       0.0       1.0
    2    1
     -10.0     -10.0       0.0     -15.0     -10.0       0.0
     -15.0     -15.0       0.0
$ ELEMENT CONNECTIVITY
    7    1    1    2    7    0    0    0    0    1    1    0    1    0    0
    7    4    4    5   10    0    0    0    0    1    1    0    1    0    0    1
    7    5    6    7   12    0    0    0    0    2    1    0    1    0    0
    7    8    9   10   15    0    0    0    0    2    1    0    1    0    0    1
    7    9   11   12   17    0    0    0    0    3    1    0    1    0    0
    7   10   12   13   18    0    0    0    0    3    1    0    1    0    0
    7   11   13   14   19    0    0    0    0    4    1    0    1    0    0
    7   12   14   15   20    0    0    0    0    4    1    0    1    0    0
    7   13   16   17   22    0    0    0    0    5    1    0    1    0    0
    7   16   19   20   25    0    0    0    0    5    1    0    1    0    0    1
    7   17    7    6    1    0    0    0    0    6    1    0    1    0    0
    7   20   10    9    4    0    0    0    0    6    1    0    1    0    0    1
    7   21   12   11    6    0    0    0    0    7    1    0    1    0    0
    7   24   15   14    9    0    0    0    0    7    1    0    1    0    0    1
    7   25   17   16   11    0    0    0    0    8    1    0    1    0    0
    7   26   18   17   12    0    0    0    0    8    1    0    1    0    0
    7   27   19   18   13    0    0    0    0    9    1    0    1    0    0
    7   28   20   19   14    0    0    0    0    9    1    0    1    0    0
    7   29   22   21   16    0    0    0    0   10    1    0    1    0    0
    7   32   25   24   19    0    0    0    0   10    1    0    1    0    0    1
$ COMPOSITE SHELL ELEMENT STACK DESCRIPTION DATA
    1    2
    1     .0315    3
    1     .0315    1
    2    2
    1     .0315    3
    1     .0315    3
    3    2
    1     .0315    4
    1     .0315    4
    4    2
    1     .0315    2
    1     .0315    2
    5    2
    1     .0315    1
    1     .0315    1
    6    2
    1     .0315    6
    1     .0315    5
    7    2
    1     .0315    6
    1     .0315    6
    8    2
    1     .0315    7
    1     .0315    7
    9    2
    1     .0315    8
    1     .0315    8
   10    2
    1     .0315    5
    1     .0315    5
```

```
$ SPECIFICATION FOR MATERIAL AXIS ORIENTATION
   1    2     0
      0.0
   2    2     0
   0.7854
   3    2     0
   1.5708
   4    2     0
   2.3562
   5    2     0
   3.1416
   6    2     0
   4.7120
   7    2     0
   5.4980
   8    2     0
   3.9260
$ ELEMENT MATERIAL PROPERTIES
   1    2
 .7966E+07 .6638E+06      0.0 .2566E+07       0.0  0.125E+7  .1042E+7
      0.0 .1042E+07   .35e-5   .114e-4       0.0  0.259E-3
$ ELEMENT TEMPERATURE DATA
   1       10.
```

STARS output summary - The results are printed in table 15.

Table 15. Natural frequencies of a square composite plate.

Mode	Natural frequency ω, rad/sec	
	T = 0	T = 10
1	505.40	373.38
2	611.98	486.78
3	967.78	851.04
4	1434.66	1275.96
5	1523.71	1361.70
6	1765.22	1643.97

4.12 Thermal Prestress Free-Free Vibration of Rectangular Plate

To illustrate the thermal prestress vibration analysis capability, a free-free rectangular plate (fig. 20) subjected to varying temperature loading and having varying material properties has been analyzed to obtain natural frequencies and modes.

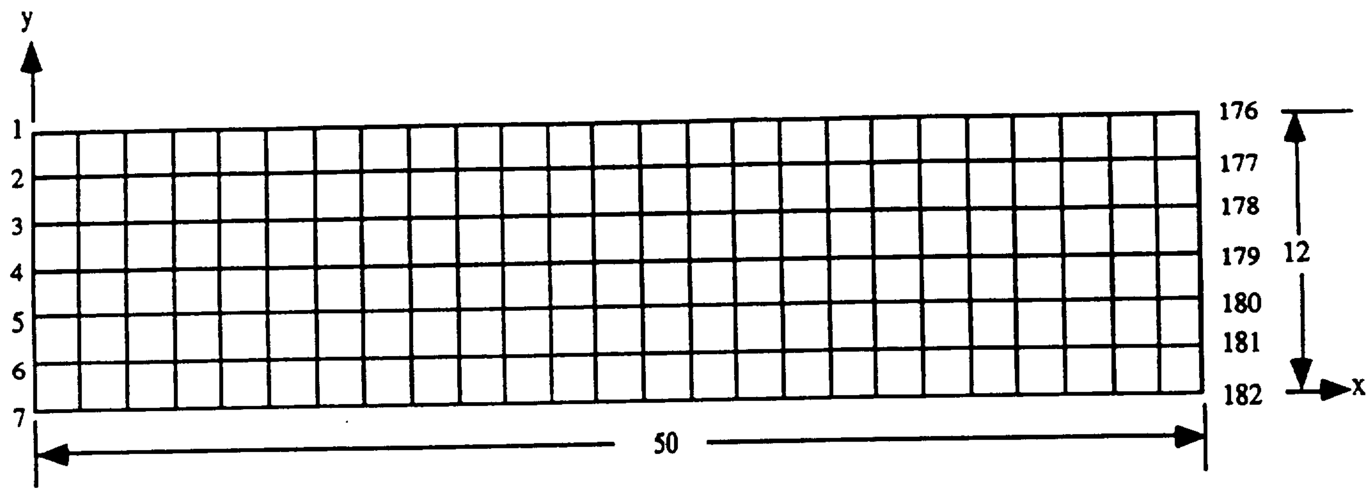

Figure 20. Rectangular plate.

Important data parameters:

Rectangular Plate	= 12 x 50
Plate thickness, t	= 0.19
Mass density, ρ	= 2.614×10^{-4}
Temperature	= varying along x-axis

STARS input data:

```
50"  x  12"  Aluminum  Plote;   NON-UNIFORM  HEAT;   Free-free
  182,  150,   15,    4,     0,      1,     0,    0,    0,    0
   15,    0,    0,    0,     0,      0,     0,    0,    0
    1,    0,    0,    0,     0,      1,     0,    0
    2,    0,    2,    0,     1,      0
    1,   20,    0,  2000.0,     0.0,    1.0E+05
$  NODAL  DATA
     1    0.0000   12.0000   0.0000   0   0   0   0   0   0   0   0   0
     7    0.0000    0.0000   0.0000   0   0   0   0   0   0   0   0   1
     8    2.0000   12.0000   0.0000   0   0   0   0   0   0   0   0   0
    14    2.0000    0.0000   0.0000   0   0   0   0   0   0   0   0   1
    15    4.0000   12.0000   0.0000   0   0   0   0   0   0   0   0   0
    21    4.0000    0.0000   0.0000   0   0   0   0   0   0   0   0   1
    22    6.0000   12.0000   0.0000   0   0   0   0   0   0   0   0   0
    28    6.0000    0.0000   0.0000   0   0   0   0   0   0   0   0   1
    29    8.0000   12.0000   0.0000   0   0   0   0   0   0   0   0   0
    35    8.0000    0.0000   0.0000   0   0   0   0   0   0   0   0   1
    36   10.0000   12.0000   0.0000   0   0   0   0   0   0   0   0   0
    42   10.0000    0.0000   0.0000   0   0   0   0   0   0   0   0   1
    43   12.0000   12.0000   0.0000   0   0   0   0   0   0   0   0   0
    49   12.0000    0.0000   0.0000   0   0   0   0   0   0   0   0   1
    50   14.0000   12.0000   0.0000   0   0   0   0   0   0   0   0   0
    56   14.0000    0.0000   0.0000   0   0   0   0   0   0   0   0   1
    57   16.0000   12.0000   0.0000   0   0   0   0   0   0   0   0   0
    63   16.0000    0.0000   0.0000   0   0   0   0   0   0   0   0   1
    64   18.0000   12.0000   0.0000   0   0   0   0   0   0   0   0   0
    70   18.0000    0.0000   0.0000   0   0   0   0   0   0   0   0   1
    71   20.0000   12.0000   0.0000   0   0   0   0   0   0   0   0   0
    77   20.0000    0.0000   0.0000   0   0   0   0   0   0   0   0   1
    78   22.0000   12.0000   0.0000   0   0   0   0   0   0   0   0   0
    84   22.0000    0.0000   0.0000   0   0   0   0   0   0   0   0   1
    85   24.0000   12.0000   0.0000   0   0   0   0   0   0   0   0   0
    91   24.0000    0.0000   0.0000   0   0   0   0   0   0   0   0   1
    92   26.0000   12.0000   0.0000   0   0   0   0   0   0   0   0   0
    98   26.0000    0.0000   0.0000   0   0   0   0   0   0   0   0   1
    99   28.0000   12.0000   0.0000   0   0   0   0   0   0   0   0   0
   105   28.0000    0.0000   0.0000   0   0   0   0   0   0   0   0   1
   106   30.0000   12.0000   0.0000   0   0   0   0   0   0   0   0   0
   112   30.0000    0.0000   0.0000   0   0   0   0   0   0   0   0   1
   119   32.0000    0.0000   0.0000   0   0   0   0   0   0   0   0   0
   120   34.0000   12.0000   0.0000   0   0   0   0   0   0   0   0   1
   126   34.0000    0.0000   0.0000   0   0   0   0   0   0   0   0   0
   127   36.0000   12.0000   0.0000   0   0   0   0   0   0   0   0   1
   133   36.0000    0.0000   0.0000   0   0   0   0   0   0   0   0   0
   134   38.0000   12.0000   0.0000   0   0   0   0   0   0   0   0   1
   140   38.0000    0.0000   0.0000   0   0   0   0   0   0   0   0   0
   141   40.0000   12.0000   0.0000   0   0   0   0   0   0   0   0   1
   147   40.0000    0.0000   0.0000   0   0   0   0   0   0   0   0   0
   148   42.0000   12.0000   0.0000   0   0   0   0   0   0   0   0   1
   154   42.0000    0.0000   0.0000   0   0   0   0   0   0   0   0   0
   155   44.0000   12.0000   0.0000   0   0   0   0   0   0   0   0   1
   162   46.0000   12.0000   0.0000   0   0   0   0   0   0   0   0   0
   168   46.0000    0.0000   0.0000   0   0   0   0   0   0   0   0   1
   169   48.0000   12.0000   0.0000   0   0   0   0   0   0   0   0   0
   175   48.0000    0.0000   0.0000   0   0   0   0   0   0   0   0   1
   176   50.0000   12.0000   0.0000   0   0   0   0   0   0   0   0   0
   182   50.0000    0.0000   0.0000   0   0   0   0   0   0   0   0   1
$  ELEMENT  CONNECTIVITY  CONDITIONS
     2    1    1    2    9    8   0   0   0   0   1   1   1   0   0   0
     2    6    6    7   14   13   0   0   0   0   1   1   1   0   0   1
     2    7    8    9   16   15   0   0   0   0   1   1   1   0   0   0
     2   12   13   14   21   20   0   0   0   0   1   1   1   0   0   1
     2   13   15   16   23   22   0   0   0   0   1   1   1   0   0   0
     2   18   20   21   28   27   0   0   0   0   1   1   1   0   0   1
     2   19   22   23   30   29   0   0   0   0   2   1   2   0   0   0
     2   24   27   28   35   34   0   0   0   0   2   1   2   0   0   1
     2   25   29   30   37   36   0   0   0   0   3   1   3   0   0   0
     2   30   34   35   42   41   0   0   0   0   3   1   3   0   0   1
     2   31   36   37   44   43   0   0   0   0   4   1   4   0   0   0
     2   36   41   42   49   48   0   0   0   0   4   1   4   0   0   1
     2   37   43   44   51   50   0   0   0   0   5   1   5   0   0   0
     2   42   48   49   56   55   0   0   0   0   5   1   5   0   0   1
     2   43   50   51   58   57   0   0   0   0   6   1   6   0   0   0
     2   48   55   56   63   62   0   0   0   0   6   1   6   0   0   1
     2   49   57   58   65   64   0   0   0   0   6   1   6   0   0   0
     2   54   62   63   70   69   0   0   0   0   6   1   6   0   0   1
     2   55   64   65   72   71   0   0   0   0   6   1   6   0   0   0
     2   60   69   70   77   76   0   0   0   0   6   1   6   0   0   1
     2   61   71   72   79   78   0   0   0   0   7   1   7   0   0   0
     2   66   76   77   84   83   0   0   0   0   7   1   7   0   0   1
     2   67   78   79   86   85   0   0   0   0   7   1   7   0   0   0
     2   72   83   84   91   90   0   0   0   0   7   1   7   0   0   1
     2   73   85   86   93   92   0   0   0   0   8   1   8   0   0   0
     2   78   90   91   98   97   0   0   0   0   8   1   8   0   0   1
     2   79   92   93  100   99   0   0   0   0   9   1   9   0   0   0
     2   84   97   98  105  104   0   0   0   0   9   1   9   0   0   1
```

```
   2   85   99  100  107  106    0    0    0    0    9    1    9    0    0    0
   2   90  104  105  112  111    0    0    0    0    9    1    9    0    0    1
   2   91  106  107  114  113    0    0    0    0   10    1   10    0    0    0
   2   96  111  112  119  118    0    0    0    0   10    1   10    0    0    1
   2   97  113  114  121  120    0    0    0    0   10    1   10    0    0    0
   2  102  118  119  126  125    0    0    0    0   10    1   10    0    0    1
   2  103  120  121  128  127    0    0    0    0   10    1   10    0    0    0
   2  108  125  126  133  132    0    0    0    0   10    1   10    0    0    1
   2  109  127  128  135  134    0    0    0    0   11    1   11    0    0    0
   2  114  132  133  140  139    0    0    0    0   11    1   11    0    0    1
   2  115  134  135  142  141    0    0    0    0   12    1   12    0    0    0
   2  120  139  140  147  146    0    0    0    0   12    1   12    0    0    1
   2  121  141  142  149  148    0    0    0    0   13    1   13    0    0    0
   2  126  146  147  154  153    0    0    0    0   13    1   13    0    0    1
   2  127  148  149  156  155    0    0    0    0   14    1   14    0    0    0
   2  132  153  154  161  160    0    0    0    0   14    1   14    0    0    1
   2  133  155  156  163  162    0    0    0    0   15    1   15    0    0    0
   2  138  160  161  168  167    0    0    0    0   15    1   15    0    0    1
   2  139  162  163  170  169    0    0    0    0   15    1   15    0    0    0
   2  144  167  168  175  174    0    0    0    0   15    1   15    0    0    1
   2  145  169  170  177  176    0    0    0    0   15    1   15    0    0    0
   2  150  174  175  182  181    0    0    0    0   15    1   15    0    0    1
$    SHELL  ELEMENT  THICKNESSES
    1    0.1900     0.0000     0.0000
$  MATERIAL  PROPERTIES
    1    1
9.909e+06       0.3205  12.9e-06 2.614e-04
    2    1
9.895e+06       0.3205  12.9e-06 2.614e-04
    3    1
9.872e+06       0.3205  12.9e-06 2.614e-04
    4    1
9.848e+06       0.3205  12.9e-06 2.614e-04
    5    1
9.832e+06       0.3205  12.9e-06 2.614e-04
    6    1
9.825e+06       0.3205  12.9e-06 2.614e-04
    7    1
9,813e+06       0.3205  12.9e-06 2.614e-04
    8    1
9.796e+06       0.3205  12.9e-06 2.614e-04
    9    1
9.793e+06       0.3205  12.9e-06 2.614e-04
   10    1
9.789e+06       0.3205  12.9e-06 2.614e-04
   11    1
9.780e+06       0.3205  12.9e-06 2.614e-04
   12    1
9.741e+06       0.3205  12.9e-06 2.614e-04
   13    1
9.677e+06       0.3205  12.9e-06 2.614e-04
   14    1
9.618e+06       0.3205  12.9e-06 2.614e-04
   15    1
9.565e+06       0.3205  12.9e-06 2.614e-04
$     TEMPERATURE   DATA
    1   37.4490          0.0        0.0     2   46.6670       0.0        0.0
    3   62.4640          0.0        0.0     4   79.2340       0.0        0.0
    5   89.9840          0.0        0.0     6   94.7030       0.0        0.0
    7  101.8660          0.0        0.0     8  109.8280       0.0        0.0
    9  111.3230          0.0        0.0    10  113.2400       0.0        0.0
   11  117.2770          0.0        0.0    12  135.4120       0.0        0.0
   13  164.4520          0.0        0.0    14  191.7370       0.0        0.0
   15  205.9110          0.0        0.0
$  NODAL   MASS   DATA
    1      1 1.792E-04     3
    4      1 1.792E-04     3
    7      1 1.792E-04     3
   36      1 1.792E-04     3
   39      1 1.792E-04     3
   42      1 1.792E-04     3
   71      1 1.792E-04     3
   74      1 1.792E-04     3
   77      1 1.792E-04     3
  106      1 1.792E-04     3
  109      1 1.792E-04     3
  112      1 1.792E-04     3
  141      1 1.792E-04     3
  144      1 1.792E-04     3
  147      1 1.792E-04     3
  176      1 1.792E-04     3
  179      1 1.792E-04     3
  182      1 1.792E-04     3
   -1
```

ORIGINAL PAGE IS
OF POOR QUALITY

STARS output summary - The results are printed in table 16.

Table 16. Natural frequencies of a rectangular free-free plate

Mode Number	Natural Frequencies, rad/sec			
	Quad Element		Triangular Element	
	Zero Temperature	Varying Temperature	Zero Temperature	Varying Temperature
1-6	0.00	0.00	0.00	0.00
7	91.11	90.42	87.60	87.17
8	217.28	213.98	211.08	208.83
9	250.38	248.31	241.36	239.56
10	445.35	440.89	433.49	428.85
11	488.57	487.77	472.26	471.35
12	693.44	695.54	677.19	678.29

4.13 Thermal Prestress Free-Free Vibration of Composite Square Plate

A composite square plate (fig. 21) subjected to temperature varying along x-axis was analyzed to yield natural freqencies and modes. The results of the vibration analysis are shown in table 17.

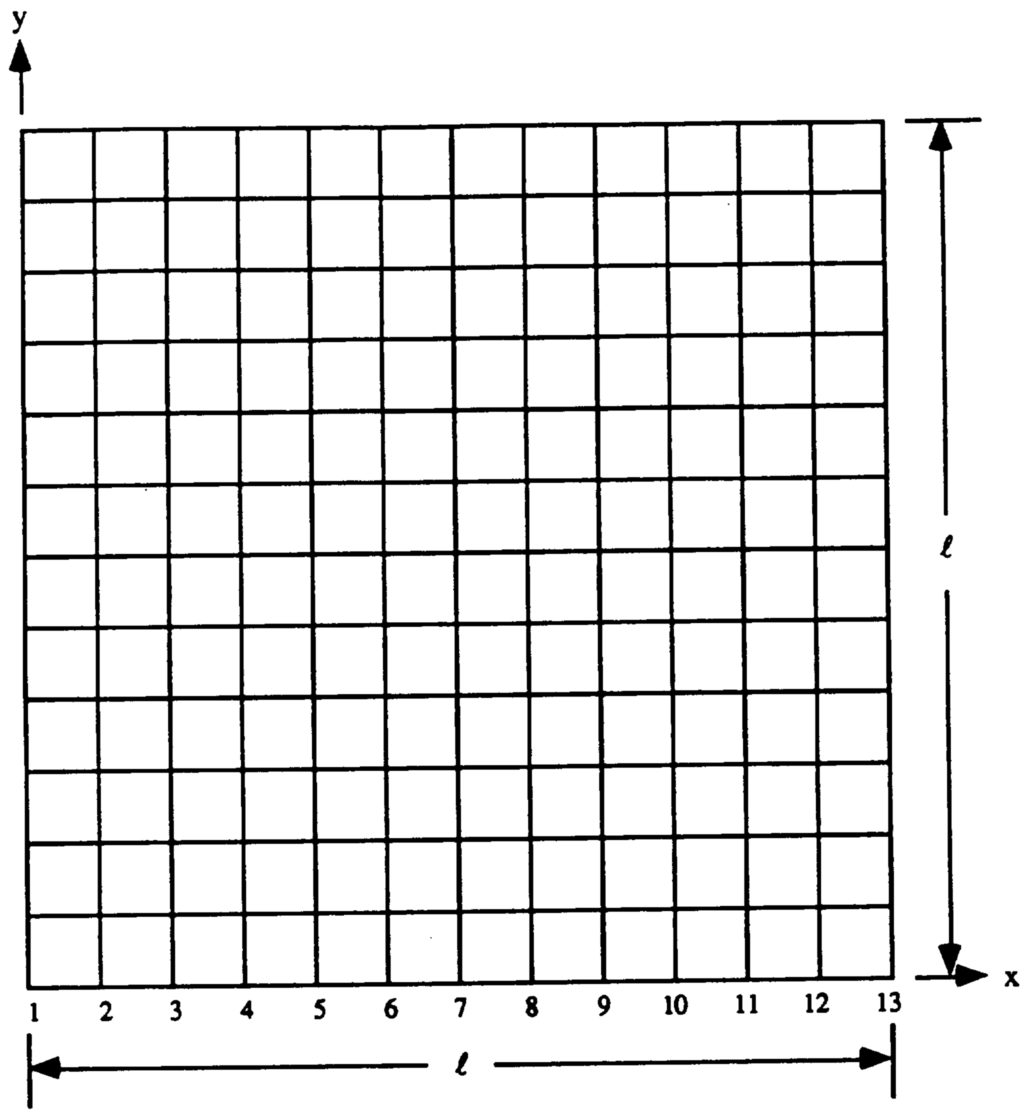

Figure 21. Free-free composite square plate.

Important data parameters:

Side length, ℓ	= 12
Plate thickness, t	= 0.24
Mass density, ρ	= 0.1475×10^{-3}
Composite stacking	= [30°/-30°/-30°/30°]

STARS input data:

```
SQUARE  12-BY-12  PLATE  /  COMPOSITE  LAYERS  /  temperature  I  case.
 169, 144,    1,  13,    0,    0,    0,    2,    1,     4
  12,    0,    0,    0,    0,    0,    0,    0,    0
   1,    1,    0,    1,    0,    0,    0,    0
   2,    0,    2,    0,    1,    0
   1,   12,    0,  6000.0,      0.0,         0.0
$  NODAL  DATA
     1    0.0000    0.0000    0.0000   0   0   0   0   0   0   0   0   0
    13   12.0000    0.0000    0.0000   0   0   0   0   0   0   0   0   1
    14    0.0000    1.0000    0.0000   0   0   0   0   0   0   0   0   0
    26   12.0000    1.0000    0.0000   0   0   0   0   0   0   0   0   1
    27    0.0000    2.0000    0.0000   0   0   0   0   0   0   0   0   0
    39   12.0000    2.0000    0.0000   0   0   0   0   0   0   0   0   1
    40    0.0000    3.0000    0.0000   0   0   0   0   0   0   0   0   0
    52   12.0000    3.0000    0.0000   0   0   0   0   0   0   0   0   1
    53    0.0000    4.0000    0.0000   0   0   0   0   0   0   0   0   0
    65   12.0000    4.0000    0.0000   0   0   0   0   0   0   0   0   1
    66    0.0000    5.0000    0.0000   0   0   0   0   0   0   0   0   0
    78   12.0000    5.0000    0.0000   0   0   0   0   0   0   0   0   1
    79    0.0000    6.0000    0.0000   0   0   0   0   0   0   0   0   0
    91   12.0000    6.0000    0.0000   0   0   0   0   0   0   0   0   1
    92    0.0000    7.0000    0.0000   0   0   0   0   0   0   0   0   0
   104   12.0000    7.0000    0.0000   0   0   0   0   0   0   0   0   1
   105    0.0000    8.0000    0.0000   0   0   0   0   0   0   0   0   0
   117   12.0000    8.0000    0.0000   0   0   0   0   0   0   0   0   1
   118    0.0000    9.0000    0.0000   0   0   0   0   0   0   0   0   0
   130   12.0000    9.0000    0.0000   0   0   0   0   0   0   0   0   1
   131    0.0000   10.0000    0.0000   0   0   0   0   0   0   0   0   0
   143   12.0000   10.0000    0.0000   0   0   0   0   0   0   0   0   1
   144    0.0000   11.0000    0.0000   0   0   0   0   0   0   0   0   0
   156   12.0000   11.0000    0.0000   0   0   0   0   0   0   0   0   1
   157    0.0000   12.0000    0.0000   0   0   0   0   0   0   0   0   0
   169   12.0000   12.0000    0.0000   0   0   0   0   0   0   0   0   1
$  ELEMENT  CONNECTIVITY
     6    1    1    2   15   14    0    0    0    1    1    0    1    0    0    0
     6    2    2    3   16   15    0    0    0    1    1    0    2    0    0    0
     6    3    3    4   17   16    0    0    0    1    1    0    3    0    0    0
     6    4    4    5   18   17    0    0    0    1    1    0    4    0    0    0
     6    5    5    6   19   18    0    0    0    1    1    0    5    0    0    0
     6    6    6    7   20   19    0    0    0    1    1    0    6    0    0    0
     6    7    7    8   21   20    0    0    0    1    1    0    7    0    0    0
     6    8    8    9   22   21    0    0    0    1    1    0    8    0    0    0
     6    9    9   10   23   22    0    0    0    1    1    0    9    0    0    0
     6   10   10   11   24   23    0    0    0    1    1    0   10    0    0    0
     6   11   11   12   25   24    0    0    0    1    1    0   11    0    0    0
     6   12   12   13   26   25    0    0    0    1    1    0   12    0    0    0
     6   13   14   15   28   27    0    0    0    1    1    0    1    0    0    0
     6   14   15   16   29   28    0    0    0    1    1    0    2    0    0    0
     6   15   16   17   30   29    0    0    0    1    1    0    3    0    0    0
     6   16   17   18   31   30    0    0    0    1    1    0    4    0    0    0
     6   17   18   19   32   31    0    0    0    1    1    0    5    0    0    0
     6   18   19   20   33   32    0    0    0    1    1    0    6    0    0    0
     6   19   20   21   34   33    0    0    0    1    1    0    7    0    0    0
     6   20   21   22   35   34    0    0    0    1    1    0    8    0    0    0
     6   21   22   23   36   35    0    0    0    1    1    0    9    0    0    0
     6   22   23   24   37   36    0    0    0    1    1    0    0    0    0    0
     6   23   24   25   38   37    0    0    0    1    1    0   11    0    0    0
     6   24   25   26   39   38    0    0    0    1    1    0   12    0    0    0
     6   25   27   28   41   40    0    0    0    1    1    0    1    0    0    0
     6   26   28   29   42   41    0    0    0    1    1    0    2    0    0    0
     6   27   29   30   43   42    0    0    0    1    1    0    3    0    0    0
     6   28   30   31   44   43    0    0    0    1    1    0    4    0    0    0
     6   29   31   32   45   44    0    0    0    1    1    0    5    0    0    0
     6   30   32   33   46   45    0    0    0    1    1    0    6    0    0    0
     6   31   33   34   47   46    0    0    0    1    1    0    7    0    0    0
     6   32   34   35   48   47    0    0    0    1    1    0    8    0    0    0
     6   33   35   36   49   48    0    0    0    1    1    0    9    0    0    0
     6   34   36   37   50   49    0    0    0    1    1    0   10    0    0    0
     6   35   37   38   51   50    0    0    0    1    1    0   11    0    0    0
     6   36   38   39   52   51    0    0    0    1    1    0   12    0    0    0
     6   37   40   41   54   53    0    0    0    1    1    0    1    0    0    0
     6   38   41   42   55   54    0    0    0    1    1    0    2    0    0    0
     6   39   42   43   56   55    0    0    0    1    1    0    3    0    0    0
     6   40   43   44   57   56    0    0    0    1    1    0    4    0    0    0
     6   41   44   45   58   57    0    0    0    1    1    0    5    0    0    0
     6   42   45   46   59   58    0    0    0    1    1    0    6    0    0    0
     6   43   46   47   60   59    0    0    0    1    1    0    7    0    0    0
     6   44   47   48   61   60    0    0    0    1    1    0    8    0    0    0
     6   45   48   49   62   61    0    0    0    1    1    0    9    0    0    0
     6   46   49   50   63   62    0    0    0    1    1    0   10    0    0    0
     6   47   50   51   64   63    0    0    0    1    1    0   11    0    0    0
     6   48   51   52   65   64    0    0    0    1    1    0   12    0    0    0
     6   49   53   54   67   66    0    0    0    1    1    0    1    0    0    0
     6   50   54   55   68   67    0    0    0    1    1    0    2    0    0    0
     6   51   55   56   69   68    0    0    0    1    1    0    3    0    0    0
```

6	52	56	57	70	69	0	0	0	1	1	0	4	0	0	0
6	53	57	58	71	70	0	0	0	1	1	0	5	0	0	0
6	54	58	59	72	71	0	0	0	1	1	0	6	0	0	0
6	55	59	60	73	72	0	0	0	1	1	0	7	0	0	0
6	56	60	61	74	73	0	0	0	1	1	0	8	0	0	0
6	57	61	62	75	74	0	0	0	1	1	0	9	0	0	0
6	58	62	63	76	75	0	0	0	1	1	0	10	0	0	0
6	59	63	64	77	76	0	0	0	1	1	0	11	0	0	0
6	60	64	65	78	77	0	0	0	1	1	0	12	0	0	0
6	61	66	67	80	79	0	0	0	1	1	0	1	0	0	0
6	62	67	68	81	80	0	0	0	1	1	0	2	0	0	0
6	63	68	69	82	81	0	0	0	1	1	0	3	0	0	0
6	64	69	70	83	82	0	0	0	1	1	0	4	0	0	0
6	65	70	71	84	83	0	0	0	1	1	0	5	0	0	0
6	66	71	72	85	84	0	0	0	1	1	0	6	0	0	0
6	67	72	73	86	85	0	0	0	1	1	0	7	0	0	0
6	68	73	74	87	86	0	0	0	1	1	0	8	0	0	0
6	69	74	75	88	87	0	0	0	1	1	0	9	0	0	0
6	70	75	76	89	88	0	0	0	1	1	0	10	0	0	0
6	71	76	77	90	89	0	0	0	1	1	0	11	0	0	0
6	72	77	78	91	90	0	0	0	1	1	0	12	0	0	0
6	73	79	80	93	92	0	0	0	1	1	0	1	0	0	0
6	74	80	81	94	93	0	0	0	1	1	0	2	0	0	0
6	75	81	82	95	94	0	0	0	1	1	0	3	0	0	0
6	76	82	83	96	95	0	0	0	1	1	0	4	0	0	0
6	77	83	84	97	96	0	0	0	1	1	0	5	0	0	0
6	78	84	85	98	97	0	0	0	1	1	0	6	0	0	0
6	79	85	86	99	98	0	0	0	1	1	0	7	0	0	0
6	80	86	87	100	99	0	0	0	1	1	0	8	0	0	0
6	81	87	88	101	100	0	0	0	1	1	0	9	0	0	0
6	82	88	89	102	101	0	0	0	1	1	0	10	0	0	0
6	83	89	90	103	102	0	0	0	1	1	0	11	0	0	0
6	84	90	91	104	103	0	0	0	1	1	0	12	0	0	0
6	85	92	93	106	105	0	0	0	1	1	0	1	0	0	0
6	86	93	94	107	106	0	0	0	1	1	0	2	0	0	0
6	87	94	95	108	107	0	0	0	1	1	0	3	0	0	0
6	88	95	96	109	108	0	0	0	1	1	0	4	0	0	0
6	89	96	97	110	109	0	0	0	1	1	0	5	0	0	0
6	90	97	98	111	110	0	0	0	1	1	0	6	0	0	0
6	91	98	99	112	111	0	0	0	1	1	0	7	0	0	0
6	92	99	100	113	112	0	0	0	1	1	0	8	0	0	0
6	93	100	101	114	113	0	0	0	1	1	0	9	0	0	0
6	94	101	102	115	114	0	0	0	1	1	0	10	0	0	0
6	95	102	103	116	115	0	0	0	1	1	0	11	0	0	0
6	96	103	104	117	116	0	0	0	1	1	0	12	0	0	0
6	97	105	106	119	118	0	0	0	1	1	0	1	0	0	0
6	98	106	107	120	119	0	0	0	1	1	0	2	0	0	0
6	99	107	108	121	120	0	0	0	1	1	0	3	0	0	0
6	100	108	109	122	121	0	0	0	1	1	0	4	0	0	0
6	101	109	110	123	122	0	0	0	1	1	0	5	0	0	0
6	102	110	111	124	123	0	0	0	1	1	0	6	0	0	0
6	103	111	112	125	124	0	0	0	1	1	0	7	0	0	0
6	104	112	113	126	125	0	0	0	1	1	0	8	0	0	0
6	105	113	114	127	126	0	0	0	1	1	0	9	0	0	0
6	106	114	115	128	127	0	0	0	1	1	0	10	0	0	0
6	107	115	116	129	128	0	0	0	1	1	0	11	0	0	0
6	108	116	117	130	129	0	0	0	1	1	0	12	0	0	0
6	109	118	119	132	131	0	0	0	1	1	0	1	0	0	0
6	110	119	120	133	132	0	0	0	1	1	0	2	0	0	0
6	111	120	121	134	133	0	0	0	1	1	0	3	0	0	0
6	112	121	122	135	134	0	0	0	1	1	0	4	0	0	0
6	113	122	123	136	135	0	0	0	1	1	0	5	0	0	0
6	114	123	124	137	136	0	0	0	1	1	0	6	0	0	0
6	115	124	125	138	137	0	0	0	1	1	0	7	0	0	0
6	116	125	126	139	138	0	0	0	1	1	0	8	0	0	0
6	117	126	127	140	139	0	0	0	1	1	0	9	0	0	0
6	118	127	128	141	140	0	0	0	1	1	0	10	0	0	0
6	119	128	129	142	141	0	0	0	1	1	0	11	0	0	0
6	120	129	130	143	142	0	0	0	1	1	0	12	0	0	0
6	121	131	132	145	144	0	0	0	1	1	0	1	0	0	0
6	122	132	133	146	145	0	0	0	1	1	0	2	0	0	0
6	123	133	134	147	146	0	0	0	1	1	0	3	0	0	0
6	124	134	135	148	147	0	0	0	1	1	0	4	0	0	0
6	125	135	136	149	148	0	0	0	1	1	0	5	0	0	0
6	126	136	137	150	149	0	0	0	1	1	0	6	0	0	0
6	127	137	138	151	150	0	0	0	1	1	0	7	0	0	0
6	128	138	139	152	151	0	0	0	1	1	0	8	0	0	0
6	129	139	140	153	152	0	0	0	1	1	0	9	0	0	0
6	130	140	141	154	153	0	0	0	1	1	0	10	0	0	0
6	131	141	142	155	154	0	0	0	1	1	0	11	0	0	0
6	132	142	143	156	155	0	0	0	1	1	0	12	0	0	0
6	133	144	145	158	157	0	0	0	1	1	0	1	0	0	0
6	134	145	146	159	158	0	0	0	1	1	0	2	0	0	0
6	135	146	147	160	159	0	0	0	1	1	0	3	0	0	0
6	136	147	148	161	160	0	0	0	1	1	0	4	0	0	0
6	137	148	149	162	161	0	0	0	1	1	0	5	0	0	0
6	138	149	150	163	162	0	0	0	1	1	0	6	0	0	0
6	139	150	151	164	163	0	0	0	1	1	0	7	0	0	0
6	140	151	152	165	164	0	0	0	1	1	0	8	0	0	0
6	141	152	153	166	165	0	0	0	1	1	0	9	0	0	0
6	142	153	154	167	166	0	0	0	1	1	0	10	0	0	0

```
    6  143  154  155  168  167    0    0    0    1    1    0   11    0    0   0
    6  144  155  156  169  168    0    0    0    1    1    0   12    0    0   0
$    COMPOSITE  SHELL  ELEMENT  STACK  DESCRIPTION  DATA
    1    4
    1      .0600    1
    1      .0600    2
    1      .0600    2
    1      .0600    1
$  SPECIFICATION  FOR  MATERIAL  AXIS  ORIENTATION
    1    2    0
    0.5236
    2    2    0
   2.61799
$  MATERIAL  PROPERTIES
    1    2
30.1169E+65,56559E+50.0000E+002.65029e+60,0000E+00T.8400e+057.8400E+05
0.0000E+007.8400E+050.2420E-050.1370E-040,0000E+000.1475E-03
$  ELEMENT  TEMPERATURE  DATA
    1    29.0278    0.0000    0.0000    2    81.8056    0.0000    0.0000
    3   124.0278    0.0000    0.0000    4   155.6945    0.0000    0.0000
    5   176.8056    0.0000    0.0000    6   187.3611    0.0000    0.0000
    7   187.3611    0.0000    0.0000    8   176.8056    0.0000    0.0000
    9   155.6944    0.0000    0.0000   10   124.0278    0.0000    0.0000
   11    81.8056    0.0000    0.0000   12    29.0278    0.0000    0.0000
```

STARS output summary - The results are printed in table 17.

Table 17. Natural frequencies of a free-free square composite plate

Mode Number	Natural Frequencies, rad/sec			
	Quad Element		Triangular Element	
	Zero Temperature	Varying Temperature	Zero Temperature	Varying Temperature
1-6	0.00	0.00	0.00	0.00
7	1367.30	1565.43	1320.18	1503.57
8	1651.18	1759.18	1584.41	1683.26
9	3618.14	3736.52	3506.99	3610.58
10	3847.03	3848.52	3702.82	3705.50
11	3955.95	4180.88	3858.03	4074.09
12	5812.83	5862.73	5630.24	5673.17

B. STARS-HEAT TRANSFER

In this section, the input data, as well as relevant outputs, of several typical heat transfer test cases are provided in some detail. The input data are prepared in accordance with the procedures described in section 3 and are defined in consistent unit form.

4.14 Cooling Fin: Convection Boundary Condition

A linear steady-state heat transfer analysis of a cooling fin (fig. 22) was performed utilizing heat transfer line elements. The results are given below.

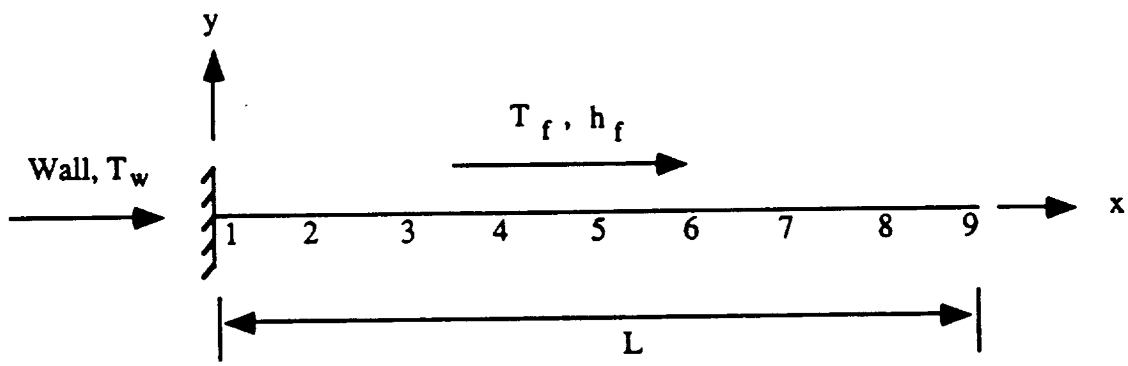

Figure 22. Cooling fin with convection

Important data parameters - Arbitrary available element and material properties data are utilized for the analysis to correlate results with existing ones expressed in parametric form.

Coefficient of conductivity, k	= 132.0
Convective heat transfer coefficient, h_f	= 1.6
Fluid temperature, T_f	= 70
Wall temperature, T_w	= 250
Length, L	= 1
Area, A	= 0.001365
Perimeter, P	= 0.13091
specific heat, c_p	= 0.2

STARS input data:

```
HEAT TRANSFER- TRUSS
10,8,1,11,1,0,0,0,0,0
0,0,0,1,1,0,0,0,0
10,0,0,1,0,0,0,0
2,0,1,0,0,0
$ NODAL DATA
   1      0.0       0.0       0.0    0    1    1    1    1    1
   2      0.125     0.0       0.0    0    1    1    1    1    1
   3      0.250     0.0       0.0    0    1    1    1    1    1
   4      0.375     0.0       0.0    0    1    1    1    1    1
   5      0.500     0.0       0.0    1    1    1    1    1    1
   6      0.625     0.0       0.0    0    1    1    1    1    1
   7      0.750     0.0       0.0    0    1    1    1    1    1
   8      0.875     0.0       0.0    0    1    1    1    1    1
   9      1.000     0.0       0.0    0    1    1    1    1    1
  10      0.0      50.0       0.0    1    1    1    1    1    1
$ ELEMENT CONNECTIVITY
   1    1    1    2   10    0    0    0    0    0    1    1    1
   1    2    2    3   10    0    0    0    0    0    1    1    1
   1    3    3    4   10    0    0    0    0    0    1    1    1
   1    4    4    5   10    0    0    0    0    0    1    1    1
   1    5    5    6   10    0    0    0    0    0    1    1    1
   1    6    6    7   10    0    0    0    0    0    1    1    1
   1    7    7    8   10    0    0    0    0    0    1    1    1
   1    8    8    9   10    0    0    0    0    0    1    1    1
$ LINE ELEMENT BASIC PROPERTIES
   1  0.001365  0. 13091
$ ELEMENT MATERIAL PROPERTIES
   1   6
  13.2E01      1.6       0      0.0      70.0      0.0      0.0
     0.0       0.0       0      0.0
$ DISPLACEMENT/TEMPERATURE BOUNDARY CONDITION DATA
   1    1    1    1      250.
```

STARS analysis results:

NODE EXT	NODE INT	TEM-SUR 1	TEM-SUR 2	TEM-SUR 3	TEM-SUR 4	TEM-SUR 5	TEM-SUR 6
1	1	0.250000E+03	0.000000E+00	0.000000E+00	0.000000E+00	0.000000E+00	0.000000E+00
2	2	0.232333E+03	0.000000E+00	0.000000E+00	0.000000E+00	0.000000E+00	0.000000E+00
3	3	0.217624E+03	0.000000E+00	0.000000E+00	0.000000E+00	0.000000E+00	0.000000E+00
4	4	0.205605E+03	0.000000E+00	0.000000E+00	0.000000E+00	0.000000E+00	0.000000E+00
5	5	0.196056E+03	0.000000E+00	0.000000E+00	0.000000E+00	0.000000E+00	0.000000E+00
6	6	0.188804E+03	0.000000E+00	0.000000E+00	0.000000E+00	0.000000E+00	0.000000E+00
7	7	0.183716E+03	0.000000E+00	0.000000E+00	0.000000E+00	0.000000E+00	0.000000E+00
8	8	0.180699E+03	0.000000E+00	0.000000E+00	0.000000E+00	0.000000E+00	0.000000E+00
9	9	0.179700E+03	0.000000E+00	0.000000E+00	0.000000E+00	0.000000E+00	0.000000E+00
10	10	0.000000E+00	0.000000E+00	0.000000E+00	0.000000E+00	0.000000E+00	0.000000E+00

4.15 Three-Dimensional Box: Specified Nodal Temperature

Figure 23 depicts a 3-D box which is characterized by orthotropic material. The results of a linear steady-state heat transfer analysis of the problem are presented herein.

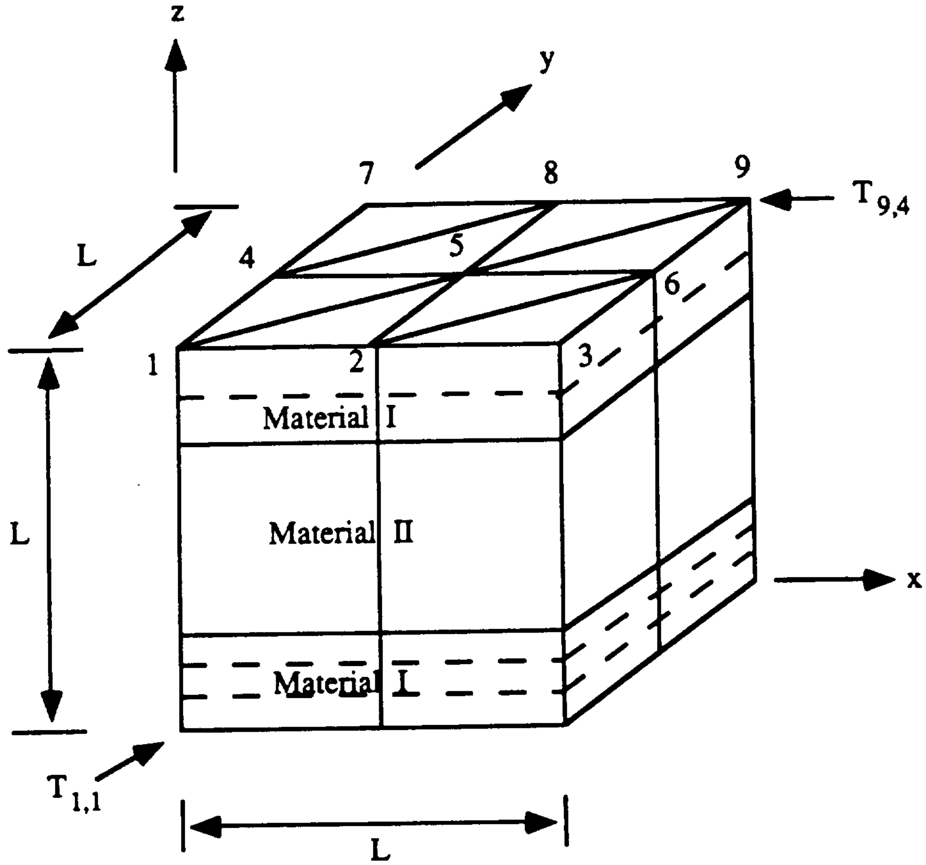

Figure 23. Three-dimensional box with conduction.

Important data parameters:

Length, L	= 1.0
Node temperature, $T_{1,1}$	= 500
Node temperature, $T_{9,4}$	= 0
Material I:	
Coefficients of conductivity, k	
k_{xx}	= 3.0
k_{yy}	= 1.0
k_{zz}	= 1.0
Thickness, t	= 0.3
Material II:	
Coefficients of conductivity, k	
k_{xx}	= 1.0
k_{yy}	= 3.0
k_{zz}	= 3.0
Thickness, t	= 0.4

STARS input data:

```
AN UNIT LENGTH FIRECLAY BRICK- 2X2 TRIANGLE MESH - HEAT TRANSFER -C2
9,8,2,44,0,0,0,2,1,6
0,0,0,1,2,0,0,0,0
10,0,0,1,0,0,0,0
2,0,2,0,1,0
$ NODAL DATA
    1   0. 0000    0. 0000     0 0000     0     0     0     0     1     1     0     0     0
    2   0. 5000    0. 0000     0 0000     0     0     0     0     1     1     0     0     0
    3   1. 0000    0. 0000     0 0000     0     0     0     0     1     1     0     0     0
    4   0. 0000    0. 5000     0 0000     0     0     0     0     1     1     0     0     0
    5   0. 5000    0. 5000     0 0000     0     0     0     0     1     1     0     0     0
    6   1. 0000    0. 5000     0 0000     0     0     0     0     1     1     0     0     0
    7   0. 0000    1. 0000     0 0000     0     0     0     0     1     1     0     0     0
    8   0. 5000    1. 0000     0 0000     0     0     0     0     1     1     0     0     0
    9   1. 0000    1. 0000     0 0000     0     0     0     0     1     1     0     0     0
$ ELEMENT CONNECTIVITY
    7     1     1     2     5     0     0     0     0     1     1     0     0     0     0
    7     2     5     4     1     0     0     0     0     1     1     0     0     0     0
    7     3     2     3     6     0     0     0     0     1     1     0     0     0     0
    7     4     6     5     2     0     0     0     0     1     1     0     0     0     0
    7     5     4     5     8     0     0     0     0     1     1     0     0     0     0
    7     6     8     7     4     0     0     0     0     1     1     0     0     0     0
    7     7     5     6     9     0     0     0     0     1     1     0     0     0     0
    7     8     9     8     5     0     0     0     0     1     1     0     0     0     0
$ COMPOSITE SHELL ELEMENT, STACKS SUBSTACKS DEFINITION
    1     6     3     3     1     2     0     0
    1     .30000     1
    2     .40000     1
    1     .30000     1
$ SPECIFICATION FOR MATERIAL AXES ORIENTATION
    1     2     0
      0.0
    2     2     0
     1.5708
$ ELEMENT MATERIAL PROPERTIES
    1     8
         3.          0.          1.          1.          0.          0.          0.
         0.          0.          0.          0.          0.          0.          0.
         0.          0.          0.          0.          0.          0.          0.
         0.          0.          0.          0.          0.          0.          0.
         0.          0.          0.          0.          0.          0.          0.
         0.          0.          0.          0.          0.          0.          0.
         0.          0.
    2     8
         1.          0.          3.          3.          0.          0.          0.
         0.          0.          0.          0.          0.          0.          0.
         0.          0.          0.          0.          0.          0.          0.
         0.          0.          0.          0.          0.          0.          0.
         0.          0.          0.          0.          0.          0.          0.
         0.          0.          0.          0.          0.          0.          0.
         0.          0.
$ DISPLACEMENT BOUNDARY CONDITION DATA
    1     1     1     1          500.
    9     4     9     4          0.
```

STARS analysis results:

NODE EXT	NODE INT	TEM-SUR 1	TEM-SUR 2	TEM-SUR 3	TEM-SUR 4	TEM-SUR 5	TEM-SUR 6
1	1	0.500000E+03	0.224775E+03	0.212283E+03	0.200333E+03	0.000000E+00	0.000000E+00
2	2	0.267260E+03	0.223166E+03	0.207237E+03	0.199651E+03	0.000000E+00	0.000000E+00
3	3	0.232398E+03	0.211402E+03	0.203162E+03	0.197953E+03	0.000000E+00	0.000000E+00
4	4	0.205148E+03	0.208393E+03	0.196695E+03	0.196979E+03	0.000000E+00	0.000000E+00
5	5	0.185295E+03	0.202975E+03	0.188997E+03	0.199701E+03	0.000000E+00	0.000000E+00
6	6	0.189722E+03	0.193493E+03	0.185473E+03	0.187941E+03	0.000000E+00	0.000000E+00
7	7	0.193992E+03	0.186909E+03	0.178882E+03	0.164663E+03	0.000000E+00	0.000000E+00
8	8	0.191341E+03	0.181805E+03	0.169013E+03	0.142837E+03	0.000000E+00	0.000000E+00
9	9	0.190919E+03	0.176588E+03	0.169369E+03	0.000000E+00	0.000000E+00	0.000000E+00

ORIGINAL PAGE IS
OF POOR QUALITY

4.16 Square Plate: Transient Heating

A heat transfer analysis of a square plate with transient internal heating, heat flow, and convective heating was performed. The results are presented here.

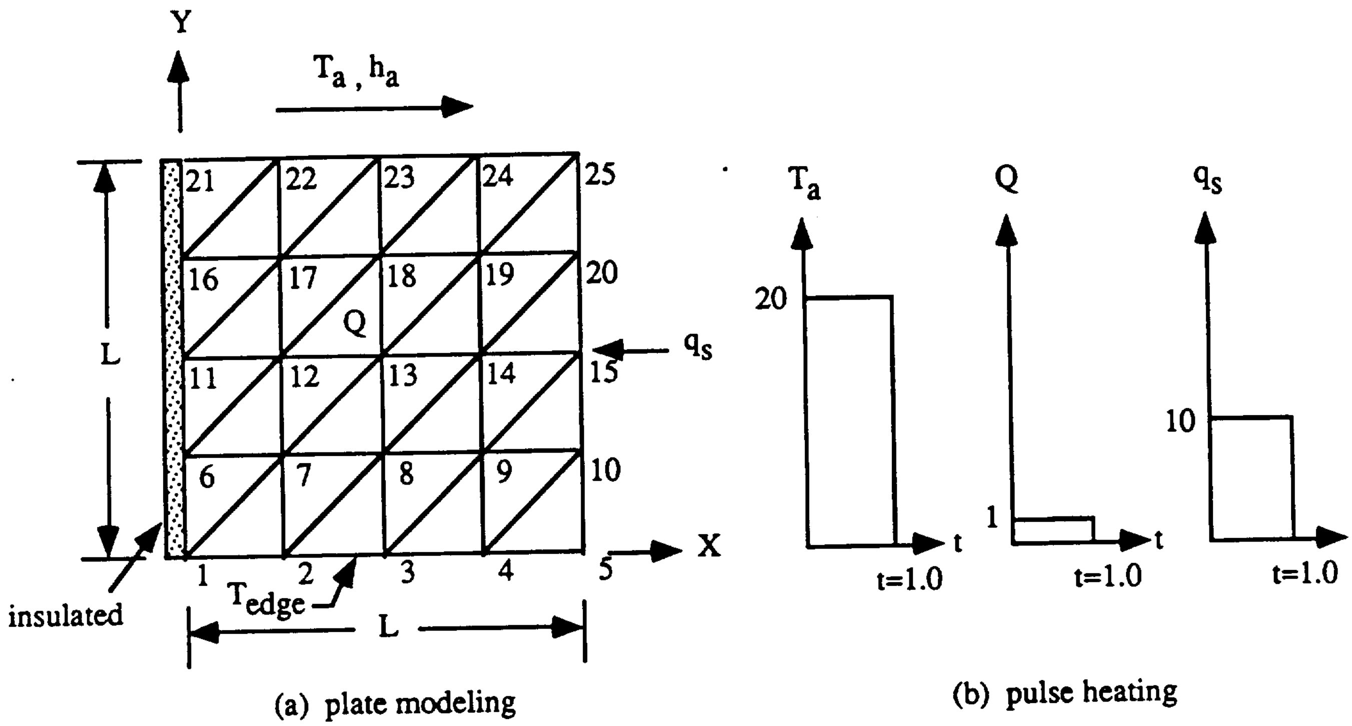

Figure 24. Square plate with transient heating.

Important data parameters:

Coefficient of conductivity, k	= 1.0
Internal heat generation rate, Q	= 1.0
Surface heat flow rate, qs	= 10.0
Convective heat transfer coefficient, h_a	= 3.0
Air temperature, T_a	= 20
Edge temperature, T_{edge}	= 10
Length, L	= 1
Thickness, t	= 0.1
Time step, Δt	= 0.05
Total time period for response	= 4.0

STARS input data:

```
SHELL-4x4- Isotropic plate - Transient heat loading
25,32,2,44,0,0,0,1,2,1
0,0,0,2,10,0,0,0,0
10,0,1,1,0,0,0,0
2,0,2,0,1,0
2,20,0,1675. ,3.0,0.0
0,1,2,2
$ NODAL DATA
    1    0.000    0.000    0.000   0   0   1   1   1   1   0   0   0
    2    0.250    0.000    0.000   0   0   1   1   1   1   0   0   0
    3    0.500    0.000    0.000   0   0   1   1   1   1   0   0   0
    4    0.750    0.000    0.000   0   0   1   1   1   1   0   0   0
    5    1.000    0.000    0.000   0   0   1   1   1   1   0   0   0
    6    0.000    0.250    0.000   0   0   1   1   1   1   0   0   0
    7    0.250    0.250    0.000   0   0   1   1   1   1   0   0   0
    8    0.000    0.250    0.000   0   0   1   1   1   1   0   0   0
    9    0.750    0.250    0.000   0   0   1   1   1   1   0   0   0
   10    1.000    0.250    0.000   0   0   1   1   1   1   0   0   0
   11    0.000    0.500    0.000   0   0   1   1   1   1   0   0   0
   12    0.250    0.500    0.000   0   0   1   1   1   1   0   0   0
   13    0.500    0.500    0.000   0   0   1   1   1   1   0   0   0
   14    0.750    0.500    0.000   0   0   1   1   1   1   0   0   0
   15    1.000    0.500    0.000   0   0   1   1   1   1   0   0   0
   16    0.000    0.750    0.000   0   0   1   1   1   1   0   0   0
   17    0.250    0.750    0.000   0   0   1   1   1   1   0   0   0
   18    0.500    0.750    0.000   0   0   1   1   1   1   0   0   0
   19    0.750    0.750    0.000   0   0   1   1   1   1   0   0   0
   20    1.000    0.750    0.000   0   0   1   1   1   1   0   0   0
   21    0.000    1.000    0.000   0   0   1   1   1   1   0   0   0
   22    0.250    1.000    0.000   0   0   1   1   1   1   0   0   0
   23    0.000    1.000    0.000   0   0   1   1   1   1   0   0   0
   24    0.750    1.000    0.000   0   0   1   1   1   1   0   0   0
   25    1.000    1.000    0.000   0   0   1   1   1   1   0   0   0
$ ELEMENT CONNECTIVITY CONDITIONS
    7   1    1    7    6   0   0   0   0   1   1   0   0   0   0   0
    7   2    7    1    2   0   0   0   0   1   1   0   0   0   0   0
    7   3    2    8    7   0   0   0   0   1   1   0   0   0   0   0
    7   4    8    2    3   0   0   0   0   1   1   0   0   0   0   0
    7   5    3    9    8   0   0   0   0   1   1   0   0   0   0   0
    7   6    9    3    4   0   0   0   0   1   1   0   0   0   0   0
    7   7    4   10    9   0   0   0   0   1   1   0   0   0   0   0
    7   8   10    4    5   0   0   0   0   1   1   0   0   0   0   0
    7   9    6   12   11   0   0   0   0   1   1   0   0   0   0   0
    7  10   12    6    7   0   0   0   0   1   1   0   0   0   0   0
    7  11    7   13   12   0   0   0   0   1   1   0   0   0   0   0
    7  12   13    7    8   0   0   0   0   1   1   0   0   0   0   0
    7  13    8   14   13   0   0   0   0   1   1   0   0   0   0   0
    7  14   14    8    9   0   0   0   0   1   1   0   0   0   0   0
    7  15    9   15   14   0   0   0   0   1   1   0   0   0   0   0
    7  16   15    9   10   0   0   0   0   1   1   0   0   0   0   0
    7  17   11   17   16   0   0   0   0   1   1   0   0   0   0   0
    7  18   17   11   12   0   0   0   0   1   1   0   0   0   0   0
    7  19   12   18   17   0   0   0   0   1   1   0   0   0   0   0
    7  20   18   12   13   0   0   0   0   1   1   0   0   0   0   0
    7  21   13   19   18   0   0   0   0   1   1   0   0   0   0   0
    7  22   19   13   14   0   0   0   0   1   1   0   0   0   0   0
    7  23   14   20   19   0   0   0   0   1   1   0   0   0   0   0
    7  24   20   14   15   0   0   0   0   1   1   0   0   0   0   0
    7  25   16   22   21   0   0   0   0   2   1   0   0   0   0   0
    7  26   22   16   17   0   0   0   0   1   1   0   0   0   0   0
    7  27   17   23   22   0   0   0   0   2   1   0   0   0   0   0
    7  28   23   17   18   0   0   0   0   1   1   0   0   0   0   0
    7  29   18   24   23   0   0   0   0   2   1   0   0   0   0   0
    7  30   24   18   19   0   0   0   0   1   1   0   0   0   0   0
    7  31   19   25   24   0   0   0   0   2   1   0   0   0   0   0
    7  32   25   19   20   0   0   0   0   1   1   0   0   0   0   0
$ COMPOSITE SHELL ELEMENT

    1    1     1    1    0    0    0    0
    1    0.1000     1
    2    1     1    1    0    0    0    0
    2    0.1000     1
$ SPECIFICATION FOR MATERIAL AXES ORIENTATION
    1    2    0
       0.0
$ ELEMENT MATERIAL PROPERTIES
    1    8
         1.       0.       1.       1.       0.       0.       0.
         0.       0.       0.       0.       0.       0.       0.
         0.       0.       0.       0.       0.       0.       0.
         0.       0.       0.       0.       0.       0.       0.
         0.       0.       0.       0.       0.       0.       0.
         0.       0.       0.       0.       0.       0.       0.
         1.       1.
    2    8
         1.       0.       1.       1.       0.       3.       0.
         0.       0.       0.       0.       0.       0.       0.
         0.       0.       0.       0.       0.       0.       0.
         0.       0.       0.       0.       0.       0.       0.
```


C-2

ORIGINAL PAGE IS
OF POOR QUALITY

```
        0.       0.       0.       0.       0.       0.       0.
        0.       0.       0.       0.       0.       0.       0.
        1.       1.
$ TEMPERATURE BOUNDARY CONDITION DATA
    1    1    1    1        10.
    1    2    1    2        10.
    2    1    2    1        10.
    2    2    2    2        10.
    3    1    3    1        10.
    3    2    3    2        10.
    4    1    4    1        10.
    4    2    4    2        10.
    5    1    5    1        10.
    5    2    5    2        10.
$ NODAL FORCE ACCELERATION/ELEMENT HEAT TRANSFER DATA
             1.0
    1    1       10.       0.0       0.0
    2    1       10.       0.0       0.0
    3    1       10.       0.0       0.0
    4    1       10.       0.0       0.0
    5    1       10.       0.0       0.0
    6    1       10.       0.0       0.0
    7    1       10.       0.0       0.0
    8    3       10.      10.0       0.0
    9    1       10.       0.0       0.0
   10    1       10.       0.0       0.0
   11    1       10.       0.0       0.0
   12    1       10.       0.0       0.0
   13    1       10.       0.0       0.0
   14    1       10.       0.0       0.0
   15    1       10.       0.0       0.0
   16    3       10.      10.0       0.0
   17    1       10.       0.0       0.0
   18    1       10.       0.0       0.0
   19    1       10.       0.0       0.0
   20    1       10.       0.0       0.0
   21    1       10.       0.0       0.0
   22    1       10.       0.0       0.0
   23    1       10.       0.0       0.0
   24    3       10.      10.0       0.0
   25    2       10.       0.0      20.0
   26    1       10.       0.0       0.0
   27    2       10.       0.0      20.0
   28    1       10.       0.0       0.0
   29    2       10.       0.0      20.0
   30    1       10.       0.0       0.0
   31    2       10.       0.0      20.0
   32    3       10.      10.0       0.0
   -1
            3.0
   -1
$ INCREMENTAL TIME DATA FOR DYNAMIC RESPONSE ANALYSIS
           0.05    20
           0.05    60
```

STARS output summary - The results are presented in table 18.

Table 18. Heat transfer analysis results of a square plate with transient heating.

Node	STARS Temperature	
	Time = 1.0	Time = 4.0
1	10.0000	10.0000
2	10.0000	10.0000
3	10.0000	10.0000
4	10.0000	10.0000
5	10.0000	10.0000
6	12.4690	8.1250
7	12.5664	8.1250
8	12.8989	8.1250
9	13.6243	8.1250
10	15.1492	8.1250
11	14.6929	6.2500
12	14.8433	6.2500
13	15.3527	6.2500
14	16.3961	6.2500
15	18.2922	6.2500
16	16.5640	4.3750
17	16.7172	4.3750
18	17.2233	4.3750
19	18.2667	4.3750
20	20.1821	4.3750
21	18.0920	2.5000
22	18.1862	2.5000
23	18.5102	2.5000
24	19.2220	2.5000
25	20.8517	2.5000

4.17 Composite Square Plate: Transient Heating

This problem repeats problem 4.16 with composite material and the solution results are given below.

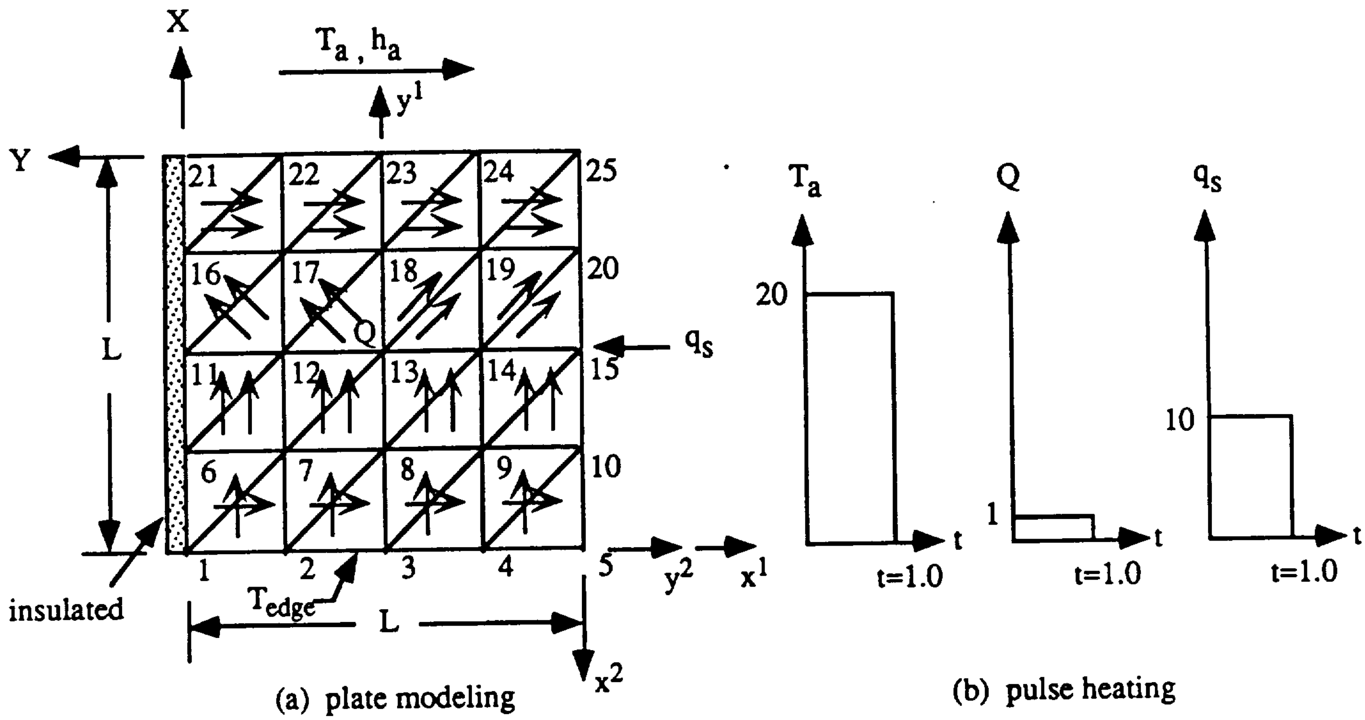

Figure 25. Composite square plate with transient heating.

Important data parameters:

Coefficient of conductivity, k_x	= 3.0
Coefficient of conductivity, k_y	= 1.0
Coefficient of conductivity, k_z	= 1.0
Internal heat generation rate, Q	= 1.0
Heat flow rate, qs	= 10.0
Convective heat transfer coefficient, h_a	= 3.0
Air temperature, T_a	= 20
Edge temperature, T_{edge}	= 10
Length, L	= 1
Thickness, t of each layer	= 0.0315
Time step, Δt	= 0.05
Total time period for response	= 4.0

STARS input data:

```
SHELL-4x4- composite element- Transient heat loading
25,32,2,44,0,0,2,4,6,2
0,0,0,2,10,0,0,0,0
10,0,1,1,0,0,0,0
2,0,2,0,1,0
2,20,0,1675. ,3.0,0.0
0,1,2,2
$ NODAL DATA
   1      -0.5       0.0      0.0   0   0   0   0   0   0   1   0   0
   5       0.5       0.0      0.0   0   0   0   0   0   0   1   0   1
   6      -0.25     -1.0      0.0   0   0   0   0   0   0   2   0   0
  10      -0.25      0.0      0.0   0   0   0   0   0   0   2   0   1
  11      -0.5       0.5      0.0   0   0   0   0   0   0   1   0   0
  15       0.5       0.5      0.0   0   0   0   0   0   0   1   0   1
  16      -0.25      0.0      0.0   0   0   0   0   0   0   0   0   0
  20      -0.25     -1.0      0.0   0   0   0   0   0   0   0   0   1
  21      -0.5       1.0      0.0   0   0   0   0   0   0   1   0   0
  25       0.5       1.0      0.0   0   0   0   0   0   0   1   0   1
$ LOCAL-GLOBAL COORDINATE SYSTEM DATA
   1   2
     -1.0      -0.5      0.0      0.0      -1.0      0.0
      1.0       0.0      0.0      0.0       0.0      1.0
   2   1
     -1.0      -1.0      0.0     -1.5      -1.0      0.0
     -1.5      -1.5      0.0
$ ELEMENT CONNECTIVITY CONDITIONS
   7   1   7   6   1   0   0   0   0   1   1   0   0   0   0   0
   7   2   1   2   7   0   0   0   0   1   1   0   0   0   0   0
   7   3   8   7   2   0   0   0   0   1   1   0   0   0   0   0
   7   4   2   3   8   0   0   0   0   1   1   0   0   0   0   0
   7   5   9   8   3   0   0   0   0   1   1   0   0   0   0   0
   7   6   3   4   9   0   0   0   0   1   1   0   0   0   0   0
   7   7  10   9   4   0   0   0   0   1   1   0   0   0   0   0
   7   8   4   5  10   0   0   0   0   1   1   0   0   0   0   0
   7   9  12  11   6   0   0   0   0   2   1   0   0   0   0   0
   7  10   6   7  12   0   0   0   0   2   1   0   0   0   0   0
   7  11  13  12   7   0   0   0   0   2   1   0   0   0   0   0
   7  12   7   8  13   0   0   0   0   2   1   0   0   0   0   0
   7  13  14  13   8   0   0   0   0   2   1   0   0   0   0   0
   7  14   8   9  14   0   0   0   0   2   1   0   0   0   0   0
   7  15  15  14   9   0   0   0   0   2   1   0   0   0   0   0
   7  16   9  10  15   0   0   0   0   2   1   0   0   0   0   0
   7  17  17  16  11   0   0   0   0   3   1   0   0   0   0   0
   7  18  11  12  17   0   0   0   0   3   1   0   0   0   0   0
   7  19  18  17  12   0   0   0   0   3   1   0   0   0   0   0
   7  20  12  13  18   0   0   0   0   3   1   0   0   0   0   0
   7  21  19  18  13   0   0   0   0   4   1   0   0   0   0   0
   7  22  13  14  19   0   0   0   0   4   1   0   0   0   0   0
   7  23  20  19  14   0   0   0   0   4   1   0   0   0   0   0
   7  24  14  15  20   0   0   0   0   4   1   0   0   0   0   0
   7  25  22  21  16   0   0   0   0   5   1   0   0   0   0   0
   7  26  16  17  22   0   0   0   0   6   1   0   0   0   0   0
   7  27  23  22  17   0   0   0   0   5   1   0   0   0   0   0
   7  28  17  18  23   0   0   0   0   6   1   0   0   0   0   0
   7  29  24  23  18   0   0   0   0   5   1   0   0   0   0   0
   7  30  18  19  24   0   0   0   0   6   1   0   0   0   0   0
   7  31  25  24  19   0   0   0   0   5   1   0   0   0   0   0
   7  32  19  20  25   0   0   0   0   6   1   0   0   0   0   0
$ COMPOSITE SHELL ELEMENENT
   1   2   1   2   0   0   0   0
   1    0.0315   3
   1    0.0315   1
   2   2   1   2   0   0   0   0
   1    0.0315   3
   1    0.0315   3
   3   2   1   2   0   0   0   0
   1    0.0315   4
   1    0.0315   4
   4   2   1   2   0   0   0   0
   1    0.0315   2
   1    0.0315   2
   5   2   1   2   0   0   0   0
   2    0.0315   1
   2    0.0315   1
   6   2   1   2   0   0   0   0
   1    0.0315   1
   1    0.0315   1
$ SPECIFICATION FOR MATERIAL AXIS ORIENTATION
   1   2   0
     0.0
   2   2   0
   0.7854
   3   2   0
   1.5708
   4   2   0
   2.3562
$ ELEMENT MATERIAL PROPERTIES
   1   8
     3.      0.      1.      1.      0.      0.      0.
```

```
          0.        0.        0.        0.        0.        0.        0.
          0.        0.        0.        0.        0.        0.        0.
          0.        0.        0.        0.        0.        0.        0.
          0.        0.        0.        0.        0.        0.        0.
          0.        0.        0.        0.        0.        0.        0.
          1.        1.
     2    8
          3.        0.        1.        1.        3.        0.        0.
          0.        0.        0.        0.        0.        0.        0.
          0.        0.        0.        0.        0.        0.        0.
          0.        0.        0.        0.        0.        0.        0.
          0.        0.        0.        0.        0.        0.        0.
          0.        0.        0.        0.        0.        0.        0.
          1.        1.
$ TEMPERATURE BOUNDARY CONDITION DATA
    1    1    1    1        10.
    1    2    1    2        10.
    2    1    2    1        10.
    2    2    2    2        10.
    3    1    3    1        10.
    3    2    3    2        10.
    4    1    4    1        10.
    4    2    4    2        10.
    5    1    5    1        10.
    5    2    5    2        10.
$ NODAL FORCE ACCELERATION/ELEMENT HEAT TRANSFER DATA
               1.0
    1    1         1.0       0.0       0.0
    2    1         1.0       0.0       0.0
    3    1         1.0       0.0       0.0
    4    1         1.0       0.0       0.0
    5    1         1.0       0.0       0.0
    6    1         1.0       0.0       0.0
    7    1         1.0       0.0       0.0
    8    2         1.0      10.0       0.0
    9    1         1.0       0.0       0.0
   10    1         1.0       0.0       0.0
   11    1         1.0       0.0       0.0
   12    1         1.0       0.0       0.0
   13    1         1.0       0.0       0.0
   14    1         1.0       0.0       0.0
   15    1         1.0       0.0       0.0
   16    2         1.0      10.0       0.0
   17    1         1.0       0.0       0.0
   18    1         1.0       0.0       0.0
   19    1         1.0       0.0       0.0
   20    1         1.0       0.0       0.0
   21    1         1.0       0.0       0.0
   22    1         1.0       0.0       0.0
   23    1         1.0       0.0       0.0
   24    2         1.0      10.0       0.0
   25    1         1.0       0.0      20.0
   26    1         1.0       0.0       0.0
   27    1         1.0       0.0      20.0
   28    1         1.0       0.0       0.0
   29    1         1.0       0.0      20.0
   30    1         1.0       0.0       0.0
   31    1         1.0       0.0      20.0
   32    2         1.0      10.0       0.0
   -1
               3.0
   -1
$ INCREMENTAL TIME DATA FOR DYNAMIC RESPONSE ANALYSIS
              0.05   20
              0.05   60
```

ORIGINAL PAGE IS
OF POOR QUALITY

Stars output summary - The results are presented in table 19

Table 19. Heat transfer analysis results of a composite square plate with transient heating

Node	STARS Temperature			
	t = 1.0		t = 4.0	
	Top	Bottom	Top	Bottom
1	10.0000	10.0000	10.0000	10.0000
2	10.0000	10.0000	10.0000	10.0000
3	10.0000	10.0000	10.0000	10.0000
4	10.0000	10.0000	10.0000	10.0000
5	10.0000	10.0000	10.0000	10.0000
6	12.5037	12.5103	8.0513	8.1142
7	12.5385	12.3414	8.2472	8.1441
8	12.6449	12.4654	8.3309	8.2436
9	13.0012	12.8188	8.4125	8.3416
10	13.8822	13.5101	8.5948	8.3604
11	13.8530	13.8371	6.9806	6.9805
12	13.7527	13.7943	7.1628	7.1481
13	13.9433	14.0115	7.2812	7.2947
14	14.4623	14.5265	7.4240	7.4281
15	15.4407	15.5770	7.5933	7.6121
16	15.3201	15.3235	5.5602	5.5597
17	15.1751	15.1724	5.7778	5.7801
18	15.2787	15.2635	5.9395	5.9397
19	16.6449	15.6294	6.0931	6.0906
20	16.3318	16.2958	6.2942	6.2905
21	17.3489	17.3478	3.2628	3.2632
22	17.3476	17.3470	3.3180	3.3176
23	17.4610	17.4654	3.3926	3.3919
24	17.7651	17.7719	3.4641	3.4646
25	18.3725	18.3864	3.5144	3.5163

4.18 Cooling Fin: Radiation Boundary Condition

A non-linear steady state radiation analysis of a cooling fin (fig. 26) was performed utilizing heat transfer line element. The results are given below.

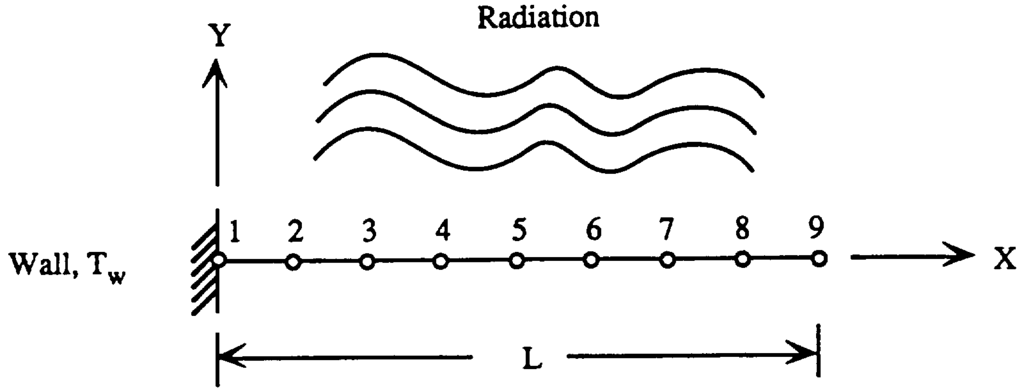

Figure 26. Cooling fin with radiation.

Important data parameters:

Coefficient of conductivity, k	= 132.0
Wall temperature, T_W	= 1500
Length, L	= 1
Area, A	= 0.001365
Stefan-Boltzmann constant, σ	= 0.1713×10^{-8}
Emissivety, ε	= 0.6

STARS input data:

```
RADIATION HEAT TRANSFER- TRUSS
10,8,1,11,1,0,0,0,0,0
0,0,0,1,1,0,0,0,0
10,0,0,1,0,0,0,0
2,0,1,0,0,0
$ NODAL DATA
    1       0.0        0.0        0.0    0    1    1    1    1    1
    2     0.125        0.0        0.0    0    1    1    1    1    1
    3     0.250        0.0        0.0    0    1    1    1    1    1
    4     0.375        0.0        0.0    0    1    1    1    1    1
    5     0.500        0.0        0.0    0    1    1    1    1    1
    6     0.625        0.0        0.0    0    1    1    1    1    1
    7     0.750        0.0        0.0    0    1    1    1    1    1
    8     0.875        0.0        0.0    0    1    1    1    1    1
    9     1.000        0.0        0.0    0    1    1    1    1    1
   10       0.0       50.0        0.0    1    1    1    1    1    1
$ ELEMENT CONNECTIVITY
    1    1    1    2   10    0    0    0    0    0    1    1    1
    1    2    2    3   10    0    0    0    0    0    1    1    1
    1    3    3    4   10    0    0    0    0    0    1    1    1
    1    4    4    5   10    0    0    0    0    0    1    1    1
    1    5    5    6   10    0    0    0    0    0    1    1    1
    1    6    6    7   10    0    0    0    0    0    1    1    1
    1    7    7    8   10    0    0    0    0    0    1    1    1
    1    8    8    9   10    0    0    0    0    0    1    1    1
$ LINE ELEMENT BASIC PROPERTIES
    1   0.001365   0. 13091
$ ELEMENT MATERIAL PROPERTIES
    1    6
      10.5        0.0        0        0.0        0.0        0.0  0.1713E-8
       0.6        0.0        0        0.0
$ DISPLACEMENT/TEMPERATURE BOUNDARY CONDITION DATA
    1    1    1    1      1500.
```

STARS ANALYSIS RESULTS:

NODAL TEMPERATURE

NODE EXT	NODE INT	TEM-SUR 1	TEM-SUR 2	TEM-SUR 3	TEM-SUR 4	TEM-SUR 5	TEM-SUR 6
1	1	.150000E+04	.000000E+00	.000000E+00	.000000E+00	.000000E+00	.000000E+00
2	2	.105848E+04	.000000E+00	.000000E+00	.000000E+00	.000000E+00	.000000E+00
3	3	.850319E+03	.000000E+00	.000000E+00	.000000E+00	.000000E+00	.000000E+00
4	4	.727245E+03	.000000E+00	.000000E+00	.000000E+00	.000000E+00	.000000E+00
5	5	.647702E+03	.000000E+00	.000000E+00	000000E+00	.000000E+00	.000000E+00
6	6	.594974E+03	.000000E+00	.000000E+00	000000E+00	.000000E+00	.000000E+00
7	7	.561119E+03	.000000E+00	.000000E+00	000000E+00	.000000E+00	.000000E+00
8	8	.542098E+03	.000000E+00	.000000E+00	000000E+00	.000000E+00	.000000E+00
9	9	.535953E+03	.000000E+00	.000000E+00	000000E+00	.000000E+00	.000000E+00
10	10	.000000E+00	.000000E+00	.000000E+00	000000E+00	.000000E+00	.000000E+00

4.19 Three Dimensional Box: Radiation Boundary Condition

Figure 27 depicts a 3-D box which is characterized by orthotropic material. The results of a nonlinear steady-state radiation heat transfer analysis of the problem are presented herein.

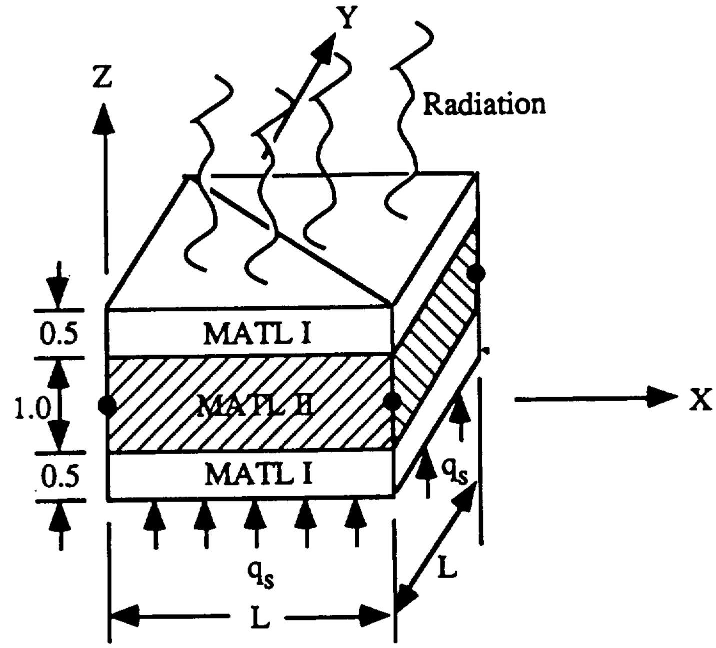

Figure 27. Three dimensional box with radiation.

Important dat parameters:

Length, L = 1.0
Stefan-Boltzmann constant, σ = $0.1713\text{x}10^{-8}$
Emissivity, ε = 0.6

Material I:
Coefficient of conductivity, k
k_{xx} = 10.5
k_{yy} = 10.5
k_{zz} = 10.5
thickness, t = 0.5

Material II:
Coefficient of conductivity, k
k_{xx} = 2.1
k_{yy} = 2.1
k_{zz} = 2.1
thickness, t = 1.0

STARS input data

```
RADIATION HEAT TRANSFER-COMPOSITE BOX
4,2,3,44,0,0,0,1,1,3
1,0,0,1,0,0,0,0,0
10,0,0,1,0,0,0,0
2,0,2,0,1,0
$ NODAL  DATA
   1    0.0000     0.0000     0.0000   0    0    0    0    1    1    0    0    0
   2    2.0000     0.0000     0.0000   0    0    0    0    1    1    0    0    0
   3    0.0000     2.0000     0.0000   0    0    0    0    1    1    0    0    0
   4    2.0000     2.0000     0.0000   0    0    0    0    1    1    0    0    0
$  ELEMENT CONNECTIVITY
   7    1    1    2    3    0    0    0    0    1    1    0    0    0    0
   7    2    4    3    2    0    0    0    0    1    1    0    0    0    0
$  COMPOSITE SHELL ELEMENT
   1    3    3    1    1    1    0    0
   3    .50000   1
   2    1.0000   1
   1    .50000   1
$  SPECIFICATION FOR MATERIAL AXES ORIENTATION
   1    2    0
      0.0
$  ELEMENT MATERIAL PROPERTIES
   1    8
     10.5        0.        10.5       10.5        0.         0.         0.
       0.        0.          0.         0.        0.         0.         0.
       0.        0.       1000.         0.        0.         0.         0.
       0.        0.          0.         0.        0.         0.         0.
       0.        0.          0.         0.        0.         0.         0.
       0.        0.          0.         0.        0.         0.         0.
       0.        0.
   2    8
      2.1        0.         2.1        2.1        0.         0.         0.
       0.        0.          0.         0.        0.         0.         0.
       0.        0.          0.         0.        0.         0.         0.
       0.        0.          0.         0.        0.         0.         0.
       0.        0.          0.         0.        0.         0.         0.
       0.        0.          0.         0.        0.         0.         0.
       0.        0.
   3    8
     10.5        0.        10.5       10.5        0.         0.         0.
       0.        0.          0.         0.        0.         0.         0.
       0.        0.          0.         0.        0.         0.         0.
       0.        0.          0.         0.        0.         0.         0.
       0.        0.          0.         0.        0.   0.1713E-8        0.
       0.        0.          0.         0.       0.6         0.         0.
       0.        0.
$    INITIAL NODAL TEMPERATURE DATA
   1    4        800.0
   2    4        800.0
   3    4        800.0
   4    4        800.0
  -1
```

STARS analysis results:

NODE EXT	NODE INT	TEM-SUR 1	TEM-SUR 2	TEM-SUR 3	TEM-SUR 4	TEM-SUR 5	TEM-SUR 6
1	1	.156460E+04	.151698E+04	.104079E+04	.993168E+03	.000000E+00	.000000E+00
2	2	.156460E+04	.151698E+04	.104079E+04	.993168E+03	.000000E+00	.000000E+00
3	3	.156460E+04	.151698E+04	.104079E+04	.993168E+03	.000000E+00	.000000E+00
4	4	.156460E+04	.151698E+04	.104079E+04	.993168E+03	.000000E+00	.000000E+00

ORIGINAL PAGE IS
OF POOR QUALITY

4.20 Composite Square Plate: Radiation Boundary Condition

A radiation heat transfer analysis of a composite square plate (fig. 28), with specified temperature, was performed. The results are presented in table 20.

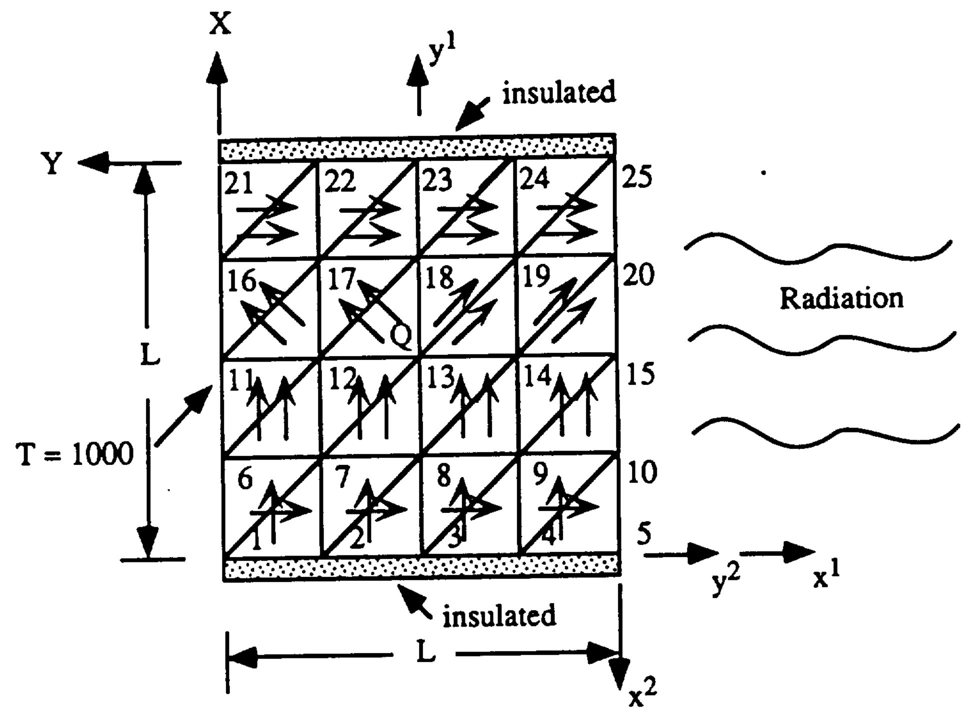

Figure 28. Composite square plate with radiation.

Important data parameters:

Coefficient of conductivity, k_x	= 3.0
Coefficient of conductivity, k_y	= 1.0
Coefficient of conductivity, k_z	= 1.0
Length, L	= 1
Thickness of each layer, t	= 0.0315
Temperature, T	= 1000
Emissivity, ε	= 0.6
Stefan-Boltzmann constant, σ	= 0.1713×10^{-8}

STARS input data

```
SHELL-4x4- composite element- Radiation
25,32,2,44,0,0,2,8,9,2
0,0,0,1,10,0,0,0,0
10,0,0,1,0,0,0,0
2,0,2,0,1,0
$ NODAL DATA
    1       -0.5        0.0        0.0    0    0    0    0    0    0  1   0   0
    5        0.5        0.0        0 0    0    0    0    0    0    0  1   0   1
    6       -0.25      -1.0        0 0    0    0    0    0    0    0  2   0   0
   10       -0.25       0.0        0 0    0    0    0    0    0    0  2   0
   11       -0.5        0.5        0 0    0    0    0    0    0    0  1   0   0
   15        0.5        0.5        0 0    0    0    0    0    0    0  1   0   1
   16       -0.25       0.0        0 0    0    0    0    0    0    0  0   0   0
   20       -0.25      -1.0        0 0    0    0    0    0    0    0  0   0   1
   21       -0.5        1.0        0 0    0    0    0    0    0    0  1   0   0
   25        0.5        1.0        0 0    0    0    0    0    0    0  1   0   1
$ LOCAL-GLOBAL COORDINATE SYSTEM DATA
    1    2
      -1.0      -0.5       0.0       0.0      -1.0       0.0
       1.0       0.0       0.0       0.0       0.0       1.0
    2    1
      -1.0      -1.0       0.0      -1.5      -1.0       0.0
      -1.5      -1.5       0.0
$ ELEMENT CONNECTIVITY CONDITIONS
    7    1    1    7    6    0    0    0    0    1    1    0    0  0    0    0
    7    2    7    1    2    0    0    0    0    1    1    0    0  0    0    0
    7    3    2    8    7    0    0    0    0    1    1    0    0  0    0    0
    7    4    8    2    3    0    0    0    0    1    1    0    0  0    0    0
    7    5    3    9    8    0    0    0    0    1    1    0    0  0    0    0
    7    6    9    3    4    0    0    0    0    1    1    0    0  0    0    0
    7    7    4   10    9    0    0    0    0    1    1    0    0  0    0    0
    7    8   10    4    5    0    0    0    0    2    1    0    0  0    0    0
    7    9    6   12   11    0    0    0    0    3    1    0    0  0    0    0
    7   10   12    6    7    0    0    0    0    3    1    0    0  0    0    0
    7   11    7   13   12    0    0    0    0    3    1    0    0  0    0    0
    7   12   13    7    8    0    0    0    0    3    1    0    0  0    0    0
    7   13    8   14   13    0    0    0    0    3    1    0    0  0    0    0
    7   14   14    8    9    0    0    0    0    3    1    0    0  0    0    0
    7   15    9   15   14    0    0    0    0    3    1    0    0  0    0    0
    7   16   15    9   10    0    0    0    0    4    1    0    0  0    0    0
    7   17   11   17   16    0    0    0    0    5    1    0    0  0    0    0
    7   18   17   11   12    0    0    0    0    5    1    0    0  0    0    0
    7   19   12   18   17    0    0    0    0    5    1    0    0  0    0    0
    7   20   18   12   13    0    0    0    0    5    1    0    0  0    0    0
    7   21   13   19   18    0    0    0    0    6    1    0    0  0    0    0
    7   22   19   13   14    0    0    0    0    6    1    0    0  0    0    0
    7   23   14   20   19    0    0    0    0    6    1    0    0  0    0    0
    7   24   20   14   15    0    0    0    0    7    1    0    0  0    0    0
    7   25   16   22   21    0    0    0    0    8    1    0    0  0    0    0
    7   26   22   16   17    0    0    0    0    8    1    0    0  0    0    0
    7   27   17   23   22    0    0    0    0    8    1    0    0  0    0    0
    7   28   23   17   18    0    0    0    0    8    1    0    0  0    0    0
    7   29   18   24   23    0    0    0    0    8    1    0    0  0    0    0
    7   30   24   18   19    0    0    0    0    8    1    0    0  0    0    0
    7   31   19   25   24    0    0    0    0    8    1    0    0  0    0    0
    7   32   25   19   20    0    0    0    0    9    1    0    0  0    0    0
$  COMPOSITE  SHELL  EIEMENT
    1         2    1    2    0    0     0    0
    1    0.0315    2
    1    0.0315    7
    2         2    1    2    0    0     0    0
    2    0.0315    2
    2    0.0315    7
    3         2    1    2    0    0     0    0
    1    0.0315    2
    1    0.0315    2
    4         2    1    2    0    0     0    0
    2    0.0315    2
    2    0.0315    2
    5         2    1    2    0    0     0    0
    1    0.0315    3
    1    0.0315    3
    6         2    1    2    0    0     0    0
    1    0.0315    1
    1    0.0315    1
    7         2    1    2    0    0     0    0
    2    0.0315    1
    2    0.0315    1
    8         2    1    2    0    0     0    0
    1    0.0315    7
    1    0.0315    7
    9         2    1    2    0    0     0    0
    2    0.0315    7
    2    0.0315    7
$  SPECIFICATION  FOR  MATERIAL  AXIS  ORIENTATION
    1    2    0
       0.0
    2    2    0
     0.7854
```

```
    3    2     0
     1.5708
    4    2     0
     2.3562
    5    2     0
     3.1416
    6    2     0
     4.7120
    7    2     0
     5.4980
    8    2     0
     3.9260
$  ELEMENT  MATERIAL  PROPERTIES
    1    8
          3.        0.        1.        1.        0.        0.        0.
          0.        0.        0.        0.        0.        0.        0.
          0.        0.        0.        0.        0.        0.        0.
          0.        0.        0.        0.        0.        0.        0.
          0.        0.        0.        0.        0.        0.        0.
          0.        0.        0.        0.        0.        0.        0.
          1.        1.
    2    8
          3.        0.        1.        1.        0.        0.        0.
          0.        0.        0.        0.        0.        0.        0.
          0.        0.        0.        0.        0.        0.        0.
          0.        0.        0.        0.        0.        0.        0.
          0.        0.        0.  0.1713E-8        0.        0.        0.
          0.        0.       0.6        0.        0.        0.        0.
          1.        1.
$    TEMPERATURE  BOUNDARY  CONDITION  DATA
    1    1    1    1      1000
    1    2    1    2      1000
    6    1    6    1      1000
    6    2    6    2      1000
   11    1   11    1      1000
   11    2   11    2      1000
   16    1   16    1      1000
   16    2   16    2      1000
   21    1   21    1      1000
   21    2   21    2      1000
```

STARS output summary - The results are presented in table 20.

Table 20. Heat transfer analysis results for a composite plate with radiation boundary condition.

Node	STARS Temperature	
	Top	Bottom
1	1000.00	1000.00
2	928.91	930.53
3	866.21	867.33
4	805.83	806.62
5	769.79	771.48
6	1000.00	1000.00
7	940.31	941.10
8	878.29	878.84
9	816.77	818.55
10	762.80	759.63
11	1000.00	1000.00
12	939.80	938.08
13	877.30	875.68
14	814.73	812.71
15	754.18	754.65
16	1000.00	1000.00
17	938.23	938.40
18	875.09	875.52
19	808.93	809.36
20	746.37	746.86
21	1000.00	1000.00
22	938.15	938.12
23	875.23	875.10
24	811.48	811.30
25	761.17	760.90

5. STARS-AERO AND ASE PROGRAM DESCRIPTION

The aeroelastic and aeroservoelastic modules (fig. 2) are recent additions to the original STARS program (ref. 1) that are capable of predicting related stability of such structures as aircraft and spacecraft. Thus, once the vibration analysis is performed utilizing the STARS-SOLIDS module, the program continues to determine flutter and divergence characteristics as well as open- and closed-loop stability analyses, as desired. In this connection, a typical feedback control system is shown in figure 29. References 15 and 16 provide some details of the current analysis techniques.

Detailed numerical formulation in connection with the present aero-structural-control analysis is given in section 5.1. The unsteady aerodynamic forces for supersonic flow are computed by a constant pressure method (CPM) (ref. 17), whereas the doublet lattice method (DLM) (refs. 18,19) is utilized for the subsonic case. Both k and p-k stability (flutter and divergence) solution procedures are available to the user.

For the ASE analysis, the aerostructural problem is recast in the Laplace domain when the generalized aerodynamic forces are curve-fitted using Padé and least squares approximations, thereby yielding the state-space matrices (ref. 20). Such matrices can then be augmented by analog elements such as actuators, sensors, prefilters, and notch filters, and also the analog controller. The associated equivalent open-loop (loop-gain) or open-loop transfer function is obtained by standard procedure, whereas the closed-loop formulation is derived similarly by appropriately taking into account the feedback equation. The system frequency responses are simply obtained from the appropriate transfer matrices. Associated modal damping and frequency values may also be derived by solving the eigenvalue problem of the augmented state-space plant dynamics matrix.

In the case of a digital controller, a hybrid equivalent open-loop or closed-loop transfer function is achieved by suitably combining the controller, the open-loop transfer function of the original analog system of the plant, and other analog elements; frequency responses are then obtained in a routine manner. The modal damping and frequency values are obtained by first transferring the augmented analog state-space plant dynamics matrix from its usual Laplace (s) to the digital z-plane, adding the same to the corresponding matrix for the controller, and finally solving the associated eigenvalue problem.

Furthermore, the open-loop stability analyses (flutter and divergence) may also be effected with or without the controller (analog or digital). This is achieved by solving eigenvalue problems of the appropriately augmented and transformed, as the case may be, plant dynamics matrix for a number of reduced frequency values and noting the change in sign of the real part of the eigenvalues. Such a solution without a controller can be compared with the aeroelastic analysis using the k and p-k methods, whereas the relevant solution in the presence of a controller proves to be useful for comparing relevant flight test results of modern, high-performance, unstable aircraft.

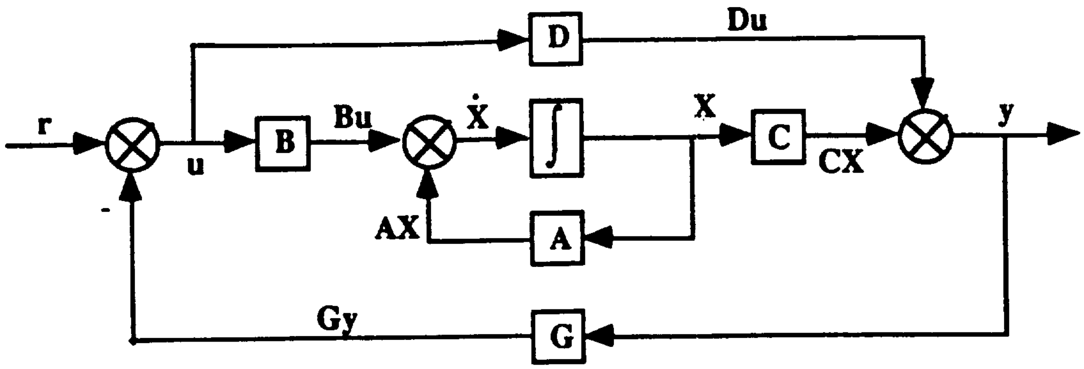

Summing junction outputs

$$u = r - Gy$$
$$\dot{X} = AX + Bu$$
$$y = CX + Du$$

Figure 29. Feedback control system.

5.1 Numerical Formulation for Aeroelastic and Aeroservoelastic Analysis

In the numerical formulation presented here, structural discretization is based on the finite element method, whereas the panel methods are adopted for computation of unsteady aerodynamic forces. The more specialized matrix equation of motion of such structures relevant to the current analysis has the form

$$\mathbf{M\ddot{q} + C\dot{q} + Kq} + \bar{q}\mathbf{A_e(k)q = P(t)} \tag{28}$$

in which relevant terms are defined as follows:

M = inertia matrix
C = damping matrix
K = elastic stiffness matrix
$\bar{q}$ = dynamic pressure $1/2\rho V^2$, ρ and V being the air density and true airspeed, respectively
k = reduced frequency $\omega b/V$, ω and b being the natural frequency and wing semichord length, respectively
$A_e(k)$ = aerodynamic influence coefficient matrix for a given Mach number M_∞ and set of k_i values
q = displacement vector
P(t) = external forcing function
s = Laplace variable (= i*ω, i* being $\sqrt{-1}$)

A solution (ref. 1) of the related free vibration problem

$$\mathbf{M\ddot{q} + kq = 0} \tag{29}$$

yields the desired roots ω and vectors Φ. Next, applying a transformation

$$\mathbf{q} = \Phi\eta \tag{30}$$

to equation (28) and premultiplying both sides by Φ^T, the generalized equation of motion is derived as

$$\hat{M}\ddot{\eta} + \hat{C}\dot{\eta} + \hat{K}\eta + \bar{q}Q(k)\eta = \hat{P}(t) \tag{31}$$

in which $\hat{M} = \Phi^T M \Phi$, etc., the modal matrix $\Phi = [\Phi_r \;\; \Phi_e \;\; \Phi_\delta]$, and the generalized coordinate $\eta = [\eta_r \;\; \eta_e \;\; \eta_\delta]$ incorporate rigid body, elastic, and control surface motions, respectively.

Expressing the generalized aerodynamic force matrix Q(k) as Padé polynomials (ref. 15) in i^*k ($=i^*\omega b/V = sb/V$), equation (31) results in

$$Q(k) = A_0 + i^*kA_1 + (i^*k)^2 A_2 + \frac{i^*k}{i^*k+\beta_1} A_3 + \frac{i^*k}{i^*k+\beta_2} A_4 + \;\; . \; . \; . \tag{32}$$

where β_j are the aerodynamic lag terms (assuming j = 1, 2), and

$$\frac{i^*k}{i^*k+\beta_j} = \frac{k^2}{k^2+\beta_j^2} + \frac{i^*k\beta_j}{k^2+\beta_j^2} \tag{32a}$$

Further, separation of the real and imaginary parts in equation (32), yields

$$\begin{aligned} \tilde{Q}_R(k) &= (Q_R(k) - A_0) \\ &= \left[-k^2 I \quad \frac{k^2}{k^2+\beta_1^2} I \quad \frac{k^2}{k^2+\beta_2^2} I \right] \begin{bmatrix} A_2 \\ A_3 \\ A_4 \end{bmatrix} \\ &= S_R(k)\tilde{A} \end{aligned} \tag{33}$$

$$\begin{aligned} \tilde{Q}_I(k) &= \frac{Q_I(k)}{k} - A_1 \\ &= \left[0 \quad \frac{\beta_1}{k^2+\beta_1^2} I \quad \frac{\beta_2}{k^2+\beta_2^2} I \right] \begin{bmatrix} A_2 \\ A_3 \\ A_4 \end{bmatrix} \\ &= S_I(k)\tilde{A} \end{aligned} \tag{33a}$$

in which for a small value of $k = k_1$, the coefficients assume the following form:

$$A_0 = Q_R(k_1) \tag{34}$$

$$A_1 = \frac{Q_I(k_1)}{k_1} - \frac{A_3}{\beta_1} - \frac{A_4}{\beta_2} \tag{34a}$$

Substituting equation (34a) in equation (33a), the unknown coefficients A_3 and A_4 can be determined; however, the resulting solution will be sensitive to the choice of β_j. On the other hand, if the elements of the A_1 matrix are replaced by measured damping coefficients without any lag terms, then the solution will be insensitive to the β_j values.

Equations (33) and (33a), computed for an NF number of values of reduced frequencies k_i, may be combined as

$$\begin{bmatrix} \bar{Q}_R(k_2) \\ \bar{Q}_I(k_2) \\ \cdot \\ \cdot \\ \cdot \\ \bar{Q}_R(k_{NF\text{-}1}) \\ \bar{Q}_I(k_{NF\text{-}1}) \end{bmatrix} = \begin{bmatrix} S_R(k_2) \\ S_I(k_2) \\ \cdot \\ \cdot \\ \cdot \\ S_R(k_{NF\text{-}1}) \\ S_I(k_{NF\text{-}1}) \end{bmatrix} \begin{bmatrix} A_2 \\ A_3 \\ A_4 \end{bmatrix} \tag{35}$$

or

$$\bar{\bar{Q}} = S\bar{A} \tag{36}$$

and a least square solution

$$\bar{A} = \left[S^T S\right]^{-1} S^T \bar{\bar{Q}} \tag{37}$$

yields the required coefficients A_2, A_3, and A_4. This procedure may be easily extended for a larger number of lag terms, if desired. Equation (31) may be rewritten as

$$\hat{M}\ddot{\eta} + \hat{C}\dot{\eta} + \hat{K}\eta + \bar{q}\left[A_0\eta + A_1\left(\frac{sb}{V}\right)\eta + A_2\left(\frac{sb}{V}\right)^2\eta + A_3X_1 + A_4X_2 + \ldots\right] = 0 \tag{38}$$

and collecting like terms, gives

$$\left(\hat{K} + \bar{q}A_0\right)\eta + \left[\hat{C} + \bar{q}\left(\frac{b}{V}\right)A_1\right]\dot{\eta} + \left[\hat{M} + \bar{q}\left(\frac{b}{V}\right)^2 A_2\right]\ddot{\eta} + \bar{q}A_3X_1 + \bar{q}A_4X_2 + \ldots = 0 \tag{39}$$

or

$$\hat{\hat{K}}\eta + \hat{\hat{C}}\dot{\eta} + \hat{\hat{M}}\ddot{\eta} + \bar{q}A_3X_1 + \bar{q}A_4X_2 + \ldots = 0 \tag{40}$$

Also

$$X_j = \frac{s\eta}{\left[s + \left(\frac{V}{b}\right)\beta_j\right]} \tag{41}$$

from which

$$\dot{X}_j + \left(\frac{V}{b}\right)\beta_j X_j = \dot{\eta} \tag{42}$$

Equations (40), (41), and (42) can be rewritten as one set of matrix equations

$$\begin{bmatrix} I & & & \\ & \hat{\hat{M}} & & \\ & & I & \\ & & & I \end{bmatrix} \begin{bmatrix} \dot{\eta} \\ \ddot{\eta} \\ \dot{X}_1 \\ \dot{X}_2 \end{bmatrix} = \begin{bmatrix} 0 & I & 0 & 0 \\ -\hat{\hat{K}} & -\hat{\hat{C}} & -\bar{q}A_3 & -\bar{q}A_4 \\ 0 & I & -\frac{V}{b}\beta_1 I & 0 \\ 0 & I & 0 & -\frac{V}{b}\beta_2 I \end{bmatrix} \begin{bmatrix} \eta \\ \dot{\eta} \\ X_1 \\ X_2 \end{bmatrix} \tag{43}$$

or

$$M'\dot{X}' = K'X' \tag{44}$$

from which

$$\begin{aligned} \dot{X}' &= (M')^{-1}K'X' \\ &= RX' \end{aligned} \tag{45}$$

Also, the state-space vector X' may be rearranged as

$$\begin{aligned} X'' &= \left[\left(\eta_r \;\; \eta_e \;\; \dot{\eta}_r \;\; \dot{\eta}_e \;\; X_1 \;\; X_2\right)\left(\eta_\delta \;\; \dot{\eta}_\delta\right)\right] \\ &= \left[\hat{X} \;\; u\right] \end{aligned} \tag{46}$$

and equation (45) may be partitioned as

$$\begin{bmatrix} \dot{\hat{X}} \\ \dot{u} \end{bmatrix} = \begin{bmatrix} R_{I,I} & R_{I,II} \\ R_{II,I} & R_{II,II} \end{bmatrix} \begin{bmatrix} \hat{X} \\ u \end{bmatrix} \tag{47}$$

where the first set of matrix equations denotes the plant dynamics, and the second set represents the dynamics of control modes. In the case of plant dynamics, the state-space equations become

$$\dot{\hat{X}} = \hat{A}\hat{X} + \hat{B}u \quad (48)$$

in which the relevant matrices and vectors are defined as

$\hat{A}$ = plant dynamics matrix

$\hat{B}$ = control surface influence matrix

$\hat{X}$ = generalized coordinates in inertial frame

u = control surface motion input into plant

and where the terms $\hat{A}\hat{X}$ and $\hat{B}u$ represent for an aircraft, for example, the airplane dynamics and forcing function on airplane due to control surface motion, respectively.

Coordinate Transformation

To incorporate control laws and feedback, it is necessary to transform equation (48) from the earth-fixed (inertial) to the body-fixed coordinate system. Since no transformations are applied to elastic and aerodynamic lag state vectors, a transformation of the form

$$\begin{aligned} \dot{X} &= \bar{T}_2^{-1}\left(\hat{A}\bar{T}_1 - \bar{T}_3\right)X + \bar{T}_2^{-1}\hat{B}u \\ &= AX + Bu \end{aligned} \quad (49)$$

in which

$$\bar{T}_1 = \begin{bmatrix} T_1 & 0 \\ 0 & I \end{bmatrix}$$

and so forth, T_1 being the 12 by 12 coordinate transformation matrix, yields the required state-space equation in the body-fixed coordinate system.

Determination of Sensor Outputs

The structural nodal displacements are related to the generalized coordinates by equation (30), and the related sensor motion can be expressed as

$$\begin{aligned} q_s &= T_s\Phi\eta \\ &= C_0 X \end{aligned} \quad (50)$$

where $C_0 = \left[T_s\Phi \;\; 0 \;\; 0 \;\; 0\right]$ and in which T_s is an interpolation matrix. Similar relations may be derived for sensor velocities and accelerations as

$$\begin{aligned} \begin{bmatrix} \dot{q}_s \\ \ddot{q}_s \end{bmatrix} &= \begin{bmatrix} T_s\Phi\dot{\eta} \\ T_s\Phi\ddot{\eta} \end{bmatrix} \\ &= C_1\dot{X} \end{aligned} \quad (51)$$

where

$$C_1 = \begin{bmatrix} T_s\Phi & 0 & 0 & 0 \\ 0 & T_s\Phi & 0 & 0 \end{bmatrix}$$

Equation (49) is next premultiplied by C_1 to yield

$$\begin{aligned} C_1\dot{X} &= C_1AX + C_1Bu \\ &= C_2X + D_2u \end{aligned} \tag{52}$$

and adjoining equations (50) and (52), the following expression is obtained

$$y = \begin{bmatrix} q_s \\ \dot{q}_s \\ \ddot{q}_s \end{bmatrix} = \begin{bmatrix} C_0 \\ C_2 \end{bmatrix} X + \begin{bmatrix} 0 \\ D_2 \end{bmatrix} u$$

or

$$y = CX + Du \tag{53}$$

which is the required sensor output relationship, the matrices C and D signifying output at sensor due to body and control surface motions, respectively.

Augmentation of Analog Elements and Controller

The complete state-space formulation for an aircraft incorporating structural and aeroelastic effects is represented by equations (49) and (53). To conduct an aeroservoelastic analysis, it is essential to augment such a formulation with associated analog elements like actuators, sensors, notch filters, and prefilters along with the controller. Thus the state-space equations of one such element can be expressed as

$$\dot{X}^{(i)} = A^{(i)}X^{(i)} + B^{(i)}u^{(i)} \tag{54}$$

$$y^{(i)} = C^{(i)}X^{(i)} + D^{(i)}u^{(i)} \tag{55}$$

these can be augmented to the original equations (49) and (53), as appropriate; typically, for the case of a connection from plant output to the external input, the relevant formulation is as follows:

$$\begin{bmatrix} \dot{X} \\ \dot{X}^{(i)} \end{bmatrix} = \begin{bmatrix} A & 0 \\ B^{(i)}C & A^{(i)} \end{bmatrix} \begin{bmatrix} X \\ X^{(i)} \end{bmatrix} + \begin{bmatrix} B \\ B^{(i)}D \end{bmatrix} [u] \tag{56}$$

or

$$\dot{X}_{(i)} = A_{(i)}X_{(i)} + B_{(i)}u \tag{57}$$

noting that $\mathbf{u}^{(1)} = \mathbf{y}$. Also

$$\begin{bmatrix} \mathbf{y} \\ \mathbf{y}^{(i)} \end{bmatrix} = \begin{bmatrix} \mathbf{C} & \mathbf{0} \\ \mathbf{D}^{(i)}\mathbf{C} & \mathbf{C}^{(i)} \end{bmatrix} \begin{bmatrix} \mathbf{X} \\ \mathbf{X}^{(i)} \end{bmatrix} + \begin{bmatrix} \mathbf{D} \\ \mathbf{D}^{(i)}\mathbf{D} \end{bmatrix} [\mathbf{u}]$$

or

$$\mathbf{y}_{(i)} = \mathbf{C}_{(i)}\mathbf{X}_{(i)} + \mathbf{D}_{(i)}\mathbf{u} \tag{58}$$

which is the new sensor output expression.

Any analog element, including a controller, can be augmented in a similar manner. Figure 29 shows a typical feedback control system. For such a system, the three sets of relevant matrix equations are

$$\dot{\mathbf{X}} = \mathbf{AX} + \mathbf{Bu} \tag{59}$$

$$\mathbf{y} = \mathbf{CX} + \mathbf{Du} \tag{59a}$$

$$\mathbf{u} = \mathbf{r} - \mathbf{Gy} \tag{59b}$$

where equation (59b) is the feedback equation. By applying Laplace transformations to equation (59), (59a), and (59b) the following relationships are obtained:

$$\mathbf{sX(s)} = \mathbf{AX(s)} + \mathbf{Bu(s)} \tag{60}$$

$$\mathbf{y(s)} = \mathbf{CX(s)} + \mathbf{Du(s)} \tag{60a}$$

$$\mathbf{u(s)} = \mathbf{r(s)} - \mathbf{G(s)y(s)} \tag{60b}$$

Further, from equation (60)

$$\mathbf{X(s)} = [\mathbf{sI} - \mathbf{A}]^{-1}\mathbf{Bu(s)} \tag{61}$$

and substitution of equation (61) into equation (60a), yields the required open-loop frequency response relationship

$$\begin{aligned} \mathbf{y(s)} &= \left[\mathbf{C}(\mathbf{sI} - \mathbf{A})^{-1}\mathbf{B} + \mathbf{D}\right]\mathbf{u(s)} \\ &= \mathbf{H(s)u(s)} \end{aligned} \tag{62}$$

H(s) being the equivalent open-loop (loop-gain) transfer function with the analog controller or the open-loop transfer function without the controller. To obtain the closed-loop frequency response relationship, equation (62) is first substituted in equation (60b), resulting in

$$\mathbf{u(s)} = \mathbf{r(s)} - \mathbf{G(s)H(s)u(s)} \tag{63}$$

or

$$\mathbf{u}(s) = [\mathbf{I} + \mathbf{G}(s)\mathbf{H}(s)]^{-1}\mathbf{r}(s) \tag{63a}$$

and again, substitution of equation (62) yields

$$\mathbf{y}(s) = \left(\mathbf{H}(s)[\mathbf{I} + \mathbf{G}(s)\mathbf{H}(s)]^{-1}\right)\mathbf{r}(s) \tag{63b}$$

$$= \hat{\mathbf{H}}(s)\mathbf{r}(s) \tag{64}$$

in which $\hat{\mathbf{H}}(s)$ is the desired closed-loop transfer function. The frequency responses plots can be simply obtained from the transfer matrices $\mathbf{H}(s)$ or $\hat{\mathbf{H}}(s)$, as the case may be. Associated damping and frequency values for the system, for the loop-gain or open-loop case, may also be calculated by solving the eigenvalue problem of the relevant **A** matrix for various k_i values, and observing the changes in sign of the real part of an eigenvalue.

In the presence of a digital controller, a hybrid approach (ref. 15) is adopted for the frequency response solution. Thus, if $\mathbf{A}'$, $\mathbf{B}'$, $\mathbf{C}'$, and $\mathbf{D}'$ are the state-space matrices associated with the controller, the related transfer function is simply given by

$$\mathbf{G}(z) = \mathbf{C}'[z\mathbf{I} - \mathbf{A}']^{-1}\mathbf{B}' + \mathbf{D}' \tag{65}$$

and the frequency response relationship for the hybrid analog/digital system can be written as

$$\mathbf{y}(s) = \mathbf{G}(z)_{\left[\text{at } z=e^{sT}\right]}\left\{\frac{\mathbf{H}(s)[\mathrm{ZOH}]}{T}\right\}\mathbf{u}(s) \tag{66}$$

$$= \mathbf{H}^*(s)\mathbf{u}(s) \tag{66a}$$

in which

$\mathbf{H}(s)$ is the open-loop transfer function for the plant and other analog elements

[ZOH] is the zero order hold complex expression $\left(= e^{-s\tau}\left(\frac{1-e^{-sT}}{s}\right)\right)$

and where $\mathbf{H}^*(s)$ is now the equivalent open-loop (loop-gain) transfer function of the hybrid system. The closed-loop frequency response relationship may be obtained as before by using equations (66a) and (60b)

$$\mathbf{y}(s) = \left\{\mathbf{H}(s)[\mathbf{I} + \mathbf{G}(s)\mathbf{H}(s)]^{-1}\right\}\mathbf{r}(s) \tag{67}$$
$$= \hat{\mathbf{H}}^*(s)\mathbf{r}(s)$$

To compute the damping and frequencies, the analog plant dynamics matrix A is first transformed into the z-plane by the standard discretization procedure which is next augmented to the A' matrix. The appropriate eigenproblem solution of the final matrix yields the required results, as before.

The STARS program has been extended to include capabilities representative of formulations presented in this section.

Figure 30 depicts the data input strategy for the entire ASE analysis procedure; such input for the solids module is described in section 3. In the following, the data pertaining to the other related analyses are given in the appropriate order, in which AERO module data input is compatible with the program described in reference 18.

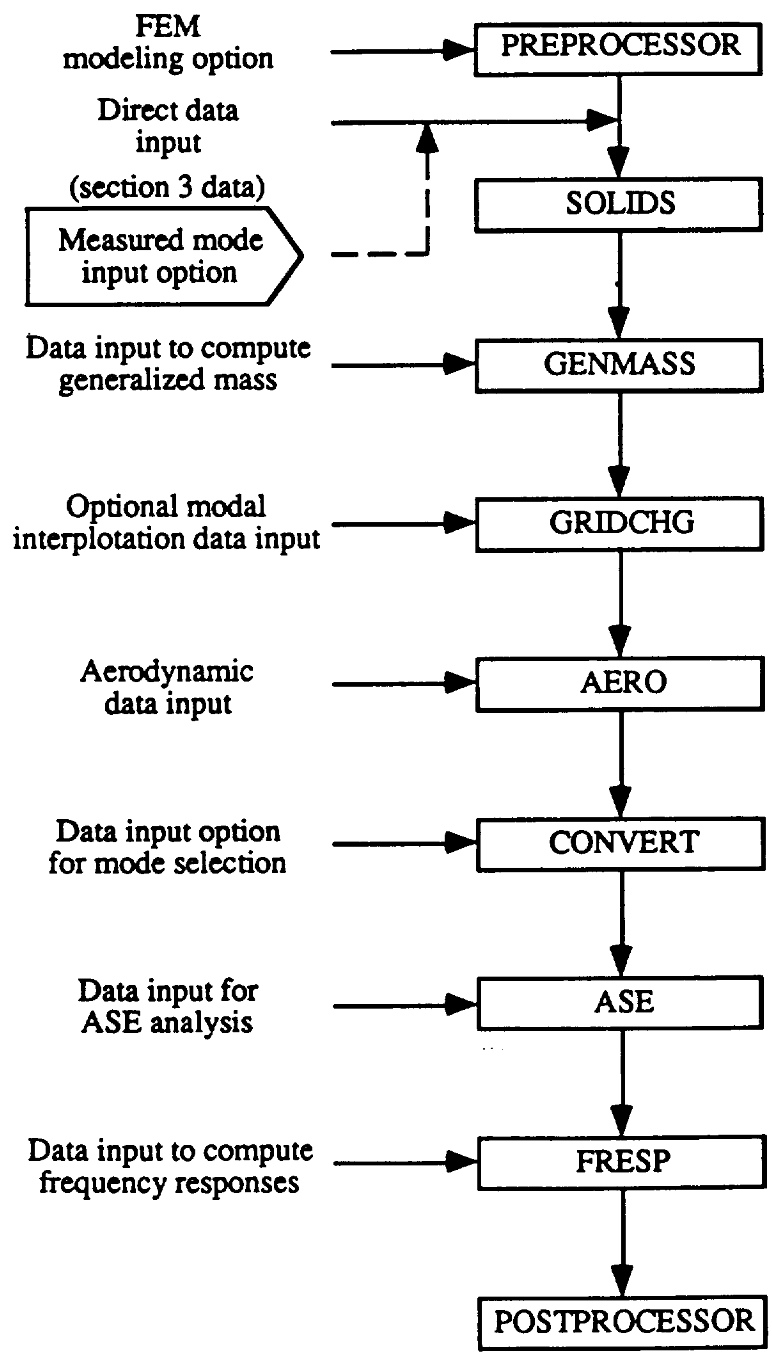

Figure 30. ASE analysis data input scheme.

6.1.1 $ JOB DESCRIPTION
Format (FREE)

6.1.2 ISTMN, NLVN, GR
Format (2I5, E10.4)

1. Description: Generalized mass matrix generation data.

2. Notes:

   ISTMN = integer specifying starting mode number

   NLVN = number of laterally vibrating nodes

   GR = gravitational constant

6.1.3 $ LATERALLY MOVING NODAL NUMBERS DATA (Required if NLVN > 0)
Format (FREE)

6.1.3.1 (LN(I), I = 1, NLVN)
Format (I5)

1. Description: NLVN number of nodes input data.

2. Notes:

   Input of a GR value is needed to convert generalized mass data into generalized weight acceptable to AERO module.

   If GRIDCHG is used, then the LN refers to STARS nodes (that is, the input vector, as defined in section 3.2.2 of the STARS manual).

   If direct STARS interpolation is used, then the LN refers to nodes as defined in STARS (that is, the output vector, as defined in section 3.5.10 of the STARS manual).

3. Note:

   The data is to be stored in the file GENMASS.DAT.

6.2.1.1 $ JOB TITLE
Format (FREE)

6.2.1.2 NELN, NLINES, NOSURF
Format (3I5)

6.2.1.3 IDELE, NMOD
Format (2I5)

6.2.1.4 NBLOCK, IRPEAT
Format (2I5)

1. Description: General input data.

2. Notes:

NELN = number of nodes eliminated from input vector

NLINES = number of output vector interpolation lines
$0 < \text{NLINES} \leq 20$

NOSURF = number of sets of input vector coordinates to be translated

IDELE = flag for deletion of interpolation elements
= 0, for no elimination of interpolation element(s)
= 1, to eliminate interpolation element(s)

NMOD = number of output points whose values are to be changed to a user-specified value (for all modes)

NBLOCK = number of blocks of added deflections

IRPEAT = flag for reuse of deflections for different modes
= 0, for user to input all blocks for all output modes
= 1, to repeat first subset of block data for all subsequent modes

6.2.2.1 $ ELIMINATED INPUT NODES (Required if NELN ≠ 0)
Format (FREE)

6.2.2.2 (NODEL(I), I = 1, NELN)
Format (I5)

1. Description: NELN indices of nodes in input vector whose deflections are not used in interpolation.

2. Notes:

NODEL(I) = node in input data that is not to be used in interpolation.

6.2.3.1 $ NUMBER OF POINTS ON OUTPUT VECTOR LINES
Format (FREE)

6.2.3.2 (NGP(I), I = 1, NLINES)
Format (I5)

1. Description: NLINES sets of numbers of output points. Each set makes up part of the output vector.

2. Notes:

NGP(I) = number of points that will be interpolated to on each line
$0 < NGP(I) \leq 12$

6.2.4.1 $ ENDPOINTS OF OUTPUT VECTOR LINES
Format (FREE)

6.2.4.2 ((XTERM1(I), YTERM1(I), XTERM2(I), YTERM2(I), XT(I), YT(I)), I = 1, NLINES)
Format (6E10.4)

1. Description: NLINES sets of endpoints for output vector interpolation lines and optional translations.

2. Notes:

XTERM1(I), YTERM1(I) = inboard coordinates of line I

XTERM2(I), YTERM2(I) = outboard coordinates of line I

XT(I), YT(I) = optional translations to be applied to line data in X- and Y-directions

6.2.5.1 $ SPANWISE COORDINATES OF POINTS ON OUTPUT VECTOR LINES
Format (FREE)

6.2.5.2 ((YGP(J,I), J = 1, NGP(I)), I = 1, NLINES)
Format (7E10.4)

1. Description: NLINES sets of spanwise coordinate of desired point in output vector.

2. Notes:

YGP(J,I) = spanwise coordinate of a point desired on an interpolation line, before any translation; translation, as defined in section 6.2.6.2, will automatically be applied

6.2.6.1 $ TRANSLATION DATA FOR INPUT VECTOR POINTS (Required if NOSURF ≠ 0)
Format (FREE)

6.2.6.2 XTRAN, YTRAN, ZTRAN
Format (3E10.4)

6.2.6.3 NODNUM
Format (I5)

1. Description: NOSURF subsets of input vector nodal data.

2. Notes:

XTRAN = value to be added to X-coordinate of input vector in set

YTRAN = value to be added to Y-coordinate of input vector in set

ZTRAN = value to be added to Z-coordinate of input vector in set

NODNUM = index of node to be translated

A data set is terminated if NODNUM is read as -1; a node should not be referenced more than once.

6.2.7.1 $ INTERPOLATION ELEMENT DATA
Format (FREE)

6.2.7.2 NXPT
Format (I5)

6.2.7.2.1 (XMESH(I), I = 1, NXPT)
Format (7E10.4)

6.2.7.3 NYPT
Format (I5)

6.2.7.3.1 (YMESH(I), I = 1, NYPT)
Format (7E10.4)

1. Description: Streamwise and spanwise finite element interpolation boundaries.

2. Notes:

NXPT	=	number of stations in X-direction for interpolation grid $2 \leq NXPT \leq 20$
XMESH(I)	=	actual X-coordinates of streamwise stations in interpolation grid, in ascending order
NYPT	=	number of stations in Y-direction for interpolation grid $2 \leq NYPT \leq 20$
YMESH(I)	=	actual Y-coordinates of spanwise stations in interpolation grid, in ascending order

6.2.8.1 $ INTERPOLATION ELEMENT DELETION DATA (Required if IDELE > 0)
Format (FREE)

6.2.8.2 IOPT
Format (I5)

6.2.8.3 NCOL, NROW (Required if IOPT = 1); or
NCOL (Required if IOPT = 2); or
NROW (Required if IOPT = 3)
Format (2I5)

1. Description: Data for elimination of finite element interpolation elements.

2. Notes:

IOPT	=	type of elimination
	=	0, to proceed to next set to be eliminated
	=	1, to eliminate following element(s)
	=	2, to eliminate following row of elements
	=	3, to eliminate following column of elements
	=	4, to quit all eliminations
NCOL	=	column of interpolation element(s)
NROW	=	row of interpolation element(s)

6.2.9.1 $ OUTPUT VECTOR MODIFICATION DATA (Required if NMOD > 0)
Format (FREE)

6.2.9.2 ((NODE(I), DEFL(NODE(I))), I = 1, NMOD)
Format (I5, E10.4)

1. Description: Sets a deflection to a user input value (for all output modes), where number of output modes NTOTAL = NR + NCNTRL - ISTMN + 1.

2. Notes:

NODE(I)	=	output point index
DEFL(NODE(I))	=	new deflection value

NR = number of analytically calculated roots (from section 3.1.6)

NCNTRL = number of rigid body control modes (from section 3.1.3)

ISTMN = integer specifying starting mode numbers

6.2.10.1 $ BLOCK SPECIFICATION OF ADDITIONAL DEFLECTION DATA (Required if NBLOCK > 0)
Format (FREE)

6.2.10.2 ((IBLOCK(I), NADD(I), IBFORE(I)), I = 1, NBLOCK)
Format (3I5)

1. Description: NBLOCK sets of description of additional deflections to be added to output vector.

2. Notes:

IBLOCK(I) = user's identification number of an added output block of output points

NADD(I) = number of points in block

IBFORE(I) = index of existing point in front of which block is to be inserted

Succeeding values of IBFORE should be greater than the previous ones.

6.2.11.1 $ DEFLECTION DATA SPECIFICATION FOR BLOCKS (Required if NBLOCK > 0)
Format (FREE)

6.2.11.2 ((NNODE(J), DADD(J)), J = 1, NADD(I))
Format (I5, E10.4)

1. Description: Added deflection data for each block.

2. Notes:

NNODE(J) = index of added point in set

DADD(J) = deflection of added point in set

This is repeated for NTOTAL modes.

If IRPEAT = 1, the same deflections are reused for all modes.

6.2.12.1 $ EIGENVALUE SPECIFICATION FOR CONTROL MODES (Required if NCNTRL > 0)
Format (FREE)

6.2.12.2 (EIGADD(I), I = 1, NCNTRL)
Format (E10.4)

1. Description: Eigenvalues for rigid body control modes from STARS.

2. Notes:

EIGADD(I) = user-input eigenvalues, in rad/sec, for rigid body control modes

6.2.13 NOTES ON PROGRAM USAGE

GRIDCHG is a versatile interpolation program that may be used as an alternative to the preferred direct interpolation option defined in section 3.1.4 of the STARS-SOLIDS module. It is utilized to interpolate deflections, obtained by a finite element code or ground vibration survey, into the straight line input points required by the aerodynamic module. Options for separate interpolation of different surfaces and for modification by the user of both the input and output vectors exist.

Input vector: The input vector is a calculated or measured vector with six degrees of freedom read from the file FOR096 (if bandwidth minimization is used) or from FOR048 (if bandwidth minimization is not used). Both files are STARS binary files. GRIDCHG normally uses only the Z-component of the vector for the interpolation. However, GRIDCHG does read the input file for the GENMASS program as part of its input, and if the variable NLVN is nonzero in that file, then it reads from the file those nodes of the input vector for which the Y-deflection is to be used (that is, a vertical surface). The GENMASS.DAT file must always be present for GRIDCHG to run, even if NLVN is zero.

Discrete element interpolation: The user defines a set of rectangular elements used for the interpolation. Each element uses the deflections within its boundaries for a surface fit, with the added stipulation that adjacent elements have identical displacements and slopes at edges. The achievable quality of interpolation is a function of number and distribution of input nodes. The output vector is obtained using a surface fit within a particular element. Separate surfaces need to be individually interpolated, and this is accomplished by letting the value of a row or column of interpolation elements or columns between the surfaces to be set to zero. If the projection of the surfaces in the X-Y plane overlap, the user has the option of temporarily modifying the coordinates of input and output vectors to separate them, thereby allowing their individual interpolation.

Output vector: The output vector occasionally needs modification, and/or additional data. This can be implemented as required.

Eigenvalues: The STARS-SOLIDS module contains an option which allows additions of user input eigenvectors to those analytically calculated. The eigenvalues for those modes are added here.

6.3.1.1 JOB TITLE - 1:6 (six lines of title cards)
Format (FREE)

6.3.2.1 (LC(I), I = 1, 40)
Format (10I5)

1. Description: Basic data parameters.

2. Notes:

LC(1) = integer defining flutter and divergence solution algorithm
= -1, p-k type of solution
= 0, pressure calculations only
= 1, k and state-space solutions
= 2, divergence analysis

LC(2) = maximum number of vibration modes to be used in analysis
$0 \leq LC(2) \leq 50$

LC(3) = number of lifting surfaces
$0 \leq LC(3) \leq 30$, for doublet lattice method (DLM) or constant pressure method (CPM)

LC(4) = number of reduced velocities, VBO, used in analysis
If LC(1) = -1, set LC(4) = 6
If LC(1) = 0 or 1, set $1 \leq LC(4) \leq 50$
If LC(1) = 2, set LC(4) = 1
LC(4) and LC(13) apply to the reduced velocities described in section 6.3.4.2 and section 6.3.4.4

LC(5) = number of air densities at which flutter and divergence solutions are to be found
$0 \leq LC(5) \leq 10$
If LC(1) = 0, set LC(5) = 0

LC(6) = print option for tested aerodynamic forces used to check aerodynamic force interpolation
= 1, print
= 0, no print

LC(7) = print option for aerodynamic pressures
= 1, print data
= 0, no print

LC(8) = print option for lift and moment coefficients
= 1, print data
= 0, no print

LC(9) = input frequency-independent additions to the aerodynamic matrix QBAR
= 1, make additions
= 0, no additions

LC(10) = print option for full set of interpolated generalized forces when used in k solutions
= 1, print data
= 0, no print

LC(11) = index of mode whose frequency is to be used in normalizing flutter determinant
Frequency chosen must be nonzero
Suggested index is 1

LC(12) = index defining flutter determinant formulation
= 1, for nonzero frequencies $[\mathbf{D} = \mathbf{K}^{-1} (\mathbf{M} + \mathbf{A_E})]$
= 0, in presence of zero frequencies $[\mathbf{D} = (\mathbf{M} + \mathbf{A_E})^{-1} \mathbf{K}]$
K = generalized stiffness matrix
M = generalized mass matrix
$\mathbf{A_E}$ = aerodynamic force matrix
If LC(1) = 0, set LC(12) = 0

LC(13) = index defining interpolation of aerodynamic forces
= 0, no interpolation, to compute at each input VBO
= 1, to compute directly at only 6 VBOs, interpolate to others
If LC(1) = -1, set LC(13) = 1
If LC(1) = 0 or 2, set LC(13) = 0
If LC(1) = 1, set LC(13) = 0 or 1, as desired

LC(14) = not used. Set = 0

LC(15) = index defining velocity scale in flutter solution output
= 1, use true airspeed, TAS
= 0, use equivalent airspeed, EAS

LC(16) = index defining addition of structural damping to complex stiffness matrix
= 1, add a single damping value to all modes
= -1, add an individual damping value to each mode
= 0, no damping added

LC(17) = print option to display number of iterations required to find each root in a p-k solution
= 1, print
= 0, no print

LC(18) = option for root extrapolation in a p-k solution
= 1, use root values at two previous velocities for initial estimation of a root
= 0, use root value at previous velocity as root estimate
If LC(1) ≠ -1, set LC(18) = 0

LC(19) = option for ordering of roots after a p-k solution
= 1, to perform ordering
= 0, no ordering required
If LC(1) ≠ -1, set LC(19) = 0

LC(20) = print option for iterated roots in p-k analysis or intermediate results in k analysis

= 1, print
= 0, no print

LC(21) = index for aerodynamics
= 1, use doublet lattice method or constant pressure method (subsonic and supersonic Mach numbers, respectively)

LC(22) = index defining generation and storage of aerodynamic influence coefficients matrix
= 0, compute and save
= 1, read precomputed values from a file

LC(23) = print option for input modal vector
= 1, print
= 0, no print

LC(24) = print option for interpolated deflections and slopes of aerodynamic elements
= 1, print
= 0, no print

LC(25) = number of modal elimination cycles
$0 \leq LC(25) \leq 25$

LC(26) = index defining additional flutter analysis
= 0, no additional cycles
> 0, perform additional flutter analysis cycles with stiffness variations applied to a mode
$0 \leq LC(26) \leq 20$

LC(27) = index of mode whose frequency and stiffness is to be varied for the LC(26) cycles
If LC(26) = 0, set LC(27) = 0

LC(28) = print option for modal eigenvectors
= 1, print
= 0, no print
If LC(1) = -1, the eigenvectors for the critical flutter root in a user-chosen velocity interval are displayed
If LC(1) = 0 or 2, set LC(28) = 0
If LC(1) = 1, the eigenvectors for all roots between user chosen reduced velocities, VBO, and real frequencies are displayed

LC(29) = print option for physical vectors corresponding to modal eigenvectors
= 1, print
= 0, no print

LC(30) = print option for k solution flutter determinant matrix analysis
= 1, print
= 0, no print
If LC(1) = -1 or 0, set LC(30) = 0

LC(31) = index defining revisions to generalized mass matrix and modal frequencies
= 1, revise
= 0, no change

LC(32) = index defining revisions to generalized stiffness matrix
= 1, revise
= 0, no change

LC(33) = index defining type of aerodynamics
= 1, steady state
= 0, oscillatory
If LC(1) = 2, set LC(33) = 1

LC(34) = not used. Set = 0

LC(35) = not used. Set = 0

LC(36) = not used. Set = 0

LC(37) = print option for aerodynamic element geometric data associated with doublet lattice and constant pressure methods
= 1, print
= 0, no print
If LC(21) ≠ 1, set LC(37) = 0

LC(38) = tape unit for ASCII printout of generalized forces and associated information. Suggest LC(38) = 99

LC(39) = not used. Set = 0

LC(40) = not used. Set = 0

6.3.3.1 INV
Format (I5)

1. Description: Input vibration data location flag.

2. Notes:

INV = integer defining location of input vectors, modal frequencies, and generalized masses
= 1, STARS binary file
= 2, this input file

6.3.3.1.1 NMDOF (Required if INV = 2)
Format (I5)

1. Description: Input vector degrees of freedom.

2. Notes:

NMDOF = total number of modal degrees of freedom used to define an input mode shape
$0 \leq \text{NMDOF} \leq 1000$

6.3.3.1.2 (QZ(I), I = 1, NMDOF) (Required if INV = 2)
Format (7E10.0)

1. Description: LC(2) sets of NMDOF input deflections.

2. Note:

QZ(I) = principal out-of-plane deflection at point I of input vector

6.3.3.1.3 NCARD (Required if INV = 2)
Format (I5)

1. Description: Mass matrix specifications.

2. Note:

NCARD = Number of nonzero generalized mass matrix elements

6.3.3.1.4 I, J, WW(I,J) (Required if INV = 2)
Format (2I5, E10.0)

1. Description: NCARD sets of data specifying nonzero generalized mass matrix elements.

2. Notes:

I = row index of generalized mass matrix
J = column index of generalized mass matrix
WW(I,J) = generalized mass (weight) matrix value, lbf

6.3.3.1.5 (OMG(I), I = LC(2)) (Required if INV = 2)
Format (7E10.0)

1. Description: LC(2) modal frequencies.

2. Note:

OMG(I) = modal frequency in proper order, Hz

6.3.4.1 BR, FMACH
Format (2E10.4)

1. Description: Reference values for aerodynamics.

2. Notes:

BR = reference semichord, in.

FMACH = reference freestream Mach number
If FMACH < 1.0, doublet lattice method is used
If FMACH ≥ 1.0, constant pressure method is used

6.3.4.2 (VBO(I), I = 1, LC(4)) (Required if LC(1) = 1)
Format (7F10.4)

1. Description: LC(4) reduced velocities.

2. Notes:

VBO(I) = reduced velocity (V/bω) for flutter-divergence analysis

If aerodynamic interpolation is chosen, then aerodynamic forces will be interpolated at each of these VBO(I) values, using the values for RVBO input in section 6.3.4.4; if direct calculation is used, the aerodynamic forces will be calculated at each of these reduced velocities. $0 \le LC(4) \le 30$

6.3.4.3 NV, V1, DV (Required if LC(1) = -1)
Format (I5, 2F10.0)

1. Description: Airspeed velocity specification for p-k analysis.

2. Notes:

NV = number of velocities used in initial analysis, knots
$1 < NV \le 20$

V1 = lowest velocity from which to start analysis, knots
$V1 \ge 200$, suggested

DV = velocity increment to be summed to V1 during initial analysis, knots
$DV \le 250$, suggested

6.3.4.4 TOLI, (RVBO(I), I = 1, 6) (Required if LC(1) = -1 or LC(13) = 1)
Format (7E10.0)

1. Description: Aerodynamic forces interpolation data.

2. Notes:

TOLI = tolerance value used for testing the interpolation fit; a nominal value of 1.0E-03 is recommended

RVBO(I) = reduced velocity at which aerodynamic forces will be computed, to be used as part of the basis in interpolating forces at other reduced velocities

If aerodynamic interpolation is used, the RVBOs should span the entire range of VBOs of section 6.3.4.2.

For LC(1) = -1, use the following approximations:

1. $RVBO(1) \le 1.69 \times 12.0 \times V1 / (BR \times WMAX)$, where
WMAX = maximum modal frequency, rad/sec.

2. $RVBO(6) \ge 1.69 \times 12.0 \times VMAX / (BR \times WMIN)$, where
$VMAX = V1 + (NV - 1) \times DV$, and
WMIN = minimum modal frequency, rad/sec.

6.3.5.1 MADD, IADD, MSYM (Required if LC(31) = 1)
Format (3I5)

1. Description: Specifications for changes to mass matrix and modal frequencies.

2. Notes:

MADD = number of changes to mass matrix

IADD = number of changes to modal frequencies

MSYM = integer specifying symmetry of mass matrix modifications
= 0, changes are symmetric
= 1, changes are nonsymmetric

6.3.5.1.1 I, J, WW(I, J) (Required if MADD > 0)
Format (2I5, F10.0)

1. Description: MADD changes to the mass matrix.

2. Notes:

I = row index of mass matrix element

J = column index of mass matrix element

WW(I,J) = value to be substituted for existing element in mass matrix, lbm

If MSYM = 0, specify only changes to upper triangular elements.

6.3.5.1.2 I, OMG(I) (Required if IADD > 0)
Format (I5, F10.0)

1. Description: IADD changes to modal frequencies.

2. Notes:

I = index of mode to be changed

OMG(I) = new frequency to be substituted for old, Hz

6.3.5.2 GDD (Required if LC(16) = 1)
Format (E10.4)

1. Description: General structural damping factor.

2. Note:

GDD = A single value for hysteretic damping to be applied to all modes; the imaginary term on the diagonal of the complex stiffness matrix will be multiplied by the term GDD

6.3.5.3 NCD (Required if LC(16) = -1)
Format (I5)

1. Description: Integer specifying individual structural damping.

2. Note:

NCD = number of individual modes for which hysteretic damping will be specified

6.3.5.3.1 (I, GDP(I)) (Required if LC(16) = -1 and NCD ≠ 0)
Format (I5, E10.0)

1. Description: NCD individual structural damping values.

2. Notes:

I = mode index

GDP(I) = hysteretic damping applied to mode I

6.3.6.1 GMAX, GMIN, VMAX, FMAX (Required if LC(1) ≠ 2)
Format (4F10.0)

1. Description: Maximum and minimum scales for V-g, V-f print plots.

2. Notes:

GMAX = maximum value of damping scales for V-g plots

GMIN = minimum value of damping scale for V-g plots

VMAX = maximum value of velocity scale for V-g and V-f plots, knots

FMAX = maximum value of frequency scale for V-f plots, Hz

6.3.7.1 (RHOR(I), I = 1, LC(5)) (Required if LC(1) ≠ 0)
Format (7F10.0)

1. Description: LC(5) values of air density ratios.

2. Notes:

RHOR(I) = density ratio with respect to sea level
$0 < RHOR(I) \leq 10$

A separate flutter and/or divergence analysis is performed at each density ratio in which the aerodynamic force matrix is multiplied by the square root of the density ratio.

6.3.8.1 NADDF, NSYM (Required if LC(9) = 1)
Format (2I5)

1. Description: Specifications for frequency-independent additions to aerodynamic matrix.

2. Notes:

NADDF = number of following additions to the flutter-determinant aerodynamic matrix

NSYM = index defining symmetry of additions
= 0, additions are symmetric. Input only upper triangular elements

= 1, additions are not symmetric

6.3.8.1.1 I, J, DETAD(I, J) (Required if LC(9) = 1)
Format (2I5, 2E10.0)

1. Description: NADDF frequency-independent additions to aerodynamic matrix.

2. Notes:

I = row index of additions

J = column index of additions

DETAD(I, J) = value of addition. DETAD(I,J) is a complex value

Additions to the aerodynamic matrix QBAR are done in the following manner:

$$\text{QBAR} = \text{QBAR} + \frac{\text{DETAD}_{\text{REAL}}}{k^2} + i^* \frac{\text{DETAD}_{\text{IMAG}}}{k},$$

where k is the reduced frequency and $i^* = \sqrt{-1}$

6.3.8.2 NADDS, NSYM (Required if LC(32) = 1)
Format (2I5)

1. Description: Specifications for changes to generalized stiffness matrix.

2. Notes:

NADDS = number of following changes to the stiffness matrix

NSYM = index specifying symmetry of changes
= 0, changes are symmetric (B(I,J) = B(J,I))
= 1, changes are not symmetric

6.3.8.2.1 I, J, B(I, J) (Required if LC(32) = 1)
Format (2I5, 2E10.0)

1. Description: NADDS changes to stiffness matrix.

2. Notes:

I = row index of changes

J = column index of changes

B(I, J) = new value of complex stiffness matrix element

If NSYM = 0, only the upper triangular elements are input.

6.3.8.3 RATOM(I) (Required if LC(26) > 0)
Format (7E10.0)

1. Description: LC(26) values of stiffness variations for an input mode.

2. Note:

RATOM(I) = ratio of modal frequency with respect to the original input value, OMG(I)

6.3.8.3.1 NOTIR, (NINZ(J), J=1, NOTIR) (Required if LC(25) ≠ 0)
Format (10I5)

1. Description: LC(25) sets of modal elimination specification for flutter and divergence analysis.

2. Notes:

NOTIR = number of deleted modes in a given modal elimination cycle

NINZ = index of individual deleted mode for a given cycle

It should be noted that the aero module always does an initial analysis without modal deletions before doing any modal elimination analyses as defined in this section.

6.3.9.1 VA, VB (Required if LC(28) = 1 and LC(1) ≠ 2)
Format (2E10.0)

1. Description: Eigenvector calculation range.

2. Notes:

VA = lower bound of the range over which the eigenvectors are to be calculated

VB = upper bound of the range over which the eigenvectors are to be calculated

If LC(1) = -1, the range is over velocity, V, knots

If LC(1) = 1, the range is over reduced velocity, $\frac{V}{B\omega}$

6.3.9.2 FLO, FHI (Required if LC(28) = 1 and LC(1) = 1)
Format (2E10.0)

1. Description: Eigenvector display range.

2. Notes:

FLO = lower bound of the frequency range over which the eigenvectors are to be displayed, Hz

FHI = upper bound of the frequency range over which the eigenvectors are to be displayed, Hz

6.3.10.1 FL, ACAP
Format (2F10.0)

1. Description: Reference length and area.

2. Notes:

FL = reference chord of model, in. (2.0 × BR, normally)

ACAP = reference area of the model, in^2

6.3.10.2 NDELT, NP, NB, NCORE, N3, N4, N7
Format (7I5)

1. Description: Doublet lattice and constant pressure methods geometrical paneling data.

2. Notes:

NDELT = index defining aerodynamic symmetry
= 1, aerodynamics are symmetrical about Y = 0
= -1, aerodynamics are antisymmetrical about Y = 0
= 0, no symmetry about Y = 0 (single surface only)

NP = total number of "panels" on all lifting surfaces

NB = body identification flag
= 0, no bodies of any kind
> 0, number of slender bodies used for doublet lattice analysis
= -1, constant pressure method body elements exist
$0 \leq NB \leq 20$ for doublet lattice method

NCORE = problem size, N × M, where
N = total number of aerodynamic elements, and
M = number of modes

N3 = print option for pressure influence coefficients
= 1, print
= 0, no print

N4 = print option for influence coefficients relating downwash on lifting surfaces to body element pressures
= 1, print
= 0, no print

N7 = index specifying calculation of pressures and generalized forces
= 1, calculate
= 0, cease computations after influence coefficients are determined
If LC(1) = -1 or 1, set N7 = 1

6.3.11.1 IBOD1, IBOD2 (Required if NB = -1)
Format (2I5)

1. Description: Aerodynamic elements defining contiguous panels which describe a supersonic body for the constant pressure method.

2. Notes:

IBOD1 = first aerodynamic element on first panel (lowest index)

IBOD2 = last aerodynamic element on last panel (highest index)

6.3.12.1 6.3.12.1.1 to 6.3.12.1.5 are repeated for NP sets of surface paneling data.

6.3.12.1.1 XO, YO, ZO, GGMAS
Format (4F10.0)

6.3.12.1.2 X1, X2, X3, X4, Y1, Y2
Format (6F10.0)

6.3.12.1.3 Z1, Z2, NEBS, NEBC, COEFF
Format (2F10.0, 1X, 2I3, 3X, F10.0)

6.3.12.1.4 (TH(I), I = 1, NEBC)
Format (6F10.0)

6.3.12.1.5 (TAU(I), I = 1, NEBS)
Format (6F10.0)

1. Description: NP sets of data defining aerodynamic panels and their component aerodynamic elements. Section 6.3.12.1.1 translates and rotates panels. Such coordinates are in the global (aircraft) system indicating position of the origin of the LCS for each panel. Section 6.3.12.1.2 contains coordinates of points defining an aerodynamic panel, while section 6.3.12.1.3 defines boundaries of "aerodynamic elements" in the panel. The panel is divided into a number of smaller trapezoids, called "aerodynamic elements," by lines of constant percent panel chord and of constant percent panel span. Section 6.3.12.1.4 defines chordwise panel stations, and 6.3.12.1.5 defines spanwise panel stations.

2. Notes:

XO = translational value to be applied to x-coordinates, in.

YO = translational value to be applied to y-coordinates, in.

ZO = translational value to be applied to z-coordinates, in.

GGMAS = panel dihedral or rotation, deg, about global x-axis

GGMAS is in a right-handed coordinate system; an upright panel would require a positive rotation of 90°.

X1 = x-coordinate of panel inboard leading edge, in.

X2 = x-coordinate of panel inboard trailing edge, in.

X3 = x-coordinate of panel outboard leading edge, in.

X4 = x-coordinate of panel outboard trailing edge, in.

Y1 = y-coordinate of panel inboard edge, in.

Y2 = y-coordinate of panel outboard edge, in.

Z1 = z-coordinate of panel inboard edge, in.

Z2 = z-coordinate of panel outboard edge, in.

Coordinates are in the local coordinate system.

NEBS = number of element boundaries in the spanwise direction
$2 \leq NEBS \leq 50$
NEBS must be set = 2 for each body interference panel

NEBC = number of element boundaries in the chordwise direction
$2 \leq NEBC \leq 50$

COEFF = entered as 0.0

TH(I) = chordwise element boundaries for the panel in fraction of chord
$0.0 \leq TH \leq 1.0$
(TH(1) = 0.0, TH(NEBC) = 1.0)

TAU(I) = spanwise element boundaries for the panel in fraction of span
$0.0 \leq TAU \leq 1.0$
(TAU(1) = 0.0, TAU(NEBS) = 1.0)

The data is to be repeated NP times in the following sequence:

1. Vertical panels or plane of symmetry (y = 0).
2. Panels on other surfaces.
3. Body interference panels. These panels must be one element wide (that is, NEBS = 2).

There are (NEBS - 1) × (NEBC - 1) aerodynamic elements on a primary or control surface.

Indices for aerodynamic elements start at the inboard leading edge element, increase while traveling aft down a strip, then outward strip by strip, ending at the outboard trailing edge element.

6.3.13.1 6.3.13.1.1 to 6.3.13.1.4 are repeated for NB sets of slender body data. (Required if NB > 0)

6.3.13.1.1 XBO, YBO, ZBO
Format (3F10.0)

6.3.13.1.2 ZSC, YSC, NF, NZ, NY, COEFF, MRK1, MRK2
Format (2F10.0, 1X, 3I2, 3X, 1F10.0, 2I3)

6.3.13.1.3 (F(I), I = 1, NF)
Format (6F10.0)

6.3.13.1.4 (RAD(I), I = 1, NF)
Format (6F10.0)

1. Description: NB sets of data defining subsonic slender bodies and their component elements. Section 6.3.13.1.1 defines X, Y, and Z global reference coordinates, and section 6.3.13.1.2 defines slender body origin, elements, and any related interference

panels. Section 6.3.13.1.3 defines slender body element stations, while section 6.3.13.1.4 defines slender body radii.

2. Notes:

XBO	=	translational value to be added to X-coordinate, in.
YBO	=	translational value to be added to Y-coordinate, in.
ZBO	=	translational value to be added to Z-coordinate, in.
ZSC	=	local z-coordinate of the body axis, in.
YSC	=	local y-coordinate of the body axis, in.
NF	=	number of slender body element boundaries along its axis $2 \leq NF \leq 50$
NZ	=	flag for body vibration in z-direction
	=	1, body vibrating
	=	0, body not vibrating
NY	=	flag for body vibration in y-direction
	=	1, body vibrating
	=	0, body not vibrating
COEFF	=	entered as 0.0
MRK1	=	index of the first aerodynamic element on the first interference panel associated with this slender body
MRK2	=	index of the last aerodynamic element on the first interference panel associated with this slender body
F(I)	=	x-coordinate of body station defining a slender body element in local coordinates, in. starting with body nose and proceeding aft
RAD(I)	=	radii of body elements at the stations F(J), in.

NZ must never equal NY.

Vertically vibrating bodies should be input before laterally vibrating ones; if both vertical and lateral body vibrations are desired in a single body, two bodies are input at the same location with corresponding NZ and NY.

A slender body, as defined here, is a frustum of a right angle cone; there are (NF - 1) slender body elements.

6.3.14.1 NSTRIP, NPR1, JSPECS, NSV, NBV, NYAW
Format (6I5)

1. Description: General aerodynamics data.

2. Notes:

NSTRIP = number of chordwise strips of panel elements on all panels.
For LC(8) = 0, set NSTRIP = 1
Printouts of lift and moment coefficients for the strips occur for NSTRIP > 1
Never set NSTRIP = 0

NPR1 = print option for pressures in subroutines QUAS or FUTSOL. Use only for debugging
= 1, print
= 0, no print

JSPECS = index describing plane's aerodynamic symmetry about Z = 0
= 1, antisymmetrical aerodynamics about Z = 0 (biplane or jet effect)
= -1, symmetrical about Z = 0 (ground effect)
= 0, no symmetry about plane Z = 0

NSV = number of strips lying on all vertical panels on the symmetric plane Y = 0

NBV = number of elements on all vertical panels lying on the plane Y = 0

NYAW = symmetry flag
= 0, if NDELT = 1 (symmetric about Y = 0)
= 1, if NDELT = -1 (antisymmetric about Y = 0)
= 0 or 1, if NDELT = 0 (asymmetric about Y = 0)

6.3.14.1.1 (LIM(I,1), LIM(I,2), LIM(I,3), I = 1, NSTRIP)
Format (3I3)

1. Description: NSTRIP sets of data defining chordwise strips for aerodynamic coefficient calculations.

2. Notes:

LIM(I,1) = index of first element on each chordwise strip

LIM(I,2) = index of last element on each chordwise strip

LIM(I,3) = 0

For NSTRIP = 1, a blank card is used.

6.3.15.1 6.3.15.1.1 and 6.3.15.1.2 are repeated for LC(3) sets of primary surface data.

6.3.15.1.1 KSURF, NBOXS, NCS
Format (1L5, 2I5)

6.3.15.1.2 NLINES, NELAXS, NICH, NISP
Format (4I5)

6.3.15.2 6.3.15.2.1 and 6.3.15.2.2 are repeated for NLINES subsets of data.

6.3.15.2.1 NGP, XTERM1, YTERM1, XTERM2, YTERM2
Format (I5, 4E10.0)

6.3.15.2.2 (YGP(I), I = 1, NGP)
Format (8E10.0)

6.3.15.3.1 DIST (Required if NELAXS = 1)
Format (E10.0)

6.3.15.3.2 (X1(I), Y1(I), X2(I), Y2(I), I = 1, NCS) (Required if KSURF = T)
Format (4E10.0)

6.3.15.3.3 NLINES, NELAXS, NICH, NISP (Required if KSURF = T)
Format (4I5)

6.3.15.4 6.3.15.4.1 and 6.3.15.4.2 are repeated for NLINES subsets of data. (Required if KSURF = T)

6.3.15.4.1 NGP, XTERM1, YTERM1, XTERM2, YTERM2
Format (I5, 4E10.0)

6.3.15.4.2 (YGP(I), I = 1, NGP)
Format (8E10.0)

6.3.15.5 DIST (Required if NELAXS = 1 and KSURF = T)
Format (E10.0)

1. Description: LC(3) sets of input modal vector data to be applied to interpolation of deflections for primary and control surface aerodynamic elements.

2. Notes:

KSURF = flag indicating control surfaces on a primary surface
= T, this surface has one or more control surfaces with forward hinge lines
= F, this surface has no control surfaces

NBOXS = number of elements on this surface, including those on control surfaces

NCS = number of control surfaces on primary surface
$0 \leq NCS \leq 5$

NLINES = number of lines along which input modal vector data are prescribed
$1 \leq NLINES \leq 50$

NELAXS = index defining input vector components
= 1, translation and pitch rotation are prescribed at each input point
= 0, only translation is prescribed

NICH = index defining chordwise interpolation/extrapolation from input vector to aerodynamic elements
= 0, linear
= 1, quadratic
= 2, cubic

NISP = index defining spanwise interpolation/extrapolation from input vector to aerodynamic elements
= 0, linear

= 1, quadratic
= 2, cubic

NGP = number of points on an input vector line
$2 \leq NGP \leq 50$

XTERM1 = X-coordinate specifying the inboard end of an input vector line in the local coordinate system

YTERM1 = Y-coordinate specifying the inboard end of an input vector line in the local coordinate system

XTERM2 = X-coordinate specifying the outboard end of an input vector line in the local coordinate system

YTERM2 = Y-coordinate specifying the outboard end of an input vector line in the local coordinate system

YGP(I) = spanwise coordinate of a point along an input vector line, going inboard to outboard in the local coordinate system

X1(I) = X-coordinate of the inboard terminus of the Ith control surface leading edge in LCS

Y1(I) = Y-coordinate of the inboard terminus of the Ith control surface leading edge in LCS

X2(I) = X-coordinate of the outboard terminus of the Ith control surface leading edge in LCS

Y2(I) = Y-coordinate of the outboard terminus of the Ith control surface leading edge in LCS

DIST = displacement reference distance

6.3.16.1 The following sets of data are repeated NB times. (Required if NB > 0)

6.3.16.1.1 NGP, NSTRIP, IPANEL
Format (3I5)

6.3.16.1.2 (XGP(I), I = 1, NGP)
Format (6F10.0)

1. Description: NB sets of data describing input modal vector to be applied to slender body aerodynamic elements deflection.

2. Notes:

NGP = number of points on a slender body axis at which input vector data are prescribed
$2 \leq NGP \leq 50$

NSTRIP = number of interference panels (or strips) associated with a slender body

IPANEL = index of the first such interference panel associated with a slender body

XGP(I) = streamwise coordinate of each point at which input modal data are prescribed, in LCS

This data is not to be input for a constant pressure method model

6.3.17.1 KLUGLB
Format (I5)

1. Description: Print option for global geometry.

2. Notes:

KLUGLB = print option for aerodynamic elements in global coordinate system
= 1, print
= 0, no print

6.3.18 NOTES ON PROGRAM USAGE

Aerodynamic Modules

The STARS aerodynamic module consists of two unsteady, linear, inviscid, aerodynamic codes: the doublet lattice method (DLM) for subsonic analyses, and the constant pressure method (CPM) (ref. 17) for supersonic analyses. Flutter and divergence solutions may be obtained by k, p-k, or state-space methods.

Aerodynamic Modeling

The aerodynamic elements on lifting and interfering surfaces consist of trapezoidal elements parallel to the free stream. The aspect ratio of an element should be, ideally, on the order of unity or less.

The number of elements required for accurate analysis varies with the model and the reduced frequency values. Increasing the number of elements will increase the computational time. Higher reduced frequencies require smaller and, therefore, more elements. A guide for element size in the streamwise direction is

$$k \, \Delta x \leq 0.04,$$

where k is reduced frequency, and Δx is element length.

Elements should be concentrated near wing tips, leading and trailing edges, control surface hinges, and so forth. As a guide, a cosine distribution of elements over the wing's chord and full span may be adopted.

The surface element may be thought of as having an unsteady horseshoe vortex bound along the quarter chord of the element and trailing aft to infinity. The downwash from the unsteady vortices are calculated at a control point located at the three-quarter chord of an element's centerline. Since the induced downwash at the center of a vortex is infinite, no control point should ever lie on any vortex line, such as along the extension of any element edge, either upstream or downstream.

Purpose: Prepare CONVERT.DAT data file; selection of desired modes.

Description: Enables selection of desired modes.

6.4.1 $ JOB TITLE
Format (FREE)

6.4.2 NM
Format (I5)

1. Description: General data.

2. Note:

NM = total number of desired modes to form reduced generalized matrices

6.4.3 $ MODAL SELECTION AND ORDERING
Format (FREE)

6.4.3.1 IOLD, INEW
Format (2I5)

1. Description: Orders the modes to be used for ASE analysis, NM sets of data.

2. Notes:

IOLD = old modal number

INEW = new modal number

3. Note:

Output is the reduced generalized force matrix and is stored in PD.DAT file for subsequent input into the ASE module.

Purpose: Prepare PADE.DAT data file.

Description: Performs Padé curve fitting of unsteady aerodynamic forces and state-space matrix formulation.

6.5.1 $ JOB TITLE
Format (FREE)

6.5.2 NRM, NEM, NCM, NG, NS, NK, NA, RHOR, VEL, CREF, IWNDT, NQD
Format (FREE)

1. Description: General input data.

2. Notes:

NRM = number of rigid body modes

NEM = number of elastic modes

NCM = number of control modes

NG = number of gusts

NS = number of sensors

NK = number of sets of input data at discrete reduced frequencies

NA = order of Padé equation
$0 \leq NA \leq 4$

RHOR = relative aerodynamic density with respect to sea level

VEL = true airspeed, ft/sec

CREF = reference chord, ft

IWNDT = wind tunnel correction index
= 0, uses formulation as in reference 16
= 1, uses wind tunnel data to modify aerodynamic generalized force matrix as in reference 16

NQD = number of velocities for flutter and divergence analysis, to be set to 0 for ASE analysis as in reference 16

6.5.3 $ TENSION COEFFICIENTS
Format (FREE)

6.5.3.1 (BETA(I), I = 1, NA)
Format (FREE)

1. Description: Padé approximate's data.

2. Note:

BETA(I) = tension coefficients

6.5.4 $ GENERALIZED MASSES
Format (FREE)

6.5.4.1 ((GMASS(I, J), J = I, NM), I = 1, NM)
Format (FREE)

1. Description: Generalized mass data, upper symmetric half, starting with diagonal element.

2. Notes:

NM = total number of modes
= NRM + NEM + NCM

GMASS(I) = generalized mass of mode I, slugs

6.5.5 $ GENERALIZED DAMPING
Format (FREE)

6.5.5.1 (DAMP(I), I = 1, NM)
Format (FREE)

1. Description: Generalized damping data.

2. Note:

DAMP(I) = generalized damping applied to mode I

6.5.6 $ NATURAL FREQUENCIES
Format (FREE)

6.5.6.1 (OMEGA(I), I = 1, NM)
Format (FREE)

1. Description: Modal frequency data.

2. Note:

OMEGA(I) = natural frequency of mode I, rad/sec

6.5.7 $ VELOCITIES FOR FLUTTER AND DIVERGENCE ANALYSES (Required if NQD > 1)
Format (FREE)

6.5.7.1 (VEL(I), I = 1, NQD) (Required if NQD > 0)
Format (FREE)

1. Description: True airspeed data for flutter and divergence analyses, ft/sec.

2. Note:

VEL(I) = airspeed values to be used to calculate the frequency and damping

6.5.8 $ AIRCRAFT ANGLES, DEGREES OF FREEDOM (Required if NQD = 0)
Format (FREE)

6.5.8.1 PHI, THETA, PSI, US, VS, WS, PS, QS, RS, PHID, THAD, PSID, NDOF (Required if NQD = 0)
Format (FREE)

1. Description: Data for transformation of earth- to body-centered coordinate systems.

2. Notes:

PHI	=	roll angle, deg
THETA	=	pitch angle, deg
PSI	=	yaw angle, deg
US, VS, WS	=	body axes velocities
PS, QS, RS	=	angular rates
PHID, THAD, PSID	=	Euler angle rates
NDOF	=	number of aircraft degrees of freedom; a negative sign indicates antisymmetric case

6.5.9 $ SENSOR DATA (Required if NQD = 0 and NS > 0)
Format (FREE)

6.5.9.1 IFLSI
Format (FREE)

1. Description: Flag for identification of sensor interpolation points in presence of GVS data only.

2. Notes:

IFLSI	=	1,	for antisymmetric case
	=	-1,	for symmetric case
	=	0,	for non-GVS case

6.5.9.2 XS, YS, ZS (Required if NQD = 0 and NS > 0)
Format (FREE)

LX, MY, NZ, THX, THY, THZ
Format (FREE)

1. Description: Sensor location and orientation; NS sets of data.

2. Notes:

XS	=	X-coordinate of sensor
YS	=	Y-coordinate of sensor

ZS	=	Z-coordinate of sensor
LX	=	direction cosine for accelerometer normal in X
MY	=	direction cosine for accelerometer normal in Y
NZ	=	direction cosine for accelerometer normal in Z
THX	=	direction cosine for pitch axis about X
THY	=	direction cosine for pitch axis about Y
THZ	=	direction cosine for pitch axis about Z

3. Notes:

For the case IFLSI $\neq 0$, the user must modify file VEC_AND_COORDS.DAT by defining appropriate sensor location. This is done by setting the fourth column of the relevant nodes in the nodal coordinates section of the data file to the appropriate value of IFLSI.

Purpose: Prepare frequency response analysis data file.

6.6.1 $ JOB TITLE
Format (FREE)

6.6.2 NX, NY, NU, NV, NXC, DELTAT, TDELAY, MAXBC, MAXPO
Format (FREE)

1. Description: System parameters.

2. Notes:

NX = number of states in the plant
= $[2\times(NRM + NEM) + NA\times(NRM + NEM + NCM)]$ (Refer to section 6.5)

NY = number of outputs from the plant
= (number of rows of C matrix)
= $(2\times NS\times 3)$

NU = number of inputs to the plant
= $(2\times NCM)$

NV = number of external inputs to the system

NXC = total number of continuous states (plant plus analog elements)

DELTAT = sample time for digital elements

TDELAY = system time delay

MAXBC = maximum number of block connectivity

MAXPO = maximum polynomial order plus one

6.6.3 NB, NYBTUV, IADDRA, IADDCB, IADDRC, NLST, NDRESP, IRP, ITRP
Format (FREE)

1. Notes:

NB = number of analog and digital elements in the system including the summing elements and excluding the plant

NYBTUV = NYTOV + NBTOU (See section 6.6.10.2 for definitions.)

IADDRA = additional rows of A due augmentation of control elements; appropriate summation of orders of polynomial of all analog elements for open- as well as closed-loop solutions to be derived from block connectivity input

IADDCB = additional columns of B due augmentation of control elements

IADDRC = additional rows of C due augmentation of control elements, equal to the number of connecting links into block/connecting junction

NLST = total number of frequency range specifications for frequency response computations

NDRESP = number of times the loops are broken for open-loop response evaluation

IRP = frequency response problem number to be evaluated

ITRP = total number of frequency response cases

6.6.4.1 $ BLOCK CONNECTIVITY
Format (FREE)

1. Note:

Analog blocks to precede digital blocks

6.6.4.2 IBN, ICN1, ICN2, ICN3, IEXI, ISLPCL, IELPCL
Format (7I5)

1. Notes:

IBN = integer defining block number

ICN1, ICN2, ICN3 = connecting block numbers, up to 3

IEXI = integer defining external input number

ISLPCL = integer defining starting block of the closed-loop system

IELPCL = integer defining closing block of the closed-loop system

2. Note:

A symbolic gain block indicating closing of loop is identified by presence of starting and closing blocks.

6.6.5.1 $ TRANSFER FUNCTION DESCRIPTION, AS ORDER OF POLYNOMIALS, FOR EACH BLOCK
Format (FREE)

1. Note:

The polynomial descriptions pertain to either analog or digital elements, as appropriate.

6.6.5.2 IBN, ICNP, ICDP
Format (3I5)

1. Notes:

ICNP = integer defining number of coefficients in the numerator polynomial

ICDP = integer defining number of coefficients in the denominator polynomial

6.6.6.1 $ LISTING OF POLYNOMIAL COEFFICIENTS
Format (FREE)

6.6.6.2 IBN, (POLCON(I), I=1, MAXPO)
Format (I5, < MAXPO > (E10.4))
IBN, (POLCOD(I), I=1, MAXPO)
Format (I5, <MAXPO > (E10.4))

1. Notes:

   1. The coefficients are to be listed in increasing order of polynomials.

   2. The numerator coefficients (POLCON) are placed in one row followed by the denominator (POLCOD) ones in the next row, for each block, one block at a time.

   3. Data to be prepared for each block, NB sets of data being the input.

6.6.7.1 $ GAIN INPUTS FOR EACH BLOCK
Format (FREE)

6.6.7.2 IBN, GAIN
Format (5(I5, E10.4))

1. Note:

   Gains may alternatively be the input as multiplier of polynomial coefficients in the numerator. NB sets of data are the input.

6.6.8.1 $ SPECIFICATION FOR SYSTEM OUTPUTS, NYB = NY + NB NUMBER OF DATA
Format (FREE)

6.6.8.2 ISO1, ISO2, . . ., ISONYB
Format (16I5)

1. Description: This data is needed for closed-loop frequency response analysis only.

2. Notes:

   1. Plant output are numbered 1 through NY.

   2. Each block output is numbered as NY + IBN.

3. Note:

   ISOI = desired output from any sensor (corresponding row of C matrix for the plant) and any control element (augmented thereafter)

6.6.9.1 $ SPECIFICATION FOR SYSTEM INPUTS, NUV = NU + NV NUMBER OF DATA
Format (FREE)

6.6.9.2 ISI1, ISI2, . . ., ISINUV
Format (16I5)

1. Notes:

    1. Plant input are numbered 1 through NU.

    2. Each block input is numbered as NU + IEXI.

2. Note:

    ISII = plant input (corresponding column of **B** matrix for the plant) and external input

6.6.10.1 $ CONNECTION DETAILS FROM PLANT TO BLOCKS
Format (FREE)

6.6.10.2 NYTOV, NBTOU, NBTOK
Format (3I5)

1. Notes:

    NYTOV = number of connections from plant outputs to external inputs

    NBTOU = number of block outputs connected to plant inputs

    NBTOK = number of digital element outputs connected to analog element inputs

6.6.10.3 IYTOV1, IYTOV2
Format (2I5)

1. Notes:

    IYTOV1 = row number of C matrix corresponding to output from plant to feedback control system

    IYTOV2 = external input number which describes connection of plant output to control system

2. Note:

    Repeat NYTOV times, ISO to IEXI.

6.6.10.4 IBTOU1, IBTOU2
Format (2I5)

1. Notes:

    IBTOU1 = block number to be connected to plant input

    IBTOU2 = column of **B** matrix to which block is connected

2. Note:

    Output NBTOU times, IBN to ISI.

6.6.10.5 IBTOK1, IBTOK2
Format (2I5)

1. Note:

Output NBTOK times, IBN (ANALOG) to IBN (DIGITAL).

6.6.11.1 $ FREQUENCY RANGE SPECIFICATION (Required if NLST ≠ 0)
Format (FREE)

6.6.11.2 FREQI, FREQF, NFREQ
Format (2F10.4,I5)

1. Notes:

FREQI = initial frequency

FREQF = final frequency

NFREQ = number of frequencies within range, logarithmically spaced

2. Note:

Data to be repeated NLST times

6.6.12.1 $ LOOP DEFINITIONS
Format (FREE)

6.6.12.2 ILOOP, IPRINT
Format (FREE)

6.6.12.3 NBRAK1, NBRAK2 (Required if ILOOP = 1)
Format (2I5)

1. Notes:

ILOOP = integer defining loop type
= 0, for closed loop case
= 1, for open loop case

IPRINT = eigensolution print option for closed loop case
= 0, prints eigenvalues only
= 1, prints eigenvalues and vectors

NBRAK1 = block having the output signal

NBRAK2 = block having the input signal

2. Note:

Data of 6.6.12.3 to be repeated NDRESP times.

7. SAMPLE PROBLEMS
(STARS Integrated Aero-Structural-Control Systems Analysis)

A simplified aircraft test model (ATM) is selected as a standard problem for the full spectrum of ASE analyses. In this section, the relevant data (fig. 30), for associated SOLIDS, AERO, and ASE modules are presented in detail. Each such data set is also followed by relevant output of results. The input data are prepared in accordance with procedures described in section 6.

Three perfect rigid body modes (Y-translation, X-rotation roll, and Z-rotation yaw about center of gravity - Φ_{PR}) and two rigid control modes (aileron and rudder deflections - Φ_C) are generated in this module along with eight elastic (Φ_E) and three usual rigid body modes (Φ_R), of which the latter are excluded from consideration as GENMASS data input. The perfect rigid body modes Φ_{PR} are moved in the front through convert data input for subsequent ASE analysis ($\Phi = \Phi_{PR} + \Phi_E + \Phi_C$).

7.1 ATM: Free Vibration Analysis (STARS-SOLIDS)

The input data pertain to the free vibration analysis of the finite element model. The direct modal interpolation option is used for subsequent flutter and ASE analyses.

The finite element model (fig. 31) of the symmetric half of the aircraft is utilized for the vibration analysis. Only the typical antisymmetric case is presented here; figure 32 shows a direct interpolation scheme for subsequent aeroelastic and aeroservoelastic analyses.

STARS-SOLIDS input data:

```
 AERO TEST MODEL
C
C ANTISYMMETRIC HALF MODEL
C IINTP  = 1, DIRECT INTERPOLATION OF NODAL DATA
C
C NCNTRL = 5, FIRST THREE TO GENERATE PERFECT RIGID BODY MODES
C Y TRANSLATION, ROLL AND YAW, PLUS AILERONS AND RUDDER CONTROL
C MODES.
C///////////////////////////////////////////////////////////////////////
   74,  149,    1,    4,   22,    5,    0,    0,    0,   0
    0,    0,    0,    0,    0,    0,    5,  132
    1,    1,    0,    0,    0,    1,    0,    1
    2,    0,    2,    0,    1
    1,   11,    0, 0.7500E+03, 0.0000E+00,   0.0
$ NODAL DATA
    1  300.0000  200.0000    0.0000    0    0    0    0    0    0    0    0
    2  312.5000  200.0000    0.0000    0    0    0    0    0    0    0    0
    3  325.0000  200.0000    0.0000    0    0    0    0    0    0    0    0
    4  337.5000  200.0000    0.0000    0    0    0    0    0    0    0    0
    5  350.0000  200.0000    0.0000    0    0    0    0    0    0    0    0
    6  287.5000  150.0000    0.0000    0    0    0    0    0    0    0    0
    7  303.1250  150.0000    0.0000    0    0    0    0    0    0    0    0
    8  318.7500  150.0000    0.0000    0    0    0    0    0    0    0    0
    9  334.3750  150.0000    0.0000    0    0    0    0    0    0    0    0
   10  350.0000  150.0000    0.0000    0    0    0    0    0    0    0    0
   11  335.3750  149.0000    0.0000    0    0    0    0    0    0    0    0
   12  350.0000  149.0000    0.0000    0    0    0    0    0    0    0    0
   13  275.0000  100.0000    0.0000    0    0    0    0    0    0    0    0
   14  293.7500  100.0000    0.0000    0    0    0    0    0    0    0    0
   15  312.5000  100.0000    0.0000    0    0    0    0    0    0    0    0
   16  331.2500  100.0000    0.0000    0    0    0    0    0    0    0    0
   17  332.2500  100.0000    0.0000    0    0    0    0    0    0    0    0
   18  350.0000  100.0000    0.0000    0    0    0    0    0    0    0    0
   19  262.5000   50.0000    0.0000    0    0    0    0    0    0    0    0
   20  284.3750   50.0000    0.0000    0    0    0    0    0    0    0    0
   21  306.2500   50.0000    0.0000    0    0    0    0    0    0    0    0
```

22	328.1250	50.0000	0.0000	0	0	0	0	0	0	0	0
23	329.1250	51.0000	0.0000	0	0	0	0	0	0	0	0
24	350.0000	51.0000	0.0000	0	0	0	0	0	0	0	0
25	350.0000	50.0000	0.0000	0	0	0	0	0	0	0	0
26	250.0000	0.0000	0.0000	1	0	1	0	1	0	0	0
27	275.0000	0.0000	0.0000	1	0	1	0	1	0	0	0
28	300.0000	0.0000	0.0000	1	0	1	0	1	0	0	0
29	325.0000	0.0000	0.0000	1	0	1	0	1	0	0	0
30	350.0000	0.0000	0.0000	1	0	1	0	1	0	0	0
31	200.0000	0.0000	0.0000	1	0	1	0	1	0	0	0
32	400.0000	0.0000	0.0000	1	0	1	0	1	0	0	0
33	150.0000	0.0000	0.0000	1	0	1	0	1	0	0	0
34	450.0000	0.0000	0.0000	1	0	1	0	1	0	0	0
35	100.0000	0.0000	0.0000	1	0	1	0	1	0	0	0
36	500.0000	0.0000	0.0000	1	0	1	0	1	0	0	0
37	50.0000	0.0000	0.0000	1	0	1	0	1	0	0	0
38	560.0000	0.0000	0.0000	1	0	1	0	1	0	0	0
39	0.0000	0.0000	0.0000	1	0	1	0	1	0	0	0
40	600.0000	0.0000	0.0000	1	0	1	0	1	0	0	0
41	520.0000	0.0000	50.0000	1	0	1	0	1	0	0	0
42	580.0000	100.0000	0.0000	0	0	0	0	0	0	0	0
43	555.0000	0.0000	50.0000	1	0	1	0	1	0	0	0
44	520.0000	20.0000	0.0000	0	0	0	0	0	0	0	0
45	580.0000	0.0000	20.0000	1	0	1	0	1	0	0	0
46	560.0000	20.0000	0.0000	0	0	0	0	0	0	0	0
47	600.0000	0.0000	20.0000	1	0	1	0	1	0	0	0
48	600.0000	20.0000	0.0000	0	0	0	0	0	0	0	0
49	540.0000	0.0000	100.0000	1	0	1	0	1	0	0	0
50	526.6666	46.6667	0.0000	0	0	0	0	0	0	0	0
51	580.0000	0.0000	50.0000	1	0	1	0	1	0	0	0
52	560.0000	46.6667	0.0000	0	0	0	0	0	0	0	0
53	581.0000	0.0000	21.0000	1	0	1	0	1	0	0	0
54	600.0000	46.6667	0.0000	0	0	0	0	0	0	0	0
55	600.0000	0.0000	21.0000	1	0	1	0	1	0	0	0
56	533.3331	73.3333	0.0000	0	0	0	0	0	0	0	0
57	565.0000	0.0000	100.0000	1	0	1	0	1	0	0	0
58	560.0000	73.3333	0.0000	0	0	0	0	0	0	0	0
59	580.0000	0.0000	80.0000	1	0	1	0	1	0	0	0
60	600.0000	73.3333	0.0000	0	0	0	0	0	0	0	0
61	581.0000	0.0000	79.0000	1	0	1	0	1	0	0	0
62	540.0000	100.0000	0.0000	0	0	0	0	0	0	0	0
63	600.0000	0.0000	79.0000	1	0	1	0	1	0	0	0
64	560.0000	100.0000	0.0000	0	0	0	0	0	0	0	0
65	600.0000	0.0000	100.0000	1	0	1	0	1	0	0	0
66	600.0000	100.0000	0.0000	0	0	0	0	0	0	0	0
67	600.0000	0.0000	80.0000	1	0	1	0	1	0	0	0
68	580.0000	73.3333	0.0000	0	0	0	0	0	0	0	0
69	580.0000	46.6667	0.0000	0	0	0	0	0	0	0	0
70	580.0000	20.0000	0.0000	0	0	0	0	0	0	0	0
71	581.0000	100.0000	0.0000	0	0	0	0	0	0	0	0
72	581.0000	73.3333	0.0000	0	0	0	0	0	0	0	0
73	581.0000	46.6667	0.0000	0	0	0	0	0	0	0	0
74	581.0000	20.0000	0.0000	0	0	0	0	0	0	0	0

$ ELEMENT CONNECTIVITY CONDITIONS

2	1	6	7	2	1	0	0	0	0	1	1	0	0	0	0
2	2	7	8	3	2	0	0	0	0	1	1	0	0	0	0
2	3	8	9	4	3	0	0	0	0	1	1	0	0	0	0
2	4	9	10	5	4	0	0	0	0	1	1	0	0	0	0
2	5	13	14	7	6	0	0	0	0	1	1	0	0	0	0
2	6	14	15	8	7	0	0	0	0	1	1	0	0	0	0
2	7	15	16	9	8	0	0	0	0	1	1	0	0	0	0
2	8	19	20	14	13	0	0	0	0	1	1	0	0	0	0
2	9	20	21	15	14	0	0	0	0	1	1	0	0	0	0
2	10	21	22	16	15	0	0	0	0	1	1	0	0	0	0
2	11	26	27	20	19	0	0	0	0	1	1	0	0	0	0
2	12	27	28	21	20	0	0	0	0	1	1	0	0	0	0
2	13	28	29	22	21	0	0	0	0	1	1	0	0	0	0
2	14	29	30	25	22	0	0	0	0	1	1	0	0	0	0
2	15	17	18	12	11	0	0	0	0	1	2	0	0	0	0
2	16	23	24	18	17	0	0	0	0	1	2	0	0	0	0
1	17	1	2	39	0	0	0	0	0	1	11	0	0	0	0
1	18	2	3	39	0	0	0	0	0	1	11	0	0	0	0
1	19	3	4	39	0	0	0	0	0	1	1	0	0	0	0
1	20	4	5	39	0	0	0	0	0	1	1	0	0	0	0
1	21	6	7	39	0	0	0	0	0	1	11	0	0	0	0
1	22	7	8	39	0	0	0	0	0	1	11	0	0	0	0
1	23	8	9	39	0	0	0	0	0	1	1	0	0	0	0
1	24	9	10	39	0	0	0	0	0	1	1	0	0	0	0
1	25	6	1	39	0	0	0	0	0	1	11	0	0	0	0
1	26	7	2	39	0	0	0	0	0	1	11	0	0	0	0
1	27	8	3	39	0	0	0	0	0	1	1	0	0	0	0

1	28	9	4	39	0	0	0	0	0	1	1	0	0	0	0
1	29	10	5	39	0	0	0	0	0	1	1	0	0	0	0
1	30	13	14	39	0	0	0	0	0	1	11	0	0	0	0
1	31	14	15	39	0	0	0	0	0	1	11	0	0	0	0
1	32	15	16	39	0	0	0	0	0	1	1	0	0	0	0
1	33	13	6	39	0	0	0	0	0	1	11	0	0	0	0
1	34	14	7	39	0	0	0	0	0	1	11	0	0	0	0
1	35	15	8	39	0	0	0	0	0	1	1	0	0	0	0
1	36	16	9	39	0	0	0	0	0	1	1	0	0	0	0
1	37	19	20	1	0	0	0	0	0	1	11	0	0	0	0
1	38	20	21	1	0	0	0	0	0	1	11	0	0	0	0
1	39	21	22	1	0	0	0	0	0	1	1	0	0	0	0
1	40	22	25	1	0	0	0	0	0	1	1	0	0	0	0
1	41	19	13	39	0	0	0	0	0	1	11	0	0	0	0
1	42	20	14	39	0	0	0	0	0	1	11	0	0	0	0
1	43	21	15	39	0	0	0	0	0	1	1	0	0	0	0
1	44	22	16	39	0	0	0	0	0	1	1	0	0	0	0
1	45	26	27	1	0	0	0	0	0	1	11	0	0	0	0
1	46	27	28	1	0	0	0	0	0	1	11	0	0	0	0
1	47	28	29	1	0	0	0	0	0	1	1	0	0	0	0
1	48	29	30	1	0	0	0	0	0	1	1	0	0	0	0
1	49	26	19	39	0	0	0	0	0	1	11	0	0	0	0
1	50	27	20	39	0	0	0	0	0	1	11	0	0	0	0
1	51	28	21	39	0	0	0	0	0	1	1	0	0	0	0
1	52	29	22	39	0	0	0	0	0	1	1	0	0	0	0
1	53	30	25	39	0	0	0	0	0	1	1	0	0	0	0
1	54	11	12	39	0	0	0	0	0	1	2	0	0	0	0
1	55	17	18	39	0	0	0	0	0	1	2	0	0	0	0
1	56	23	24	39	0	0	0	0	0	1	2	0	0	0	0
1	57	23	17	39	0	0	0	0	0	1	2	0	0	0	0
1	58	17	11	39	0	0	0	0	0	1	2	0	0	0	0
1	59	24	18	39	0	0	0	0	0	1	2	0	0	0	0
1	60	18	12	39	0	0	0	0	0	1	2	0	0	0	0
1	61	11	9	39	0	0	0	0	0	1	5	0	0	0	0
1	62	16	17	39	0	0	0	0	0	1	5	0	0	0	0
1	63	22	23	1	0	0	0	0	0	1	5	0	0	0	0
2	64	56	58	64	62	0	0	0	0	1	3	0	0	0	0
2	65	58	68	42	64	0	0	0	0	1	3	0	0	0	0
2	66	50	52	58	56	0	0	0	0	1	3	0	0	0	0
2	67	52	69	68	58	0	0	0	0	1	3	0	0	0	0
2	68	44	46	52	50	0	0	0	0	1	3	0	0	0	0
2	69	46	70	69	52	0	0	0	0	1	3	0	0	0	0
1	70	62	64	1	0	0	0	0	0	1	3	0	0	0	0
1	71	64	42	1	0	0	0	0	0	1	3	0	0	0	0
1	72	56	58	1	0	0	0	0	0	1	3	0	0	0	0
1	73	58	68	1	0	0	0	0	0	1	3	0	0	0	0
1	74	56	62	1	0	0	0	0	0	1	3	0	0	0	0
1	75	58	64	1	0	0	0	0	0	1	3	0	0	0	0
1	76	60	66	1	0	0	0	0	0	1	2	0	0	0	0
1	77	50	52	1	0	0	0	0	0	1	3	0	0	0	0
1	78	52	69	1	0	0	0	0	0	1	3	0	0	0	0
1	79	50	56	1	0	0	0	0	0	1	3	0	0	0	0
1	80	52	58	1	0	0	0	0	0	1	3	0	0	0	0
1	81	54	60	1	0	0	0	0	0	1	2	0	0	0	0
1	82	44	46	1	0	0	0	0	0	1	3	0	0	0	0
1	83	46	70	1	0	0	0	0	0	1	3	0	0	0	0
1	84	44	50	1	0	0	0	0	0	1	3	0	0	0	0
1	85	46	52	1	0	0	0	0	0	1	3	0	0	0	0
1	86	48	54	1	0	0	0	0	0	1	2	0	0	0	0
3	87	36	38	43	0	0	0	0	0	1	4	0	0	0	0
3	88	36	43	41	0	0	0	0	0	1	4	0	0	0	0
2	89	41	43	57	49	0	0	0	0	1	4	0	0	0	0
2	90	38	45	51	43	0	0	0	0	1	4	0	0	0	0
2	91	43	51	59	57	0	0	0	0	1	4	0	0	0	0
2	92	38	40	47	45	0	0	0	0	1	4	0	0	0	0
2	93	59	67	65	57	0	0	0	0	1	4	0	0	0	0
2	94	53	55	63	61	0	0	0	0	1	5	0	0	0	0
1	95	36	41	1	0	0	0	0	0	1	4	0	0	0	0
1	96	41	49	1	0	0	0	0	0	1	4	0	0	0	0
1	97	36	43	1	0	0	0	0	0	1	4	0	0	0	0
1	98	43	57	1	0	0	0	0	0	1	4	0	0	0	0
1	99	49	57	1	0	0	0	0	0	1	4	0	0	0	0
1	100	38	43	1	0	0	0	0	0	1	4	0	0	0	0
1	101	38	45	1	0	0	0	0	0	1	4	0	0	0	0
1	102	45	51	1	0	0	0	0	0	1	4	0	0	0	0
1	103	41	43	1	0	0	0	0	0	1	4	0	0	0	0
1	104	43	51	1	0	0	0	0	0	1	4	0	0	0	0
1	105	51	59	1	0	0	0	0	0	1	4	0	0	0	0
1	106	59	57	1	0	0	0	0	0	1	4	0	0	0	0
1	107	59	67	1	0	0	0	0	0	1	4	0	0	0	0
1	108	57	65	1	0	0	0	0	0	1	4	0	0	0	0

```
1 109 67 65  1  0 0 0 0 0 1   4 0 0 0 0
1 110 40 47  1  0 0 0 0 0 1   4 0 0 0 0
1 111 45 47  1  0 0 0 0 0 1   4 0 0 0 0
1 112 53 55  1  0 0 0 0 0 1   9 0 0 0 0
1 113 53 61  1  0 0 0 0 0 1   9 0 0 0 0
1 114 55 63  1  0 0 0 0 0 1   9 0 0 0 0
1 115 61 63  1  0 0 0 0 0 1   9 0 0 0 0
1 116 45 53  1  0 0 0 0 0 1  10 0 0 0 0
1 117 61 59  1  0 0 0 0 0 1  10 0 0 0 0
1 118 38 46  1  0 0 0 0 0 1   8 0 0 0 0
1 119 36 44  1  0 0 0 0 0 1   8 0 0 0 0
1 120 39 37  1  0 0 0 0 0 1 120 0 0 0 0
1 121 37 35  1  0 0 0 0 0 1 121 0 0 0 0
1 122 35 33  1  0 0 0 0 0 1 122 0 0 0 0
1 123 33 31  1  0 0 0 0 0 1 123 0 0 0 0
1 124 31 26  1  0 0 0 0 0 1 124 0 0 0 0
1 125 26 28  1  0 0 0 0 0 1 125 0 0 0 0
1 126 28 30  1  0 0 0 0 0 1 126 0 0 0 0
1 127 30 32  1  0 0 0 0 0 1 127 0 0 0 0
1 128 32 34  1  0 0 0 0 0 1 128 0 0 0 0
1 129 34 36  1  0 0 0 0 0 1 129 0 0 0 0
1 130 36 38  1  0 0 0 0 0 1 130 0 0 0 0
1 131 38 40  1  0 0 0 0 0 1 131 0 0 0 0
2 132 72 60 66 71 0 0 0 0 1   2 0 0 0 0
2 133 73 54 60 72 0 0 0 0 1   2 0 0 0 0
2 134 74 48 54 73 0 0 0 0 1   2 0 0 0 0
1 135 42 71  1  0 0 0 0 0 1   5 0 0 0 0
1 136 68 72  1  0 0 0 0 0 1   5 0 0 0 0
1 137 69 73  1  0 0 0 0 0 1   5 0 0 0 0
1 138 70 74  1  0 0 0 0 0 1   5 0 0 0 0
1 139 74 73  1  0 0 0 0 0 1   2 0 0 0 0
1 140 73 72  1  0 0 0 0 0 1   2 0 0 0 0
1 141 72 71  1  0 0 0 0 0 1   2 0 0 0 0
1 142 70 69  1  0 0 0 0 0 1   3 0 0 0 0
1 143 69 68  1  0 0 0 0 0 1   3 0 0 0 0
1 144 68 42  1  0 0 0 0 0 1   3 0 0 0 0
1 145 71 66 65  0 0 0 0 0 1   2 0 0 0 0
1 146 72 60 65  0 0 0 0 0 1   2 0 0 0 0
1 147 73 54 65  0 0 0 0 0 1   2 0 0 0 0
1 148 74 48 65  0 0 0 0 0 1   2 0 0 0 0
1 149 40 70 65  0 0 0 0 0 1   8 0 0 0 0
$ LINE ELEMENT BASIC PROPERTIES
   1     1.5000    37.5000    18.8000    18.8000
   2     0.5300     3.8000     1.9000     1.9000
   3     0.7500    19.0000     9.0000     9.0000
   4     0.0600     1.5000     0.7500     0.7500
   5     0.4000     1.5000     0.7500     0.7500
   6    19.0000   750.0000   375.0000   375.0000
   8     3.7500  1500.0000   750.0000   750.0000
   9     0.0300     0.8000     0.4000     0.4000
  10     0.0100     0.4000     0.2000     0.2000
  11     1.1250    28.1250    14.0600    14.0600
 120    11.2500      675.0      338.0      338.0
 121    18.7500      900.0      900.0      900.0
 122    18.7500     1050.0     1575.0     1575.0
 123    18.7500     1200.0     2250.0     2250.0
 124    18.7500     1650.0     2625.0     2625.0
 125    18.7500     1875.0     1875.0     1875.0
 126    18.7500     2250.0     1125.0     1125.0
 127    18.7500     3000.0     1275.0     1275.0
 128    18.7500     3000.0     1275.0     1275.0
 129    18.7500     3000.0     1275.0     1275.0
 130    16.5000     2250.0      975.0      975.0
 131    15.0000     1500.0      675.0      675.0
$ SHELL ELEMENT THICKNESSES
   1    0.1130
   2    0.0530
   3    0.0900
   4    0.0400
   5    0.0100
$ MATERIAL PROPERTIES
   1   1
  1.0E+07       0.30          0.   .259E-03
$ NODAL MASS DATA
  39   1    0.0195    3
  37   1    0.0389    3
  35   1    0.0584    3
  33   1    0.0972    3
  31   1    0.1943    3
  26   1    0.2915    3
  28   1    0.2915    3
```

ORIGINAL PAGE IS
OF POOR QUALITY

```
 30   1   0.2915   3
 32   1   0.2915   3
 34   1   0.2915   3
 36   1   0.2915   3
 38   1   0.2915   3
 40   1   0.1943   3
 -1
$ OUTPUT POINT SPECIFICATION FOR DIRECT INTERPOLATION OF MODAL DATA
  1  36
  2  36  36  41
  3  36  41  41  41
  4  41
  5  41  49
  6  41  49  49
  7  49
  8  36  38
  9  38  38  43
 10  38  43  43  43
 11  43
 12  43  57
 13  43  57  57
 14  57
 15  38  40
 16  45
 17  45  51  51
 18  51
 19  51  59  59  59
 20  59
 21  57  65
 22  67
 23  65
 24  53
 25  61
 26  55
 27  63
 28  26
 29  19  26
 30  19
 31  13  19  19
 32  13  13  19
 33  13
 34   6  13
 35   6
 36   1   6   6
 37   1   1   6
 38   1
 39  27
 40  20  27
 41  20
 42  14  20  20
 43  14  14  20
 44  14
 45   7  14
 46   7
 47   2   7   7
 48   2   2   7
 49   2
 50  28
 51  21  28
 52  21
 53  15  21  21
 54  15  15  21
 55  15
 56   8  15
 57   8
 58   3   8   8
 59   3   3   8
 60   3
 61  29
 62  22  29
 63  22
 64  16  22  22
 65  16  16  22
 66  16
 67   9  16
 68   9
 69   4   9   9
 70   4   4   9
 71   4
 72  30
 73  25  30
 74  25
 75  10
 76   5  10  10
 77   5   5  10
 78   5
 79  23
 80  17  23  23
 81  17  17  23
 82  17
 83  11  17
 84  11
```

ORIGINAL PAGE IS
OF POOR QUALITY

```
 85   24
 86   18   24   24
 87   18   18   24
 88   18
 89   12   18
 90   12
 91   44
 92   44   50   50   50
 93   50   50   56
 94   56
 95   56   62
 96   62
 97   46
 98   46   52   52   52
 99   52   52   58
100   58
101   58   64
102   64
103   70
104   69   70   70   70
105   68   68   69
106   68
107   42   68
108   42
109   74
110   73   74   74   74
111   72   72   73
112   72
113   71   72
114   71
115   48
116   48   54   54   54
117   54   54   60
118   60
119   60   66
120   66
121   39
122   35
123   33
124   31
125   26
126   28
127   30
128   32
129   34
130   36
131   38
132   40
$ RIGID BODY CONTROL MODE DATA
   1    2      -1.0   74    1      <--- RIGID BODY Y TRANSLATION

   1    2   -0.6908                <--- RIGID BODY X ROTATION (ROLL)
   1    3   16.6089
   1    4    1.0000
   2    2   -0.6908
   2    3   16.6089
   2    4    1.0000
   3    2   -0.6908
   3    3   16.6089
   3    4    1.0000
   4    2   -0.6908
   4    3   16.6089
   4    4    1.0000
   5    2   -0.6908
   5    3   16.6089
   5    4    1.0000
   6    2   -0.5181
   6    3   12.4567
   6    4    1.0000
   7    2   -0.5181
```

7	3	12.4567
7	4	1.0000
8	2	-0.5181
8	3	12.4567
8	4	1.0000
9	2	-0.5181
9	3	12.4567
9	4	1.0000
10	2	-0.5181
10	3	12.4567
10	4	1.0000
11	2	-0.5147
11	3	12.3737
11	4	1.0000
12	2	-0.5147
12	3	12.3737
12	4	1.0000
13	2	-0.3454
13	3	8.3045
13	4	1.0000
14	2	-0.3454
14	3	8.3045
14	4	1.0000
15	2	-0.3454
15	3	8.3045
15	4	1.0000
16	2	-0.3454
16	3	8.3045
16	4	1.0000
17	2	-0.3454
17	3	8.3045
17	4	1.0000
18	2	-0.3454
18	3	8.3045
18	4	1.0000
19	2	-0.1727
19	3	4.1522
19	4	1.0000
20	2	-0.1727
20	3	4.1522
20	4	1.0000
21	2	-0.1727
21	3	4.1522
21	4	1.0000
22	2	-0.1727
22	3	4.1522
22	4	1.0000
23	2	-0.1762
23	3	4.2353
23	4	1.0000
24	2	-0.1762
24	3	4.2353
24	4	1.0000
25	2	-0.1727
25	3	4.1522
25	4	1.0000
26	4	1.0000
27	4	1.0000
28	4	1.0000
29	4	1.0000
30	4	1.0000
31	4	1.0000
32	4	1.0000
33	4	1.0000
34	4	1.0000
35	4	1.0000
36	4	1.0000
37	4	1.0000
38	4	1.0000
39	4	1.0000
40	4	1.0000
41	2	-4.1522
41	3	-0.1727
41	4	1.0000
42	2	-0.3454
42	3	8.3045
42	4	1.0000
43	2	-4.1522
43	3	-0.1727
43	4	1.0000
44	2	-0.0691

44	3	1.6609
44	4	1.0000
45	2	-1.6609
45	3	-0.0691
45	4	1.0000
46	2	-0.0691
46	3	1.6609
46	4	1.0000
47	2	-1.6609
47	3	-0.0691
47	4	1.0000
48	2	-0.0691
48	3	1.6609
48	4	1.0000
49	2	-8.3045
49	3	-0.3454
49	4	1.0000
50	2	-0.1612
50	3	3.8754
50	4	1.0000
51	2	-4.1522
51	3	-0.1727
51	4	1.0000
52	2	-0.1612
52	3	3.8754
52	4	1.0000
53	2	-1.7439
53	3	-0.0725
53	4	1.0000
54	2	-0.1612
54	3	3.8754
54	4	1.0000
55	2	-1.7439
55	3	-0.0725
55	4	1.0000
56	2	-0.2533
56	3	6.0899
56	4	1.0000
57	2	-8.3045
57	3	-0.3454
57	4	1.0000
58	2	-0.2533
58	3	6.0899
58	4	1.0000
59	2	-6.6436
59	3	-0.2763
59	4	1.0000
60	2	-0.2533
60	3	6.0899
60	4	1.0000
61	2	-6.5605
61	3	-0.2729
61	4	1.0000
62	2	-0.3454
62	3	8.3045
62	4	1.0000
63	2	-6.5605
63	3	-0.2729
63	4	1.0000
64	2	-0.3454
64	3	8.3045
64	4	1.0000
65	2	-8.3045
65	3	-0.3454
65	4	1.0000
66	2	-0.3454
66	3	8.3045
66	4	1.0000
67	2	-6.6436
67	3	-0.2763
67	4	1.0000
68	2	-0.2533
68	3	6.0899
68	4	1.0000
69	2	-0.1612
69	3	3.8754
69	4	1.0000
70	2	-0.0691
70	3	1.6609
70	4	1.0000
71	2	-0.3454

71	3	8.3045	
71	4	1.0000	
72	2	-0.2533	
72	3	6.0899	
72	4	1.0000	
73	2	-0.1612	
73	3	3.8754	
73	4	1.0000	
74	2	-0.0691	
74	3	1.6609	
74	4	1.0000	
-1			
1	1	16.5227	<--- RIGID BODY Z ROTATION (YAW) at 275 in.
1	2	-2.7670	
1	6	1.0000	
2	1	16.4795	
2	2	-3.8050	
2	6	1.0000	
3	1	16.4364	
3	2	-4.8431	
3	6	1.0000	
4	1	16.3932	
4	2	-5.8812	
4	6	1.0000	
5	1	16.3500	
5	2	-6.9192	
5	6	1.0000	
6	1	12.4137	
6	2	-1.5562	
6	6	1.0000	
7	1	12.3596	
7	2	-2.8538	
7	6	1.0000	
8	1	12.3057	
8	2	-4.1514	
8	6	1.0000	
9	1	12.2517	
9	2	-5.4489	
9	6	1.0000	
10	1	12.1978	
10	2	-6.7465	
10	6	1.0000	
11	1	12.1652	
11	2	-5.5285	
11	6	1.0000	
12	1	12.1147	
12	2	-6.7431	
12	6	1.0000	
13	1	8.3045	
13	2	-0.3454	
13	6	1.0000	
14	1	8.2398	
14	2	-1.9025	
14	6	1.0000	
15	1	8.1750	
15	2	-3.4596	
15	6	1.0000	
16	1	8.1102	
16	2	-5.0167	
16	6	1.0000	
17	1	8.1068	
17	2	-5.0998	
17	6	1.0000	
18	1	8.0455	
18	2	-6.5738	
18	6	1.0000	
19	1	4.1955	
19	2	0.8654	
19	6	1.0000	
20	1	4.1199	
20	2	-0.9512	
20	6	1.0000	
21	1	4.0443	
21	2	-2.7679	
21	6	1.0000	
22	1	3.9688	
22	2	-4.5845	
22	6	1.0000	
23	1	4.0483	
23	2	-4.6710	
23	6	1.0000	

24	1	3.9763
24	2	-6.4046
24	6	1.0000
25	1	3.8932
25	2	-6.4011
25	6	1.0000
26	1	0.0863
26	2	2.0761
26	6	1.0000
27	1	0.0000
27	2	0.0000
27	6	1.0000
28	1	-0.0864
28	2	-2.0761
28	6	1.0000
29	1	-0.1727
29	2	-4.1523
29	6	1.0000
30	1	-0.2591
30	2	-6.2284
30	6	1.0000
31	1	0.2591
31	2	6.2284
31	6	1.0000
32	1	-0.4318
32	2	-10.3807
32	6	1.0000
33	1	0.4318
33	2	10.3807
33	6	1.0000
34	1	-0.6045
34	2	-14.5330
34	6	1.0000
35	1	0.6045
35	2	14.5330
35	6	1.0000
36	1	-0.7772
36	2	-18.6852
36	6	1.0000
37	1	0.7772
37	2	18.6852
37	6	1.0000
38	1	-0.9845
38	2	-23.6680
38	6	1.0000
39	1	0.9499
39	2	22.8375
39	6	1.0000
40	1	-1.1227
40	2	-26.9898
40	6	1.0000
41	1	-0.8463
41	2	-20.3461
41	6	1.0000
42	1	7.2510
42	2	-25.6743
42	6	1.0000
43	1	-0.9672
43	2	-23.2527
43	6	1.0000
44	1	0.8146
44	2	-20.4152
44	6	1.0000
45	1	-1.0536
45	2	-25.3289
45	6	1.0000
46	1	0.6765
46	2	-23.7371
46	6	1.0000
47	1	-1.1227
47	2	-26.9898
47	6	1.0000
48	1	0.5383
48	2	-27.0589
48	6	1.0000
49	1	-0.9154
49	2	-22.0071
49	6	1.0000
50	1	3.0061
50	2	-21.0610
50	6	1.0000

51	1	-1.0536	
51	2	-25.3289	
51	6	1.0000	
52	1	2.8910	
52	2	-23.8291	
52	6	1.0000	
53	1	-1.0570	
53	2	-25.4119	
53	6	1.0000	
54	1	2.7528	
54	2	-27.1510	
54	6	1.0000	
55	1	-1.1227	
55	2	-26.9898	
55	6	1.0000	
56	1	5.1977	
56	2	-21.7067	
56	6	1.0000	
57	1	-1.0017	
57	2	-24.0832	
57	6	1.0000	
58	1	5.1056	
58	2	-23.9212	
58	6	1.0000	
59	1	-1.0536	
59	2	-25.3289	
59	6	1.0000	
60	1	4.9674	
60	2	-27.2431	
60	6	1.0000	
61	1	-1.0570	
61	2	-25.4119	
61	6	1.0000	
62	1	7.3892	
62	2	-22.3525	
62	6	1.0000	
63	1	-1.1227	
63	2	-26.9898	
63	6	1.0000	
64	1	7.3201	
64	2	-24.0134	
64	6	1.0000	
65	1	-1.1227	
65	2	-26.9898	
65	6	1.0000	
66	1	7.1819	
66	2	-27.3352	
66	6	1.0000	
67	1	-1.1227	
67	2	-26.9898	
67	6	1.0000	
68	1	5.0365	
68	2	-25.5822	
68	6	1.0000	
69	1	2.8219	
69	2	-25.4901	
69	6	1.0000	
70	1	0.6074	
70	2	-25.3980	
70	6	1.0000	
71	1	7.2475	
71	2	-25.7573	
71	6	1.0000	
72	1	5.0330	
72	2	-25.6652	
72	6	1.0000	
73	1	2.8185	
73	2	-25.5731	
73	6	1.0000	
74	1	0.6039	
74	2	-25.4810	
74	6	1.0000	
-1			
11	3	0.0833	<--- AILERON DEFLECTION, T.E. UP
17	3	0.0833	
23	3	0.0833	
24	3	1.8229	
18	3	1.5625	
12	3	1.3020	
11	5	1.0	
17	5	1.0	

```
23   5        1.0
24   5        1.0
18   5        1.0
12   5        1.0
-1
53   2    -.08333          <--- RUDDER DEFLECTION, T.E. NEGATIVE
53   6   1.00000
61   2    -.08333
61   6   1.00000
55   2  -1.66667
55   6   1.00000
63   2  -1.66667
63   6   1.00000
-1
```

ORIGINAL PAGE IS
OF POOR QUALITY

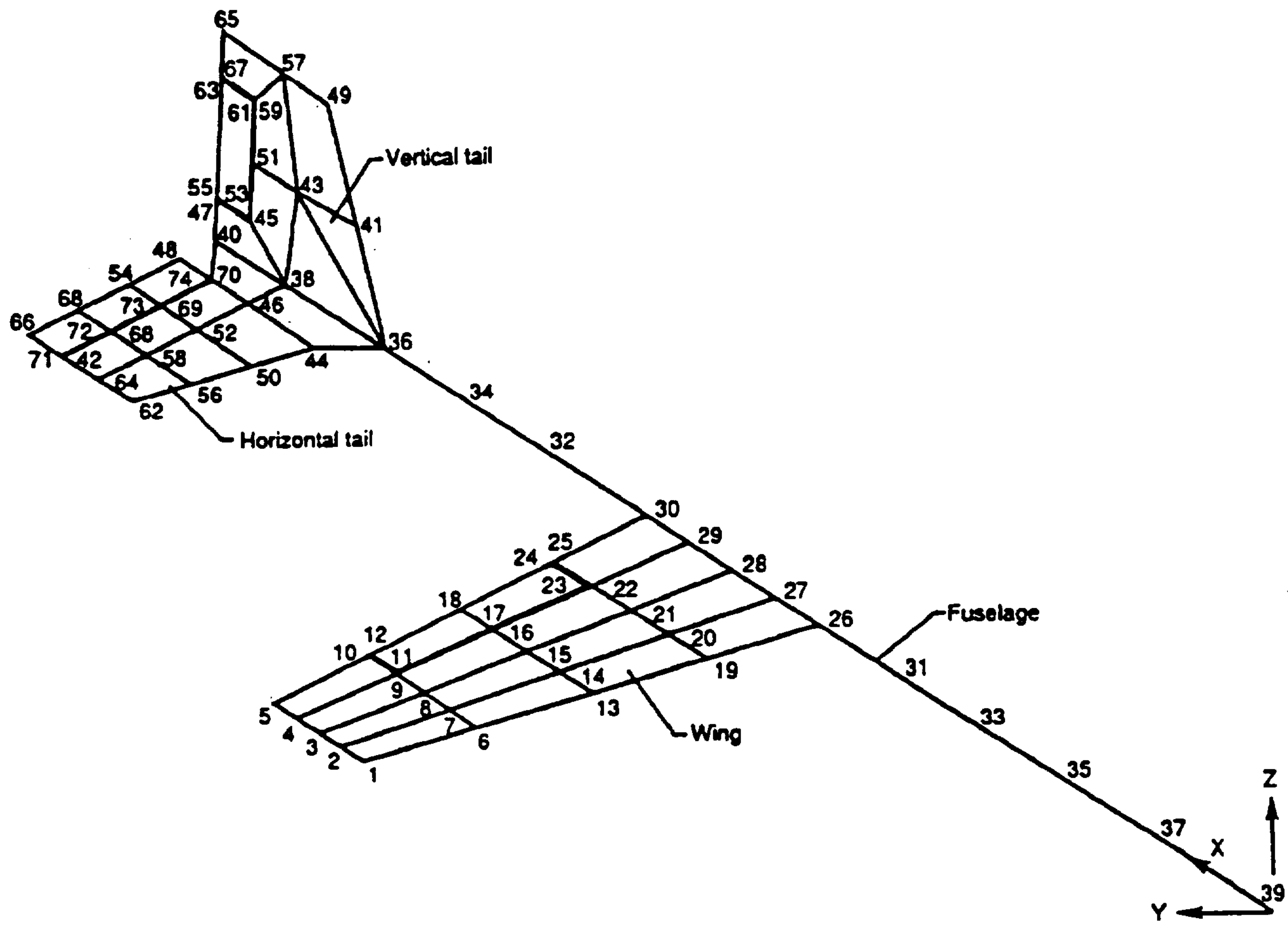

Figure 31. ATM symmetric half finite element model with nodes.

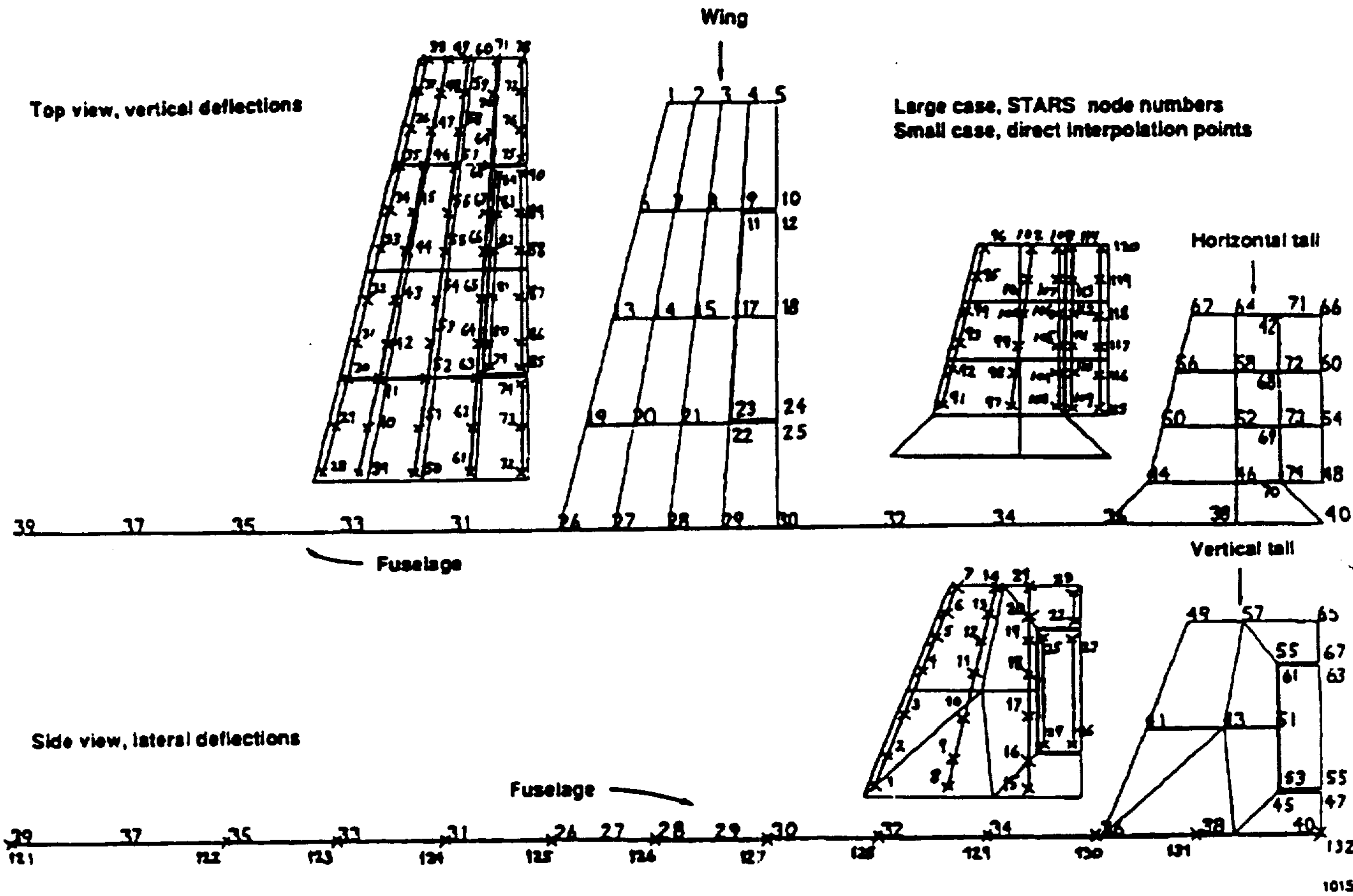

Figure 32. ATM antisymmetric case, direct-surface interpolation scheme.

ATM STARS-SOLIDS analysis results:

Table 21 depicts the results of the free vibration analysis. Figure 33 shows the eight elastic mode shapes, whereas the three perfect rigid body and the two control modes are shown in figure 34. In order to effect correct response from the controllers, the perfect rigid body and control modes need to be defined in the fashion shown in table 22.

Table 21. AERO test model (ATM): Antisymmetric free vibration analysis results.

Mode shape		Eigenvalue		Generalized mass, lb	Mode shape
SOLIDS	AERO-ASE	Hz	rad/sec		
1	---	---	---	113.8	Rigid body X-rotation
2	---	---	---	2,384	Rigid body Y-translation
3	---	---	---	111.6	Rigid body Z-rotation
4	1	10.175	63.931	8.2	Vertical fin first bending
5	2	12.448	78.217	235.1	Fuselage first bending
6	3	14.632	91.934	44.62	Wing first bending
7	4	28.741	180.584	60.53	Wing second bending
8	5	29.810	187.301	204.3	Fuselage second bending
9	6	32.450	203.890	47.87	Wing first torsion
10	7	35.815	225.030	3.233	Fin first torsion
11	8	51.138	321.309	239.3	Fuselage third bending
12	9	---	---	2,534	Rigid body Y-translation
13	10	---	---	151,200	Rigid body roll
14	11	---	---	589,000	Rigid body yaw at 275 in.
15	12	---	---	128.60	Flap deflection
16	13	---	---	14.22	Rudder deflection

Table 22. ATM rigid body and control mode generation parameters.

Motion	Symmetric analysis	Antisymmetric analysis
X-translation	1.0 in X	
Y-translation		1.0 in Y
Z-translation	-1.0 in Z	
X-rotation		-Δ in Z
Y-rotation	-Δ in Z	
Z-rotation		-Δ in Y
Flap	-Δ in Z	
Aileron		+Δ in Z
Elevator	-Δ in Z	
Rudder		-Δ in Y

In the table, the term Δ is defined as $\Delta = (d_N - d_A)/12$, where d_N and d_A represent the coordinates of the node under consideration and the axis of rotation, respectively.

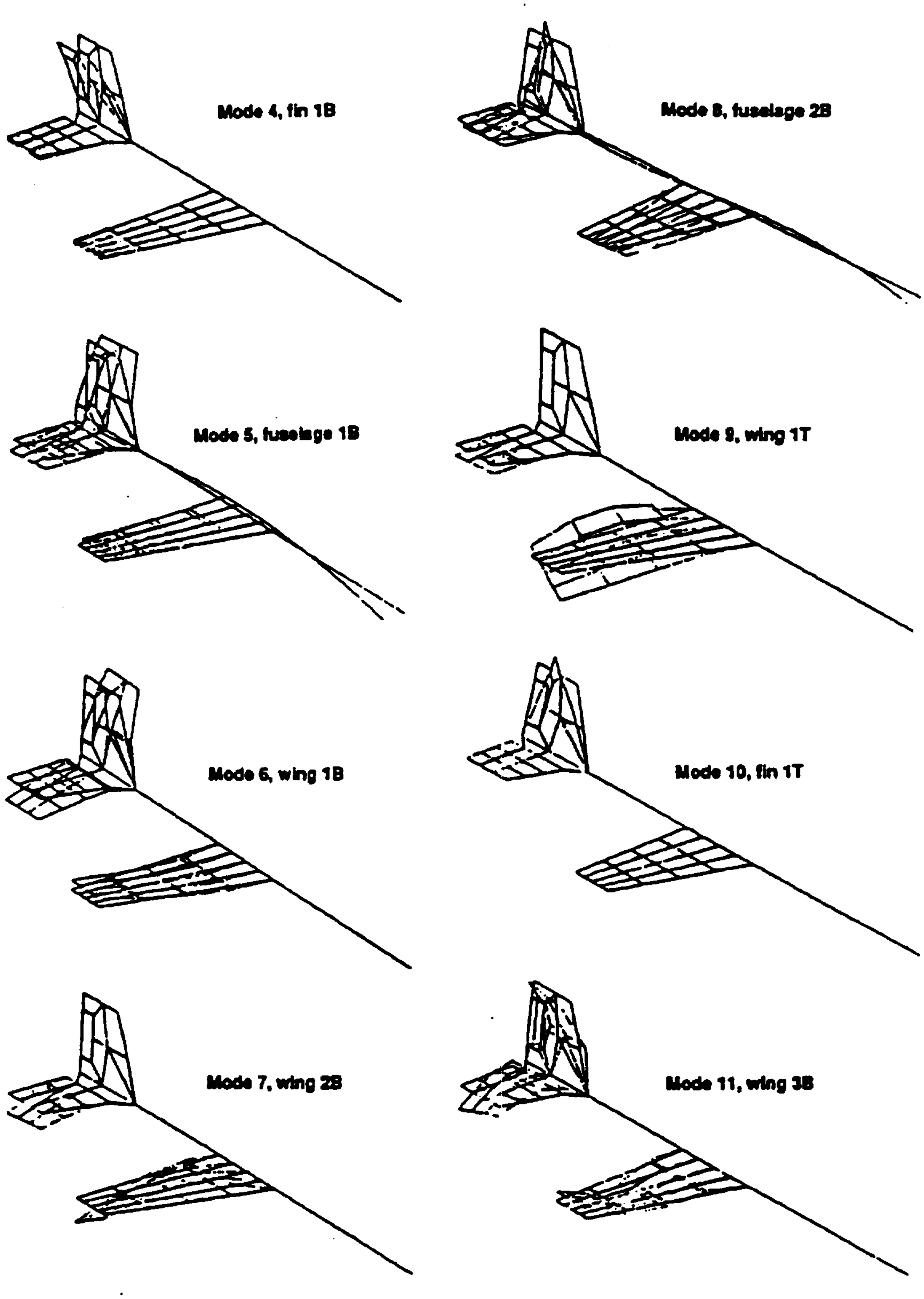

Figure 33. ATM antisymmetric case, elastic (Φ_E) mode shapes.

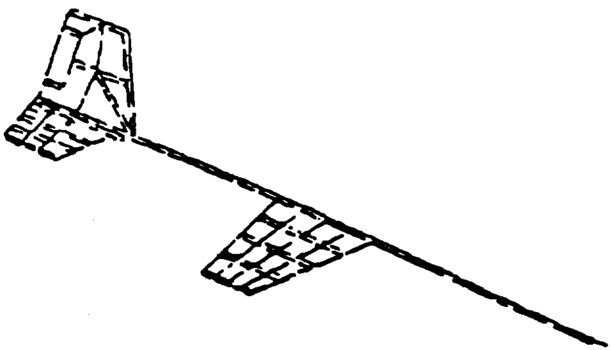

(a) Rigid body mode, X-Y plane motion.

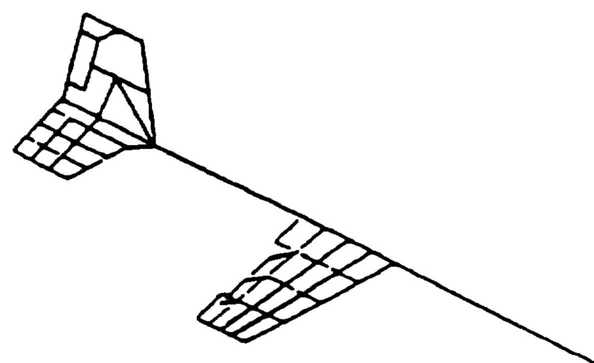

(b) Control mode, flap motion.

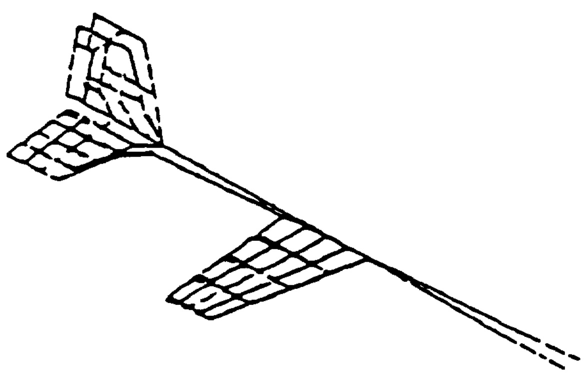

(c) Rigid body mode, Z-rotation motion.

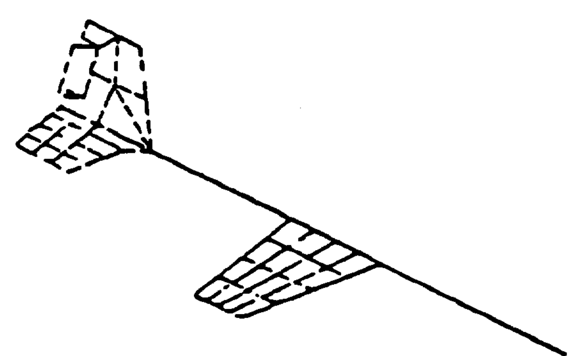

(d) Control mode, rudder motion.

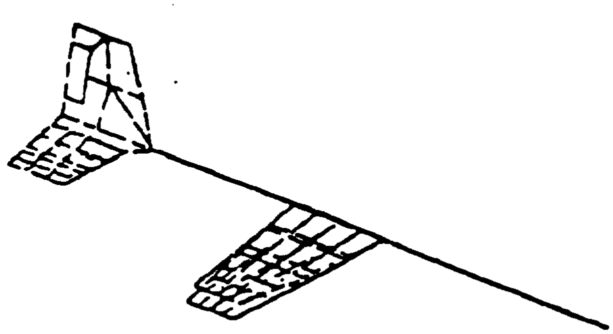

(e) Rigid body mode, X-rotation motion.

Figure 34. ATM antisymmetric case, perfect rigid body (Φ_{PR}) and control (Φ_C) modes.

This run is made by deleting the first three rigid body modes so that

$$\Phi = \Phi_E + \Phi_{PR} + \Phi_C$$

STARS-AERO-GENMASS input data:

```
$  AERO TEST MODES, ANTISYMMETRIC VERSION
   4   39   386.008
$ LATERALLY MOVING direct interpolation output NODE NUMBERS
    1
    2
    3
    4
    5
    6
    7
    8
    9
   10
   11
   12
   13
   14
   15
   16
   17
   18
   19
   20
   21
   22
   23
   24
   25
   26
   27
  121
  122
  123
  124
  125
  126
  127
  128
  129
  130
  131
  132
```

The calculated generalized mass is depicted in table 23.

The input data used for eventual ASE response analysis are given in this section. These data also enable flutter and divergence analysis of the aircraft. For a k or p-k method of flutter solution, the number of reduced frequencies in the data is increased from 10 to 28, and rigid body and control modes are eliminated. Figures 35 through 37 show the ATM relevant aerodynamic element arrangements.

STARS-AERO input data - ASE analysis:

```
AERO TEST MODEL - ANTISYMMETRIC CASE - NCNTRL = 5
SET UP FOR ASE SOLUTION.
DIRECT SURFACE INTERPOLATION.
EIGHT ELASTIC MODES, PLUS FIVE ADDED RIGID BODY-CONTROL MODES;
REVISED RIGID BODY Y TRANSLATIONS, ROLL, YAW,  PLUS AILERON AND RUDDER MODES.
MACH NO.= 0.90            ALTITUDE: SEA LEVEL
  1  13    3   10    1    0    0    0    0    0
  1   0    0    0    0    0    0    0    0    0
  1   0    0    0    0    0    0    0    0    0
  0   0    0    0    0    0    0   99    0    0
  1
   38.89      0.90
 11000.0    1000.0      100.0       50.0       10.0        5.0        1.0
   0.667     0.500       0.25
     .10      -.40      1400.       80.0
     1.0
   77.78    15000.
 -1   15    1 1200    0    0    1
                                    90.0
   508.0     580.0      532.0      580.0       20.0       80.0
     0.0       0.0   4  4            0.0
     0.0    0.3333     0.6666        1.0
     0.0    0.3333     0.6666        1.0
                                    90.0
   532.0     600.0      540.0      600.0       80.0      100.0
     0.0       0.0   2  5            0.0
     0.0    0.2353     0.4705     0.7059        1.0
     0.0       1.0
                                    90.0
   580.0     600.0      580.0      600.0       20.0       80.0
     0.0       0.0   4  2            0.0
     0.0       1.0
     0.0    0.3333     0.6666        1.0

   255.0     350.0      262.5      350.0       20.0       50.0
     0.0       0.0   3  5            0.0
     0.0      0.25       0.50       0.75        1.0
     0.0       0.5        1.0

   262.5   328.125      275.0     331.25       50.0      100.0
     0.0       0.0   4  4            0.0
     0.0    0.3333     0.6666        1.0
     0.0      0.34       0.66        1.0

   275.0    331.25      287.5    334.375      100.0      150.0
     0.0       0.0   4  4            0.0
     0.0    0.3333     0.6666        1.0
     0.0      0.34       0.66        1.0

   287.5     350.0      300.0      350.0      150.0      200.0
     0.0       0.0   4  5            0.0
     0.0      0.25       0.50       0.75        1.0
     0.0      0.34       0.66        1.0

 328.125     350.0     331.25      350.0       50.0      100.0
     0.0       0.0   4  2            0.0
     0.0       1.0
     0.0      0.34       0.66        1.0

  331.25     350.0    334.375      350.0      100.0      150.0
     0.0       0.0   4  2            0.0
     0.0       1.0
     0.0      0.34       0.66        1.0

   520.0     580.0      527.5      580.0       20.0       50.0
     0.0       0.0   3  3            0.0
     0.0    0.4167        1.0
     0.0       0.5        1.0

   527.5     580.0      540.0      580.0       50.0      100.0
     0.0       0.0   4  3            0.0
     0.0    0.4167        1.0
     0.0      0.34       0.66        1.0

   580.0     600.0      580.0      600.0       20.0       50.0
```

```
    0.0       0.0  3  2         0.0
    0.0       1.0
    0.0       0.5       1.0

  580.0     600.0     580.0     600.0      50.0     100.0
    0.0       0.0  4  2         0.0
    0.0       1.0
    0.0      0.34      0.66       1.0

   -5.0     600.0      -5.0     600.0       0.0      20.0
  -20.0       0.0  2 11         0.0
    0.0    0.1074    0.2149    0.3223    0.4298    0.5083
 0.5868    0.6777    0.7769    0.8678    1.0000
    0.0       1.0

   -5.0     600.0      -5.0     600.0      20.0       0.0
    0.0      20.0  2 11         0.0
    0.0    0.1074    0.2149    0.3223    0.4298    0.5083
 0.5868    0.6777    0.7769    0.8678    1.0000
    0.0       1.0

    0.0       0.0 14 1 0        0.0 76 95
-15.000    25.000    85.000   145.000   205.000   245.000
295.000   335.000   365.000   425.000   485.000   565.000
605.000   645.000
    0.0      10.0      20.0      20.0      20.0      40.0
   40.0      40.0      40.0      30.0      30.0      20.0
   20.0      15.0
 1    0    0    2   16    0

 T   16    1
 4    0    1    1
 7     502.0      2.0     542.0     100.0
   2.0      17.0      37.0      50.0      75.0      85.0     100.0
 7     542.0      2.0     560.0     100.0
   2.0      17.0      37.0      50.0      75.0      85.0     100.0
 7     578.0      2.0     578.0     100.0
   2.0      17.0      40.0      50.0      73.0      82.0     100.0
 2     598.0     82.0     598.0     100.0
  82.0     100.0
 580.0      20.0     580.0      80.0
 2    0    1    1
 2     582.0     22.0     582.0      78.0
  22.0      78.0
 2     598.0     22.0     598.0      78.0
  22.0      78.0
 T   44    1
 6    0    1    1
11     252.0      2.0     302.0     200.0
   2.0      25.0      50.0      67.0      83.0     102.0     125.0     150.0
 167.0     183.0     200.0
11     270.0      2.0     313.0     200.0
   2.0      25.0      50.0      67.0      83.0     102.0     125.0     150.0
 167.0     183.0     200.0
11     298.0      2.0     324.0     200.0
   2.0      25.0      50.0      67.0      83.0     102.0     125.0     150.0
 167.0     183.0     200.0
11     323.0      2.0     336.0     200.0
   2.0      25.0      50.0      67.0      83.0     102.0     125.0     150.0
 167.0     183.0     200.0
 3     348.0      2.0     348.0      48.0
   2.0      25.0      48.0
 4     348.0    152.0     348.0     200.0
 152.0     167.0     183.0     200.0
328.125     50.0   334.375     150.0
 2    0    1    1
 6     330.0     52.0     336.0     148.0
  52.0      67.0      83.0     102.0     125.0     148.0
 6     348.0     52.0     348.0     148.0
  52.0      67.0      83.0     102.0     125.0     148.0
 T   15    1
 3    0    1    1
 6     522.0     20.0     542.0     100.0
  20.0      40.0      55.0      72.0      87.0     100.0
 6     550.0     20.0     562.0     100.0
  20.0      40.0      55.0      72.0      87.0     100.0
 6     578.0     20.0     578.0     100.0
  20.0      40.0      55.0      72.0      87.0     100.0
 580.0      20.0     580.0     100.0
 2    0    1    1
 6     582.0     20.0     582.0     100.0
  20.0      40.0      55.0      72.0      87.0     100.0
 6     598.0     20.0     598.0     100.0
  20.0      40.0      55.0      72.0      87.0     100.0
12    2   14
   0.0     100.0     150.0     200.0     250.0     300.0
 350.0     400.0     450.0     500.0     560.0     600.0
 0
```

ORIGINAL PAGE IS
OF POOR QUALITY

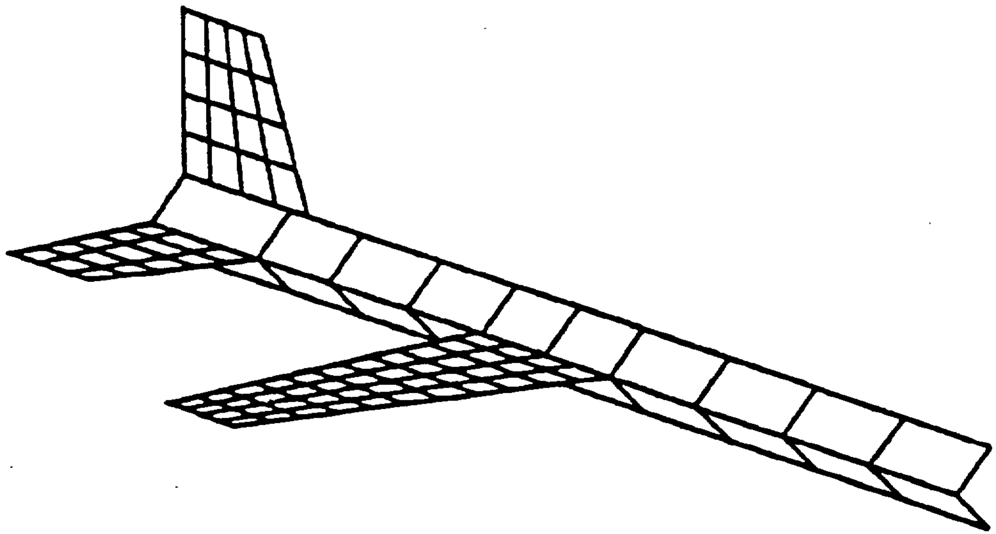

Figure 35. ATM antisymmetric case, half aircraft aerodynamic boxes.

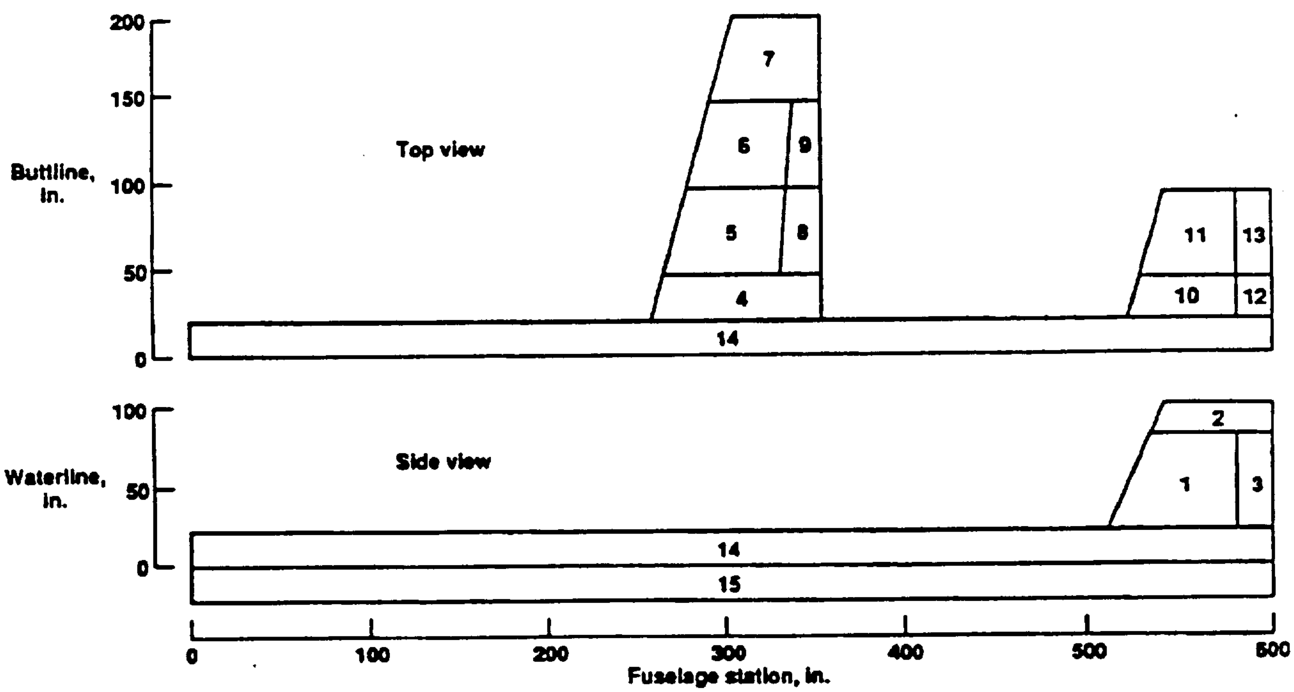

Figure 36. ATM antisymmetric case, aerodynamic panels.

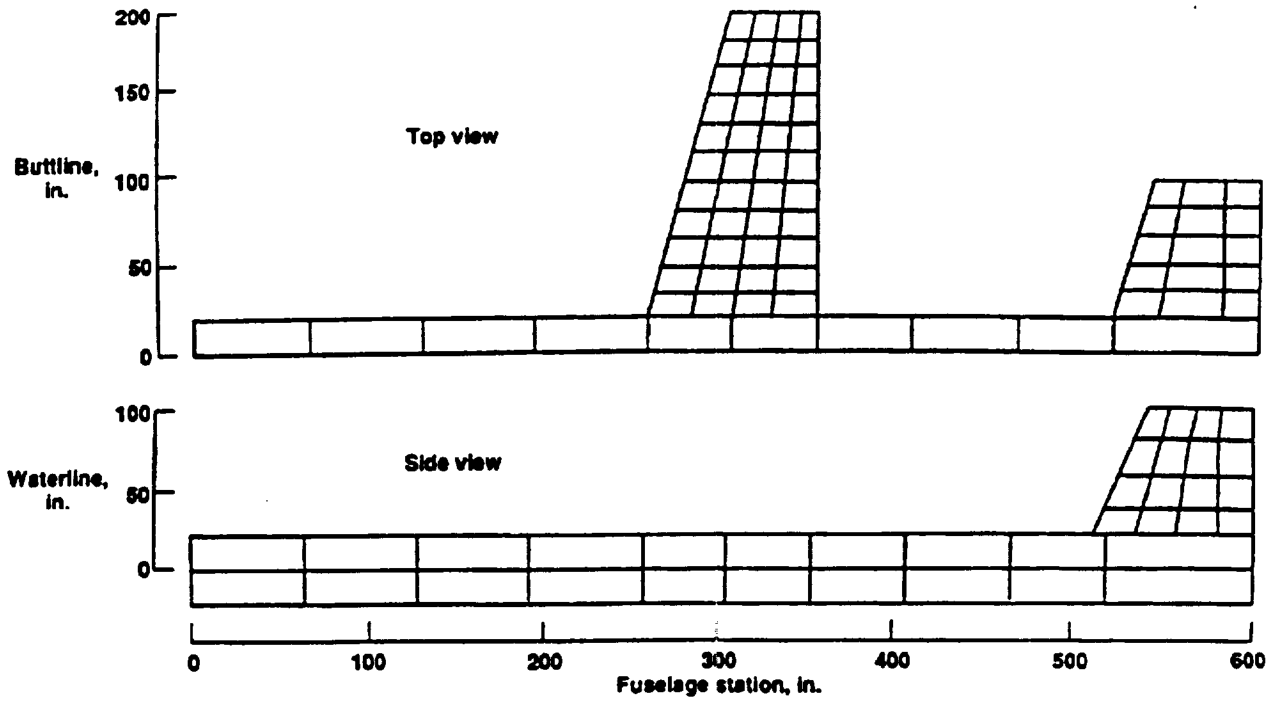

(a) Aerodynamic boxes.

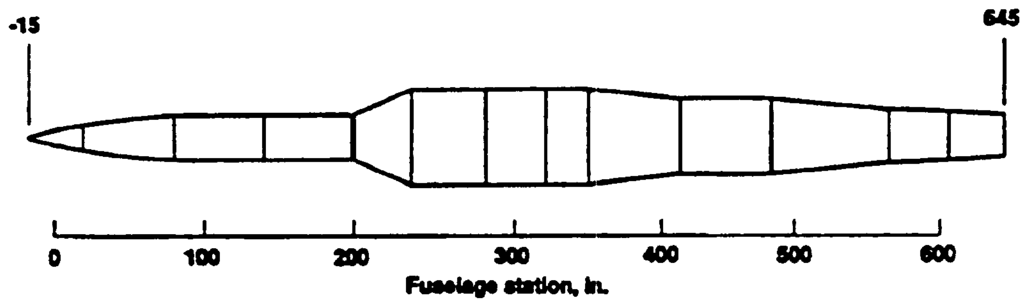

(b) Slender body definitions.

Figure 37. ATM antisymmetric case, aerodynamic boxes.

STARS-AERO input data–k-type flutter analysis:

The data presented here pertain only to changes required in the corresponding ASE analysis case, and occur within the first 16 lines.

```
AERO TEST MODEL - ANTISYMMETRIC CASE -
K-FLUTTER SOLUTION
ELASTIC MODE 8 - DIRECT FROM SOLID MODEL 11  (-3 GENMASS)
DIRECT SURFACE INTERPOLATION /// CORRECTED INTERP FORMAT AND POINTS
STARS STRUCTURAL MODEL, BYPASS RIGID BODY MODES IN GENMASS
MACH NO.-0.90            ALTITUDE: SEA LEVEL
    1    8    3   28    1    0    0    0    0    0
    1    1    0    0    0    0    0    0    0    0
    1    0    0    0    0    0    0    0    0    0
    0    0    0    0    0    0    0   99    0    0
    1
  38.89      0.90
   .350      .745      .940     1.491     1.615     1.698     1.864
  2.000     2.450     2.750     3.150     3.270     3.400     3.850
  4.150     4.551     5.250     7.000     9.000    11.110    15.000
 19.000    24.070    50.000   140.000   315.774   616.746  1200.000
```

STARS-AERO analysis results:

Table 23 provides the results of flutter analysis by various methods using direct interpolation of modal data. The flutter solution based on the ASE method utilizing state-space formulation employs a data file as in section 6.5. Figures 38 through 40 depict the pattern of root location as a function of velocity for the k, p-k, and ASE methods. In this connection it may be noted that only the elastic modes are considered in these analyses. In the ASE method, the real (a) and imaginary (b) parts of the eigenvalues, termed as damping and frequencies, of the state-space plant dynamics matrix (A) are plotted against the air speed. In the k and p-k methods, the damping term is expressed as $g' = 2ab / \omega_n^2$ where ω_n is the relevant natural frequency.

Table 23. ATM: An aeroelastic antisymmetric analysis using a direct interpolation for AERO paneling.

Mode	Instability number	k - SOLN Velocity, keas	k - SOLN Frequency, rad/sec	p-k Velocity, keas	p-k Frequency rad/sec	ASE Velocity, keas	ASE Frequency rad/sec
Fuselage first bending	F1	445.6	77.9	444.0	77.4	434.8	77.4
Wing second bending	F2	859.3	147.4	861.2	147.1	727.6	136.3
Fin first bending	D1	650.6	0.0	---	---	653.7	0.0
Fin first torsion	D2	729.3	0.0	---	---	727.6	0.0

Analysis notes:
1) F - Flutter point
2) Mach = 0.90
3) Altitude = Sea level

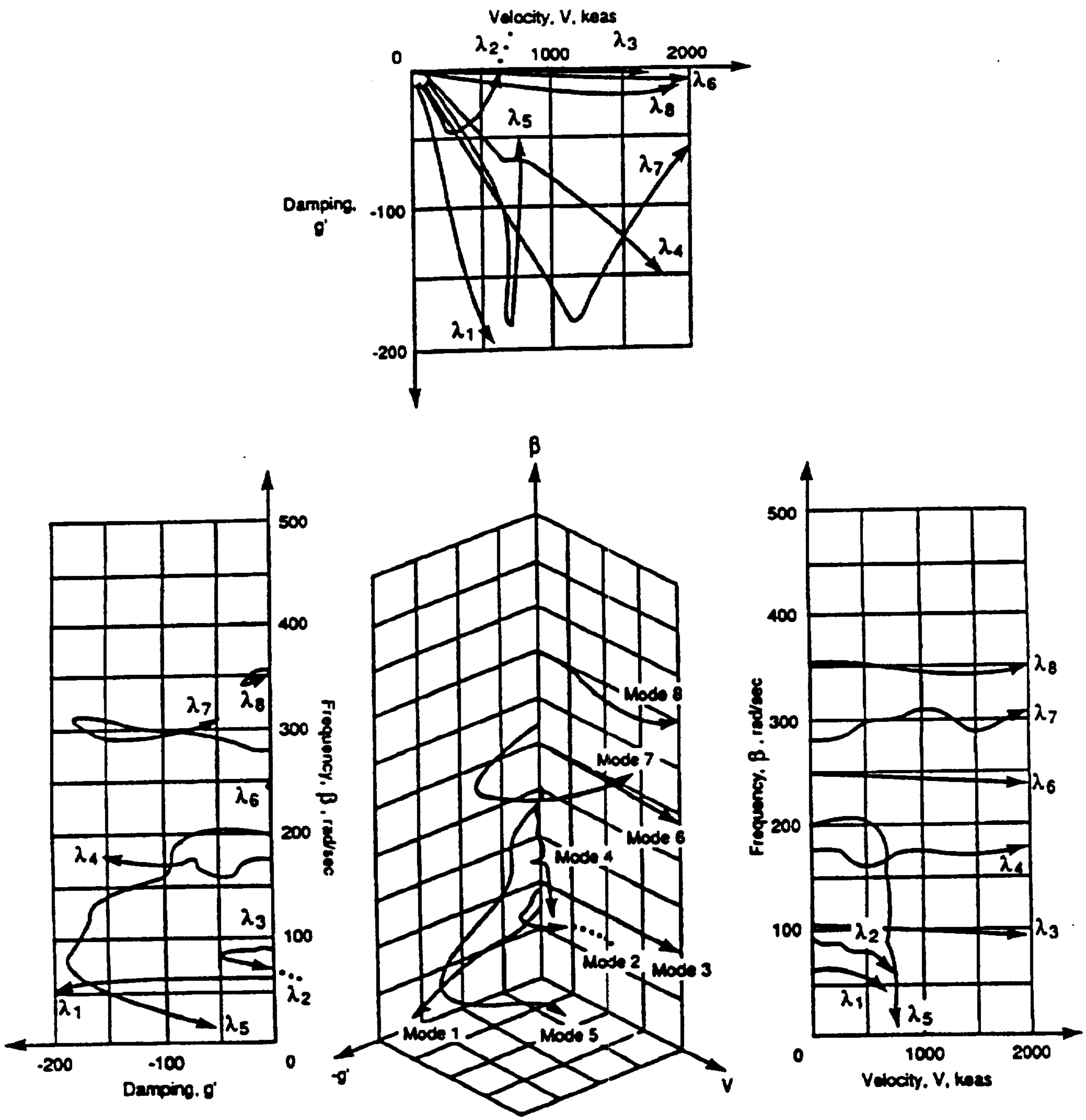

Figure 38. STARS ATM-k flutter analysis—damping (g'), frequency (β), velocity (v) plot, antisymmetric case, using direct interpolation where g' = g x 200.

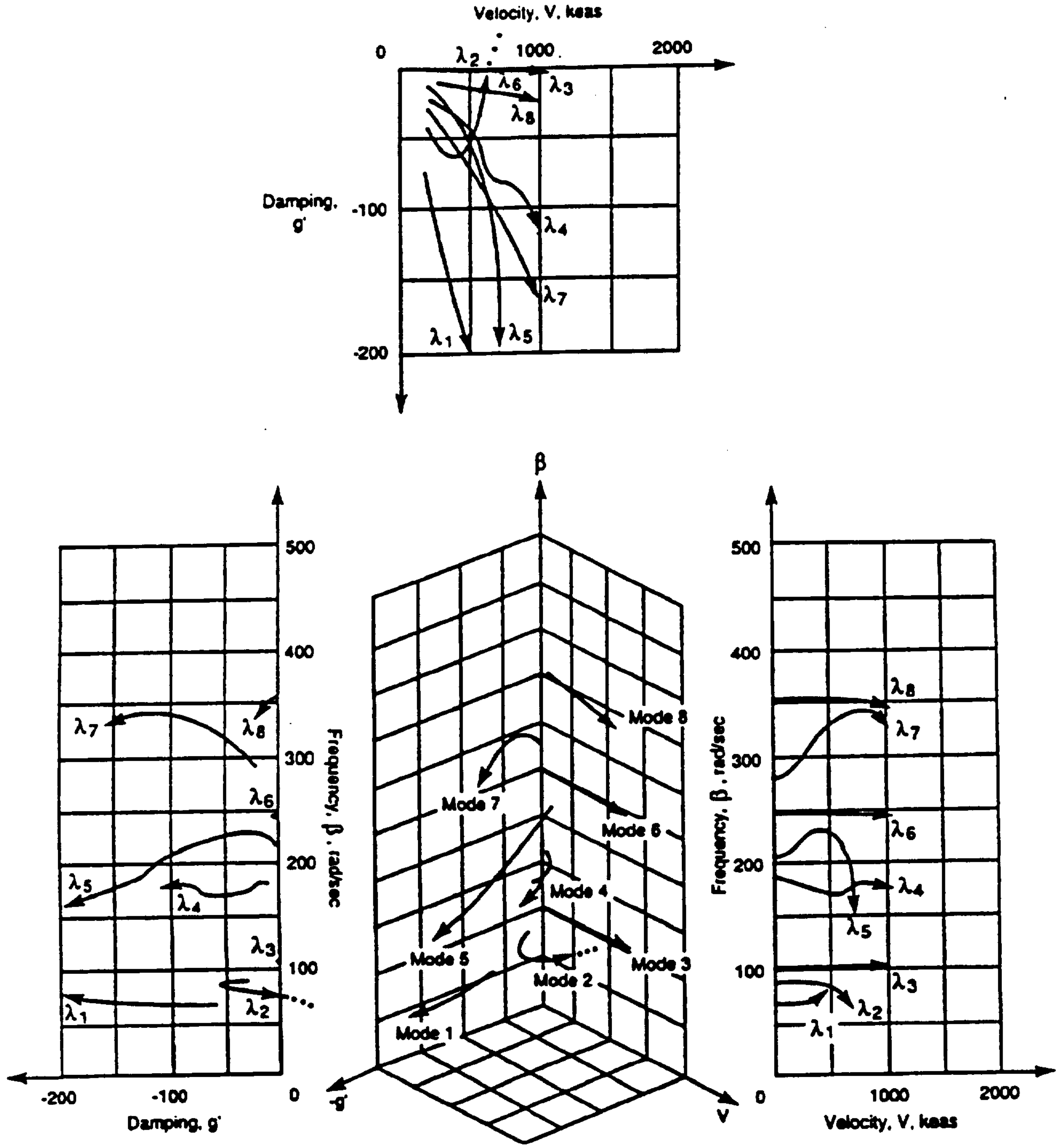

Figure 39. STARS ATM-pk flutter analysis—damping (g'), frequency (β), velocity (v) plot, antisymmetric case, using direct interpolation where g' = g x 200.

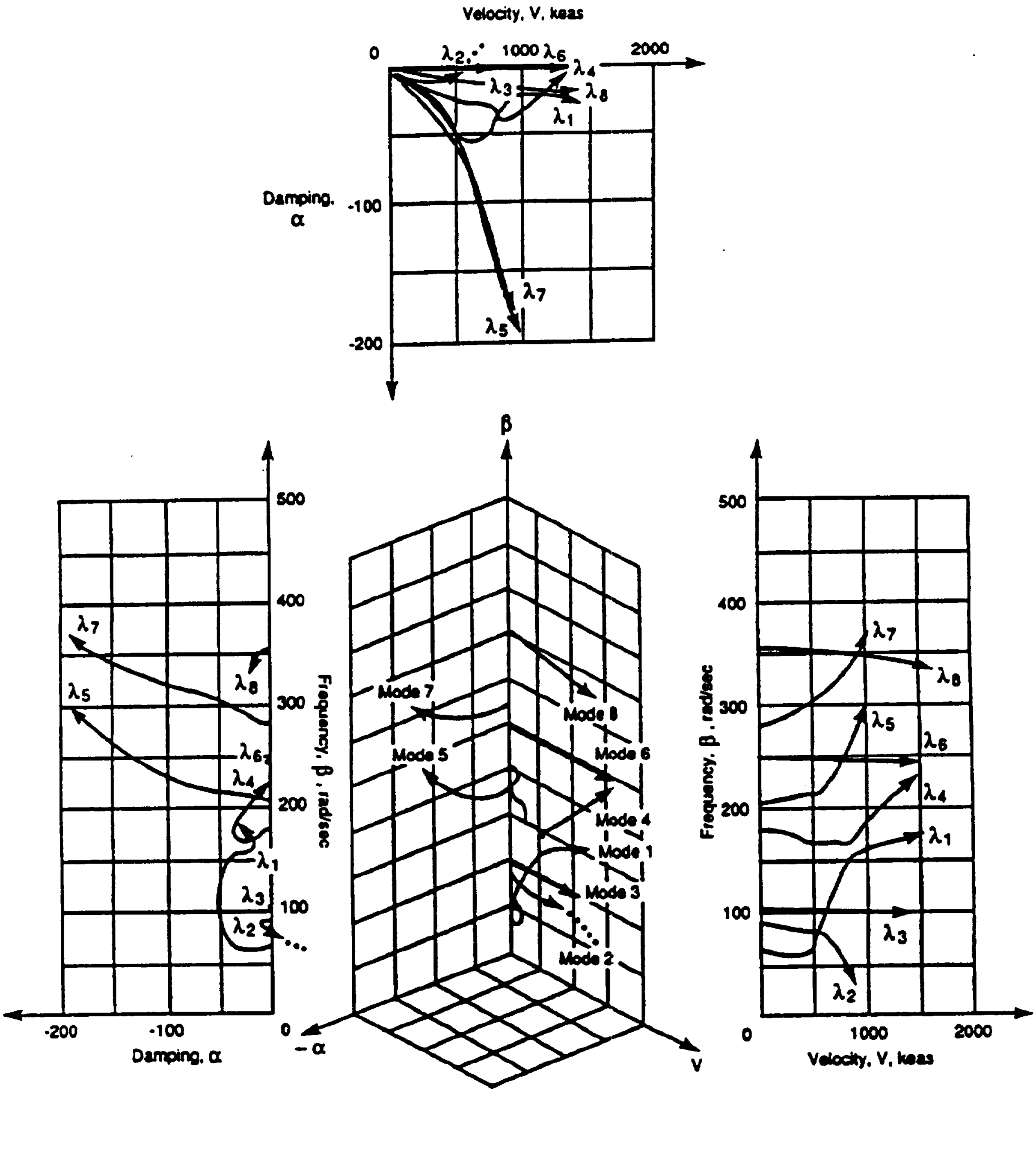

Figure 40. STARS ATM-ASE flutter analysis—damping (a), frequency (b), velocity (v) plot, antisymmetric case, using direct interpolation.

The input data presented here enable appropriate reordering of generalized matrices. Thus, the three perfect rigid body modes (Φ_{PR}) are placed in the front, followed by eight elastic modes (Φ_E) and two rigid control modes (Φ_C) for the ASE solution. For the flutter analysis, only the eight elastic modes (Φ_E) are used.

STARS-ASE-CONVERT input data:

```
$ CONVERT FILE FOR ASE SOLUTION
   13
$ MODAL SELECTION AND ORDERING
   9,1
  10,2
  11,3
   1,4
   2,5
   3,6
   4,7
   5,8
   6,9
   7,10
   8,11
  12,12
  13,13
```

```
$ CONVERT FILE FOR ASE FLUTTER AND DIVERGENCE SOLUTION
    8
$ MODAL SELECTION AND ORDERING
   1,1
   2,2
   3,3
   4,4
   5,5
   6,6
   7,7
   8,8
```

The input data presented here effect curve fitting of unsteady aerodynamic forces employing Padé polynomials. The state-space matrices are also formed in this module. Version I of the input file pertains to the ASE flutter solution, whereas version II corresponds to subsequent ASE frequency response and damping solution.

STARS-ASE-PADÉ input data:

```
$ ATM ASE FLUTTER ANALYSIS, 0.9 MACH AT SEA LEVEL - VERSION I DATA
              0,  8,  0,  0,  0, 10,  2,  1.0, 1004.76, 3.2,  0,  69
$ TENSION COEFFICIENTS
     0.4    0.2
$ GENERALIZED MASS
  .2570E+00  0.0  0.0  0.0  0.0  0.0  0.0  0.0
  .7314E+01  0.0  0.0  0.0  0.0  0.0  0.0
  .1386E+01  0.0  0.0  0.0  0.0  0.0
  .1881E+01  0.0  0.0  0.0  0.0
  .6350E+01  0.0  0.0  0.0
  .1488E+01  0.0  0.0
  .1005E+00  0.0
· .7429E+01
$ GENERALIZED DAMPING
  .00000000E+00  .00000000E+00  .00000000E+00  .00000000E+00
  .00000000E+00  .00000000E+00  .00000000E+00  .00000000E+00
$ Natural Frequencies (radians)
  .63933857E+02  .78230537E+02  .91933533E+02  .18058362E+03
  .18729909E+03  .20388907E+03  .22502760E+03  .32130740E+03
$ VELOCITIES FOR FLUTTER AND DIVERGENCE ANALYSIS
    1.0
  100.0
  200.0
  300.0
  400.0
  500.0
  600.0
  700.0
  800.0
  900.0
 1000.0
 1100.0
 1200.0
 1210.0
 1220.0
 1230.0
 1240.0
 1250.0
 1260.0
 1270.0
 1280.0
 1290.0
 1300.0
 1400.0
 1500.0
 1600.0
 1700.0
 1800.0
 1900.0
 2000.0
 2050.0
 2100.0
 2150.0
 2200.0
 2250.0
 2300.0
 2350.0
 2400.0
 2450.0
 2500.0
 2550.0
 2600.0
 2650.0
 2700.0
 2710.0
 2730.0
 2740.0
 2750.0
 2760.0
 2780.0
 2790.0
 2800.0
 2850.0
 2875.0
 2900.0
 2950.0
 3000.0
```

```
3050.0
3100.0
3150.0
3200.0
3250.0
3300.0
3350.0
3400.0
3450.0
3500.0
3550.0
3600.0


$ ATM ASE ANALYSIS, 0.9 MACH AT 40K FEET - VERSION II DATA
              3,  8,  2,  0,  2, 10,  2,  0.247, 871.0, 3.2,     0,   0
$ TENSION COEFFICIENTS
     0.4    0.2
$ GENERALIZED MASS
0.7878E+02  0.0  0.0  0.0  0.0  0.0  0.0  0.0  0.0  0.0  0.0  0.0  0.0
0.4701E+04  0.0  0.0  0.0  0.0  0.0  0.0  0.0  0.0  0.0  0.0  0.0
0.1831E+05  0.0  0.0  0.0  0.0  0.0  0.0  0.0  0.0  0.0  0.0
0.2570E+00  0.0  0.0  0.0  0.0  0.0  0.0  0.0  0.0  0.0
0.7314E+01  0.0  0.0  0.0  0.0  0.0  0.0  0.0  0.0
0.1386E+01  0.0  0.0  0.0  0.0  0.0  0.0  0.0
0.1881E+01  0.0  0.0  0.0  0.0  0.0  0.0
0.6350E+01  0.0  0.0  0.0  0.0  0.0
0.1488E+01  0.0  0.0  0.0  0.0
0.1005E+00  0.0  0.0  0.0
0.7429E+01  0.0  0.0
0.3998E+01  0.0
0.4419E+00
$ GENERALIZED DAMPING
0.00000000E+00 0.00000000E+00 0.00000000E+00 0.00000000E+00
0.00000000E+00 0.00000000E+00 0.00000000E+00 0.00000000E+00
0.00000000E+00 0.00000000E+00 0.00000000E+00 0.00000000E+00
0.00000000E+00
$ Natural Frequencies (radians)
         0.0             0.0             0.0   .63933857E+02
 .78230537E+02  .91933533E+02  .18058362E+03  .18729909E+03
 .20388907E+03  .22502760E+03  .32130740E+03             0.0
         0.0
$ PHI,THETA, PSI,    US,  VS,  WS,  PS,  QS,  RS, PHID, THAD, PSID, NOOF
 0.0,  0.0, 0.0, 871.0, 0.0, 0.0, 0.0, 0.0, 0.0,  0.0,  0.0,  0.0,   -3
$ SENSOR DATA
 0
    300.00          0.0          50.0
       0.0          0.0           0.0          1.0          0.0          0.0
    300.00          0.0          50.0
       0.0          0.0           0.0          0.0          0.0          1.0
```

STARS-ASE-PADÉ analysis results:

The state-space matrices generated in this module by the Version I data file are utilized for the flutter solution; the results are given in table 24. Results derived through utilization of Version II data are used for subsequent ASE frequency response and damping analyses in the next section.

The input data presented here pertain to the frequency response analysis of the ATM at Mach 0.9 and 40,000 ft altitude. Thus, phase and gain margins as well as damping and frequency values are generated from this module. Figure 41 shows the block diagram for the ATM lateral mode analog control system.

STARS-ASE-FRESP input data:
Open-loop case-

```
$ ATM ANTISYMMETRIC THREE RIGID, EIGHT ELASTIC, AND TWO CONTROL MODES, OPEN LOOP ROLL RESPONSE
C LOOP OPEN BETWEEN BLOCKS 3 AND 9 AS WELL AS BETWEEN 4 AND 10
 48, 12, 4, 4, 58, 0.0, 0.0
 10  4  10  6  10  4  2  1  1
$ BLOCK CONNECTIVITY
    1    3    0    0    0    0    0
    2   10    0    0    0    0    0
    3   -9    7    0    0    0    0
    4    6    0    0    0    0    0
    5    0    0    0    1    0    0
    6    0    0    0    2    0    0
    7    0    0    0    3    0    0
    8    0    0    0    4    0    0
    9    5    0    0    0    0    0
   10   -4    8    0    0    0    0
$ TRANSFER FUNCTION DESCRIPTIONS
    1    1    2
    2    1    2
    3    2    2
    4    2    2
    5    1    3
    6    1    3
    7    1    1
    8    1    1
    9    1    3
   10    1    1
$ LISTING OF POLYNOMIAL COEFFICIENTS
 .2000E+02 .0000E+00 .0000E+00 .0000E+00 .0000E+00
 .2000E+02 .1000E+01 .0000E+00 .0000E+00 .0000E+00
 .2000E+02 .0000E+00 .0000E+00 .0000E+00 .0000E+00
 .2000E+02 .1000E+01 .0000E+00 .0000E+00 .0000E+00
 .5000E+01 .1000E+00 .0000E+00 .0000E+00 .0000E+00
 .0000E+00 .1000E+01 .0000E+00 .0000E+00 .0000E+00
 .0000E+00 .1000E+01 .0000E+00 .0000E+00 .0000E+00
 .1000E+00 .1000E+01 .0000E+00 .0000E+00 .0000E+00
 .1877E+05 .0000E+00 .0000E+00 .0000E+00 .0000E+00
 .1877E+05 .1930E+03 .1000E+01 .0000E+00 .0000E+00
 .1877E+05 .0000E+00 .0000E+00 .0000E+00 .0000E+00
 .1877E+05 .1930E+03 .1000E+01 .0000E+00 .0000E+00
 .1000E+01 .0000E+00 .0000E+00 .0000E+00 .0000E+00
 .1000E+01 .0000E+00 .0000E+00 .0000E+00 .0000E+00
 .1000E+01 .0000E+00 .0000E+00 .0000E+00 .0000E+00
 .1000E+01 .0000E+00 .0000E+00 .0000E+00 .0000E+00
 .1000E+00 .0000E+00 .0000E+00 .0000E+00 .0000E+00
 .1000E+02 .1100E+02 .1000E+01 .0000E+00 .0000E+00
 .1000E+01 .0000E+00 .0000E+00 .0000E+00 .0000E+00
 .1000E+01 .0000E+00 .0000E+00 .0000E+00 .0000E+00
$ GAIN INPUTS FOR EACH BLOCK
 .1000E+01 .1000E+01 .1000E+01 .1000E+00 .1000E+01 .1000E+01 .1000E+01 .1000E+01
 .1000E+01 .1000E+01
$ SPECIFICATION FOR SYSTEM OUTPUTS
    7    8    0    0    0    0    0    0    0    0    0    0    0    0    0    0
    0    0    0    0    0    0
$ SPECIFICATION FOR SYSTEM INPUTS
    7    8    0    0    0    0    0    0
$ CONNECTION DETAILS FROM PLANT TO BLOCKS
    2    2    0
    7    1
    8    2
    1    1
    2    2
$ FREQUENCY RANGE SPECIFICATIONS
 0.1,  500.0,  100
$ LOOP DEFINITIONS
    1
    3,   1
```

ORIGINAL PAGE IS
OF POOR QUALITY

STARS-ASE-FRESP input data:
Closed-loop case-

```
$ ATM ANTI-SYMMETRIC-THE ROLL AND YAW CLOSED LOOP CASE
C
   48,  12,   4,   4,  53, 0.0, 0.0,   3,   3
   12    4   10    6   10    0    0    1    1
$ BLOCK CONNECTIVITY
    1    3    0    0    0    0    0
    9    5    0    0    0    0    0
   11    0    0    0    0    3    9
    3    7    0    0    0    0    0
    5    0    0    0    1    0    0
    7    0    0    0    3    0    0
    2   10    0    0    0    0    0
    4    6    0    0    0    0    0
   12    0    0    0    0   10    4
    6    0    0    0    2    0    0
    8    0    0    0    4    0    0
   10    8    0    0    0    0    0
$ TRANSFER FUNCTION DESCRIPTIONS
    1    1    2
    2    1    2
    3    2    2
    4    2    2
    5    1    3
    6    1    3
    7    1    1
    8    1    1
    9    1    3
   10    1    1
   11    1    1
   12    1    1
$ LISTING OF POLYNOMIAL COEFFICIENTS
    1 .2000E+02 .0000E+00 .0000E+00
    0 .2000E+02 .1000E+01 .0000E+00
    2 .2000E+02 .0000E+00 .0000E+00
    0 .2000E+02 .1000E+01 .0000E+00
    3 .5000E+01 .1000E+00 .0000E+00
    0 .0000E+00 .1000E+01 .0000E+00
    4 .0000E+00 .1000E+01 .0000E+00
    0 .1000E+00 .1000E+01 .0000E+00
    5 .1877E+05 .0000E+00 .0000E+00
    0 .1877E+05 .1930E+03 .1000E+01
    6 .1877E+05 .0000E+00 .0000E+00
    0 .1877E+05 .1930E+03 .1000E+01
    7 .1000E+01 .0000E+00 .0000E+00
    0 .1000E+01 .0000E+00 .0000E+00
    8 .1000E+01 .0000E+00 .0000E+00
    0 .1000E+01 .0000E+00 .0000E+00
    9 .1000E+00 .0000E+00 .0000E+00
    0 .1000E+02 .1100E+02 .1000E+01
   10 .1000E+01 .0000E+00 .0000E+00
    0 .1000E+01 .0000E+00 .0000E+00
   11 .1000E+01 .0000E+00 .0000E+00
    0 .1000E+01 .0000E+00 .0000E+00
   12 .1000E+01 .0000E+00 .0000E+00
    0 .1000E+01 .0000E+00 .0000E+00
$ GAIN INPUTS FOR EACH BLOCK
    1 .1000E+01    2 .1000E+01    3 .1000E+01    4 .1000E+00    5 .1000E+01
    6 .1000E+01    7 .1000E+01    8 .1000E+01    9 .1000E+01   10 .1000E+01
   11 -.100E+01   12 -.100E+01
$ SPECIFICATION FOR SYSTEM OUTPUTS
    7    8    0    0    0    0    0    0    0    0    0    0    0    0    0    0
    0    0    0    0    0    0    0    0
$ SPECIFICATION FOR SYSTEM INPUTS
    7    8    0    0    0    0    0    0
$ CONNECTION DETAILS FROM PLANT TO BLOCKS
    2    2    0
    7    1
    8    2
    1    1
    2    2
$ LOOP DEFINITIONS
    0    0
```

ORIGINAL PAGE IS
OF POOR QUALITY

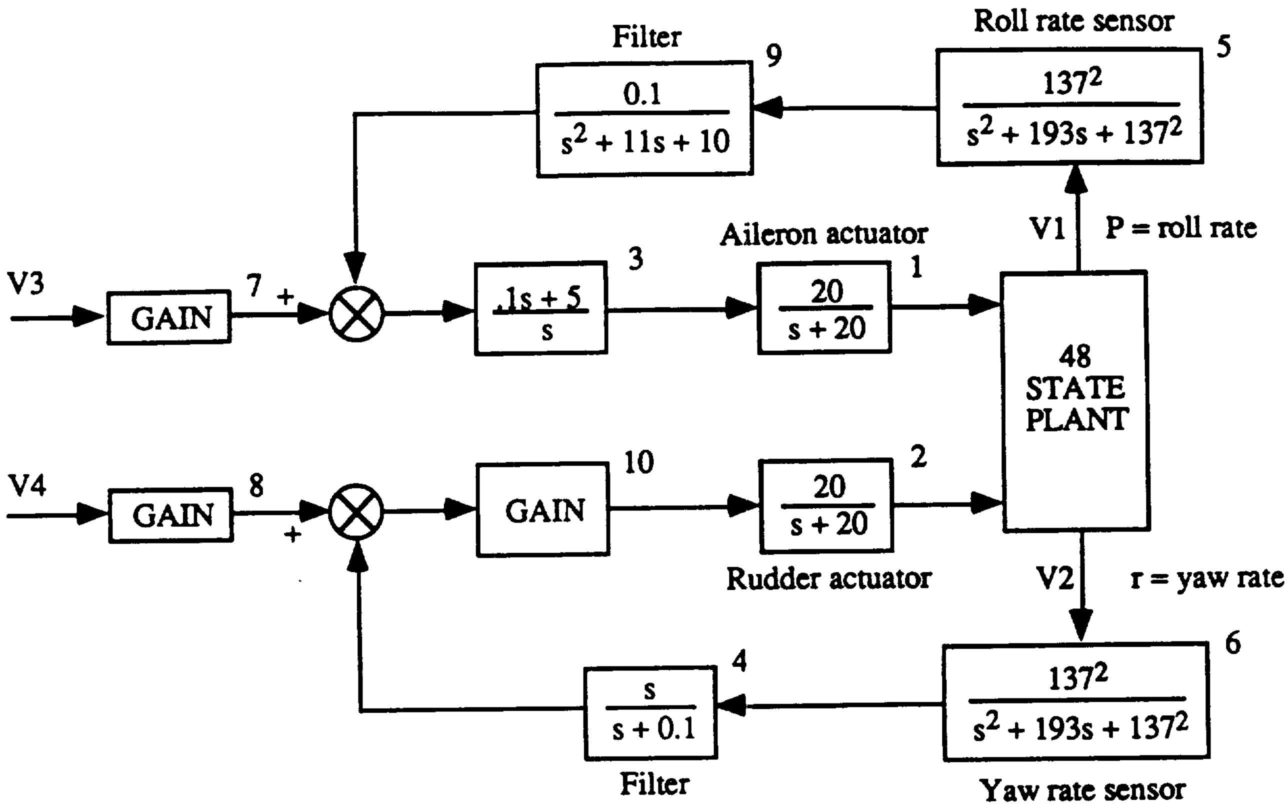

Figure 41. ATM lateral mode analog control system.

STARS-ASE-PADÉ analysis results:

Figures 42 and 43 depict the lateral loop gains for the roll and yaw modes, respectively. The gain margins are tabulated in table 24.

Table 24. ATM gain and phase margins.

Mode	Phase crossover, rad	Gain margin, dB
Roll	19.88	79.59
Yaw	2.48	-5.25

The closed loop damping and frequency plots are shown in figure 44.

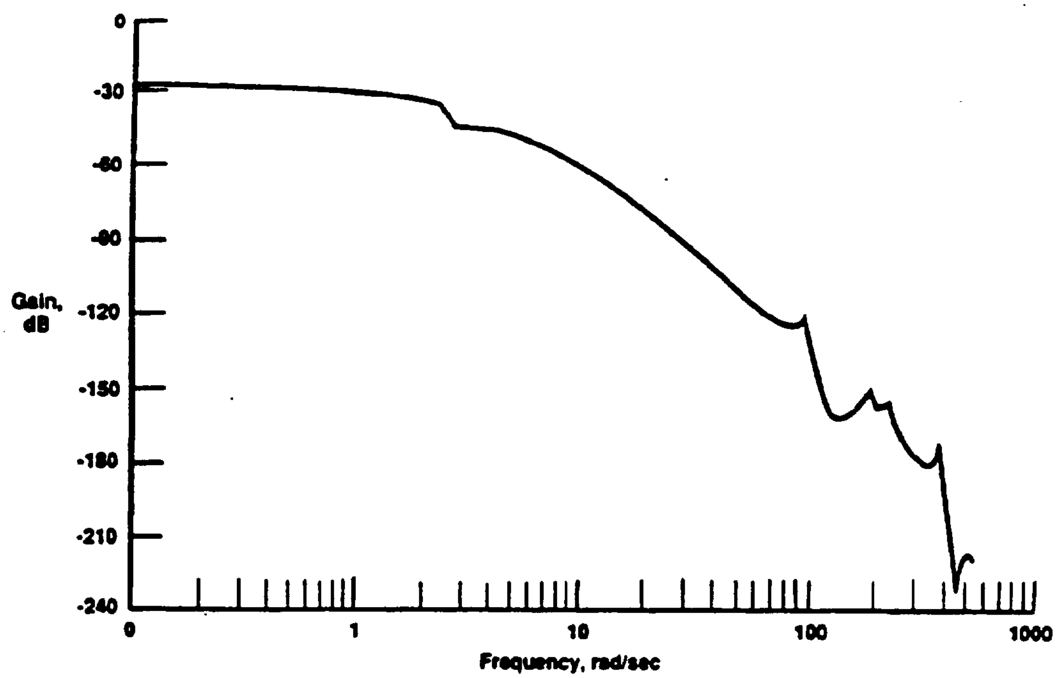

(a) Gain.

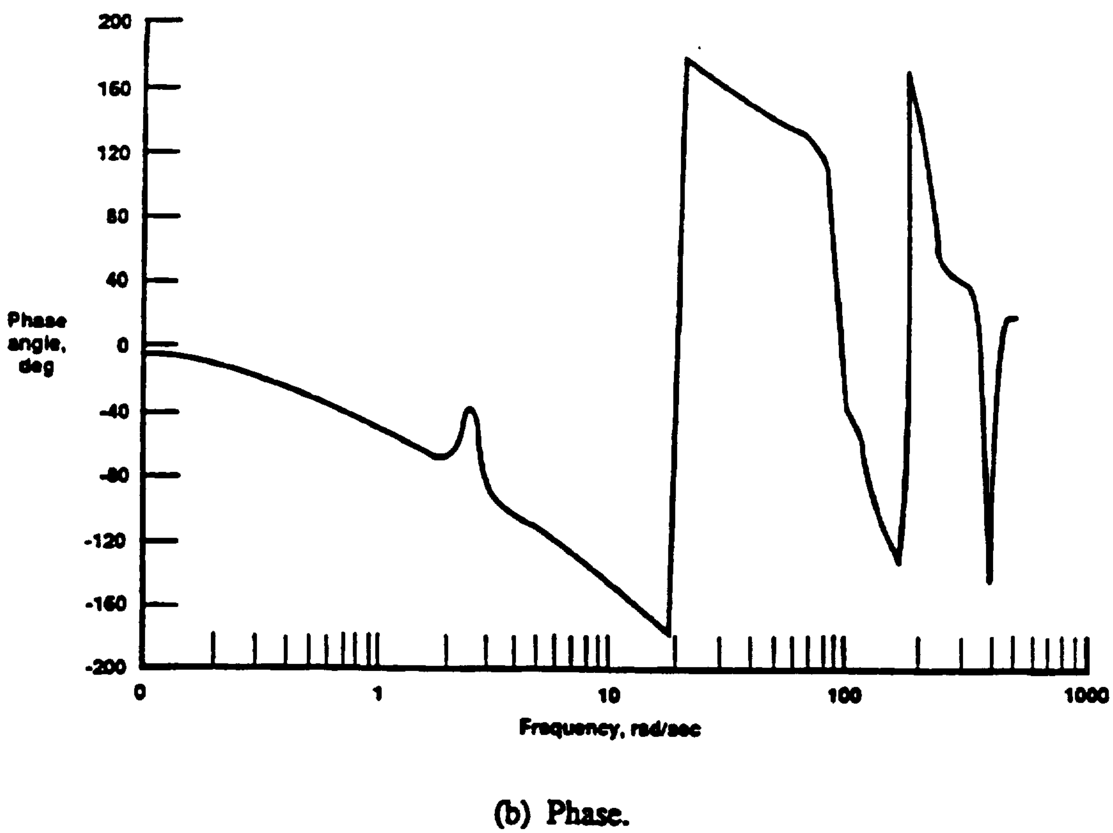

(b) Phase.

Figure 42. ATM lateral loop gains, roll mode.

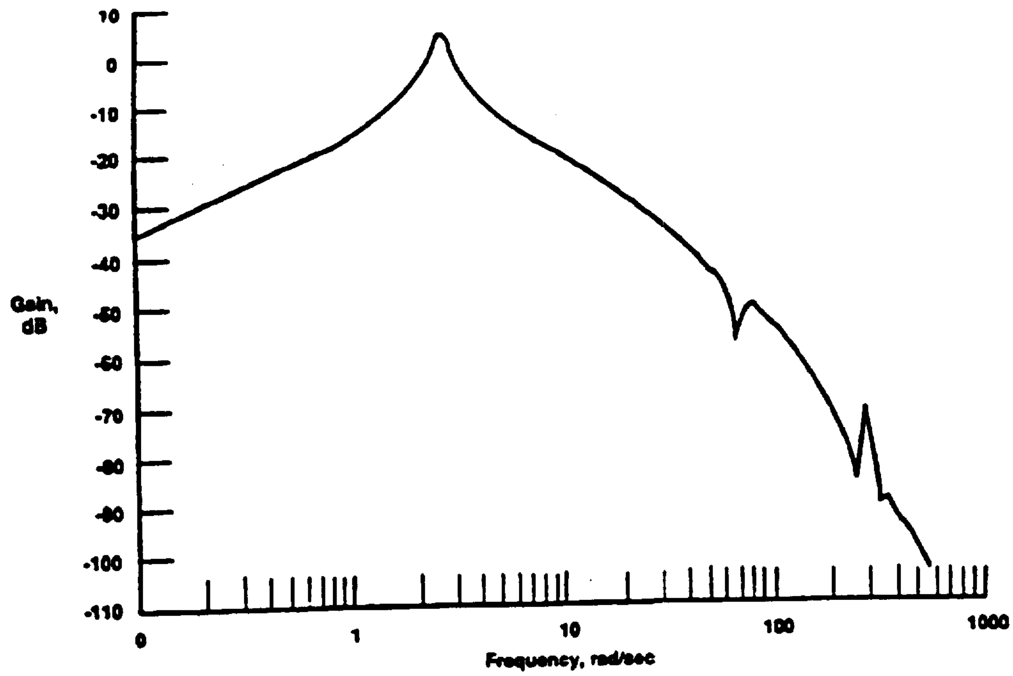

(a) Gain.

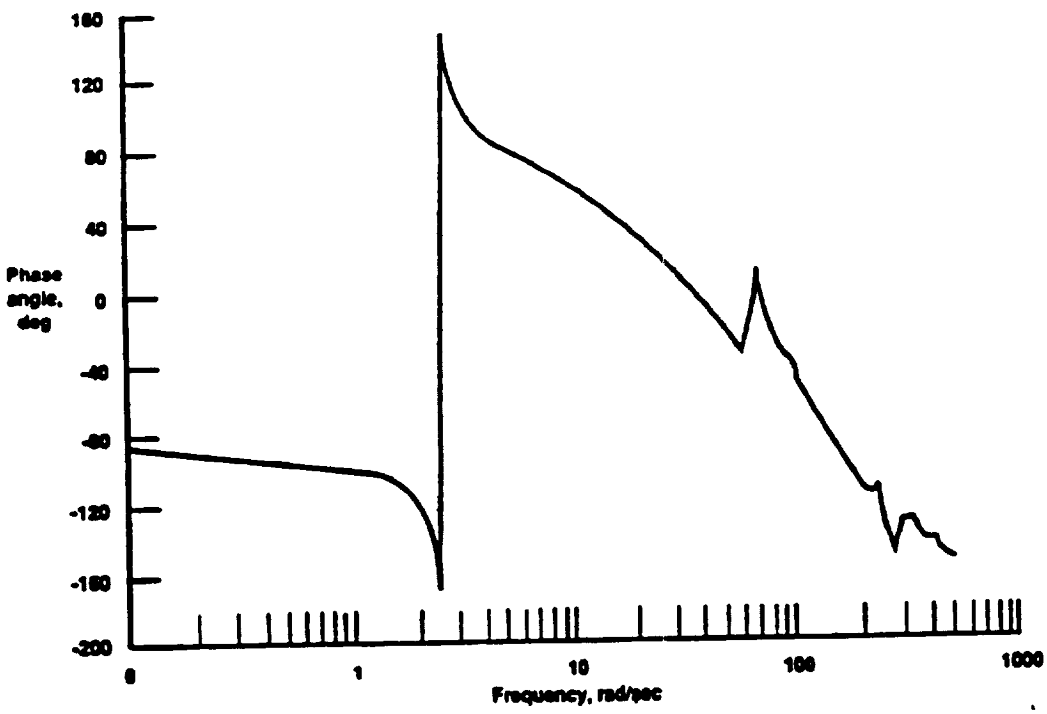

(b) Phase.

Figure 43. ATM lateral loop gains, yaw mode.

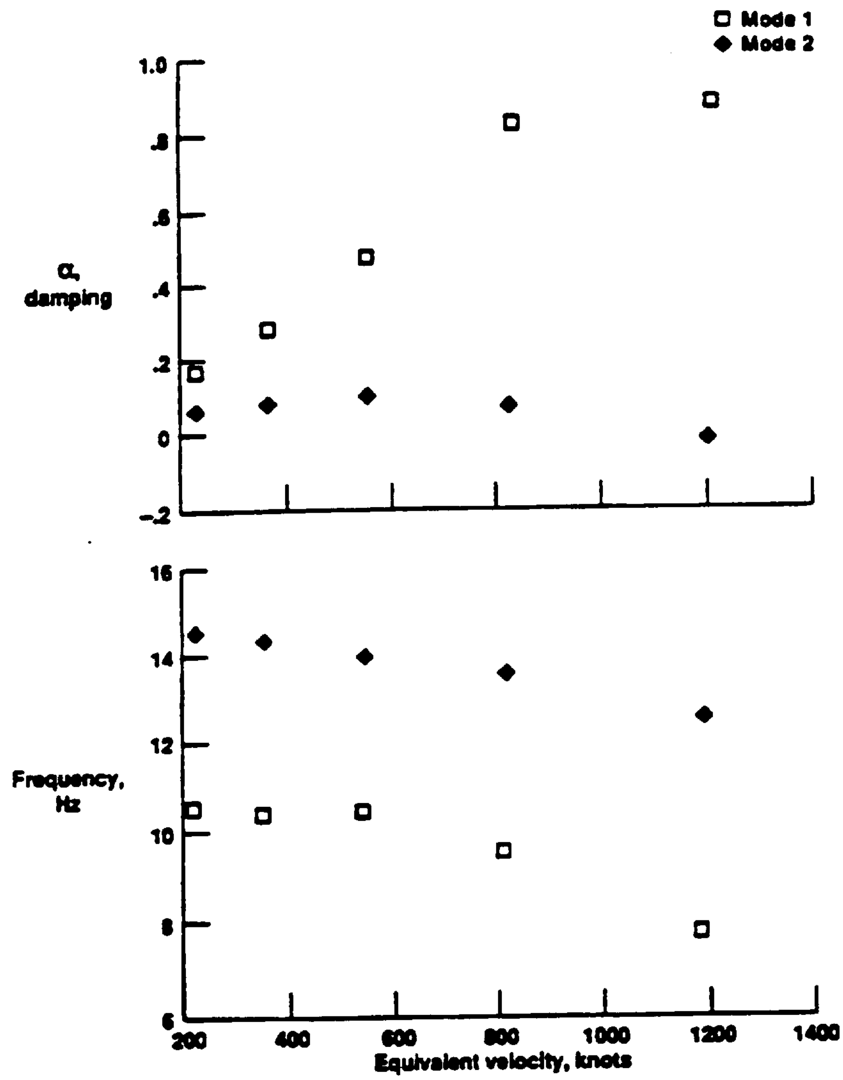

Figure 44. ATM closed-loop damping, v-g, and frequency, v-f.

8. STARS NONLINEAR MULTIDISCIPLINARY ANALYSIS - CFD, AEROELASTICITY AND AEROSERVOELASTICITY

A number of consistent disciplines and innovative algorithms must be incoporated into an integrated system required to simulate nonlinear peformance characteristics of advanced engineering systems such as aerospace vehicles. Since the finite element technique can be commonly utilized to discretize relevant solids and fluids continua, its employment ensures accurate interaction of various disciplines. Figure 1 depicts a number of disciplines that are involved in the multidisciplinary modeling simulation of such systems. Some relevant details of finite element formulations, adopted for computational fluid dynamics (CFD) as well as nonlinear stability analysis, are presented next.

8.1 Finite Element Computational Fluid Dynamics (CFD)

The CFD analysis requies two major fundamental solution capabilities:

1. Effective generation of unstructured and solution adaptive fluids domain meshes

2. Finite element analysis of the relevant flow problem

and effective development of related numerical tools that are vital to the efficient solution of complex practical problems; these have been appropriately incorportated in the STARS program.

8.1.1 Mesh Generation

An advancing front technique, developed for automated generation of unstructured meshes, has been found to be rather suitable for discretization of complex domains. This procedure has the following advantages:

1. Flexibilty with regard to specification of arbitrary shapes and varying grid density throught the domain

2. Facility in adaptive mesh generation in accordance with solution trend

Such an algorithm was initially developed[21] for arbitrary, multi-connected, planar domains in which the interior nodes are generated first, then suitably linked to yield the best possible triangulation; during this process, the generation front is continually updated each time a new element is constructed. Further improvement and extension of this technique in three dimensions is described in reference [22]; here the nodes and triangles are formed simultaneously for all boundary surfaces. This is followed by generation of tetrahedra by the advancing front approach to fill the entire solution domain. Suitable background grids are utilized to specify important mesh parameters defining node spacing, stretching parameters and directions.

The 3-D automated unstructured mesh generation scheme, as above, has been found to be rather versatile for modeling of practical CFD solution domain around complex structural forms such as an aircraft. However, since the advancing front technique involves a rather extensive search for nodes and faces on the front, the grid generation time tends to be rather large for such complex configurations. A simple modification of the procedure, implemented during our current effort, proves to be rather efficient and economical. In this method, the usual technique is first utilized to generate a grid whose cells have linear dimensions about twice the desired size, and then each cell is reduced locally to its desired size (ref. 23).

8.1.2 Finite Element CFD Analysis

The dynamic equation for a viscous, heat-conducting, compressible fluid obeying conservation of mass, momentum, and energy can be expressed by a set of partial differential equations

$$\frac{\partial V}{\partial t}+\frac{\partial F_i}{\partial x_i}=f_b, \qquad i=1,2,3 \tag{68}$$

where the solution, flux and body forces column vectors as well as the viscous stress tensor are defined as below

$$V=\{\rho \;\; \rho u_j \;\; \rho E\} \tag{69}$$

$$F_i=\left\{\rho u_i \;\; \rho u_i u_j+p\delta_{ij}+\sigma_{ij} \;\; u_i(\rho E+p)+u_l\sigma_{li}+k\frac{\partial T}{\partial x_i}\right\} \tag{70}$$

$$f_b=\{0 \;\; f_{b_j} \;\; u_l f_{b_l}\} \tag{71}$$

$$\sigma_{ij}=-\frac{2}{3}\mu\frac{\partial u_k}{\partial x_k}\delta_{ij}+\mu\left(\frac{\partial u_i}{\partial x_j}+\frac{\partial u_j}{\partial x_i}\right) \tag{72}$$

in which ρ, p, E are the density, average pressure intensity and total energy, respectively, δ_{ij} the Kronecker delta; u_j the velocity component in the direction x_j of a cartesian coordinate system, μ the viscosity, k the thermal conductivity, and f_b the body forces. The above equations are supplemented with state equations

$$p=(\gamma-1)\rho\left[E-\frac{1}{2}u_i u_i\right] \tag{73}$$

$$T=\left[E-\frac{1}{2}u_i u_i\right]c_v \tag{74}$$

for a complete solution, in which γ is the ratio of specific heats and c_v is the specific heat at constant volume, such a formulation being valid for a perfect gas.

Solution of the non-viscous form of equation (68) is achieved by first obtaining a Taylor series expansion of V in time domain. The spatial domain Ω is next discretized by unstructured meshes consisting of 3-D tetrahedron elements. Using linear finite element approximations $V=a\hat{V}$, $\hat{V}$ being nodal variable values, and employing Galerkin weighted residual procedure, a time-dependent form of the governing equations may be obtained as below

$$M\delta\hat{V}=-\Delta\left[C\hat{V}\right]+R \tag{75}$$

in which **R** includes artifical viscosity effects essential for capturing shocks. Solution of equation (75) is effected by advancing this time-dependent form until steady conditions are obtained; an explicit time-stepping iterative scheme as well as an alternative quasi-implicit solution scheme has been implemented in the STARS program to that effect. An accelerated Euler solution procedure based on the Aitken acceleration technique has recently been implemented (ref. 24) that effects considerable improvement in solution convergence rate.

8.2 Nonlinear Aeroelastic and Aeroservoelastic Analysis

Such a process starts with the finite element structural modeling and subsequently computes the natural frequencies (ω) and modes (ϕ) that consist of rigid body, elastic, and control surface motions, by solving

$$\mathbf{M}\ddot{\mathbf{u}} + \mathbf{K}\mathbf{u} = \mathbf{0} \tag{76}$$

in which **M** and **K** are the inertial and stiffness matrices, respectively, and **u** is the displacement vector. This is achieved by an efficient block Lanczos procedure that fully exploits matrix sparsity.[7,25] Next, a steady-state Euler solution is effected in which optimum solution convergence is achieved through an explicit or an alternative quasi-implicit, local time-stepping solution procedure that also employs a residual smoothing strategy. The resulting vehicle equation of motion is then cast into the frequency domain as follows:

$$\hat{\mathbf{M}}\ddot{\mathbf{q}} + \hat{\mathbf{C}}\dot{\mathbf{q}} + \hat{\mathbf{K}}\mathbf{q} + \hat{\mathbf{f}}_a(t) + \hat{\mathbf{f}}_I(t) = \mathbf{0} \tag{77}$$

in which the generalized matrices and vectors are as below:

$\hat{\mathbf{M}}$	=	inertia matrix ($=\mathbf{\Phi}^T\mathbf{M}\mathbf{\Phi}$), and similarly
$\hat{\mathbf{K}}, \hat{\mathbf{C}}$	=	stiffness and damping matrices
$\mathbf{q}$	=	displacement vector ($=\mathbf{\Phi}^T\mathbf{u}$)
$\hat{\mathbf{f}}_a(t)$	=	aerodynamic (CFD) load vector ($=\mathbf{\Phi}_a^T pA$), where p is the Euler pressure, A the appropriate surface area, and $\mathbf{\Phi}_a$ the modal vector pertaining to areodynamic grid points interpolated from relevant structural nodes
$\hat{\mathbf{f}}_I(t)$	=	impulse force vector ($=\mathbf{\Phi}^T\mathbf{f}_i$)

where $\mathbf{f}_I$ is the user input that contains a number of modes of interest. Equation (77) may next be formulated in the state-space matrix equation form as

$$\dot{\mathbf{X}} = \mathbf{A}\mathbf{X} + \mathbf{b}_a(t) + \mathbf{b}_I(t) \tag{78}$$

where

$$\mathbf{X} = \begin{bmatrix} \mathbf{q} \\ \dot{\mathbf{q}} \end{bmatrix}$$

$$\mathbf{A} = \begin{bmatrix} \mathbf{0} & \mathbf{I} \\ -\hat{\mathbf{M}}^{-1}\hat{\mathbf{K}} & -\hat{\mathbf{M}}^{-1}\hat{\mathbf{C}} \end{bmatrix}$$

$$b_a(t) = \begin{bmatrix} 0 \\ -\hat{M}^{-1}\hat{f}_a(t) \end{bmatrix}$$

$$b_I(t) = \begin{bmatrix} 0 \\ -\hat{M}^{-1}\hat{f}_I(t) \end{bmatrix}$$

and a time response solution of equation (78) in an interval Δt (= $t_{n+1} - t_n$) is obtained as

$$X_{n+1} = e^{A\Delta t}X_n + A^{-1}\,[e^{A\Delta t} - I]\,[b_a(t_n) + b_I(t_n)] \tag{79}$$

Data consisting of q and $\dot{q}$ vectors are next stored for later processing. The structural deformations u and velocities $\dot{u}$ are then computed from q and $\dot{q}$, respectively, and the aerodynamic mesh is updated only if large motions are encountered. Such u and $\dot{u}$ values are next fed into the CFD code to change velocity boundary conditions at the solid boundary. This is then followed by a one-step Euler solution using a global time-stepping scheme, and the entire solution process is then repeated for the required number of time steps.

The response data, as above, may next be resolved into modal components utilizing an FFT, as below:

$$X = \sum_{m=1}^{p} e^{\varsigma_m t}(a_m \cos \omega_m t + b_m \sin \omega_m t) \tag{80}$$

yielding the damping (ζ) and frequency (ω) values. This process is repeated for a number of dynamic pressure values, $\bar{q} = \frac{1}{2}\rho V^2$ and the ζ and ω values plotted against $\bar{q}$ or Mach number. Such a plot depicting stability characteristics of the vehicle enables prediction of onset of flutter or divergence occurring within the entire flight regime. Figure 45 depicts a flowchart of the nonlinear flutter analysis methodology adopted in the STARS program. Alternatively, the generalized modal velocity values are also plotted as a function of time and an onset of flutter may also be predicted from their pattern of convergence. Similar solution is also effected by a root tracking procedure that identifies coalescence of the roots.

In aeroservoelastic analysis, assuming that a control law has been designed based on linear characteristics of the control derivatives, such a control law may be interfaced with the CFD analysis procedure. Thus, the input to the control law will consist of angle of attack, α, and also, q, $\dot{q}$, $\ddot{q}$, and the control hinge moment, M_c. Based on such input, the flight control derives the necessary control surface deflections to alleviate the aircraft response.

For the more realistic case, where the control derivatives are not known *a priori*, since the nonlinear CFD analysis has been used, an autoregression procedure may be utilized to reconstruct a model based on past history of aircraft input and output information. Thus, for a small incremental motion of a control surface, the vehicle body forces and moments are first computed from the surface pressure distribution. This is followed by an estimation of such parameters as angle of attack (α), side slip (β), control surface deflections and hinge moments, as well as roll, pitch, and yaw rates employing q and $\dot{q}$ values computed from appropriate equations of motion. These calculations are to be performed for a

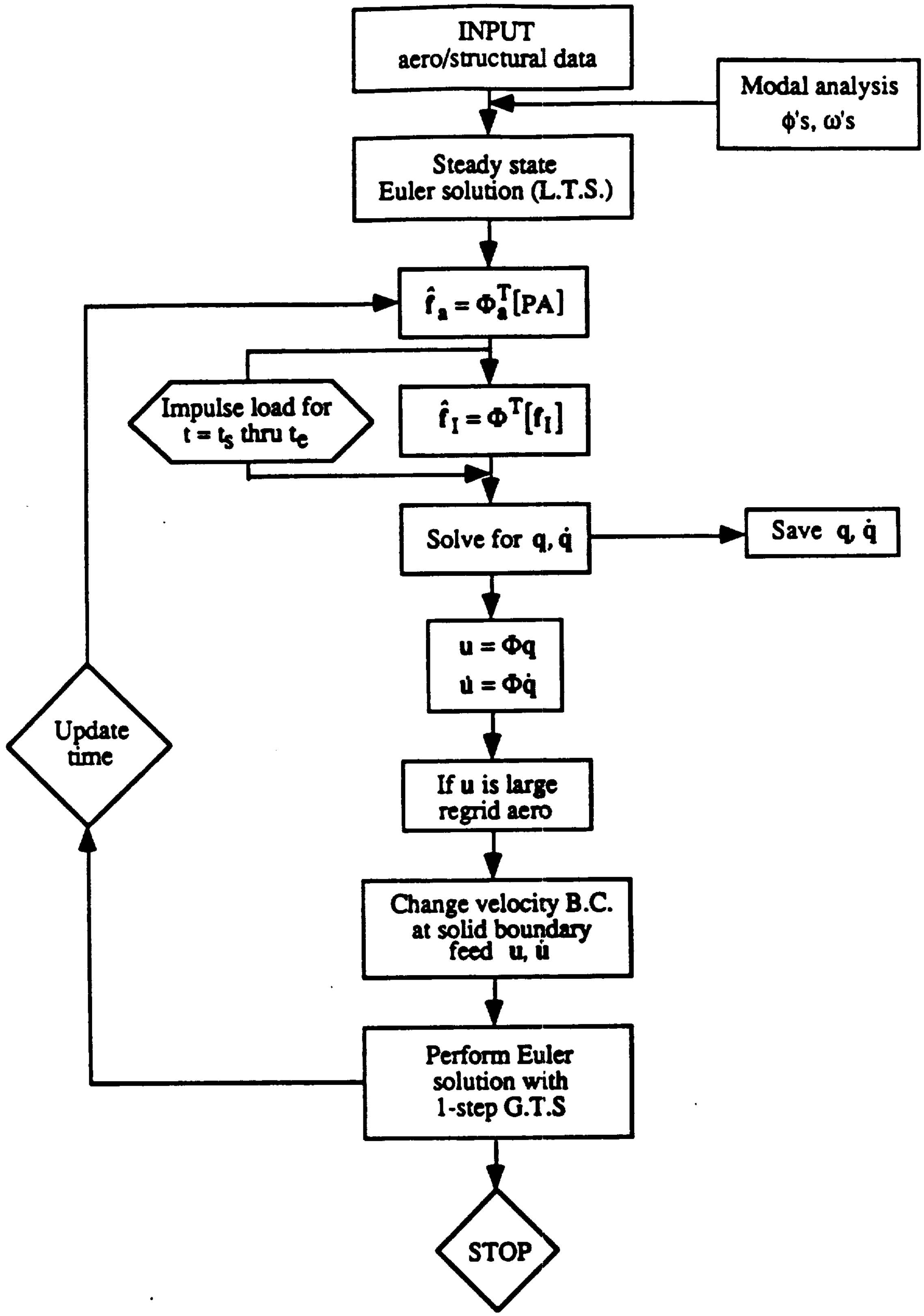

Figure 45 Nonlinear Flutter Analysis Methodolgy

large number of time steps that represent the entire range of control surface motion, and the resulting data are then employed to obtain static and dynamic stability derivatives for the vehicle simulation analysis.

8.3 Numerical Examples

A large number of CFD analyses has been performed in support of such NASA projects as PEGASUS, SR71, SR71-HALO, High Speed Civil Transport (HSCT), National Aerospace Plane (NASP), and generc hypersonic vehicle, among others. Some such analysis results have also been correlated with those obtained from flight testing. In the area of aeroelasticity, the associated solution module has been checked out by comparing such results with those obtained from tests as well as other analysis methods. Some of these analysis results are presented next.

8.3.1 PEGASUS Vehicle - CFD Analysis

An Euler solution for the vehicle was achieved for Mach 5.0 and angle of attack (α) of 0.5 degrees. The aerodynamic model has the following details:

1. Number of tetrahedral elements = 728,022
2. Number of nodes = 128,600

and figure 46 depicts the external surface grid. Detailed calculaions were made to extract the CFD pressure data and such values in the fillet region were compared with flight test data, and also with results from a parallel analysis employing a Navier-Stokes finite difference flow solver code[26]. Such results are compared in table 25, whereas figure 47 depicts the pressure (p/p_i) distribution on the vehicle surface that includes the fillet area.

Table 25. PEGASUS vehicle - comparison of numerical and flight pressure (lb/ft^2) data, Mach = 5.0, α = 0.5 deg

Sensor #	Flight data	STARS	Parc 3D
1	28	28	29
2	31		
3	17	22	26
4	16		
5	32	23	22
7	30	23	24

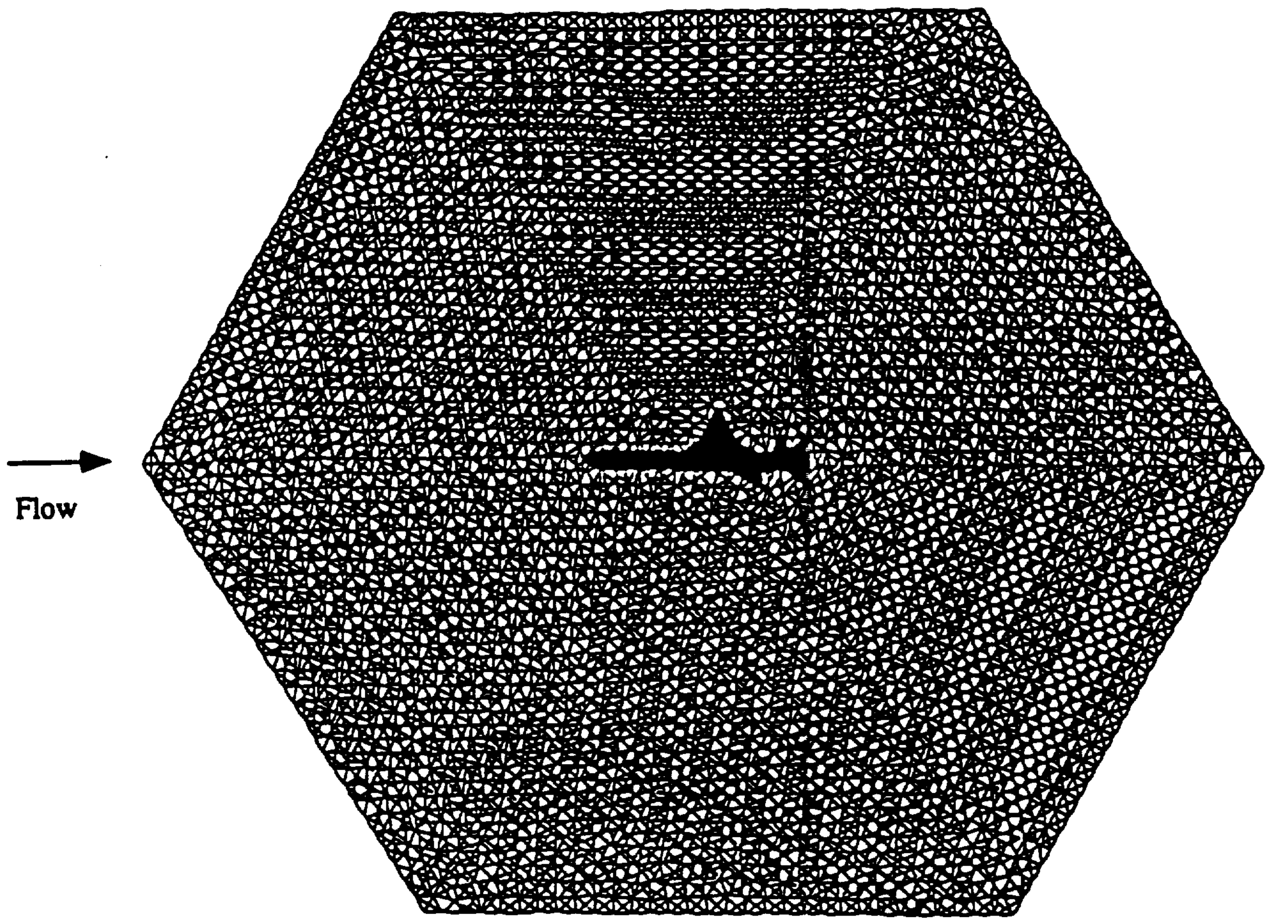

Figure 46. PEGASUS external aerodynamic surface grid

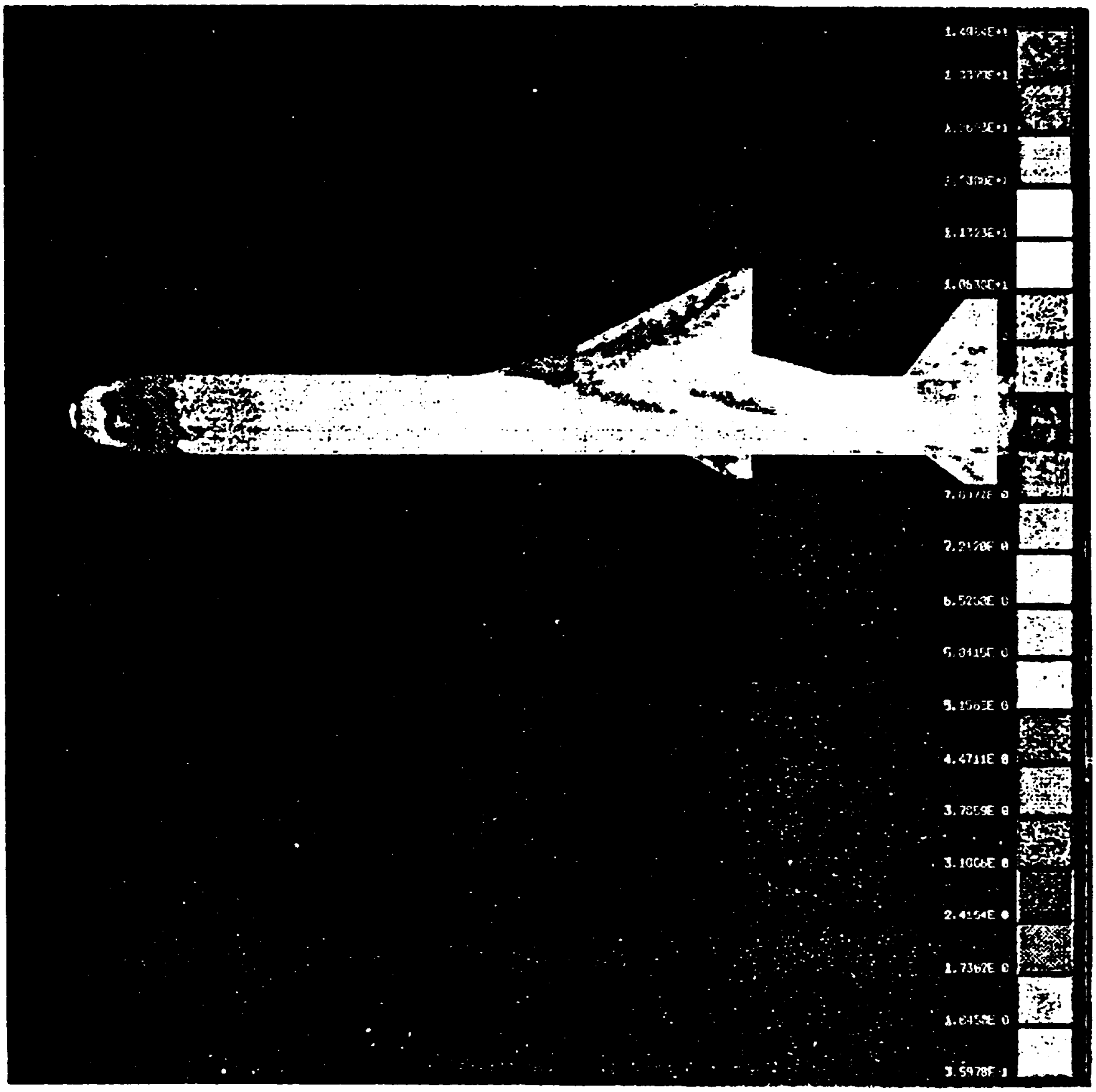

Figure 47. PEGASUS CFD solution - pressure distribution (p/p_i), Mach = 5.0, alpha = 0.5

8.3.2 Generic Hypersonic Vehicle - CFD Analysis

A generic hypersonic vehicle (fig. 48) was chosen for some aeroelastic analyses. The 3-D aerodynamic grid (fig. 49) developed in this connection has the following details:

1. Number of tetrahedral elements = 1,293,112
2. Number of nodes = 221,893

An Euler solution was effected for Mach of 7.0, and figure 50 depicts a typical density distribution on and around the top surface of the vehicle.

8.3.3 Oscillating Double Wedge Airfoil - Unsteady Aerodynamic Forces Computation

To check the STARS nonlinear aeroelastic and ASE analysis capabilities, a double wedge airfoil[24] (length = 2, depth = 0.092, span = 2.5) undergoing pitching motion along the trailing edge (fig. 51) and oscillating at a frequency of 670 rad/sec was analyzed using STARS-ASE(NL) module. The associated aerodynamic grid (fig. 52) consists of 33,850 tetrahedron elements. The unsteady aerodynamic forces were computed for an airspeed of Mach 3.0, the maximum pitching angle being 0.1 rad. Figure 53 compares such results with those obtained by the simple piston theory.

8.3.4 Clamped Plate - Nonlinear Flutter Analysis

Some parametric flutter solution studies were performed on a clamped rectangular panel of length-width ratio, a/b and uniform thichness h, with air flowing over the surface and along the length at a Mach number, M. The panel aerodynamic model consisted of over 100,000 elements, and STARS unsteady CFD calculations were performed for a number of flutter parameters for each panel test case pertaining to a specific aspect ratio. A comparison of such nonlinear flutter solution results with experimental and approximate aerodynamic theory[27] is shown in figure 54; λ is the flutter parameter defined as

$$\lambda = 2qa^3/\beta D$$

in which

q = airstream dynamic pressure ($=1/2\rho V^2$), V being velocity

β = $\sqrt{M^2-1}$, M being the Mach numberr

D = panel stiffness parameter ($=Eh^3/12(1-\nu^2)$), E is the elastic modulus and ν the Poisson's ratio.

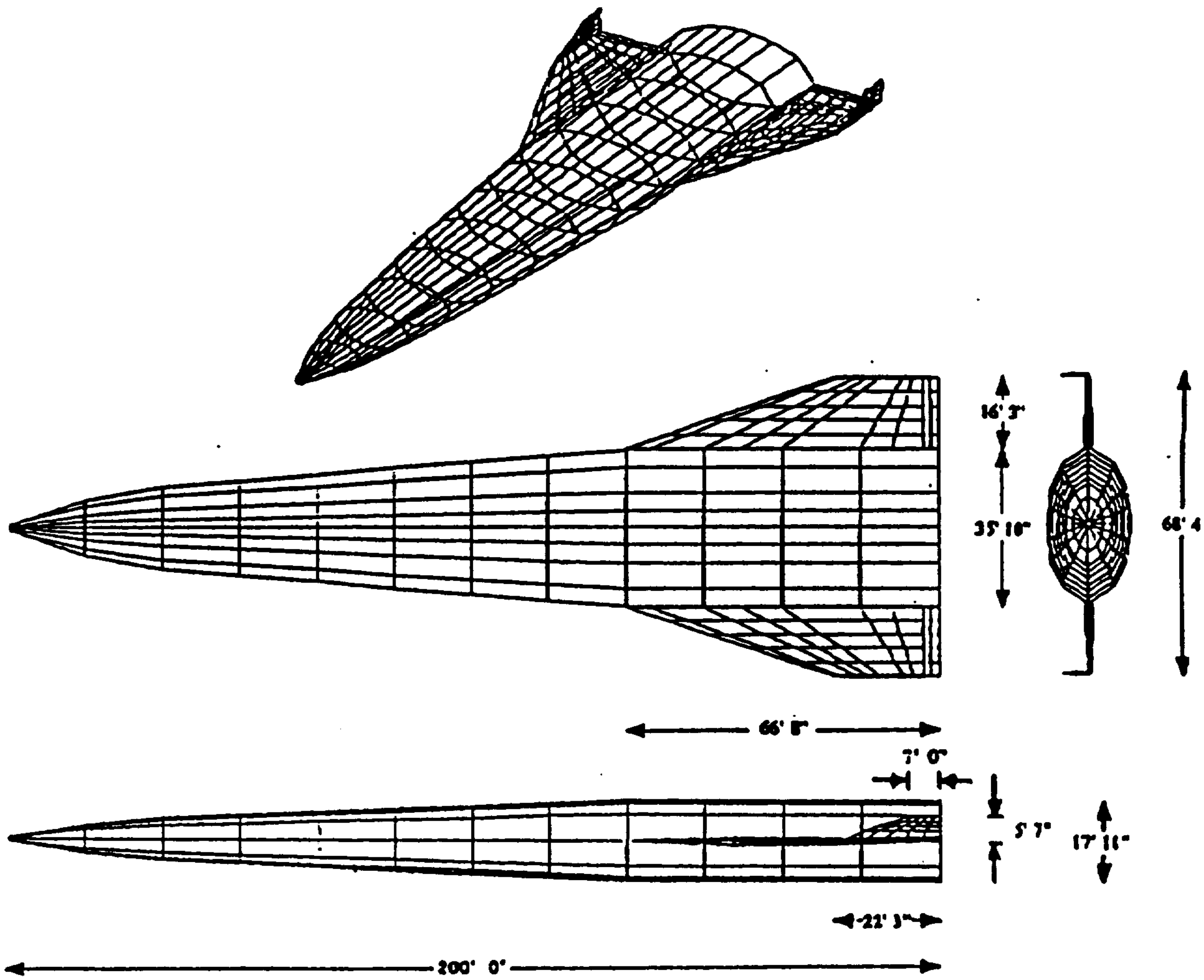

Figure 48. Generic hypersonic vehicle

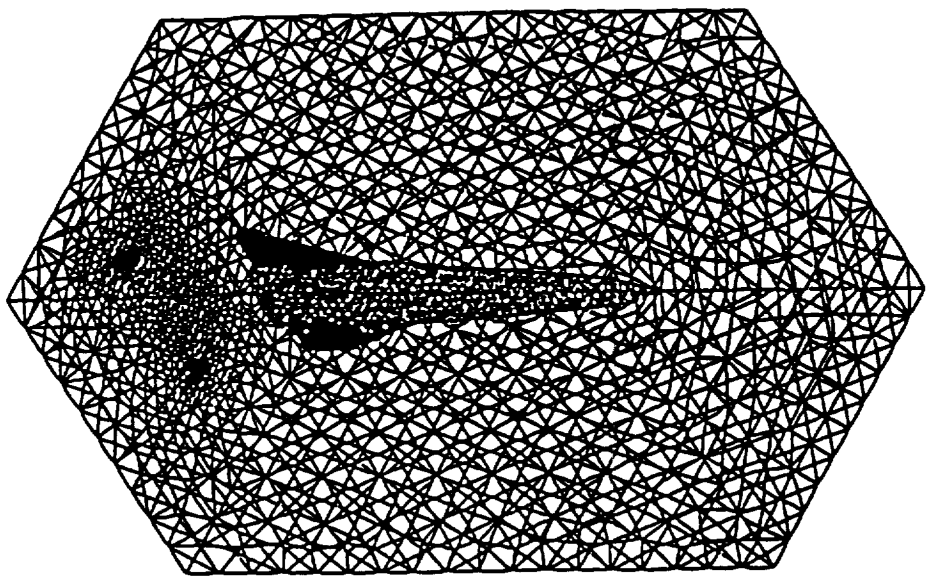

Figure 49. Generic hypersonic vehicle - surface mesh

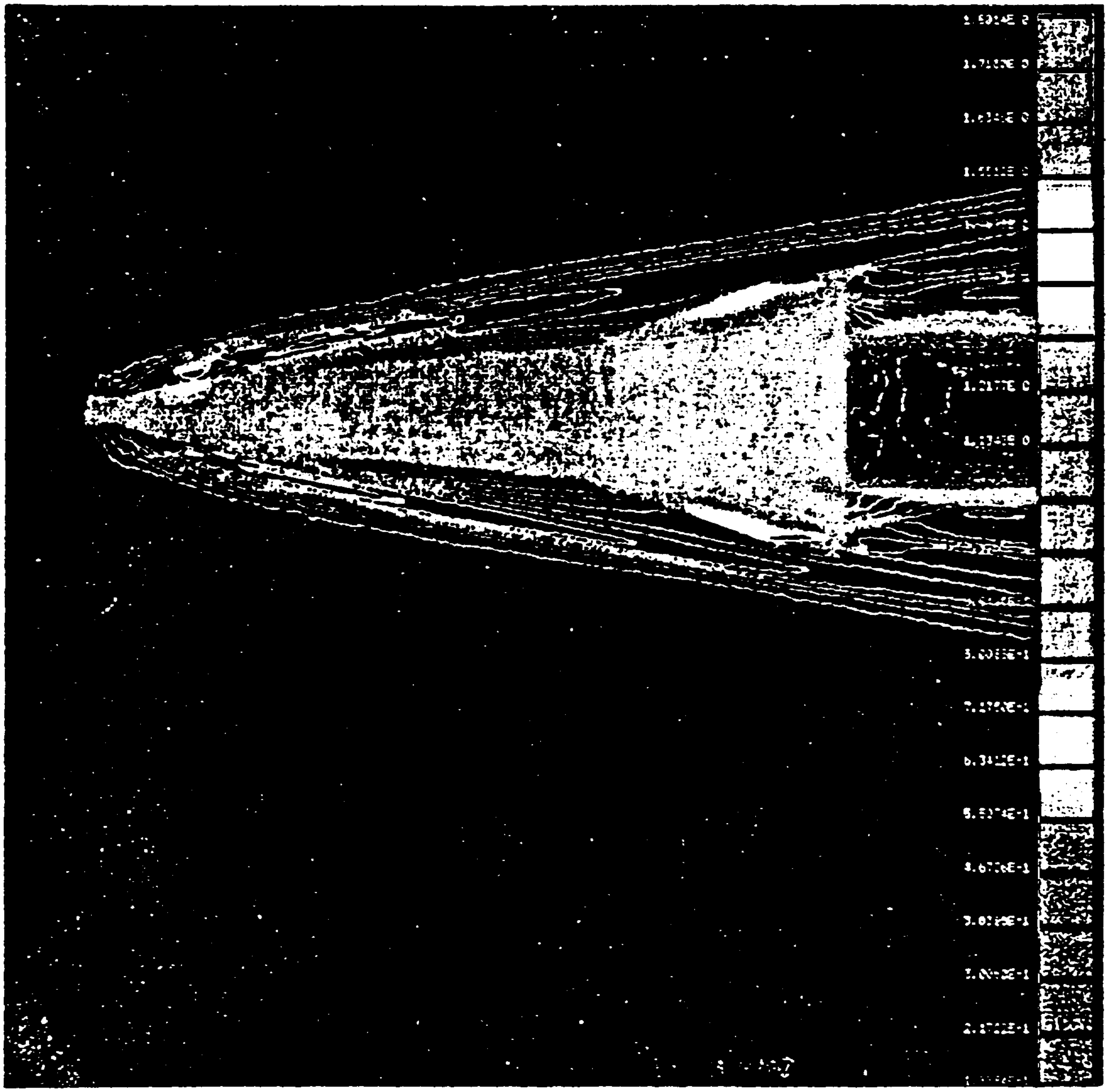

Figure 50. Generic hypersonic vehicle - density distribution

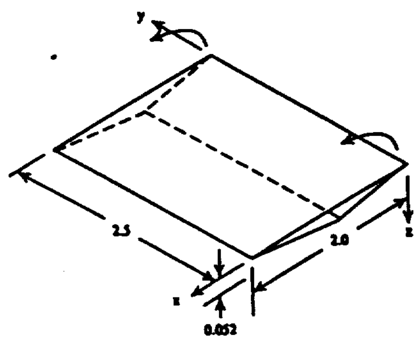

Figure 51. Oscillating vane

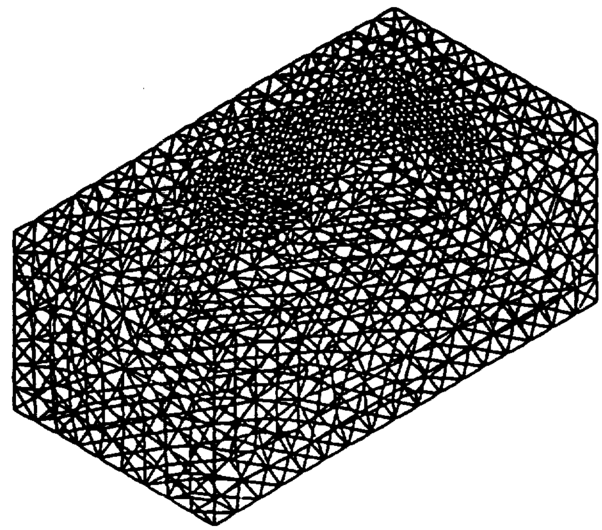

Figure 52. CFD surface grid

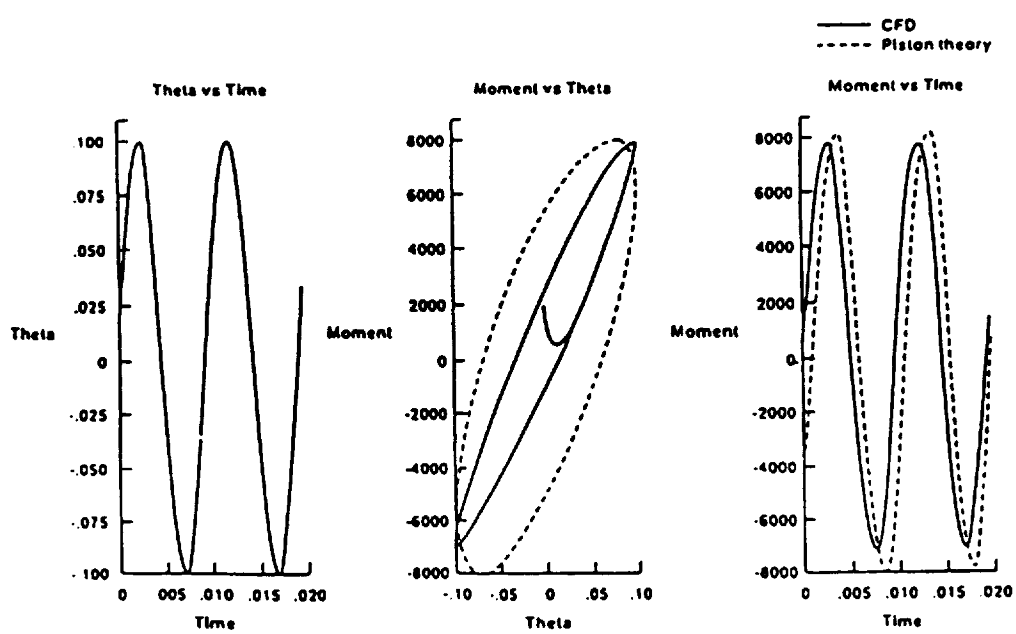

Figure 53. Double wedge airfoil - comparison of unsteady aerodynamic forces obtained from CFD and piston theory solution

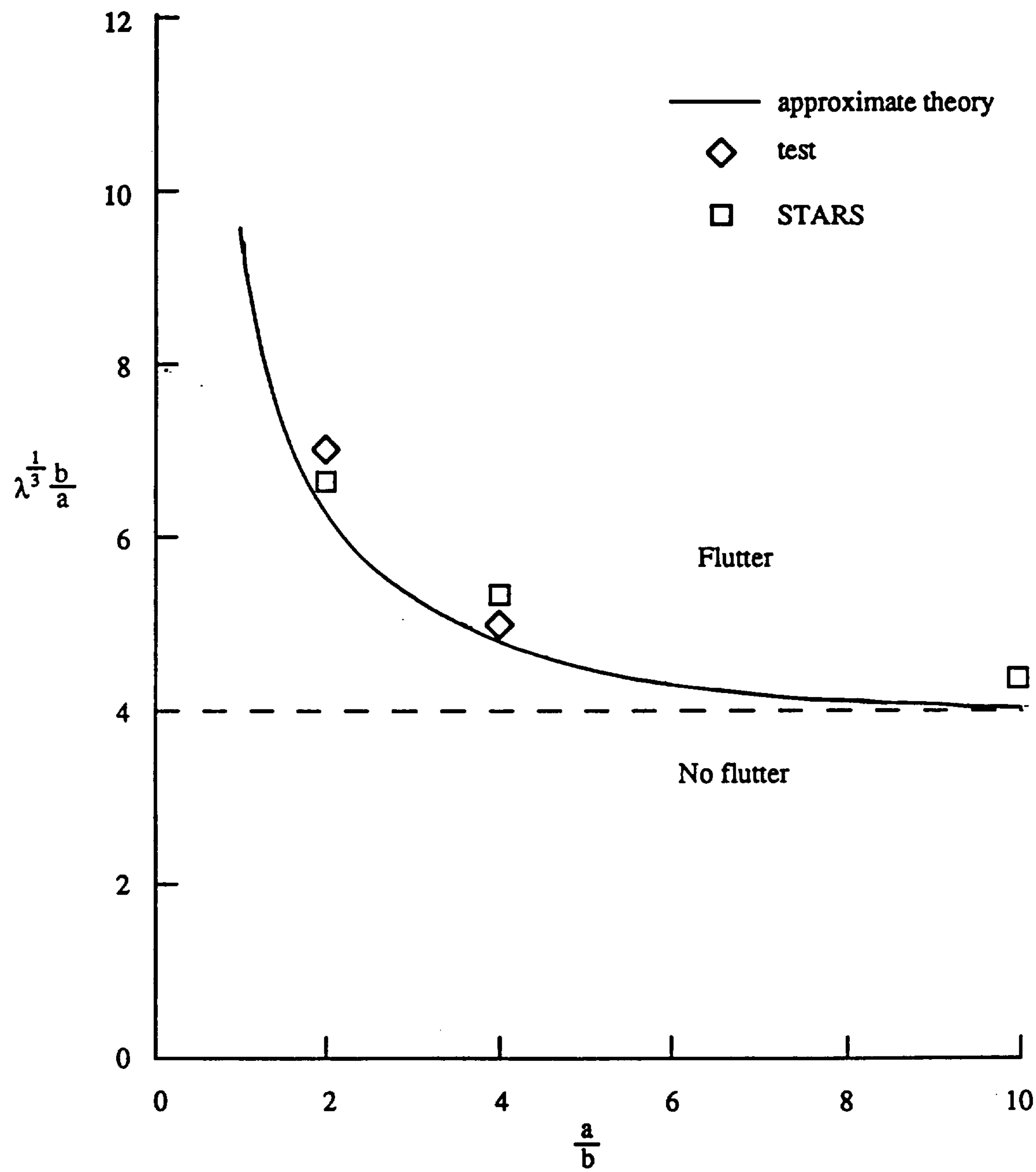

Figure 54. Clamped rectangular panel - comparison of experimental, approximate aerodynamic theory and STARS nonlinear aeroelastic solution

APPENDIX A — PREPROCESSOR MANUAL

The preprocessor routine PREPROC is an integral part of the set of routines that form the STARS program. It has been developed to automate generation of finite element models and corresponding data files. Instead of defining a complete structure by independently describing each node and element, the preprocessor allows the formation of such data automatically. The preprocessor minimizes data input, eliminates data editing, and thereby enhances the efficiency of the STARS program.

To run the preprocessor, the user may type the command GRUN followed by the command PREPROC; the program will prompt a list of different terminals. The user may then choose the type of terminal to be used, namely E/S PS390, Tektronix, and various compatible terminals. Next, the user will be prompted with menu options in a progressive fashion. At any level of the menu, the user may exit by entering Control-Z.

Only a brief description of the primary menu is given here; because of the interactive nature of the program, the user is automatically exposed to more extensive details.

PREPROC MENU

MENU OPTIONS:

0 STOP
stop the program

1 COMPUTER AIDED DESIGN
generate graphics objects

2 PROPERTIES AND ANALYSIS SPECIFICATION
specify STARS data

3 READ
read STARS data file

4 WRITE
write STARS data file

5 DELETE
delete the current structure

1 COMPUTER-AIDED DESIGN

DESIGN OPTIONS:

0 QUIT
quit this menu

1 LINES
generate line segments

2 SURFACES
generate surface segments

3 SOLIDS
generate solid segments

4 SYNTHESIS
generate surfaces from existing line segments

5 REPRODUCE
generate new segments using existing ones

6 DRAW
plot the current structure

7 EDITOR
modify existing data

1.1 LINES

0 QUIT
quit this menu

1 STRAIGHT LINE
generate straight line segment

2 PARABOLIC CURVE
generate parabolic line segment

3 CIRCULAR CURVE
generate circular line segment

4 ELLIPTIC CURVE
generate elliptical line segment

1.2 SURFACES

0 QUIT
quit this menu

1 SIMPLE SURFACE
generate four node surface segment

2 COMPLEX SURFACE
generate nine node surface segment

3 ELLIPTICAL SURFACE
generate elliptical surface segment

1.3 SOLIDS

0 QUIT
quit this menu

1 8 POINT SOLID
generate eight node segment

2 ELLIPTICAL SOLID
generate solid cylinder

3 4 POINT SOLID
generate four node segment

4 6 POINT SOLID (PRISM)
generate six node segment

1.4 SYNTHESIS

0 QUIT
quit this menu

1 ARC: LINE SEGMENT --> SURFACE
generate surface segments by moving a line segment along a curve

2 GLIDE: 2 LINE SEGMENT --> SURFACE
generate surface segments using two line segments

1.5 REPRODUCE

0 QUIT
quit this menu

1 COPY
reproduce by method of direct copying

2 MIRROR
produce a mirror image

3 ROTATE
reproduce by rotating the original about an axis

1.6 DRAW

The preprocessor will draw the generated structure on a standard terminal with multiple options.

2 PROPERTIES AND ANALYSIS

This option enables automatic generation of a complete STARS data set in which the user is prompted for appropriate input.

APPENDIX B — POSTPROCESSOR MANUAL

The POSTPLOT routine is designed to provide graphic depiction of analysis results pertaining to the three major modules, namely SOLIDS, AEROS, ASE, and CFD. This is effected by the main command GRUN, followed by the POSTPLOT command. The program runs on a variety of terminals such as E/S PS390, Tektronix, and other PLOT10/PHIGS-compatible machines.

1.0 Basic Menu

- 1.1 On-off switches
- 1.2 Load Database
- 1.3 Delete Database
- 1.4 Miscellaneous
- 1.5 Exit

1.1 On-off switches

- 1.1.1 Original structure
- 1.1.2 Deformed structure
- 1.1.3 Dynamic response
- 1.1.4 Displacement as a function of time
- 1.1.5 Stress as a function of time
- 1.1.6 Node number
- 1.1.7 Element number
- 1.1.8 Element group
- 1.1.9 Depth clipping

1.2 Load Database

- 1.2.1 Deformed or mode shape
- 1.2.2 Rendering deformed or mode shape
- 1.2.3 Dynamic response
- 1.2.4 Rendering stress
- 1.2.5 Rendering deformation

1.2.6 Displacement as a function of time

1.2.7 Stress as a function of time

1.2.8 Node numbers

1.2.9 Element numbers

1.2.10 Numerical renumbering

1.2.11 Aerodynamic paneling plots

1.2.12 Interpolated mode shape for aerodynamic load calculation

1.2.13 Aerodynamic pressure distribution

1.2.14 Frequency-damping-velocity plots, k, p-k, and ASE solutions

1.2.15 Phase and gain plots as a function of frequency for analog and digital systems

1.2.16 ASE damping and frequency plots as a function of velocity

1.2.17 CFD density, Mach, and pressure plots.

1.3 Delete Database

Essentially any one of the loaded databases, given above.

1.4 Miscellaneous

A host of additional options.

APPENDIX C — SYSTEMS DESCRIPTION

The STARS computer program is set up using a main directory and many subdirectories. The setup described in this section uses the directory names employed on various computer system at NASA. The top-level directories are shown in figure 55. [KGUPTA.STARS] is the main directory which contains the five major subdirectories named as COMMANDS, SOURCES, OBJECTS, EXECUTIONS, and TESTCASES. The COMMANDS subdirectory contains the command files which are used to guide the user in running the STARS program system. The SOURCES subdirectory contains the source elements for the program. It is further subdivided into the SOLIDS, AERODYNAMICS (linear), ASE (linear), CFD, ASE (nonlinear), CONTROLSD (Control law design)and associated GRAPHICS subdirectories. The OBJECTS subdirectory contains the object elements required for creating the execution elements. The object elements have been combined into various object libraries to ease the linking process. The EXECUTIONS subdirectory contains the execution elements used to run the program. The TESTCASES subdirectory contains a variety of representative example problems that facilitate the learning and debugging of the program.

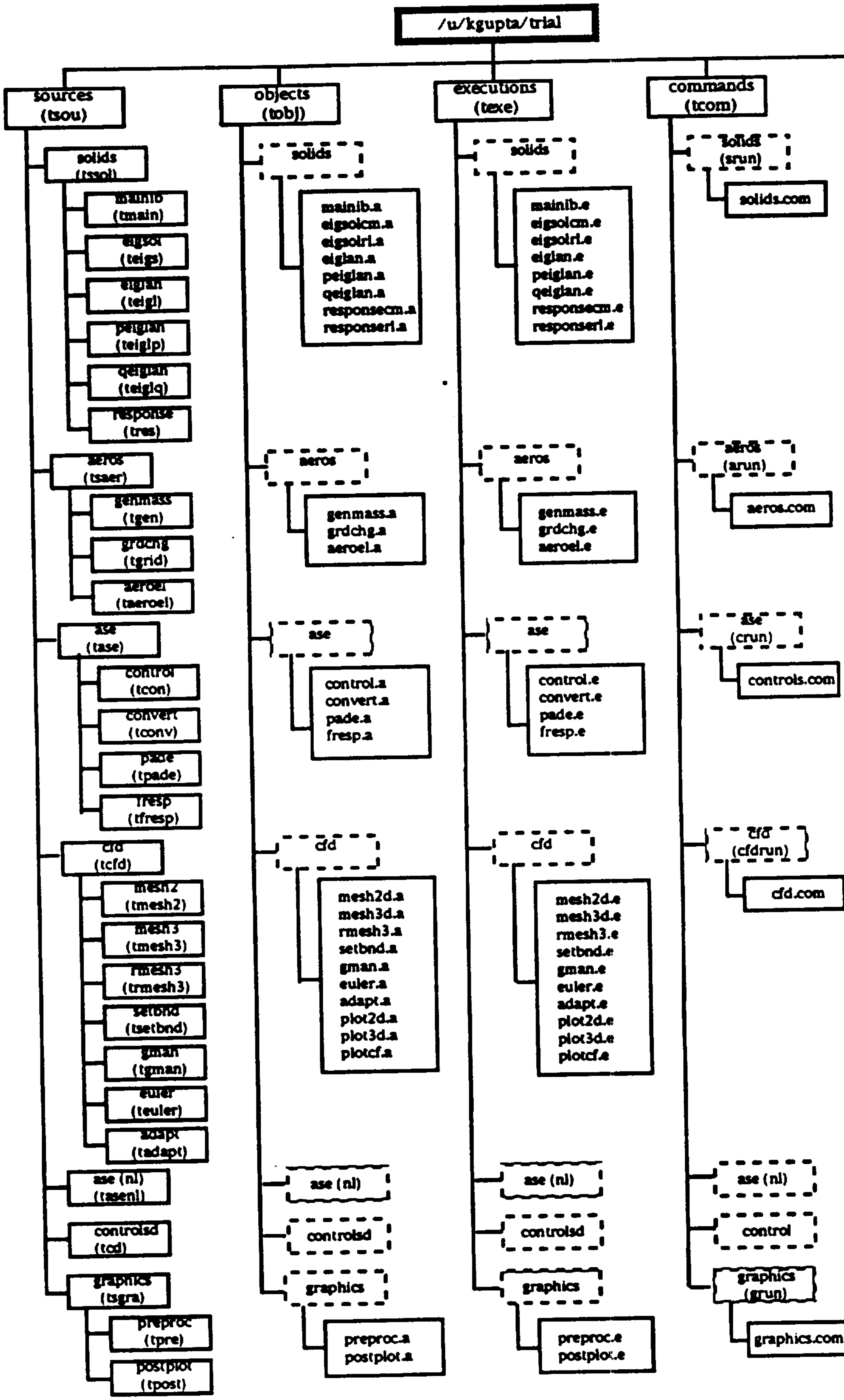

Figure 55 STARS system description

REFERENCES

1. Gupta, K.K., *STARS—A General-Purpose Finite Element Computer Program for Analysis of Engineering Structures*, NASA RP-1129, 1984.

2. Collins, R.J., "Bandwidth Reduction by Automatic Renumbering," *Inter. J. Numer. Methods Eng.*, vol. 6, 1973, pp. 345-356.

3. Gupta, K.K., "Development of a Unified Numerical Procedure for Free Vibration Analysis of Structures," *Inter. J. Numer. Methods Eng.*, vol. 17, 1981, pp. 187-198.

4. Gupta, K.K., "On a Finite Dynamic Element Method for Free Vibration Analysis of Structures," *Comput. Methods Appl. Mech. Eng.*, vol. 9, 1976, pp. 105-120.

5. Przemieniecki, J.S., *Theory of Matrix Structural Analysis*, McGraw-Hill, New York, 1968.

6. Gupta, K.K., "Formulation of Numerical Procedures for Dynamic Analysis of Spinning Structures," *Inter. J. Numer. Methods Eng.*, vol. 23, 1986, pp. 2347-2357.

7. Gupta, K.K., and C.L. Lawson, "Development of a Block Lanczos Algorithm for Free Vibration Analysis of Spinning Structures," *Inter. J. Numer. Methods Eng.*, vol. 26, 1988, pp. 1029-1037.

8. Zienkiewicz, O.C., *The Finite Element Method in Engineering Science*, McGraw Hill, United Kingdom, 1989.

9. Huebner, K.H., and E.A. Thornton, *The Finite Element Method for Engineers*, John Wiley and Sons, New York, 1982.

10. *The NASTRAN Theoretical Manual*, NASA SP-221(06), 1981.

11. Meriam, L., *Statics*, 2d ed., John Wiley and Sons, New York, 1971.

12. Ross, C.T.F., *Computer Methods in Engineering*, Elis Howard Publishers, United Kingdom, 1982.

13. Tezcan, S.S., *Application of Matrix Algebra to Problems of Plane Stress, Plane Strain, Bending of Plates and Cylindrical Shells*, Wiss. Z. Hochsch. Architek. Bauw, Weimar, Germany, 1965.

14. Rutkowski, M.J., *The Vibration Characteristics of a Coupled Helicopter Rotor-Fuselage by a Finite Element Analysis*, NASA TP-2118, 1983.

15. Gupta, K.K., M.J. Brenner, and L.S. Voelker, "Integrated Aeroservoelastic Analysis Capability with X-29A Comparisons," *J. Aircraft*, vol. 26, no. 1, 1989, pp. 84-90.

16. Abel, I., *An Analytical Technique for Predicting the Characteristics of a Flexible Wing Equipped With an Active Flutter-Suppression System and Comparison With Wind-Tunnel Data*, NASA TP-1367, 1979.

17. Appa, K., "Constant Pressure Panel Method for Supersonic Unsteady Airload Analysis," *J. Aircraft*, vol. 24, no. 10, 1987, pp. 696-702.

18. Taylor, R.F., K.L. Miller, and R.A. Brockman, *A Procedure for Flutter Analysis of FASTOP-3 Compatible Mathematical Models, Vol. 1—Theory and Application*, Air Force Wright Aeronautical Labs., TR81-3063, June 1981.

19. Geising, J.P., T.P. Kalman, and W.P. Rodden, *Subsonic Unsteady Aerodynamics for General Configurations, vols. 1 and 2*, AFFDL-TR-71-5, rev. Oct. 1977.

20. Gupta, K.K., M.J. Brenner, and L.S. Voelker, *Development of an Integrated Aeroservoelastic Analysis Program and Correlation with Test Data*, NASA TP-3120, May 1991.

21. Lo, S.H., "A New Mesh Generation Scheme for Arbitrary Planar Domains", *Inter. J. Numer. Methods Eng.*, vol. 21, 1985, pp. 1403-1426.

22. Peraire, J., Peiro, J., Formaggia, L., Morgan, K., and Zienkiewicz, O.C., "Finite Element Euler Computations in Three Dimensions, *Inter. J. Numer. Methods Eng.*, vol. 26, 1988, pp 2135-2159.

23. Gupta, K.K., and C.L. Lawson, "Multidisciplinary Modeling and Dynamic Response Analysis for Hypersonic Vehicles," paper no. AIAA-91-5015, AIAA 3rd International Aerospace Planes Conference, December 3-5, 1991, Orlando, Fl.

24. Gupta, K.K., Peterson, K., and Lawson, C., "On Some Recent Advances in Multidisciplinary Analysis of Hypersonic Vehicles", paper no. AIAA-92-5026, AIAA 4th International Aerospace Planes Conference, December 1-4, 1992, Orlando, Fl.

25. Parlett, B.N. and Scott, D.S., "The Lanczos Algorithm with Selective Orthogonalization", Math. Comp. 33, 1979, pp. 217-238.

25. Cooper, G.K., and Sirbaugh, J.R., "The PARC Code: Theory and Usage," AEDC-TR-89-15, Arnold Engineering and Development Center, Arnold AFB, TN, Dec. 1989

27. Dixon, Sidney C., *Comparison of Panel Flutter Results From Approximate Aerodynamic Theory with Results From Exact Inviscid Theory and Experiment*, NASA TND-3649, NASA LaRC, 1966.

ACKNOWLEDGEMENTS

The Eloret Institute personnel in general and Mr. S. Hozaki in particular contributed heavily in the preparation of this document, which will be published shortly as a NASA publication.

APPENDIX B

NO_X EMISSIONS FROM AIRCRAFT ENGINES

Exhaust Emissions

and

Engine Efficiency

for Aircraft Gas Turbine Engines

A Literature Review

Paul Arentzen

Eloret Institute, Claremont, California

May 1994

INTRODUCTION

The purpose of this literature study was initially to give a brief overview on recent research projects related to aircraft gas turbine engines, fuel consumption, combustion and emissions. Papers and reports that have been consulted in this research with almost no exception, point out the importance and necessity of reducing the volume of pollutant exhaust gas components. This is a general environmental concern, and in near future one will probably have to face strict national and international regulations and requirements regarding aircraft pollution. Considering this situation the study was focusing mainly on how to reduce the exhaust gas emission without suffering significant losses in the combustion efficiency and engine performance.

There are at least four more or less obvious ways to search for a solution:

1. introducing a new combustor concept that is able to burn the fuel in such a way that the amount of harmful emissions is reduced,

2. conducting a direct treatment of the exhaust gases to remove certain species,

3. performing a more fuel efficient operation and control of the aircraft. Again, less total fuel burnt means reduced emissions,

4. designing and building a more fuel efficient engine, this engine will burn less fuel for the same thrust, and generate less pollution.

In this paper my investigation will mainly concentrate on the first of these options, but I will also give a few examples related to the other three.
The volume of written material on these subjects is large and therefore my research is mainly reflecting work that has been documented during the last 5 - 10 years.

Access to the NASA Dryden library was my opportunity to perform literature search in the NASA library computer catalog and the manual systems that are available there. The "NASA Open Volumes on Aerospace", NOVA and "Scientific and Technical Aerospace Reports", STAR have also been extremely useful. For a listing of the search objects see Appendix 1.

1. THE COMBUSTION PROCESS

1.1 COMBUSTION PRODUCTS

NO_X, CO and CO_2 are the exhaust emission components causing the greatest concern. These gases are posing a threat to the ozone layer and they are causing the so-called greenhouse effect. Particulate emissions, smoke, from aircraft engines may also be a problem in certain phases of engine operation. One of my references (16) is showing an increase in smoke with higher power. Other papers say that in most regular operation conditions such emission is almost non existent.

The NO_X mainly consists of NO and NO_2 (42). In the combustion process the nitrogen oxides for the most part develop as the nitrogen in the air reacts with free oxygen atoms in the air. This product is called thermal NO_X (2). Nitrous components in the fuel will also contribute, and this part is called the prompt NO_X. According to (4) the fuels for aeroengines have practically no fuel bound nitrogen, and the thermal NO_X formation is dominant. To a cer-tain extent one is able to control several parameters that have influence on the total amount of NO_X being developed.

When burning fossil fuels, carbon dioxide CO_2, like water vapor, is a main product. If sufficient oxygen is not available, the combustion is incomplete and some of the carbon forms mono-oxide CO. Avoiding CO in the exhaust stream is therefore possible in most operating conditions by letting enough air into the combustion zone. CO_2 on the other hand is always present. The only ways to reduce CO_2 are by burning less fuel, or eventually find some other source of

energy, a different kind of fuel (20).
Based on these facts the efforts to reduce exhaust emissions should concentrate on lowering the NO_X. This has been the case with most of recent research (20) and will also be the essence of this paper.

1.2 COMBUSTION EFFICIENCY

Ideally all the energy potential in the fuel should be utilized. No pressure losses or temperature losses should occur. Starting and relighting capability and a wide operating range are other important concerns, in aircraft engines in particular. Combustors in modern gas turbine engines are optimized very close to the ideal limits.
Modifying a design to incorporate capabilities not considered in the past will most likely lead to a reduction in the efficiency originally built in.This is so crucial in all attempts of improving the combustor design. It is important to keep an eye on figures like NO_X level per power unit and NO_X per thrust, rather than just watching the NO_X per fuel, or mass percentage of NO_X in the exhaust gas. Many of the references, when discussing new combustion concepts, do not take the efficiency into consideration in their presentations. The efficiency may be reduced and the mass fraction g[NO_X]/kg[fuel] alone does not necessarily give the true and complete picture of the total emission level when this combustor becomes part of a jet engine.

1.3 THE COMBUSTOR

Developing more advanced combustor designs is said to be the only relevant option for aircraft engines (20).
From this study it is evident that temperature, pressure and time are essential to the NO_X emission (1). The availability of free oxygen in the hot zone is also necessary for the NO_X to form, and one paper is reporting that radiation from the burning gases has an impact on NO_X.In this case temperature means the actual temperature in the burning zone and in the hot areas close to that

zone. The higher the temperature the more the tendency of the nitrogen to form oxides.
The combustor inlet pressure is by some of the references said to have an influence (1, 40). A relation $NO_X \sim p0.4$ (g/kg fuel) is found, while other papers claim that the NO_X level is independent of the inlet pressure (and inlet temperature) except for their effect on the flame temperature.
Time is the residence time, when the air/fuel mixture is in the combustion zone. As NO_X formation takes time, the level increases with the residence time. Reference (13) gives a rather complicated expression for the NO_X reaction rate where the influence of system pressure, reaction temperature, mass concentrations of oxygen and carbon mono-oxide, and residence time are all included.

The relations that are mentioned above are the governing rules in all low NO_X combustor design proposals documented in the literature. The practical consequences can be found in five different principles developed for low NO_X burning. These principles are all based on one or more of the governing rules, and they are:

1. A very lean mixture (low fuel/air) combustion:
   all the cold dilution air mixed in will keep the temperature low and causing little nitrogen to react.

2. Premixing and/or prevaporization:
   the fuel/air is prepared for burning as it reaches the hot zone. The fuel is either free molecules or small particles evenly distributed in the air. When the fuel mixture reaches the flame zone it will burn much faster then a fuel sprayed directly into the combustion zone. There will be no extremely hot spots in the flame zone and the residence time is reduced.

3. A very rich (high fuel/air) combustion:
   the major part of the combustion occurs at richer then stoichiometric mixture (fuel exceeds air by 20 % - 80 % (4)). NO_X is not likely to

form because so little free oxygen atoms are available. This very rich combustion of course requires a second stage of burning to complete the combustion.

4. Introducing rotating motion, swirl, in the combustion chamber:
   that will contribute to a better mixing upstream and downstream from the combustion zone. The reason why this is giving a low NO_X level is probably that the residence time is reduced and high temperature spots are not likely to form. A more extreme way to introduce motions and thus encourage mixing in the burner is by letting strong jets of air hit the fuel sprays when entering the chamber. By doing this, so-called shear layers are generated. The flames will be located in these shear layers, and it appears to give a low NO_X combustion.

5. Varying the combustor geometry along with changing operating conditions:
   by being able to do this one can optimize the fuel/air mixture, where and how much dilution air is dumped in, how much air motions, what the residence time is etc., and such obtain control of the parameters that are influential to fuel consumption and emissions.

2. THE COMBUSTOR, GEOMETRY AND DESIGN

These five principles have been incorporated in several combustors that are evaluated with respect to NO_X through numerical analyses and experiments. This is well documented. A closer description of the most common designs will be given here.

2.1 STAGING

Most frequently mentioned are probably the staged combustors. The rich, quench, lean combustor (RQL) and the lean/lean combustor are both staged combustors.

2.1.1 The RQL Combustor

The rich, quench, lean concept has a rich fuel/air mixture primary zone followed by a quench zone where cold dilution air is mixed in to stop the burning and cool the gases, and finally a lean burn zone where the combustion is completed at a relatively low temperature.
This burner has shown good NO_X characteristics, though not quite as good as some other concepts. A NO_X reduction of 50 % compared to conventional combustors is indicated (1). It also has a wide rage of operation where stability is still acceptable. One disadvantage is the complexity and the length of this combustor. For the quench zone it is difficult to match the optimum amount of air, therefore much of NO_X develops here (25).

2.1.2 The Lean/lean Combustor

The lean/lean burner as presented in the references usually has two primary zones where the fuel is mixed with air and where also the reaction is taking place. The two stages are called the pilot burner and the main burner, and they are partly separated by a wall. Only the pilot burner will operate at low power then as a lean burner. At higher power the main burner is lit, also burning a lean mixture. The lean combustors in general do not have a wide range of operation because of problems with flame stability. The two stages will extend this range, make the combustor far more flexible. The lean/lean combustor is documented to have low NO_X levels and the efficiency is said to be good.

2.1.3 The Variable Geometry Combustor

This combustor concept in some way belongs in the staged combustion category. Some designs have several combustion stages, some are running rich/lean and some are the lean/lean concept. The key feature though is that the variable geometry combustor will adjust its size and shape according to the current conditions. The NO_X potential is a 40-50 % reduction (35).

2.2 MIXING

2.2.1 Premixing/Prevaporization

In the one stage lean mixture combustor mixing of air and fuel aerosol / fuel vapor is completed before the mixture enters the flame zone. A pre-chamber is sometimes fitted to accommodate the mixing. The LPP, lean/premixed/pre-vaporized combustor has good NO_X characteristics, according to (4) better than the RQL. Reference (13) is indicating a NO_X level at 70 % of that for the RQL, and according to (34) the level is 1 - 2 g[NO_X]/kg[fuel]. Conventional combustors are running at 3 - 5 g/kg (28).
The disadvantage with this kind of combustor, as mentioned above, is its narrow range of operation.

2.2.2 Swirlers

Several of the references are documenting the advantage of generating a rotational motion in the flow inside the burner. Through either radial or axial vanes the air is given velocity component transverse of the main flow. Depending on how the airflow encounters the fuel spray, this will contribute to a better mixing of the two, and probably also better mixing of the hot and cold air downstream from the flame zone. Both effects are positive with respect to NO_X.

Reference (10) is suggesting one further step by introducing what is called vane fuel injection, the fuel is injected into the air in the vane region. The conclusion in the report though, is that there is no significant influence on the NO_X level.

2.2.3 Jet Shear Layer Combustion

A different mixing principle is presented in reference (9), the shear layer combustion. Air and fuel are both injected, through axial and radial jets respectively. A simultaneous mixing occurs, which is supposed to cause allow NO_X emission, 4 - 7 ppm NO_X in the exhaust according to (27). The principle has proven to give very good flame stability. The emission characteristics are dependent on geometric parameters like the distance the fuel have to travel before it hits the air jets.
This combustion concept is sometimes called the lean direct injection, LDI (28).

3. COMBUSTOR INDEPENDENT NO_X ABATEMENT

In gas turbine and aerospace research and development achievements are made that may lead to a reduction on NO_X and other emissions, directly or indirectly.

3.1 EXHAUST GAS SCAVENGING

Reference (12) is a discussion on how nitrogen oxides will dissolve in water that has condensed in the exhaust stream. Water vapor will condense on carbonaceous particles as the temperature decreases downstream of the aircraft. Methods for laboratory measurements and simulations are presented, yet no NO_X level reduction is quantified.

3.2 NO_X REDUCING ADDITIVES

A study on how additives such as ammonia to the exhaust can reduce the NO_X emissions is documented (14). This method has been used in stationary gas turbines and is now mainly being investigated for the High Speed Civil Transport project. A simulation is performed which shows that from 40 % to 60 % reduction of NO_X is achievable. The big question mark though, as pointed out in the paper, is whether excess ammonia, that may be present at times, has any detrimental effect on the atmosphere.

3.3 ENGINE AND AIRCRAFT OPERATION

Recent work at NASA Dryden (43, 44) shows that through a more careful control of the flight, the fuel consumption can be lowered considerably. Integrated controllers for flight and engine operation will assist the pilot, and tests prove that a reduction in thrust specific fuel consumption of approximately 15 % is achievable.
If such controller devices are implemented in flying airplanes it will of course pay a great contribution to the effort on exhaust emission abatement.

4. EVALUATION AND SUGGESTIONS

There is still lot of research work to be done to develop the usable low NO_X combustor for aircraft applications. This is emphasized in many of the reference papers. Many important results have been obtained. To incorporate

these achievements into an applicable design is still ahead it seams. Several new concepts are found to be useful in stationary gas turbines, where size and weight are not critical. Still they may not be useful in aircraft engines.
In this last chapter I will pinpoint a few aspects that my background literature do not cover and suggest some topics for further investigation.

4.1 EFFICIENCY CONSIDERATIONS

Like I pointed out earlier, the effort on low NO_X abatement so far has very much been on

how to perform mixing of fuel and air,
the principals of combustion and governing parameters,
how and where to supply the dilution air.

Not so much has yet been done investigating how much energy is left in the gas when leaving the combustor. The number one requirement for an engine will still be on the power it is capable to deliver or what thrust it can supply in different conditions.
The new combustor concepts that are introduced in many of my references are complicated and sophisticated compared to traditional combustors. They prove to be low NO_X, they are also capable of reasonable stability and reliability in certain ranges of operation.
What we do not see so much is how well these combustors perform in transforming energy from the fuel into increase of air temperature. Some of the papers though (8, 9), present what is called the inefficiency, an efficiency loss. The inefficiency indicated for low NO_X industrial combustors is in the range of 0.05 -0.35 %. So we can not necessarily assume that a complete low NO_X combustion is the most efficient way to utilize all the available fuel energy.
I do suggest a more close look into these capabilities of the new combustor concepts to investigate how well they supply high energy air. I would like to see if there are significant correlation between NO_X emissions and combustor

efficiency. Major energy transformations are taking place in shear layers, turbulence, mixing processes, multistage combustion and in the nitrogen-oxygen reaction itself. It is the total amount of NO_X dumped in the atmosphere that matters. And going back to the introduction, we see the need to limit CO_2 emissions as well. Especially because of the direct relation between CO_2 and fuel consumption we would not like to see our attempts to reduce NO_X emissions leading to an increased overall fuel consumption.
Relevant questions are:

- Do these advanced low NO_X combustor designs allow us not to increase the specific fuel consumption for the combustor, and the engine?

- Low NO_X burners tend to be bigger than the conventional. Will the larger burners give wider/longer engines, leading to increased drag and reduced aircraft performance, and thus higher fuel consumption? And if so, what is this increase going to be?

To limit this discussion to just deal with the combustor itself I will only address the first question here.

A series of tests must be carried out to evaluate the efficiency of one or more of the low NO_X combustor concepts:

rich lean combustor
lean/lean combustor
premixed/prevaporized lean combustor
jet shear layer lean combustor.

The results from these tests should be compared to similar figures from a traditional combustor of same size and for the same range of fuel consumption and operating conditions. Many parameters may be interesting to evaluate in this investigation, the basic ones being:

* pressure drop over the combustor (P_{t4}/P_{t3})

* total temperature increase over the combustor (T_{t4}/T_{t3})

* emission level of NO_X, g[NO_X]/kg[fuel]

Based on such experiments it will be possible to go one step further in the evaluation of low nitrogen oxide combustors.

4.2 HIGH SPEED COMBUSTION AND COOLING

Considering temperature, residence time and possibly pressure, the more important parameters in the development of nitrogen oxides, one should search for alternative ways to manipulate these parameters.
For a subsonic airflow though a convergent nozzle both temperature and pressure will drop, while the speed is increasing. This is common knowledge, and just to show some figures:

> reducing the duct area for an isentropic air flow by 40 %, when Mach number is initially 0.3, we will obtain an increase in flow velocity close to 100 %, and the pressure and temperature will drop 16 % and 4 % respectively.
> A 65 % area reduction will give a Mach number increase from 0.1 to 0.3 and a pressure drop of 5 %.

The temperature alone is not going to have any significant influence on the NO_X level, and the flame will be unstable at high speeds.
Reference (8) is a research on flameholders. The flow duct itself is diverging, but the report only evaluates the combustion and NO_X regarding the sudden pressure drop over the flameholder. I have not seen any other study on the use of nozzle flow associated with combustion, and here may be a potential. I will describe two possible applications.

4.2.1 Quenching at High Speed/Low Pressure

The RQL combustor is a stable low NO_X combustor, with a wide range of operation. From reference (25) it is clear that the quench zone is where lot of the NO_X is produced. The quenching air meets hot, burning gases, and leaves free oxygen for NO_X to form. The quenching process must be conducted without using cold air, or at least cold air alone. Two of my written sources emphasize the prospects:

Ref.(25) quote:

> "- if an effective (low NO_X producing) technique to rapidly mix the secondary air with the fuel-rich primary mixture can be determined, then this concept may become practically feasible."

and ref.(34) quote:

> "It is likely that innovative quick-quench mixing schemes can significantly reduce the overall RQL NO_X levels."

By leading the hot gases from the rich burning reaction zone directly into a converging duct, the pressure will drop, speed will increase and even the temperature will fall slightly. These three phenomena together will contribute to a prompt quenching of the combustion. The convergent duct should be followed by a divergence to slow down the flow. In the divergent section (after quenching) some cold air must be added to limit the inlet temperature in the lean combustion stage. See sketch on figure 1.

4.2.2 Divergent Duct Burning

The PPL combustion is amongst the most efficient to obtain NO_X abatement. The problem with this concept is the stability at varying conditions. This stability problem could possibly be overcome by letting the combustion take place in a diverging duct. See figure 2.

The premixed fuel/air would decelerate through this duct and two advantages can be seen:

1. At some stage downstream, the flow velocity is equal to the flame propagation speed. The flame will position itself at that point. When the combustor inlet conditions are changed, higher/lower speeds and pressures occur, the flame front will move upstream and downstream accordingly. The flame front surface area will automatically adjust relating to speed/amount of mixture entering the combustor.

2. The flame front is going to be wide, probably curved and semi spherical if the duct is designed correctly. The fuel/air mixture will flow through the flame zone uniformly and fast giving a short residence time.

The combustor duct probably ought to diverge further downstream from the flame zone, due to gas expansion and the dilution air that will be mixed. No degree of stagnation causing temperature rise must happen in the hot gas zone.

There seems to be many unanswered questions in the area of combustion associated with converging and diverging flow. Especially related to NO_X abatement there may be a potential for some achievement.

ACKNOWLEDGEMENTS

This study has been supported by the Eloret Institute. I would like to thank Dr. K. Gutpa and Eloret for the invitation to come to Claremont.
Thanks to the NASA Dryden library personnel for all assistance during this time.

REFERENCES

1. Zaralis N., Joos F., Glaeser B., Ripplinger T.;
No(x) Reduction by Rich-Lean Combustion
AIAA, 28th Joint Propulsion Conference and Exhibit 1992

2. Kundu K.P., Deur J.M.;
A Simplified Reaction Mechanism for Prediction of NO(x) in the Combustion of Hydrocarbons
AIAA, 28th Joint Propulsion Conference and Exhibit 1992

3. Rizk N.K., Mongia H.C.;
NO(x) Model for Lean Combustion Concept
AIAA, 28th Joint Propulsion Conference and Exhibit 1992

4. Gupta A.;
The Effect of Combustor Dome Geometry on the Structure of Flame and NO(x) Emission
AIAA, 28th Joint Propulsion Conference and Exhibit 1992

5. Jones B.;
Requirements in the Development of Gas Turbine Combustors
Rolls-Royce, 1988

6. Moss J.E.;
Exhaust Emissions Survey of a Turbofan Engine for Flame-Holder and Swirl-Type Augmenters at Simulated Altitude Flight Conditions
NASA, TM 82787

7. Mellor A.M., Fritsky K.J.;
Turbine Combustor Preliminary Design Approach
J. Propulsion, May-June 1990

8. Duerr R.A., Lyons V.J.;
Effect of Flameholder Pressure Drop on Emissions and Performance of Premixed-Prevaporized Combustors
NASA, TP 2131

9. Hussain U.S., Andrews G.E., Cheng W.G., Shahabadi A.R.;
Low NO(x) Primary Zones Using Jet Mixing Shear Layer Combustion
The University of Leeds, UK (1988)

10. Alkabie H.S., Andrews G.E., Ahmad N.T.;
Lean Low NO(x) Primary Zones Using Radial Swirlers
The University of Leeds, UK (1988)

11. Al Dabbagh N.A., Andrews G.E.;
The Influence of Premixed Combustion Flame Stabilizer Geometry on Flame Stability and Emissions
The University of Leeds, UK (1981)

12. Whitefield P.D. el al.;
NO(x) Scavenging on Carbonaceous Aerosol Surfaces in Aircraft Exhaust Plumes, Part I
University of Missouri - Rolla

13. Rizk N.K., Mongia H.C.;
Three-dimensional Emission Modeling for Diffusion Flame, Rich/Lean, and Lean Gas Turbine Combustors
Allison Gas Turbine Division, GM, Indianapolis (1993)

14. Adelman H.G., Menees G.P., Cambier J-L.;
NO(x) Reduction Additives for Aircraft Gas Turbine Engines
Eloret Institute, NASA-Ames (1993)

15. Beck J.P. et al.;
Effect of Aircraft Emissions on Atmospheric Ozone in the Northern Hemisphere
Ministerie van Volkshuisvesting, Netherlands (1990)

16. Wassell A.B.;
Commercial Aircraft and the Environment
Rolls-Royce (1990)

17. Wuebbles D.J.;
Designing a Methodology for Future Air Travel Scenarios
Lawrence Livermore National Laboratory, CA (1992)

18. Snape D.M., Metcalfe M.T.
Emissions form Aircraft: Standards and Potential for Improvement
Rolls-Royce (1991)

19. Lee, Chi-Ming et al.;
Nitric Oxide Formation in a Lean, Premixed-Prevaporized Jet A/Air Flame Tube: An Experimental and Analytical Study
NASA-Lewis, 1993

20. Bahr D.W.;
Turbine Engine Developers Explore Ways to Lower NO(x) Emissions Levels
GE Aircraft Engines / The Environment

21. Motevalli V.;
Effects of Gas Turbine Combustor Geometry Variation on Pollutant Emission using a Multi-annular, Telescopic, Swirl Combustor
ASME Paper 90-GT-280 [Abstract]

22. Metcalfe M.T., Eaton R.A., Snape D.M.;
The Impact of Air Transport on the Environment
10th ISABE, (1991)[Abstract]

23. Bahr D.W.;
Aircraft Engine NO(x) Emissions - Abatement Progress and Prospects
10th ISABE, (1991)[Abstract]

24. Kinnison D.E., Wueeles D.J.;
Future Aircraft and Potential Effects on Stratospheric Ozone and Climate
Lawrence Livermore National Laboratory, CA (1992)

25. Menon S. et al.;
A New Unsteady Mixing Model to Predict NO(x) Production During Rapid Mixing in a Dual-Stage Combustor
30th Aerospace Sciences Meeting & Exhibit, 1992

26. Chen C.P. et al.;
A Novel Gas-Droplet Numerical Method for Spray Combustion
Dept. of Chemical Engineering, Univ. of AL. (1991)

27. Al Dabbagh et al.;
Shear Layer Combustion: Influence of the Method of Fuel Injection on Stability and Emissions
University of Leeds, UK

28. Colantonio R.O.;
Application of Jet-Shear-Layer Mixing and Effervescent atomization to the Development of a Low-NO(x) Combustor
NASA TM 105888

29. Gupta A., King M.K., Daily J., Sabla P.;
Combustion Faces Environmental Challenges
Aerospace America, Jul 1990

30. Ma Y., Van Moorhem W.K., Shorthill R.W.;
Experimental Investigation of Velocity Coupling in Combustion Instability
University of Utah, UT / J. Propulsion

31. Odgers J, et al.;
The Combustion of Droplets within Gas Turbine Combustors - Some Recent Observations
ASME, 37th Int. Congress 1992 [Abstract]

32. Alkabie H.S. et al.;
The Influence of Fuel Placement on NO(x) Emissions From Flames Stabilized by Radial Swirlers
10th ISABE, (1991) [Abstract]

33. Ohkubo et al.;
Ignition and Exhaust Emission Characteristics of Spray Combustion in a Prechamber Type Vortex Combustor
ASME, 37th Int. Congress 1992 [Abstract]

34. Lyons V.J., Niezwiecki R.W.;
Combustor Technology for Future Small Gas Turbine Aircraft
NASA-Lewis, (1993)

35. Desaulty M.;
Turbine Engine Combustor Design at SNECMA
10th ISABE, (1991)

36. Senechal P.J.;
New Approaches for a Second Generation Supersonic Transport Propulsion System
SNECMA
2nd Int. Aerospace Symp. 1991

37. Lee C-M. et al.;
Simplified Jet Fuel Reaction Mechanism for Lean Burn Combustion Application
NASA-Lewis (1993)

38. Sivashinsky G.I.;
Studies in Premixed Combustion
The City University of New York (1992)

39. Turns S.R., Bandaru R.V.
Oxides of Nitrogen Emissions from Turbulent Hydrocarbon/Air Jet Diffusion Flames
The Pennsylvania State University, PA, 1992

40. Rizk N.K., Mongia H.C.;
Three-dimensional NO(x) Model for Rich/Lean Combustor
31st Aerospace Sciences Meeting & Exhibit, 1993

41. Wu M-Z.B.;
Velocity and Temperature Measurements in a Non-Premixed Reacting Flow Behind a Backward Facing Step
Pn.D. Georgia Inst. of Tech. [Abstract]

42. Scheid J. et al.;
Measurements of Jet Aircraft Emissions at Cruise Altitude.
I - The Odd-Nitrogen Gases ----.
ISSN 0094-8276, 1992 [Abstract]

43. Myers L.P., Connors T.R.;
Flight Evaluation of an Extended Engine Life Mode on an F-15 Airplane
NASA-Dryden, 1992

44. Stewart J.F.
Integrated Flight Propulsion Control Research Results Using the NASA F-15 HIDEC Flight Research Facility
NASA-Dryden, NASA TM 4394

APPENDIX 1

THE LITERATURE SEARCH

The entries I have been using in the computer search are based on the following objects:

combustion efficiency
combustion products
exhaust emissions
exhaust gases
gas turbine
burning rate
fuel/air ratio
pressure dependence
subsonic aircraft
air pollution
environmental effects

A number of combinations in groups of two, three and four of the objects formed the entities.

In the NOVA and STAR I have more specifically looked for references related to single key objects and their sub objects. These key objects are:

combustion
efficiency
exhaust
fuel
performance
emission
environment
nitrogen
pollution

The search in NOVA and STAR goes back two years only.

APPENDIX 2

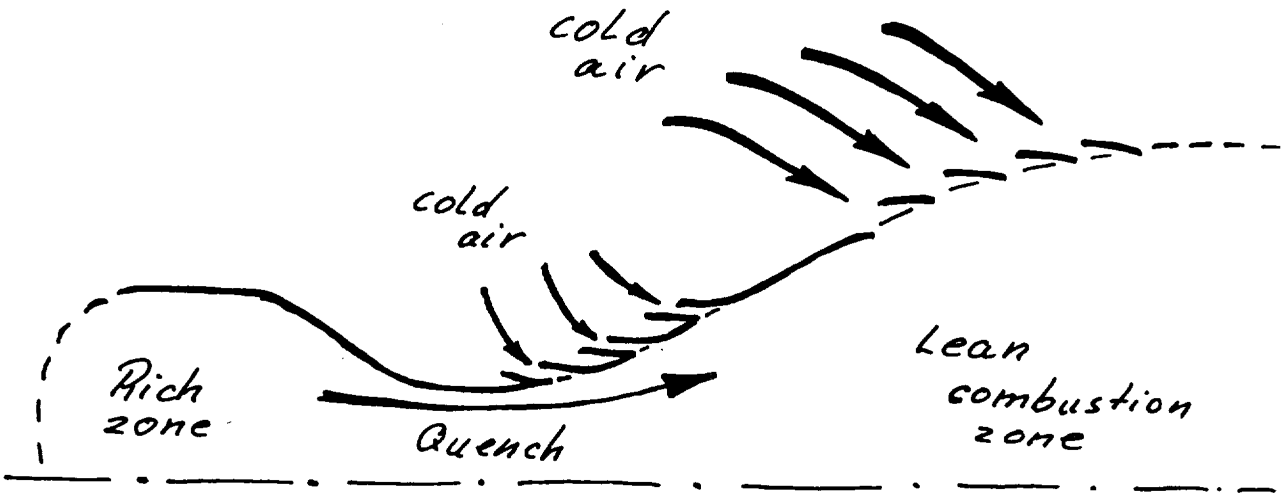

FIGURE 1. **High speed guenching.**

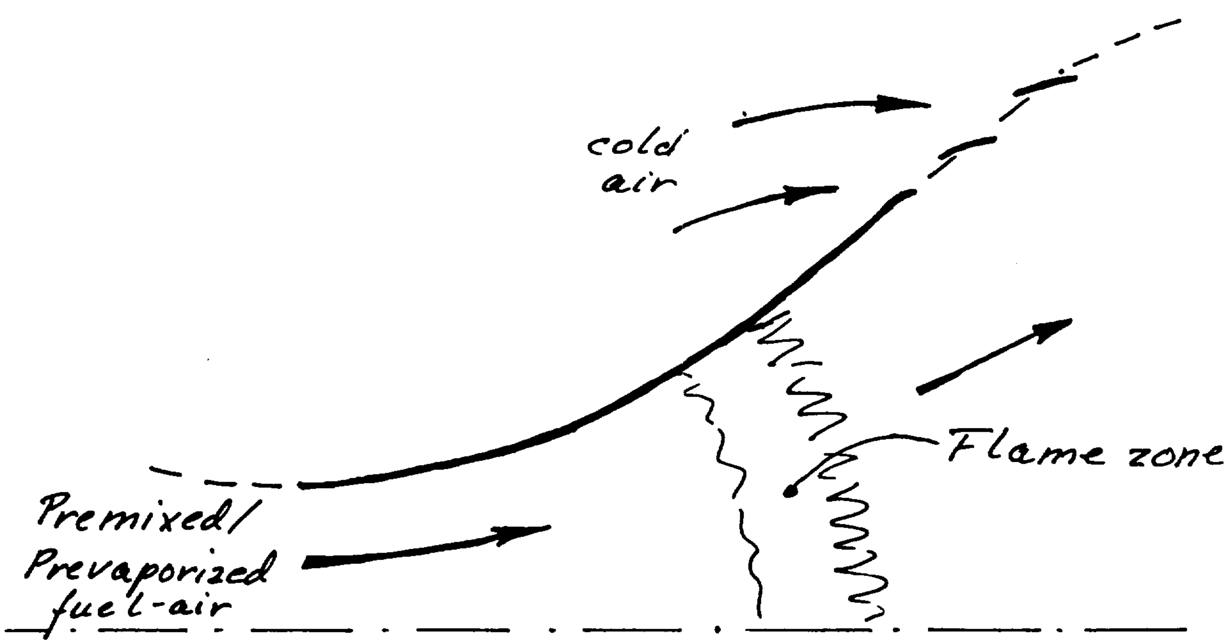

FIGURE 2. **Divergent duct burning.**